

University of Massachusetts Medical School

eScholarship@UMMS

GSBS Dissertations and Theses

Graduate School of Biomedical Sciences

2011-05-16


Blocking the Notch Pathway with Gamma-Secretase Inhibitors Enhances Temozolomide Treatment of Gliomas through Therapy-Induced Senescence: A Dissertation

Candace A. Gilbert

University of Massachusetts Medical School

Let us know how access to this document benefits you.

Follow this and additional works at: https://escholarship.umassmed.edu/gsbs_diss

 Part of the [Amino Acids, Peptides, and Proteins Commons](#), [Cancer Biology Commons](#), [Heterocyclic Compounds Commons](#), [Neoplasms Commons](#), [Pharmaceutical Preparations Commons](#), and the [Therapeutics Commons](#)

Repository Citation

Gilbert CA. (2011). Blocking the Notch Pathway with Gamma-Secretase Inhibitors Enhances Temozolomide Treatment of Gliomas through Therapy-Induced Senescence: A Dissertation. GSBS Dissertations and Theses. <https://doi.org/10.13028/a7fz-f103>. Retrieved from https://escholarship.umassmed.edu/gsbs_diss/534

This material is brought to you by eScholarship@UMMS. It has been accepted for inclusion in GSBS Dissertations and Theses by an authorized administrator of eScholarship@UMMS. For more information, please contact Lisa.Palmer@umassmed.edu.

BLOCKING THE NOTCH PATHWAY WITH GAMMA-SECRETASE INHIBITORS
ENHANCES TEMOZOLOMIDE TREATMENT OF GLIOMAS THROUGH
THERAPY-INDUCED SENESENCE

A Dissertation Presented

By

CANDACE ANN GILBERT

Submitted to the Faculty of the
University of Massachusetts Graduate School of Biomedical Sciences, Worcester
in partial fulfillment of the requirements for the degree of

DOCTOR OF PHILOSOPHY

May 16, 2011

CANCER BIOLOGY

BLOCKING THE NOTCH PATHWAY WITH GAMMA-SECRETASE INHIBITORS
ENHANCES TEMOZOLOMIDE TREATMENT OF GLIOMAS THROUGH
THERAPY-INDUCED SENESENCE

A Dissertation Presented

By

CANDACE ANN GILBERT

The signatures of the Dissertation Defense Committee signifies
completion and approval as to style and content of the Dissertation

Alonzo Ross, Ph.D., Thesis Advisor

Stephen Lyle, Ph.D., M.D., Member of Committee

Lucio Castilla, Ph.D., Member of Committee

Merav Socolovsky, Ph.D., MBBS, Member of Committee

Jeremy Rich, M.D., Member of Committee

The signature of the Chair of the Committee signifies that the written dissertation meets
the requirements of the Dissertation Committee

JeanMarie Houghton, Ph.D., M.D., Chair of Committee

The signature of the Dean of the Graduate School of Biomedical Sciences signifies
that the student has met all graduation requirements of the school.

Anthony Carruthers, Ph.D.,
Dean of the Graduate School of Biomedical Sciences

Cancer Biology Program

May 16, 2011

Dedication:

This thesis is dedicated with love to those who are no longer with us.
Claudia Gilbert, Granny Gilbert Glezen, Grandpa Strecker,
Nanny Bush, and Poppy Bush.

Acknowledgements:

First and foremost, I would like to thank my amazing family for being there with me every step of the way. My mom and dad have been continuously supportive. I count my blessings everyday that I have a family that raised me to have the morals and dedication that they did, and I know that this would not be possible without them! My brother and sister have also supported me from day one, and they have all put up with endless phone calls about science and snow storms. Thank you Mom, Dad, Lewis and Katie!

I would also like to thank Alonzo for being an amazing mentor. I never imagined that I could have learned so much in the time here, and a large majority of that, I owe to him. He has always been there to provide guidance when needed, while still allowing me to have my freedom to focus on topics that I found interesting in the field. We have an amazing lab atmosphere that has become my separate work family, with Alonzo at the head of the table. His personality, intellect and work ethic have taught me what it will take to succeed in science.

There have been so many people that have provided additional support and guidance throughout the years. I would like to thank my committee, JeanMarie Houghton, Steve Lyle, Lucio Castilla, and Merav Socolovsky. I would specifically like to thank Dr. Rick Moser for his support throughout the years, and always being willing to provide advice and fresh tumor samples. Yulian, Jess and Marie-Claire for guidance in the lab and Denise, Steve, Karen and Kshama for being my adopted lab family.

Finally, I would not have survived without my friends. It is amazing to think that we all showed up here in 2005 (some of you in 2006) as complete strangers, definitely not knowing what to expect. It's been an amazing ride thanks to you guys! Yulian, you have been there through it all, and I will never be able to thank you enough for all the laughs and very late nights! Christine, Mike, Kyle, Ryan, Jamie, James, Nate, and Jay, I would never have survived without you! Linzy, Lindsey and Derek, I am going to miss all our times together! You have all been such a support system throughout the years. Thank you for the wonderful memories and the crazy times!

Abstract:

Glioma therapy relies on induction of cytotoxicity; however, the current combination of surgery, irradiation (IR) and temozolomide (TMZ) treatment does not result in a long-term cure. Our lab previously demonstrated that a small population of glioma cells enters a transient cell cycle arrest in response to chemotherapy. Treatment with TMZ significantly decreases initial neurosphere formation; however, after a short recovery period, a small number of cells resume neurosphere formation and repopulate the culture. This recovery of neurosphere growth recapitulates the inevitable glioma recurrence in the clinic. The focus of our laboratory is to study direct-target therapies that can be combined with TMZ to inhibit neurosphere recovery. The Notch pathway is a promising target because it is involved in cell growth and survival. Here, we demonstrate that blocking the Notch pathway using gamma-secretase inhibitors (GSIs) enhances TMZ treatment. The combination of TMZ and GSI treatments targets the cells capable of recovery. TMZ + GSI treated cells do not recover and are no longer capable of self-renewal. Interestingly, recovery is inhibited when the GSI is administered 24 hrs after TMZ treatment, demonstrating a sequence-dependent mechanism. TMZ + GSI treatment also decreases tumorigenicity. When glioma cell lines were treated *in vitro* and implanted in NU/NU nude mice, TMZ + GSI treatment extended latency and greatly increased survival. In addition, *in vivo* TMZ + GSI treatment completely blocked tumor progression and resulted in the loss of a palpable tumor in 50% of mice, while none of the TMZ-only treated mice survived. TMZ + GSI treated cultures and xenografts display a senescent phenotype. Cultures treated with TMZ + GSI have decreased proliferation, but no increase in cell death. We observed an increase in the number of cells expressing senescence-associated β -galactosidase *in vitro* and *in vivo*. This demonstrates that inhibition of the Notch pathway shifts TMZ-treated cells from a transient cell cycle arrest into a permanent senescent state. Senescent cells can stimulate the innate immune system. Here we demonstrate that TMZ + GSI treatment increases phagocytosis *in vitro*. New therapy combinations, such as TMZ + GSI, are arising in the field of therapy-induced senescence (TIS). Overall, this data demonstrates the importance of the Notch pathway in chemoprotection and maintenance of TMZ-treated gliomas. The addition of GSIs to current treatments is a promising target-directed therapy to decrease the rate of brain tumor recurrence by inducing senescence and tumor clearance.

Table of Contents:

Dedication.....	iii
Acknowledgements.....	iv
Statement of Contribution.....	vi
Abstract.....	v
Table of Contents.....	vi
List of Tables.....	ix
Table of Figures.....	x
List of Abbreviations.....	xii
Preface.....	xv
CHAPTER I: Introduction.....	1
Gliomas.....	2
<i>Glioma therapy.....</i>	3
<i>Glioma recurrence and survival rates.....</i>	4
Cancer Stem Cells.....	6
<i>Clonal Evolution versus the cancer stem cell hypothesis.....</i>	6
<i>Discovery of neural stem cells.....</i>	11
<i>Glioma stem cells.....</i>	14
<i>Glioma stem cell cultures.....</i>	16
Neurosphere cultures.....	18
Laminin-coated cultures.....	23
Invincible Glioma Stem Cells?	24
<i>Chemoresistance and radioresistance.....</i>	24
<i>Notch signaling pathway.....</i>	30
<i>Notch signaling in gliomas.....</i>	34
Senescence: An Irreversible Cell Cycle Arrest.....	37
<i>Pathways of senescence.....</i>	39
<i>The senescent phenotype.....</i>	41

<i>Senescence and cancer</i>	43
<i>Senescence and Notch</i>	46
Research Framework and Objectives.....	46
CHAPTER II: Gamma-Secretase Inhibitors Enhance Temozolomide Treatment by Inhibiting Neurosphere Repopulation and Xenograft Recurrence	48
Introduction.....	49
Results.....	51
<i>Establishment of glioma neurosphere cultures</i>	51
<i>Glioma neurosphere cell lines express Notch receptors and downstream targets</i>	55
<i>TMZ + DAPT treatment inhibits neurosphere recovery and secondary neurosphere formation</i>	57
<i>Serum cultures are more sensitive to TMZ and do not recover</i>	65
<i>Constitutive expression of NICD protects neurosphere cultures from TMZ + DAPT treatment</i>	70
<i>TMZ + DAPT treatment response is schedule-dependent</i>	74
<i>TMZ + DAPT ex vivo treatment greatly reduces tumor formation</i>	79
<i>TMZ + LY in vivo treatment inhibits tumor regrowth</i>	82
Discussion.....	87
Materials and Methods.....	93
CHAPTER III: Combined Treatment with Temozolomide and Gamma-Secretase Inhibitors Target Glioma-Propagating Cells by Inducing Senescence	102
Introduction.....	103
Results.....	104
<i>TMZ + DAPT treatment does not increase cell death in neurosphere cultures</i>	104
<i>SA-β-galactosidase is increased in TMZ + DAPT treated cultures</i>	106
<i>TMZ + DAPT-induced senescence is schedule-dependent in vitro</i>	112
<i>TMZ + LY treated xenografts have decreased proliferation</i>	116

<i>SA-β-galactosidase is induced in xenografts by in vivo TMZ + LY treatment</i>	119
<i>TMZ + DAPT treatment enhances macrophage phagocytosis of neurosphere cells</i>	124
Discussion.....	128
Materials and Methods.....	132
CHAPTER IV: Final Conclusions and Future Directions	139
What population is targeted by TMZ + GSI treatment?	140
<i>Glioma cancer stem cells</i>	140
<i>Notch-expressing subpopulation</i>	143
Multifaceted Effects of TMZ + GSI Treatment.....	145
<i>Senescence and the immune system in gliomas</i>	147
<i>Notch signaling and the glioma vasculature</i>	151
Future Directions	152
Final Thoughts.....	153
APPENDIX: Preliminary Data	156
<i>p21 is persistently upregulated in TMZ + DAPT treated neurosphere cultures</i>	157
<i>Cytokine secretion is upregulated in TMZ + GSI treated cultures</i>	159
<i>TMZ-only treated gliomas progress after in vivo treatment in an intracranial xenograft model</i>	160
REFERENCES	165

List of Tables:

2.1: Neurosphere cultures established from patient gliomas.....	54
2.2: Tumor formation in subcutaneous xenografts after <i>ex vivo</i> drug treatment.....	81
2.3: List of PCR primer sequences.....	98

List of Figures:

1.1: Neural stem cell hierarchy.....	12
1.2: Glioma stem cell differentiation.....	15
1.3: Glioma culture methods.....	17
1.4: Glioma therapy cancer stem cell hypothesis.....	26
1.5: Notch Signaling Pathway.....	35
1.6: p53 and Rb signaling in senescence.....	40
2.1: Neurosphere formation in established primary neurosphere cultures.....	52
2.2: Notch pathway gene expression in glioma cultures.....	56
2.3: Neurosphere recovery assay schematic.....	58
2.4: DAPT does not significantly decrease neurosphere formation.....	59
2.5: Neurosphere size is inhibited by TMZ + DAPT treatment.....	60
2.6: TMZ + DAPT treatment blocks recovery and secondary neurosphere formation...	61
2.7: LY411,575 alone does not significantly decrease neurosphere formation.....	64
2.8: TMZ + LY blocks neurosphere recovery and secondary neurosphere formation...	66
2.9: MGMT expression levels by real time PCR in neurosphere converted cultures and primary lines	67
2.10: MGMT ⁺ lines are not responsive to TMZ treatment	68
2.11: Adherent glioma cultures do not recover after TMZ or TMZ + DAPT treatment.	69
2.12: Expression of constitutively active NICD blocks GSI knockdown of Notch targets.....	71
2.13: Expression of constitutively active NICD attenuates the TMZ + DAPT treatment synergy.....	73
2.14: Neurosphere recovery assay drug schedule treatment schematic	75
2.15: Schedule treatment affects recovery and secondary neurosphere formation	76
2.16: Neurosphere size after the schedule treatment assay	78
2.17: <i>Ex vivo</i> TMZ + DAPT treatment decreases tumorigenicity.....	80
2.18: <i>In vivo</i> TMZ and LY chow treatment effects on toxicity and gene expression.....	84

2.19: <i>In vivo</i> TMZ + LY treatment blocks tumor progression	85
2.20: Individual tumor volumes from <i>in vivo</i> TMZ + LY treatment.....	86
2.21: <i>In vivo</i> TMZ + LY treatment leads to tumor regression in 50% of treated mice...88	
3.1: TMZ + DAPT treatment does not increase cell death.....	105
3.2: TMZ + DAPT induces SA- β -galactosidase in neurosphere cultures.....	107
3.3: TMZ + DAPT induces SA- β -galactosidase in U87NS and U373NS cultures	108
3.4: SA- β -galactosidase in the U87NS NICD-expressing culture.....	111
3.5: Therapy-induced senescence in the neurosphere assay schedule treatment is unique to DAPT post-treatment in U87NS	113
3.6: Therapy-induced senescence in the neurosphere assay schedule treatment is unique to DAPT post-treatment in U373NS.....	114
3.7: Therapy-induced senescence in the neurosphere assay schedule treatment is unique to DAPT post-treatment.....	115
3.8: Ki67 expression decreases in TMZ + LY treated U87NS xenografts.....	117
3.9: Ki67 expression in DMSO and LY chow treated U87NS xenografts.....	118
3.10: Ki67 expression in TMZ-only and TMZ + LY treated U87NS xenografts.....	120
3.11: DMSO <i>in vivo</i> control treatment and SA- β -galactosidase staining.....	121
3.12: LY chow-only <i>in vivo</i> treatment and SA- β -galactosidase.....	122
3.13: TMZ <i>in vivo</i> treatment induces SA- β -galactosidase.....	123
3.14: TMZ + LY <i>in vivo</i> treatment induces SA- β -galactosidase.....	125
3.15: TMZ + LY <i>in vivo</i> treatment induces SA- β -galactosidase.....	126
3.10: TMZ + DAPT treated cells are more susceptible to macrophage phagocytosis....	127
3.11: TMZ + DAPT treated cells are more susceptible to macrophage phagocytosis....	129
4.1: TMZ + GSI Treatment Mechanism.....	141
4.2: TMZ + GSI treatment model.....	146
A.1: TMZ + DAPT treatment induces a persistent upregulation of p21 transcript levels	158
A.2: Secretion of IL-6 and IL-8 are highest in TMZ + DAPT treated cultures.....	161
A.3: TMZ-only treated intracranial xenografts are capable of tumor progression.....	163

List of Abbreviations:

AA,	anaplastic astrocytoma
ABC,	adenosine triphosphate-binding cassette
BCNU,	1,3-bis(2-chloroethyl)-1-nitrosourea
bFGF,	basic fibroblast growth factor
BrdU,	bromodeoxyuridine
CDK,	cyclin-dependent kinase
CFSE,	carboxyfluorescein succinimidyl ester
CKI,	cyclin kinase inhibitors
CSC,	cancer stem cell
CSF,	cerebrospinal fluid
CSL,	CBF1/Suppressor of Hairless/Lag1
CT-B	cholera toxin subunit B
DAPI,	4'-6-Diamindino-2-phenylindole
DAPT,	N-[N-(3,5-difluorophenacetyl)-L-alanyl]-5-phenylglycine t-butyl ester
DDR,	DNA damage response
dn,	dominant negative
DSL,	Delta and Serrate/Jagged
EGF,	epidermal growth factor
EMT,	epithelial-mesenchymal transition
GBM,	glioblastoma multiforme
GFAP,	glial fibrillary acidic protein
GM-CSF,	granulocyte/macrophage colony stimulating factor
GSI,	gamma-secretase inhibitor
hESC,	human embryonic stem cell
hTERT,	human telomerase
i.c.,	intracranial
IL,	interleukin
i.p.,	intraperitoneal injection

IR,	irradiation
LY,	LY411,575; N-2((2S)-2-(3,5-difluorophenyl)-2-hydroxyethanoyl)-N1 ((7S)-5-methyl-6-oxo-6,7-dihydro-5H-dibenzo[b,d]azepin-7-yl)-L- alaninamide
M1,	classically-activated macrophage
M2,	alternatively-activated macrophage
MCP,	monocyte chemotactic proteins
MGMT,	O-6-methylguanine-DNA methyltransferase
MMR,	mismatch repair
MTIC,	(5-(3-methyltriazen-1-yl)imidazol-4-carboxamide)
NICD,	Notch Intracellular Domain
NK,	natural killer
NSC,	neural stem cell
OIS,	oncogene-induced senescence
PBMC,	peripheral blood mononuclear cells
PCNA,	proliferating cell nuclear antigen
PI,	propidium iodide
PML,	promyelocytic leukemia
Rb,	Retinoblastoma
ROS,	reactive oxygen species
RT,	reverse transcription
SA,	senescence associated
SAHF,	senescence associated heterochromatin foci
SASP,	senescence associated secretory phenotype
s.c.,	subcutaneous
SD,	standard deviation
T-ALL,	T-cell acute lymphoblastic leukemia
TAM,	tumor-associated microglia
TIS,	therapy-induced senescence

TMZ, temozolomide
VEGF, vascular endothelial growth factor
WHO, World Health Organization
wt, wild type

Preface:

Parts of this thesis represent work submitted as:

CHAPTER I and IV:

Candace A. Gilbert^a and Alonzo H. Ross^{a,b}. Cancer Stem Cells: Cell Culture, Markers and Targets for New Therapies. *Journal of Cellular Biochemistry*. 2009 Dec 1; 108:1031–1038, review.

Candace A. Gilbert^a and Alonzo H. Ross^{a,b}. “Glioma Stem Cells: Cell Culture, Markers and Targets for New Combination Therapies.” *Cancer Stem Cells Theories and Practice*, Stanley Shostak (Ed.). InTech. 2011 March; ISBN 978-953-307-225-8, book chapter. Available from: <http://www.intechopen.com/articles/show/title/glioma-stem-cells-cell-culture-markers-and-targets-for-new-combination-therapies>.

CHAPTER II:

Candace A. Gilbert^a, Marie-Claire Daou^a, Richard P. Moser^c, and Alonzo H. Ross^{a,b}. GSIs Enhance Temozolomide Treatment of Human Gliomas by Inhibiting Neurosphere Repopulation and Xenograft Recurrence. *Cancer Research*. 2010 Sep 1;70(17):6870-9.

CHAPTER III:

Candace A. Gilbert^a, Yulian P. Ramirez^a, Jessica L. Weatherbee^a, Christopher MacKay^d, Evelyn A. Kurt-Jones^d, and Alonzo H. Ross^{a,b}. Enhancing Temozolomide Treatment by Inhibition of Notch Signaling Induces Senescence in Gliomas. Manuscript in preparation.

Departments of ^aCancer Biology, ^bBiochemistry and ^cMolecular Pharmacology, Neurosurgery, and ^dMedicine, University of Massachusetts Medical School, Worcester, Massachusetts, USA.

CHAPTER I:

Introduction

CHAPTER I:

Introduction

Gliomas

Every year, approximately 19,000 new primary brain cancers are diagnosed in the United States (www.cancer.gov). Gliomas are the most common type of brain cancers, accounting for 32% of all brain and central nervous system tumors and 80% of all malignant brain tumors (CBTRUS, 2010). Gliomas are divided into subcategories based on their similarity to normal brain tissue. These subcategories include astrocytomas, oligodendrogliomas, ependymoma, and mixed gliomas, with astrocytomas being the most common. Astrocytomas are further grouped by their malignancy and tumor characteristics using the World Health Organization (WHO) classification system. The most common gliomas, are the WHO grade III anaplastic astrocytoma (AA) and grade IV glioblastoma multiforme (GBM). AAs make up 2% and GBMs make up 17% of all primary brain tumors in the United States, with incidences of 0.40 and 3.17 cases per 100,000 persons per year, respectively (CBTRUS, 2010). AAs and GBMs are infiltrative tumors with highly vascular and necrotic regions. GBMs are further delineated by the presence of hyperplastic microvascular regions and necrotic regions surrounded by anaplastic cells, known as pseudopalisades.

Glioma therapy

Current clinical treatment for gliomas consists of a combination of surgical resection, radiotherapy and chemotherapy. In both low- and high-grade gliomas, surgery provides the most benefit to the patient. More extensive resections commonly increase patient survival times (Sanai and Berger, 2008); however, due to the infiltrative nature of AAs and GBMs, even complete macroscopic removal of the tumor is not curative. Following surgery, patients receive conventional radiation treatment, with a dosage of up to 60 Gy given daily in 2 Gy fractions (Buatti et al., 2008). Patients also receive concomitant chemotherapy treatments. The most commonly used chemotherapy drug is currently temozolomide (TMZ; Temodar®). TMZ is an alkylating agent that is taken orally and readily penetrates the blood-brain barrier (Ostermann et al., 2004). In glioma patients, TMZ is administered both concurrently with and adjuvantly to radiotherapy. Cellular toxicity from TMZ treatment results from DNA methylation (Sarkaria et al., 2008). TMZ is an imidazotetrazine derivative that, at physiological pH, spontaneously converts to MTIC (5-(3-methyltriazene-1-yl)imidazol-4-carboxamide) (Newlands et al., 1997). MITC is responsible for methylation of N⁷-guanine, N³-adenine and O⁶-guanine. In replicating cells, O⁶-methylguanine mispairs with thymine and is highly toxic (Gerson, 2002). This leads to futile cycles of the DNA mismatch repair pathway, which induces cell cycle arrest and apoptosis (Gunther et al., 2003; Hirose et al., 2001). O⁶-methylguanine can be repaired by O-6-methylguanine-DNA methyltransferase (MGMT). However, approximately 70% of GBMs have low or negative MGMT expression (Friedman et al., 1998). MGMT can be silenced in glioma tissues by methylation of the

promoter, which results in increased sensitivity to alkylating agents (Dresemann, 2010). MGMT-negative status is a positive prognostic factor. However, TMZ is currently used for both MGMT-positive and MGMT-negative GBMs, because TMZ is still more efficacious in MGMT-positive patients than irradiation (IR) alone (Dresemann, 2010).

Phase I and II clinical trials have demonstrated that TMZ treatment decreases tumor burden and neurological symptoms with manageable side effects (Bower et al., 1997; Brada et al., 1999; Newlands et al., 1992; O'Reilly et al., 1993; Yung et al., 1999). Preclinical data demonstrating a synergistic effect by combining TMZ and IR was shown in 1997 (Wedge et al., 1997). In 2005, Stupp and colleagues provided a comprehensive study demonstrating the synergy of TMZ and IR in the clinic. Their treatment regimen, known as the EORTC/NCIC-protocol, has become the standard of care. After surgery, TMZ is administered daily at 75 mg/m² body surface during conventional fractionated IR treatment. This is followed by 6 cycles of adjuvant TMZ administered at 150 to 200 mg/m² for 5 consecutive days, on a 28-day schedule, referred to as the 5/28-regimen (Dresemann, 2010). TMZ has a very short half-life *in vitro* (1.24 h), in mouse models (1.29 h), and in patients (1.81 h) (Newlands et al., 1997). The TMZ concentrations in patients can vary from 0.1 to 14.0 µg/ml in the plasma and 0.2 to 1.9 µg/ml in the cerebrospinal fluid (CSF) (Baker et al., 1999; Ostermann et al., 2004; Spiro et al., 2001).

Glioma recurrence and survival rates

Long-term survival for glioma patients remains uncommon, despite advances in glioma treatment and increased knowledge of glioma biology over the past decade. Stupp

and colleagues have provided the most detailed clinical studies on the benefits of IR with concurrent and adjuvant TMZ treatment in GBM patients (Stupp et al., 2009; Stupp et al., 2005). TMZ treatment increases the two-year overall survival rate to 26.5%, compared to a 10.4% survival rate with radiotherapy alone (Stupp et al., 2005). The median five-year overall survival rate is 9.8% for the patient group treated with concurrent and adjuvant TMZ, while the group treated with IR-alone yields only a 1.9% survival (Stupp et al., 2009). In the United States, the current five-year and ten-year overall survival rates for GBM patients are 4.5% and 2.7%, respectively (CBTRUS, 2010). For AA patients, the current five-year and ten-year overall survival rates are 27.4% and 21.3%, respectively (CBTRUS, 2010). Despite increased survival rates over the past decade, glioma patients quickly succumb to very aggressive recurrent tumors. The median progression free survivals in GBM and AA patients are 6.9 months (Stupp et al., 2005) and 15.2 months (Chamberlain et al., 2008), respectively. In some instances, recurrent gliomas can be treated with additional surgery or radiation. Many patients with recurrent gliomas receive adjustments to their TMZ regimens, which can include: dose-dense (7/7-regimen), with 150 mg/m² on days 1 through 7, repeated with no break on day 8; prolonged (21/28-regimen), with 75 to 100 mg/m² for 21 consecutive days on a 28 day schedule; and metronomic (28/28-regimen), with continuous treatment of TMZ at 50 mg/m². Other options for recurrent glioma patients include treatment with nitrosourea chemotherapy, topoisomerase inhibitors, VEGF (vascular endothelial growth factor) inhibitors, such as bevacizumab (Avastin®), and enrollment in various clinical trials (Desjardins et al., 2008; Dresemann, 2010; Friedman et al., 2009; Kreisl et al., 2009; Zuniga et al., 2009).

Despite aggressive treatment after the initial diagnosis and tumor relapse, the current median overall survival times are only 14.6 months for GBM patients (Stupp et al., 2005) and approximately 3 years for AA patients (Chaichana et al., 2010). Relapse after TMZ treatment results in tumors with an increased occurrence of somatic mutations (Chin et al., 2008; Hunter et al., 2006). These recurrent tumors commonly have mutations in genes from the mismatch repair (MMR) pathway, such as *MSH6*, *MSH2*, *MLH1*, and *PSM2* (Cahill et al., 2007; Hunter et al., 2006; Yip et al., 2009). This suggests a role for the loss of the MMR pathway that leads to increased mutations after TMZ treatment, as well as TMZ resistance. Another mechanism that may contribute to TMZ resistance of recurrent gliomas is a change in the MGMT promoter methylation status. In tumors that had unmethylated MGMT at the time of first surgery, 62% of the recurrent cases were methylated when analyzed from the second surgery after TMZ and IR treatment (Brandes et al., 2010).

Cancer stem cells

Clonal evolution versus the cancer stem cell hypothesis

Current glioma therapies fail to cure patients because certain cells evade treatments and promote tumor regrowth. There are two competing models describing the cells responsible for tumor formation and relapse. First, is the clonal evolution theory, and second, is the cancer stem cell (CSC) hypothesis. The clonal evolution theory, also referred to as the stochastic model, states that cancer is a multi-step disease that arises from clones that have acquired multiple mutations. These clonal populations possess

enhanced tumorigenicity, metastasis and anti-apoptotic properties. Based on this theory, tumorigenicity is due strictly to genetic mutations, and does not discriminate based on different cell populations. The clonal evolution model states that within the tumor, any cell can become resistant to therapy by the acquisition of additional mutations, and it does not rely on a hierarchical organization (Shackleton et al., 2009). One example of a cancer believed to follow the clonal evolution model is melanoma. A recent study demonstrated that the percent of tumor-propagating cells harvested from patient melanomas can depend on the model systems used (Quintana et al., 2008). While melanoma-propagating cells are relatively rare when grafted into NOD/SCID mice, with only 1 cell in 837,000 being tumorigenic, in NOD/SCID that lack the interleukin (IL)-2 gamma receptor 1 in 9 melanoma cells are capable of tumor formation. Importantly, there is no difference in tumorigenicity among any populations based on marker expression. In some types of cancer, the majority of the cells within a tumor have similar tumorigenic potential, and this potential is due to genetic or epigenetic changes, and not hierarchical organization. These data support the key concept that separates this model from the CSC model.

In the second model, the CSC hypothesis, tumors follow a hierarchical model, and contain a unique population of CSCs, transit amplifying (progenitor) cells, and differentiated cells. The seminal belief behind the CSC theory is that the tumor is initiated and maintained by cells with stem cell-like properties. Many pathways that regulate normal functions of embryonic and adult stem cells are altered in cancer cells. There are three essential properties a CSC should possess (Rich, 2008). First, the cell

must be capable of self-renewal. Self-renewal is a property unique to embryonic stem cells, adult stem cells, and CSCs (Buick et al., 1979; Kawaguchi et al., 2001). Self-renewal allows for the continued production of differentiated progeny, without exhausting the pool of undifferentiated CSCs. A CSC will also possess high proliferative potential. Like normal adult stem cells, the CSC may remain quiescent, but still have the ability to re-enter the cell cycle and demonstrate high proliferative potential. The final requirement of a CSC is that it must be capable of tumor initiation. There are additional characteristics that are commonly associated with CSCs, but are not required. These characteristics include: 1) their cell of origin, 2) rarity, 3) potency, 4) the presentation of stem cell markers and 5) chemoresistance. These phenotypes are not consistent in all CSCs and can vary among different tumor types, grades and individual patients' tumors.

1) It is not necessary that a CSC originate from an adult stem cell (Akala et al., 2008; Barker et al., 2009; Holland et al., 2000; McCormack et al., 2010). It is unclear whether CSCs are derived from adult stem cells, or if mutations in a progenitor or even a terminally differentiated cell will lead to a tumor cell with stem cell characteristics. 2) CSCs may make up a rare population of the tumor, while the majority of the tumor cells are non-tumorigenic (Holyoake et al., 1999). However, recent publications find that the percent of CSCs can vary greatly in different cancers, depending on tumor type and possibly the tumor microenvironment (Eaves, 2008; Kelly et al., 2007). 3) Although multilineage differentiation is a characteristic of normal stem cells, CSCs do not normally retain the same pluripotency. CSCs are capable of differentiating into multiple cell types, but they commonly follow the lineage of the parent tumor (Canoll and Goldman, 2008;

Hill and Perris, 2007). 4) Not all cells that function as CSCs express similar markers (Lottaz et al., 2010). Normal embryonic and adult stem cells have been associated with specific markers; however, CSCs have proven to be more complicated in their marker expression. 5) A very important field of study in CSC research is therapy resistance. Since the CSC hypothesis states that only CSCs are capable of tumor formation, the CSC hypothesis postulates that these cells are responsible for tumor recurrence after treatment. Many laboratories have demonstrated the chemoresistance and radioresistance of the CSC population (Bao et al., 2006a; Ghods et al., 2007; Haraguchi et al., 2006; Kang and Kang, 2007; Liu et al., 2006; Ma et al., 2008; Salmaggi et al., 2006; Shafee et al., 2008; Wang et al., 2010a); however, it has not been demonstrated if all resistant cells are CSCs, or if every CSC has a resistant phenotype. It is important to note that the fundamental concept of the CSC hypothesis is that there is a functionally distinct group of cells with stem cell characteristics that are capable of tumor growth, while the remaining cells in the tumor are not tumorigenic (Clarke et al., 2006; Kennedy et al., 2007).

In the literature, CSC is commonly used interchangeably with the terms tumor-initiating cell and tumor-propagating cell (Venere et al., 2011). However, the term tumor-initiating cell can also specifically refer to the initial cell that forms the primary tumor in the patient, while tumor-propagating cell can refer to any cell within a patient tumor, xenograft, or tissue culture that is capable of forming a tumor. As previously described, the quintessential tests for CSCs is to examine self-renewal, proliferative potential and tumor formation. The CSC hypothesis postulates that the CSC population are capable of tumor initiation, therapy-resistant, and metastatic (Diehn and Majeti, 2010). Since patient

cancers are not detected until later stages, the original tumor-initiating cell cannot be elucidated, and this is currently only a putative term. It is also not known if the original tumor-initiating cell is involved in propagation of the recurrent tumor, or if it can form xenografts when isolated from the patient tumor. In contrast, tumor-propagating cells can be examined based solely on their ability to form tumors in mouse models. The tumor-propagating cells do not necessarily include the original tumor-initiating cells, but it is likely that these cells include a set of therapy-resistant cells that help drive tumor recurrence.

The existence of CSCs was first demonstrated in acute myeloid leukemia (Bonnet and Dick, 1997), and more recently in solid tumors, such as breast (Al-Hajj et al., 2003), prostate (Tang et al., 2007), colon (O'Brien et al., 2007), and brain cancers (Singh et al., 2003; Singh et al., 2004). Accumulating evidence suggests that CSCs play major roles in tumor initiation, angiogenesis, maintenance, and metastasis. CSCs are also clinically important, because they are more resistant to radiation and chemotherapy treatments than the bulk tumor cells, and therefore, are likely the drivers of tumor recurrence (Bao et al., 2006a; Liu et al., 2006).

Despite the arguments supporting each model, it is possible that both theories are applicable, depending on the tumor type, and there may also be variation within each tumor type. In leukemias, it has been strongly documented that only a small percentage of cells are capable of recapitulating the disease (Hope et al., 2004), which supports the CSC hypothesis, while in melanomas most cells are tumorigenic (Quintana et al., 2008), which has been used to argue against the CSC hypothesis. In addition, these two theories

do not need to be mutually exclusive (Shackleton et al., 2009). It is very likely that clonal evolution occurs in CSCs, resulting in more aggressive CSCs and making it more difficult to separate these two models of tumor propagation (Barabe et al., 2007).

Discovery of neural stem cells

The discovery of adult NSCs paved the way for the glioma CSC field (Altman, 1963; Altman and Das, 1965; Johansson et al., 1999a; Johansson et al., 1999b). Until the mid-20th century, the consensus in the neuroscience field was that adult NSCs did not exist. The former dogma was that the brain contained mitotic cells only during development. It is now known that neurogenesis persists throughout life. In the adult brain, NSCs are located primarily in the subventricular zone of the lateral ventricle (Altman, 1963) and the dentate gyrus of the hippocampus (Altman and Das, 1965). In the subventricular zone, adult NSCs are termed type B cells, and the transit amplifying cells are type C cells (Kriegstein and Alvarez-Buylla, 2009) (Fig. 1.1). The type B NSCs are mostly quiescent, are derived from embryonic and neonatal radial glial cells, and resemble astrocytes (Doetsch et al., 1997). NSCs and transit amplifying cells are closely associated with blood vessels in the subventricular zone (Tavazoie et al., 2008). In the hippocampus, the NSCs are located in the subgranular zone of the dentate gyrus. These cells are referred to as either radial astrocytes or type I progenitors (Fukuda et al., 2003; Seri et al., 2004). The subgranular zone is also located next to a vascular network, which may be a niche for adult NSCs (Palmer et al., 2000). Adult NSCs from both the

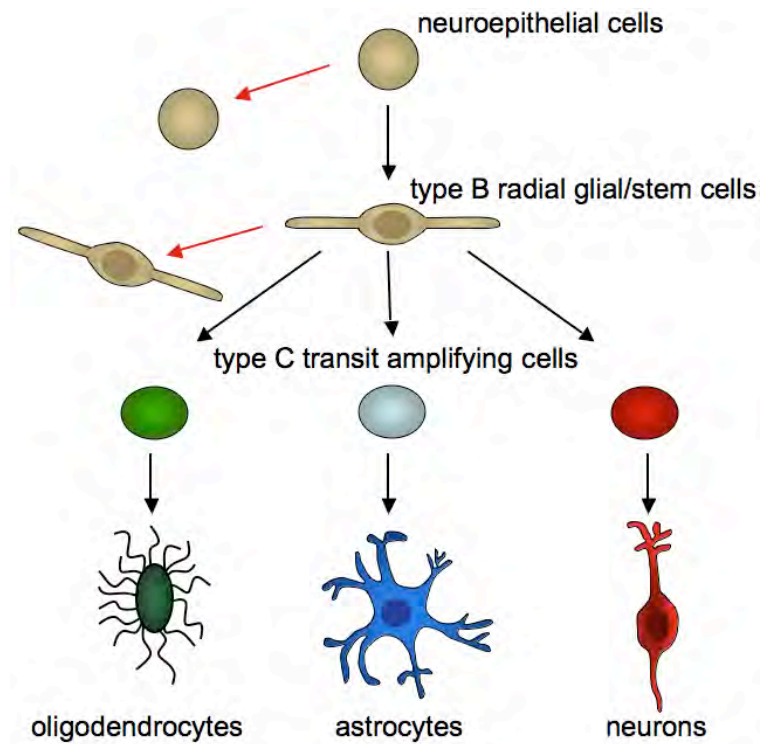


Figure 1.1 **Neural stem cell hierarchy.** Embryonic neuroepithelial cells divide symmetrically (red arrows) to maintain the stem cell population, and can also produce the type B radial glial progeny. These cells are the adult stem cells in the brain. Type B cells are also capable of symmetric and asymmetric division. The type C cells are the transit amplifying progenitor cells. These cells are multipotent and capable of dividing into the three main lineages in the brain, oligodendrocytes, astrocytes, and neurons.

subventricular and subgranular zones express the embryonic NSC markers nestin and Sox2, in addition to the astrocytic marker, glial fibrillary acidic protein (GFAP) (Doetsch et al., 1999; Lendahl et al., 1990; Seri et al., 2004; Suh et al., 2007). In the human fetal brain, CD133 is a marker for NSCs (Uchida et al., 2000). CD133 expression has also been observed in intermediate radial glial cells in the early postnatal brain, and in ependymal cells in the adult brain (Coskun et al., 2008), but not in neurogenic astrocytes in the NSC region of the subventricular zone CD133 (Pfenninger et al., 2007). CD15 (also known as SSEA-1 and Lewis-X Antigen) is also a NSC marker (Barraud et al., 2007; Pruszak et al., 2007).

In 1992, it was discovered that NSCs can be expanded as neurospheres in defined, serum-free media supplemented with growth factors (Reynolds et al., 1992; Reynolds and Weiss, 1992). These cultures maintain their self-renewal properties, have high proliferation potential and are capable of differentiation into neurons, astrocytes and occasionally oligodendrocytes. The neurospheres are non-adherent, heterogeneous aggregates that are derived from single cells. Under serum-free conditions, NSCs and transit amplifying cells are the neurosphere-initiating cells. This allows the neurosphere formation assay to measure the percentage of these undifferentiated cells in culture. NSCs have a greater, long-term proliferation potential than the transit amplifying cells and can maintain neurosphere cultures over a large number of serial dissociations, while the transit amplifying cells have a limited ability to continuously form neurospheres (Reynolds and Weiss, 1996). When neurospheres are dissociated into single-cell

suspensions and re-plated, secondary and tertiary neurosphere formation is used to measure self-renewal potential.

Glioma stem cells

While NSCs are necessary for normal neurological development and repair, cells with aberrant stem cell characteristics have been detected in brain tumors (Galli et al., 2004; Singh et al., 2003; Son et al., 2009). Glioma CSCs are capable of self-renewal and can divide asymmetrically to maintain the CSC population and produce progeny (Fig. 1.2). Gliomas display a hierarchical organization, which demonstrates the differentiation potential of the glioma CSCs (Piccirillo et al., 2006). NSCs and glioma CSCs share many additional characteristics. Both cell types are capable of migrating through normal brain tissue. Glioma CSCs have been associated with a vascular stem cell niche, similar to the NSC microenvironment niche (Calabrese et al., 2007; Sanai et al., 2005). Brain tumor cells expressing nestin and CD133 stem cell markers were consistently located in the proximity of the tumor's vascular system (Calabrese et al., 2007). It has been demonstrated that xenografts from CD133⁺ glioma cells form highly vascular tumors compared to xenografts from CD133⁻ cells (Bao et al., 2006b). The vascular niche may regulate glioma CSC proliferation and provide a protective shield against treatments. Therefore, therapies targeting the fundamental angiogenic factors could indirectly target glioma CSCs. Normal NSCs and glioma CSCs also share similar undifferentiated gene expression profiles, including *nestin*, *EGFR*, and *PTEN*. However, the nomenclature 'stem cell' in gliomas refers to their function and not their origin. It is currently unknown

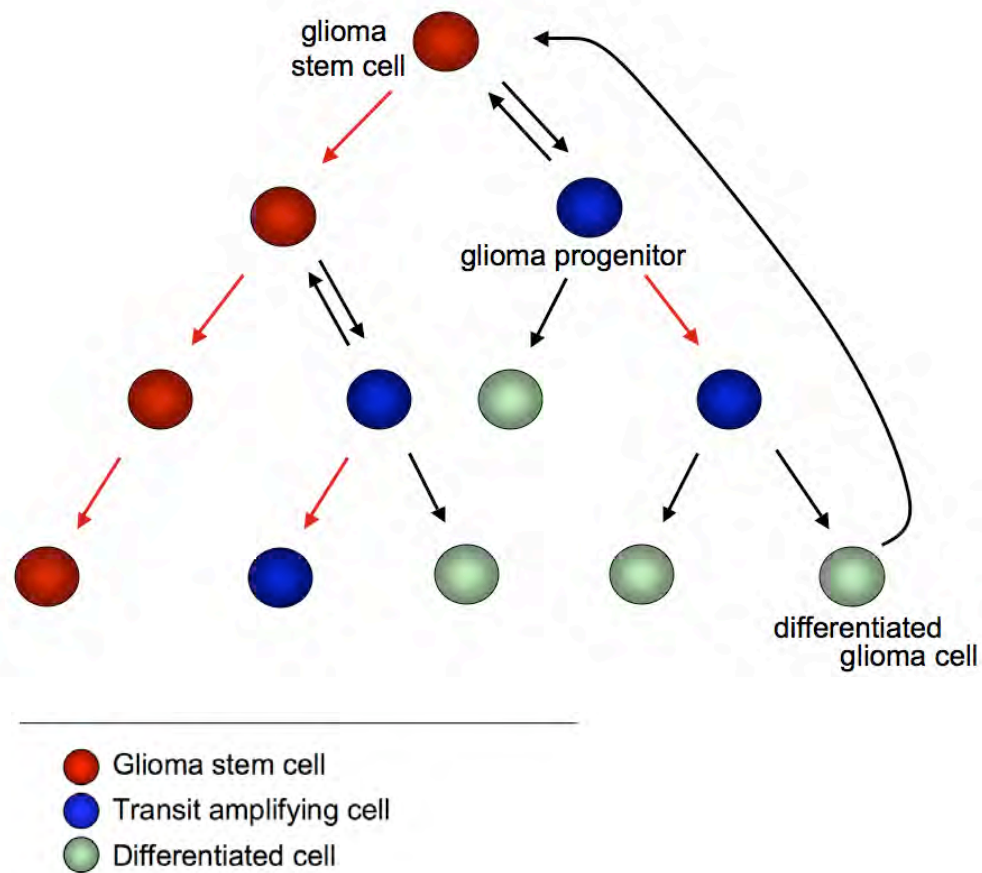


Figure 1.2 **Glioma stem cell differentiation.** Glioma CS are capable of symmetric division (red arrows) and maintain the CSC population. The glioma CSCs are also capable of asymmetric division (black arrows), which result in the progenitor glioma transit amplifying cells. The transit amplifying cells are capable of symmetric division and asymmetric division, which yields the differentiated, non-tumorigenic glioma cells. Both transit amplifying cells and the differentiated glioma cells can undergo de-differentiation into glioma CSCs.

which cell is the cell of origin for glioma CSCs. Glioma CSCs may originate from normal NSCs that have acquired tumorigenic mutations or from more differentiated transit amplifying or terminally differentiated neural cells that have acquired multiple mutations that allow the cells to be tumorigenic and revert to stemness properties (Fig. 1.2). NSCs are probably target cells for malignant transformation. When rodent brains are exposed to avian sarcoma virus or carcinogens, tumors form in the subventricular zone, where normal NSCs are believed to reside (Sanai et al., 2005). In addition, neural progenitor cells can be transformed by expression of oncogenes, such as *Akt* and *K-ras* (Holland et al., 2000) and *EGFRvIII* combined with loss of *PTEN* expression (Li et al., 2009a). Conversely, several laboratories have demonstrated that genetic alterations can dedifferentiate terminally differentiated astrocytes and induce tumorigenesis (Bachoo et al., 2002; Holland et al., 1998). Due to the substantial heterogeneity among gliomas, it is likely that tumors from different patients originate from different cells of the adult neural hierarchy. The different cell origins for these tumors may cause the inconsistencies of glioma CSC marker expression and lead to the presence of distinct molecular subclasses observed in gliomas (Phillips et al., 2006).

Glioma stem cell cultures

Traditionally, glioma cells were grown as adherent cultures in the presence of serum (Fig. 1.3). The serum-grown cultures are tumorigenic, but result in circumscribed tumors in intracranial xenograft models, unlike the infiltrative, diffuse tumors seen in glioma patients (Radaelli et al., 2009). The gene expression profile of serum cultures can

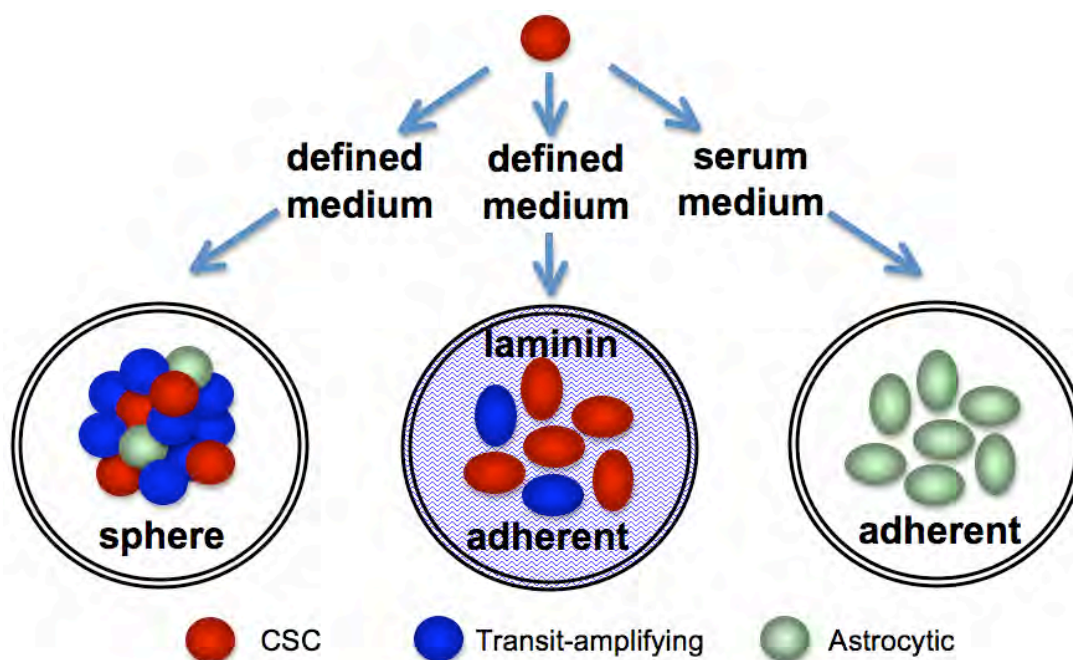


Figure 1.3 **Glioma culture methods.** Glioma CSCs can be isolated from primary tumors and grown in different culture media. Glioma CSCs can be grown in defined, serum-free media supplemented with growth factors. Under normal conditions, the glioma CSCs form neurospheres in defined medium. The neurospheres are heterogeneous and contain CSCs, transit amplifying cells, and differentiated glioma cells; however, if these cells are seeded on laminin-coated plates in defined medium, the cells grow as an adherent monolayer. The cells in laminin-coated cultures are less differentiated than the neurosphere cultures. Finally, the traditional way to grow glioma cultures is in serum-supplemented media. These cultures are adherent, differentiated cultures, that have minimal expression of glioma CSC genes.

be drastically different from the original tumor (Lee et al., 2006b). In addition, serum-supplemented glioma cultures have a very low proportion of CSCs. Similar to normal NSC cultures, several laboratories have cultured glioma tissues in defined serum-free media supplemented with growth factors. These cultures form non-adherent spheroids and have an enhanced population of glioma CSCs (Fig. 1.3) (Galli et al., 2004; Hemmati et al., 2003; Singh et al., 2003). The glioma neurospheres are a good *in vitro* model, because the cells maintain genetic profiles similar to the original patients' tumors and form diffuse tumors in intracranial xenografts (Ernst et al., 2009; Lee et al., 2006b; Singh et al., 2004). Neurosphere cultures are currently the most common method used to propagate glioma CSCs, but a new *in vitro* technique to grow adherent glioma CSCs is emerging, which utilizes laminin-coated plates with serum-free media (Pollard et al., 2009).

Neurosphere cultures

Neurosphere cultures were originally developed for propagation of normal NSCs (Reynolds and Weiss, 1992). This serum-free culture method is now applied to cancers, including breast cancers, colon cancers, and gliomas (Galli et al., 2004; Ponti et al., 2005; Ricci-Vitiani et al., 2007; Singh et al., 2003). When plated at a low cell density, each neurosphere arises from an individual glioma CSC or transit amplifying cell. Despite their clonal origin, neurospheres are heterogeneous aggregates that consist of glioma CSCs, transit amplifying cells, and more differentiated glioma cells. Malignant transformation can increase neurosphere formation (Li et al., 2009a). The percentage of

neurosphere-initiating cells can vary greatly among glioma cultures, from 1-30%. Interestingly, the majority of neurosphere-initiating cells are transit amplifying cells (Ahmed, 2009). When neurosphere cultures are dissociated to single cells, a percentage of the cells can form secondary and tertiary neurospheres for many passages (Chen et al., 2010b; Reynolds and Weiss, 1996). This demonstrates the presence of cells in the neurosphere cultures that possess a high capacity for proliferation and self-renewal.

When exposed to fetal bovine serum, glioma neurosphere cells differentiate down the lineage of the parent tumor (Singh et al., 2003). Therefore, gliomas preferentially differentiate to astrocytes (Fig. 1.3), but multilineage differentiation can occasionally be observed with neuronal lineages and some abnormal cells with mixed phenotypes (Varghese et al., 2008). However, as it is rare for an individual glioma to exhibit the full neural hierarchy, it is not expected that each glioma CSC can differentiate into all lineages (Sanai et al., 2005). It should be noted that these lineages are based on markers but not function. For example, the crucial criterion for a neuron is the action potential, but to our knowledge, this has not been tested in differentiated cells from glioma neurosphere cultures. A significant difference between NSC and glioma CSC cultures is that serum differentiation of normal NSCs is permanent (Lee et al., 2006b), while glioma lines established as serum cultures can be converted to neurospheres in serum-free media (Qiang et al., 2009).

Neurosphere cultures derived from primary tumors express known NSC genes, such as *Musashi1*, *Sox2*, *Bmi1*, and *Nestin* (Fan et al., 2010; Hemmati et al., 2003). Many laboratories have used the expression of stem cell markers to identify and isolate CSCs;

however, there is currently no universally accepted collection of markers for isolation of a pure population of CSCs for all gliomas. NSC cell surface markers, such as CD133, CD15 and A2B5, are expressed in neurosphere cultures and can be used to isolate neurosphere-initiating cells. Expression of CD133 in AA and GBM varies among patients and tumor grade, with reports of 0 – 64% in tumors and neurosphere cultures (Ogden et al., 2008; Singh et al., 2003; Singh et al., 2004; Son et al., 2009). Singh et al. (2003) were the first to demonstrate that CD133⁺ cells from gliomas are capable of multilineage differentiation and have a high capacity for neurosphere formation. The corresponding CD133⁻ cells do not proliferate in neurosphere cultures. Tumor formation and serial transplantation of xenografts in immunocompromised mice is the gold standard used to confirm that a marker identifies the glioma CSC population. CD133⁺ glioma cells have an increased capacity for tumor initiation after intracranial transplantation into mice (Singh et al., 2004). Injection of only 100 CD133⁺ cells results in tumors capable of serial transplantation, while 100,000 CD133⁻ injected cells do not form tumors. It is important to note that the laboratories that have had the most success studying glioma CSCs based on CD133 expression have isolated the cells directly from primary patient tissue and fresh xenograft samples (Bao et al., 2006a; Singh et al., 2004; Venere et al., 2011; Wang et al., 2010a). A rising concern for CD133 as a glioma CSC marker is that up to 40% of freshly isolated glioma tumors do not express CD133 (Son et al., 2009). Tumors negative for CD133 expression still contain cells with stem cell-like properties, such as self-renewal, multilineage differentiation, and xenograft tumor formation (Beier et al., 2007). Also, Ogden et al. (2008) reported that even in primary tumors with CD133 expression,

CD133 only selects for a fraction of the tumor-initiating cells. In addition, CD133 expression may be cell cycle-dependent and only identify a subset of glioma CSCs that are actively proliferating, and CD133⁺ populations may include progenitor cells (Grey et al., 2009; Jaksch et al., 2008; Snippert et al., 2009).

In freshly isolated GBM tissues, expression of a second NSC marker, CD15, can vary from 2.4 – 70% (Son et al., 2009). CD15⁺ cells form neurospheres in serum-free, defined medium, while CD15⁻ cells have minimal neurosphere formation (Mao et al., 2009). CD15⁺ cells isolated from GBMs are highly tumorigenic, while CD15⁻ cells display limited tumor formation in mouse intracranial xenografts. Additionally, tumors negative for CD133 possess CD15⁺ cells (Son et al., 2009). Importantly, 23 out of 24 primary GBMs analyzed contain a subpopulation of CD15⁺ cells. These results suggest that CD15 is an additional glioma CSC marker, and may help to identify new CD133⁻ glioma CSCs. A2B5 is a third NSC marker that is expressed in gliomas. A2B5 expression varies in AAs and GBMs, from 33 - 90% (Ogden et al., 2008). A2B5⁺ cells are capable of neurosphere formation and intracranial tumor formation, while A2B5⁻ cells do not initiate tumors (Ogden et al., 2008; Tchoghandjian et al., 2010). Since glioma cells expressing A2B5 form tumors regardless of their CD133 status, A2B5 appears to identify a broader population of glioma CSCs. Despite many successes using cell surface markers to identify glioma CSCs, it has become increasingly clear that gliomas are very heterogeneous and vary greatly from patient to patient (Phillips et al., 2006).

There are two new promising glioma CSC markers. The first, podoplanin, is a mucin-type transmembrane glycoprotein. It is overexpressed in a variety of cancers,

including squamous cell carcinomas, colorectal carcinomas and brain tumors (Cortez et al., 2010). For glioblastomas, podoplanin is expressed both in tumors and primary neurospheres in culture (Christensen et al., 2010). The second new marker, integrin alpha 6, plays an important role in normal NSCs (Lathia et al., 2010). Integrin alpha 6 binds laminin and plays a role in maintaining the stem cells in the subventricular zone. Lathia et al. provided strong evidence that integrin alpha 6-positive cells have CSC characteristics. These cells are more proliferative and potent for neurosphere and tumor formation.

Because of the lack of consensus, markers should not be the sole measure of stemness. Functional analysis, such as neurosphere and tumor formation, should also be used to confirm the CSC phenotype. However, there are caveats with using neurosphere cultures to analyze glioma CSC content. As mentioned above, both glioma CSCs and transit amplifying cells are capable of forming neurosphere. Therefore, neurosphere formation cannot be used to delineate the composition of CSCs and their early progeny. After extended periods of growth in serum-free media (> 20 passages), we have observed a change in the morphology of neurospheres in many cultures. In some lines, early passaged cultures contain densely packed neurospheres with almost indiscernible individual cells, which become more loosely packed neurospheres at later passages. The rate of neurosphere formation is also increased at higher passages. Other labs have observed these changes after 4 months of neurosphere culture, suggesting that although serum-free cultures are a better *in vitro* system than serum cultures, neurosphere tumor cells also change with time in culture (Zhang et al., 2006). An additional issue to be aware of is that the neurosphere assay is a fastidious assay. The time between

dissociation of neurospheres can affect the reproducibility of the results. While splitting neurospheres too early can result in an increase in the percentage of neurosphere-initiating cells, waiting too long to dissociate neurospheres increases the likelihood of cell death. In addition, neurospheres aggregate and fuse with one another when the cells are plated at higher densities (Singec et al., 2006). Therefore, neurosphere assays measure both the number of both glioma CSCs and transit amplifying cells and are accurate only when the cells are plated at low densities. In addition, as with any *in vitro* system, a pressing limitation with studying CSC behavior and pathways using neurosphere cultures is the absence of the CSC niche. The glioma CSC microenvironment is a hypoxic region (Heddleston et al., 2009; Li et al., 2009b) that includes a perivascular niche (Calabrese et al., 2007) and infiltrating immune cells (Humphries et al., 2010; Wu et al., 2010a). Despite these concerns, neurosphere cultures remain a valuable tool in glioma CSC research.

Laminin-coated cultures

A key aspect of the neurosphere culture system is that the serum-free, defined media maintains the CSC phenotype. However, the condensed structure of neurospheres hinders the diffusion of the growth factors to the innermost cells, which results in the presence of differentiated progeny and regions of cell death (Woolard and Fine, 2009). Differentiation and cell death decrease if glioma cultures are grown as a monolayer in the presence of serum-free, defined medium. This is achieved by culturing glioma cells in the serum-free, defined medium on laminin-coated cell culture plates (Fig. 1.3) (Pollard et

al., 2009). When seeded on laminin-coated plates, cells that normally form neurospheres under serum-free conditions grow as an adherent culture, which allows the cells equal access to growth factors. The adherent glioma CSC lines are less heterogeneous than the neurosphere cultures, with almost all of the cells express glioma CSC genes, including *Sox2*, *Nestin*, *CD133* and *CD44*. There is minimal expression of differentiation markers, such as *GFAP*, *Tuj-1* and *O4*, and the cultures grown on the laminin-coated plates also have less cell death compared to neurosphere cultures (Pollard et al., 2009). The adherent, laminin cultures are capable of tumor formation when as few as 100 cells are intracranially injected into immunocompromised mice, demonstrating the high percentage of tumor-propagating glioma CSCs. An additional benefit of the laminin glioma CSC culture system is the high success rate of establishing cultures. All patient tissues that possessed good cell viability could be established as long-term cell lines. Despite the benefit of having an increased purity of CSCs, one large caveat to the laminin culture system is its lack of heterogeneity. An important characteristic of CSCs is the ability of the cells to form a hierarchy of tumorigenic and non-tumorigenic cells, which is restricted in laminin CSC cultures (Venere et al., 2011).

Invincible Glioma Stem Cells?

Chemoresistance and radioresistance

Tumor recurrence is due to the presence of glioma cells that can escape chemotherapy- and radiotherapy-induced cytotoxicity. In patient tumors, these cells can stay dormant for extended periods after treatment. When the resistant cells eventually re-

enter the cell cycle, they contribute to local tumor recurrence. It has been proposed that CSCs are the resistant cells responsible for drug resistance and tumor re-growth in multiple cancers (Fig. 1.4). Current glioma treatments are insufficient because they only target the bulk of the tumor (Fig. 1.4). Since tumor recurrence is attributed to glioma CSCs resistant to therapy, treatments that directly target glioma CSCs could yield long-term cures. Many have hypothesized that once the glioma CSCs have been eliminated, the bulk tumor will not be able to sustain itself and will wither; however, in gliomas, it has been hypothesized that some differentiated tumor cells have the ability to revert to cells with stem cell-like properties (Fig. 1.2) (Chen et al., 2010b; Gupta et al., 2009). This would result in the eventual regrowth of the tumor. Therefore, targeting CSCs in combination with current therapies that kill the bulk of the tumor could enhance the patients' chances for long-term survival (Fig. 1.4).

The stem cell character of glioma CSCs may contribute to resistance of tumor cells to therapy through multiple mechanisms. Therapy resistance has been attributed to the quiescent phenotype and enhanced DNA repair in CSCs, as well as the expression of drug efflux pumps and anti-apoptotic proteins. First, despite their high proliferative capacity, normal stem cells can assume a quiescent state that is regulated by the stem cell niche. Cells that are not proliferating have less toxicity from chemotherapy- and radiation-induced DNA damage. Several groups have proposed that proliferating CSCs can readily assume a quiescent state and later, following DNA repair, repopulate the tumor (Mellor et al., 2005; Scopelliti et al., 2009).

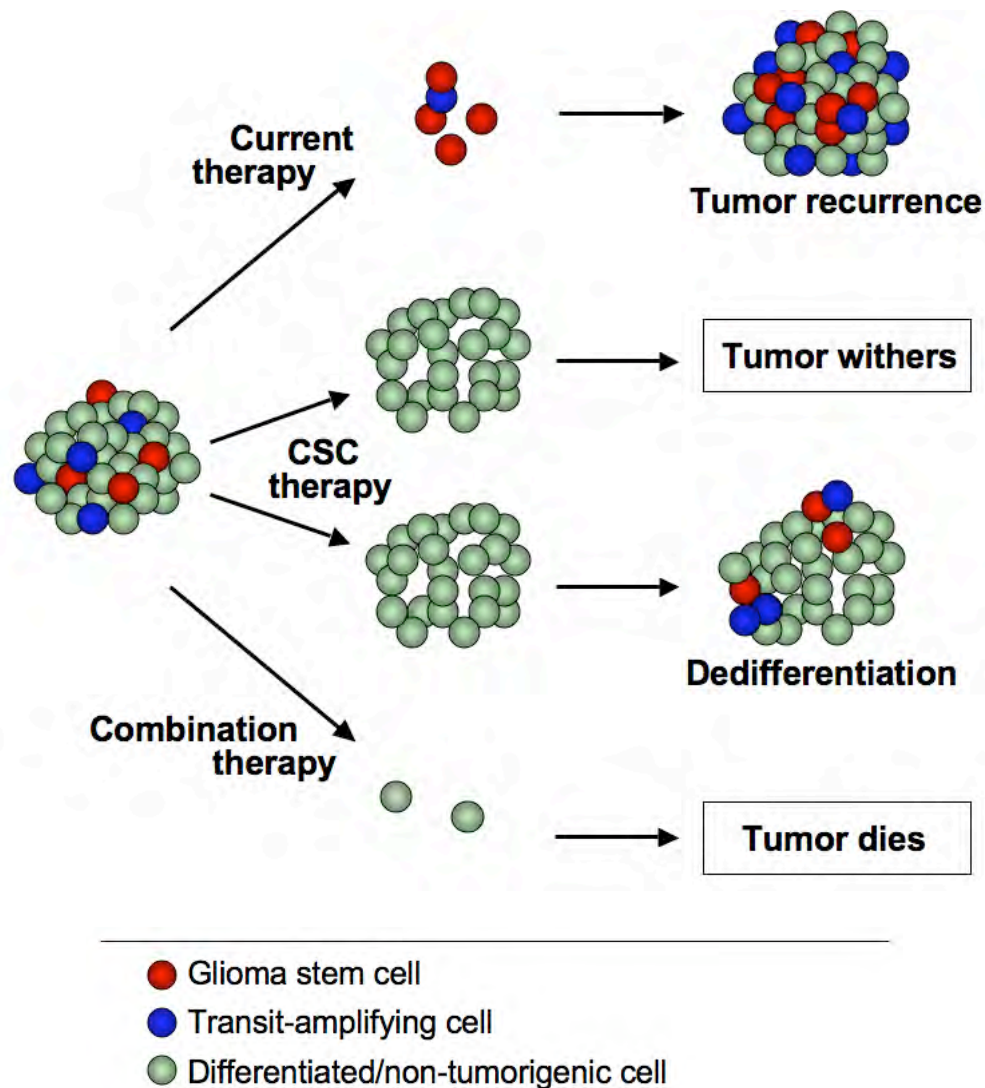


Figure 1.4 **Glioma therapy cancer stem cell hypothesis.** High-grade gliomas are difficult tumors to treat, because current therapies always result in tumor recurrence. This is due to a population of therapy-resistant cells that are believed to be glioma CSCs. These cells remain dormant after therapy, but quickly re-enter the cell cycle and drive tumor recurrence. Therefore, treatments directed against CSCs are promising therapies. Killing the CSCs will inhibit tumor growth. This may result in shrinking of the tumor; however, non-tumorigenic cells may have the ability to de-differentiate into glioma CSCs, which would lead to tumor regrowth. Instead, combination therapy that targets both the glioma CSCs and the non-tumorigenic glioma cells has the potential to inhibit tumor recurrence.

Our laboratory recently demonstrated that two commonly used chemotherapy agents, TMZ and BCNU (1,3-bis(2-chloroethyl)-1-nitrosourea; carmustine; BiCNU®), can induce a transient cell cycle arrest in neurosphere cells followed by a robust recovery of the culture (Mihaliak et al., 2010). TMZ has become the staple for chemotherapy treatment in glioma patients, while BCNU is an older alkylating agent that has been administered both by intravenous infusion and implantation of Gliadel® dissolvable wafers into the tumor bed after surgical debulking (Grossman et al., 1992). We demonstrated that TMZ and BCNU drastically diminishes initial neurosphere formation in many glioma cultures; however, some of these cultures eventually recover and form a robust number of secondary neurospheres (Mihaliak et al., 2010). TMZ-treated neurospheres also retain their tumorigenicity, and form large tumors in mouse subcutaneous xenografts. The ability of the neurosphere cells to repopulate the culture and form tumors after chemotherapy suggests that some cells undergo a transient cell cycle arrest. Analysis of cell cycle profiles demonstrates that a significant G2 arrest was observed 3 days after chemotherapy treatment, but the treated cells re-enter the cell cycle by day 7. This suggests that the cell cycle arrest allows a small percent of the neurosphere-initiating cells to evade cell death and eventually resume proliferation. Although we did not observe any changes in stem cell marker expression after TMZ treatment, the cells retain the benchmark CSCs phenotypes of self-renewal and tumor formation.

Several laboratories have published data supporting the chemoresistance of glioma CSCs, based on CD133 expression. CD133⁺ cells are more resistant than CD133⁻

cells to multiple chemotherapeutic agents, including TMZ, carboplatin, VP16, and Taxol (Liu et al., 2006). In an additional study, glioma cells that survive BCNU treatment express high levels of CD133⁺ and retain their tumorigenic potential in intracranial mouse xenografts (Kang and Kang, 2007). The glioma CSC cultures are more resistant to chemotherapy than normal NSC cultures (Gong et al., 2011). After TMZ or cisplatin treatment, the number of surviving glioma CSCs is significantly greater than the number of surviving NSCs. Cell death is also lower in the chemotherapy-treated glioma CSCs compared to the NSCs. Resistance to radiotherapy has also been observed in glioma CSCs. IR enriches the CD133⁺ population of human glioma cultures derived from xenografts and GBM patient samples (Bao et al., 2006a). Based on these data, CD133⁺ populations are more resistant to IR in colony formation assays compared to the corresponding CD133⁻ populations. In CD133⁺ cells, IR treatment only moderately decrease cell growth (Wang et al., 2010a). In addition, *ex vivo* IR treatment does not inhibit tumor formation in a subcutaneous xenograft model. Glioma patients that undergo radiotherapy treatments have increased levels of CD133 expression, demonstrating that these cells are also resistant to treatment in the clinical setting (Tamura et al., 2010).

In contrast, other laboratories have shown that number of CD133⁺ glioma cells can decrease or show no significant change after chemotherapy treatment (Beier et al., 2008; Mihaliak et al., 2010). There may be several explanations for these inconsistent results. First, these differences could indicate that CD133 is not a stem cell marker for all gliomas. Second, they could be due to different sources of the glioma CSCs, for example, neurosphere cultures versus xenografts or freshly isolated patient tissue (Venere et al.,

2011). Finally, the disparate results may be on account of the time points after treatments and the drug concentrations for these treatments. Our laboratory previously demonstrated that the chemotherapy treatments induce a cell cycle arrest in the neurosphere-initiating cells at clinically relevant doses, but require higher concentrations to induce cell death in the bulk of the cells (Mihaliak et al., 2010). The drug concentrations needed to achieve this cell cycle arrest vary between cell lines. Overall, these data support the theory that CSCs are resistant to current glioma therapies; however, due to recent data suggesting that CD133 does not identify all CSCs in glioma cultures, experiments using additional markers are needed.

Glioma CSCs have several hypothesized mechanisms to evade chemotherapy and IR treatments. Drug efflux pumps, such as adenosine triphosphate-binding cassette (ABC) pumps, ABCG2 and P-glycoprotein, are expressed on glioma CSCs (Lu and Shervington, 2008). It has been suggested that these efflux pumps remove the drugs from the CSCs, limiting DNA damage; however, in a model system, ABCG2-positive and -negative cells show no difference in their ability to form tumors mice, suggesting that these pumps are not expressed on all CSCs (Patrawala et al., 2005). The ABC transporters are often proposed to enhance survival of glioma CSCs by efflux of chemotherapy drugs, but TMZ is not a substrate for ABCG2, and expression of ABCG2 did not provide resistance to TMZ treatment (Bleau et al., 2009).

Glioma CSCs express a variety of proteins that promote survival following cancer treatment. The major drug resistance protein, MGMT, and anti-apoptotic genes such as *FLIP*, *BCL-2*, *BCL-XL*, *cIAP1* and *Survivin* are upregulated in CD133+ glioma cells

(Ghods et al., 2007; Liu et al., 2006). IR results in a greater activation of DNA checkpoint responses in CD133⁺ cells by phosphorylation of Rad15, ATM, Chk1 and Chk2 than in the autologous CD133⁻ cells (Bao et al., 2006a). This indicates that the CD133⁺ glioma CSCs' resistance to radiotherapy is partially due to enhanced DNA repair. As a result, pathways related to glioma CSC functions and resistance to therapy are promising targets for novel therapies.

A corollary to the CSC model is that signaling pathways associated with stem cells could be targeted to enhance therapy. The most effective treatments would consist of IR and chemotherapy against the bulk tumor combined with directly targeting the glioma CSC population (Fig. 1.4). Signaling pathways associated with either mechanisms of resistance or pathways required for the function of glioma CSCs could be targeted to enhance therapy.

Notch signaling pathway

The Notch signaling pathway is a promising target in gliomas. Notch regulates proliferation, differentiation, and survival, while deregulation of the pathway has been implicated in multiple types of cancer (Allenspach et al., 2002; Koch and Radtke, 2007; Roy et al., 2007). In NSCs, Notch activity maintains stemness and regulates fate determination during development and in the adult brain (Ables et al., 2010; Breunig et al., 2007; Gaiano et al., 2000; Hitoshi et al., 2002; Johnson et al., 2009; Namihira et al., 2009).

Notch was first discovered in flies with a mutated copy of the gene, which manifested as visibly ‘notched’ wings (Radtke and Raj, 2003). There are four mammalian Notch receptors (Notch1 through 4) and five membrane-associated ligands in the Delta and Serrate/Jagged (DSL) family. The Notch receptors and the ligands are single-pass transmembrane proteins that contain up to 36 tandem EGF-like repeats in their extracellular domains (Fortini, 2009). The Notch receptor begins as single protein precursor that is cleaved by a furin-like convertase (proteolytic cleavage S1) into N- and C-terminal fragments (Logeat et al., 1998). These fragments are non-covalently linked to form a mature, membrane-bound Notch receptor. Activation of the pathway occurs through direct cell-cell (*trans*) interactions with one cell expressing a Notch receptor and the other cell expressing a membrane-bound ligand (Fig. 1.5) (Fortini, 2009; Pannuti et al., 2010). In contrast, when the ligand and receptor are expressed on the same cell and interact in *cis*, Notch signaling is inhibited (Heitzler and Simpson, 1993; Jacobsen et al., 1998). When a ligand binds to a Notch receptor through a *trans* interaction, the metalloprotease ADAM protein cleaves the extracellular domain of Notch (proteolytic cleavage S2), which initiates endocytosis of the remaining membrane-bound Notch fragment. The final intracellular cleavage (proteolytic cleavage S3) of Notch occurs by gamma-secretase (Stockhausen et al., 2010). Gamma-secretase is an aspartyl protease made up of four membrane proteins, presenilin, nicastrin, PEN2, and APH1 (Wolfe, 2010). Gamma-secretase cleavage releases the Notch intracellular domain (NICD), allowing NICD to be translocated into the nucleus (Fortini, 2009; Miele, 2006). In the canonical Notch signaling pathway, the NICD forms a complex on DNA with CSL

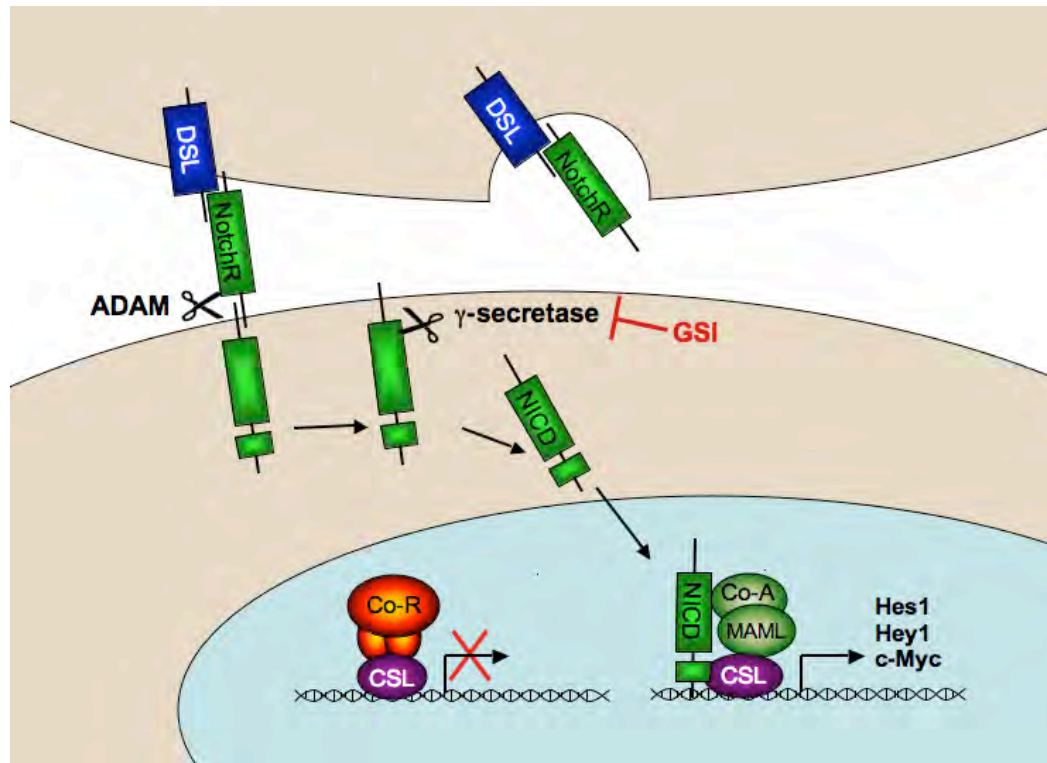


Figure 1.5 Notch Signaling Pathway. The Notch pathway requires cell-cell interactions. Notch signaling is activated when a mature Notch receptor binds to a DSL ligand on a neighboring cell. This interaction results in the S2 cleavage of the Notch receptor by the ADAM metalloprotease. This is followed by intracellular S3 cleavage by γ -secretase. The S3 cleavage results in the translocation of the NICD to the nucleus, where it binds to the CSL complex. This leads to transcription of the downstream Notch targets, such as *Hes1*, *Hey1* and *c-Myc*. The Notch pathway can be blocked by treatment with GSIs. The GSI blocks the activity of γ -secretase, thereby, preventing the translocation of NICD to the nucleus. In the absence of the NICD, the CSL is bound to a co-repressor complex, which represses transcription of the downstream Notch targets.

(CBF1/Suppressor of Hairless/Lag1, also known as RBP-J) and Mastermind. This complex recruits transcription factors p300 and PCAF, facilitating the transcription of downstream Notch targets, including members of the Hairy enhancer of split (*Hes*) and Hes-related repressor protein (*HERP/Hey*) families (Iso et al., 2003), *cyclin D* (Ronchini and Capobianco, 2001), *c-myc* (Palomero et al., 2006; Sharma et al., 2006), *p21* (Guo et al., 2009), and *NFκB* (Oswald et al., 1998). In the absence of NICD, the CSL interacts with corepressors blocking target gene transcription. Notch signaling also can occur through the non-canonical pathway, which is independent of the CSL complex (Sanalkumar et al., 2010). In this pathway, the NICD interacts with other coactivator complexes and pathways to activate downstream targets. The non-canonical pathway is a less established aspect of Notch signaling.

Aberrant Notch signaling has been associated with multiple types of cancer. It was first identified as an oncogene in T-cell acute lymphoblastic leukemia (T-ALL). In many T-ALL patients, Notch1 is constitutively active due to translocations or mutations (Ellisen et al., 1991; Weng et al., 2004). Upregulation of the Notch pathway has also been demonstrated in models for solid tumors, such as breast cancer (Dievart et al., 1999; Robbins et al., 1992), cervical cancer (Zagouras et al., 1995), lung cancer (Dang et al., 2000), and gliomas (Chen et al., 2010a; Jiang et al., 2011; Kanamori et al., 2007); however, upregulation in solid tumors is not due to Notch mutations, and is likely due to ligand-mediated hyperactivation of the pathway or upregulation of different upstream targets, such as the Id4 protein (Jeon et al., 2008). Directed therapy against Notch signaling is promising because this pathway is involved in development and survival and

can be blocked at multiple stages of the pathway (Rizzo et al., 2008). The most common approach to block the Notch pathway in basic research and in Phase I and Phase II clinical trials, is via small molecule inhibitors of gamma-secretase (Miele, 2006). Gamma-secretase inhibitors (GSIs) block the S3 cleavage of all four Notch receptors, causing the NICD to remain bound to the cell membrane, thereby halting the Notch signaling cascade (Fig. 1.5). Treatment with GSIs can induce goblet cell metaplasia of the small intestine and lead to gastrointestinal tract cytotoxicity (Barten et al., 2006; Wong et al., 2004); however, these side effects can be controlled with intermittent administration of low doses of the GSI (Rizzo et al., 2008).

Notch signaling in gliomas

The Notch receptors, their ligands, and downstream targets are commonly over-expressed in glioma tissue and cell lines (Chen et al., 2010a; Fischer and Gessler, 2007; Jiang et al., 2011; Kanamori et al., 2007; Shih and Holland, 2006). There have been several studies demonstrating a correlation between glioma grade and Notch activity. Notch1 transcripts and protein levels progressively increase from grade I to grade IV gliomas, and high expression is associated with poor prognosis (Jiang et al., 2011; Li et al., 2011). GBM tissues possess increased levels of the Notch target, *Hes1* (Chen et al., 2010a; Somasundaram et al., 2005). In addition, *Hash-1*, a gene negatively regulated by Hes1, is upregulated in grade II and III gliomas, but not in primary grade IV GBMs (Somasundaram et al., 2005). Inhibition of the Notch pathway with siRNA or a GSI, LLNle-CHO, greatly decreases the ability of adherent glioma cultures to form colonies in

soft agar and increases differentiation (Kanamori et al., 2007). Loss of Notch in adherent glioma lines decreases the number of dividing cells and results in increased apoptosis (Purow et al., 2005). Conversely, increased Notch signaling enhances glioma cell survival. Adherent glioma lines expressing Notch siRNA also have decreased tumor growth and increased survival in an intracranial xenograft mouse model.

Inhibiting the Notch signaling pathway can specifically target the glioma CSC population. In adherent glioma cultures, Notch receptors and the downstream target, *Hey*, are upregulated in the CD133⁺ population (Ulasov et al., 2011). Components of the Notch signaling pathway, have also been associated with neurosphere cultures derived from both patient GBMs and adherent glioma lines (Fan et al., 2010; Gunther et al., 2008; Zhang et al., 2008). Glioma neurosphere cultures with upregulated Notch signaling have higher growth rates than those with low levels of Notch pathway transcripts (Zhang et al., 2008). In addition, exogenous overexpression of the constitutively active NICD into neurosphere cultures further increases cell growth and neurosphere formation (Fan et al., 2010; Zhang et al., 2008). Notch signaling directly activates transcription of the stem cell marker, nestin (Shih and Holland, 2006). Likewise, knockdown of Notch by shRNAs or GSIs decreases the expression of the stem cell markers nestin and CD133 in neurosphere cultures (Fan et al., 2010; Jeon et al., 2008; Lin et al., 2010b). The GSIs, GSI-18 (2-10 μ M) or MRK-003 (2-10 μ M), decreases the downstream Notch target, *Hes1*, by 80-100% and greatly suppressed cell growth in glioma cultures (Fan et al., 2010). *Ex vivo* treatment with GSI-18 also decreases subcutaneous and intracranial xenograft tumor formation, while *in vivo* treatment with GSI-18-soaked beads in intracranial xenografts inhibits

tumor formation. This study was confirmed by similar data demonstrating that expression of a dominant negative mastermind-like 1 decreases neurosphere formation (Chen et al., 2010a). GSI treatment with MRK-003 results in a dose-dependent decrease of neurosphere formation, with high concentrations (20 μ M) inhibiting growth by almost 100%. These data demonstrate that blocking the Notch pathway can suppress growth and survival of glioma CSCs, as measured by neurosphere cell growth, tumor formation, and stem cell marker expression.

Two laboratories have demonstrated that Notch inhibition, through shRNA or treatment with GSIs, sensitizes glioma neurosphere cultures to radiotherapy (Lin et al., 2010b; Wang et al., 2010a). When GSI treatment was combined with IR, neurosphere formation is significantly impaired. The decreased neurosphere formation in GSI + IR treated glioma cultures is due to enhanced cell death, and the response is unique to the CD133⁺ population. In addition, cells with Notch knockdown by shRNA that are treated with IR have decreased tumorigenicity in a subcutaneous xenograft model. In the Wang et al. study, treatment with GSIs, DAPT (2 μ M) or L685,458 (0.5 μ M), alone has minimal affect on neurosphere formation. This disparity among data showing a strong effect from treatment with GSIs alone (Fan et al., 2010) or lack of an affect (Wang et al., 2010a) is likely due to both the potency of the inhibitor and the drug concentration. Low concentrations of GSIs would be less likely to induce GI toxicity, and are, therefore, more clinically relevant. Although these low concentrations of GSIs have a minimal affect on glioma cultures when administered as single agents, they may enhance the potency of other treatments. Together, these results suggest that an active Notch pathway

maintains the glioma CSC population and promotes radioresistance. Therefore, therapies targeting Notch receptors, ligands and downstream targets may enhance current glioma treatments.

Senescence: An Irreversible Cell Cycle Arrest

The cell cycle consists of G1 (gap 1), S (synthesis), and G2 (gap 2), and M (mitotic) phases (Schafer, 1998). Eventually, normal cells enter a terminally differentiated state. Anti-mitotic signals can drive a cell to temporarily exit the cell cycle into the G0 phase, known as quiescence. Embryonic stem cells and adult stem cells commonly reside in this phase (Jude et al., 2008; Lugert et al., 2010; Shin et al., 2009). In culture, quiescence stimuli for normal cells include cell-cell contact inhibition, loss of adhesion, and mitogen withdrawal. Quiescence is a transient cell cycle arrest, in which cells are viable, metabolically active, and can resume proliferation. Entrance into quiescence occurs during the G1 phase (Hartwell et al., 1974; Pardee, 1974), and is distinct from G1/S and G2/M cell cycle arrests (Coller et al., 2006).

Current cancer treatments target the rapidly dividing cells and rely on the induction of cell death. However, in many cancers, including gliomas, these treatments are not producing long-term cures. Cancer cells that are originally in a quiescent state before treatment, or enter into a transient cell cycle arrest after treatment are capable of evading the radiation- and chemotherapy-induced cell death (Mellor et al., 2005; Scopelliti et al., 2009). Therapy-induced senescence (TIS) is an avant-garde concept for cancer treatments that relies on the induction of cytostasis. Cellular senescence is a

permanent cell cycle arrest that occurs both *in vitro* and *in vivo*, are distinct from terminal differentiation, quiescence, and transient G1/S and G2/M cell cycle arrests. Senescence can occur at either cell cycle checkpoint transitions, G1/S or G2/M (Aviv et al., 2001; Blagosklonny, 2006, 2011). Despite their inability to re-enter the cell cycle, senescent cells remain viable and metabolically active. Senescence was first described in normal human diploid cells, where the cells were only capable of a finite number of passages in culture (Hayflick and Moorhead, 1961). This characteristic was termed the 'Hayflick Limit', and is now referred to as replicative senescence (Evan and d'Adda di Fagagna, 2009). In normal human cells, replicative senescence occurs naturally when telomeres reach a critical minimal length. Telomeres are disposable regions of repetitive DNA at the end of each chromosome that are shortened after each cell division (Harley et al., 1990). The telomere normally forms a loop structure at the ends of chromosomes, known as the 5' DNA cap, which protects them from fusion with other chromosomes. Progressive shortening eventually makes the telomerase incapable of forming the protective cap structure. This triggers a DNA damage response (DDR) signaling cascade that leads to an irreversible cell cycle arrest. Replicative senescence can be deterred by expression of telomerase (hTERT), which adds DNA sequence repeats to increase the length of telomeres (Counter et al., 1998). Since the discovery of the Hayflick limit, it has been shown that senescence can also be induced by reactive oxygen species (ROS), DNA damage (Gunther et al., 2003; Mirzayans et al., 2005; te Poele et al., 2002), oncogene overexpression (Grandori et al., 2003; Lazzerini Denchi et al., 2005; Michaloglou et al., 2005; Serrano et al., 1997), and loss of tumor suppressors, (Alimonti et al., 2010;

Courtois-Cox et al., 2006; Lin et al., 2010a). Non-replicative senescence, induced by signals other than shortening of telomeres, is commonly referred to as premature senescence, and cannot be blocked by the expression of telomerase.

Pathways of senescence

Regardless of the initial stimuli, p53 and Rb (Retinoblastoma) are the main pathways associated with all types of senescence (Fig. 1.6). While p53 and/or Rb are critical for senescence, there are many different intermediary genes and signaling forks involved. In mice, both the p53 and Rb tumor suppressor pathways are required for induction of senescence; however, in humans either pathway is sufficient (Dirac and Bernards, 2003; Shay et al., 1991). p14^{Arf} (p19^{Ink4d} in mice; encoded by *CDKN2A*) can be activated by the DNA damage response and other senescence stimuli. p14^{Arf} blocks the p53 negative regulator, HDM2 (MDM2 in mice), thereby, activating p53 and its downstream target, p21^{Waf/Cip1} (encoded by *CDKN1A*). Functional p21^{Waf/Cip1} binds to and inhibits cyclin/CDK complexes, which promotes G1 arrest (Abbas and Dutta, 2009). p21^{Waf/Cip1} has also been associated with G2 arrest in certain cell types, including tumor cells (Medema et al., 1998; Niculescu et al., 1998). Senescence signals also upregulate cyclin-dependent kinases inhibitors that regulate the Rb pathway, including p16^{Ink4a} (encoded by *CDKN2A*), p27^{Kip1} (encoded by *CDKN1B*) and p15^{Ink4b} (encoded by *CDKN2B*). p16^{Ink4a}, p15^{Ink4b}, and p14^{Arf} bind to the cyclin-D dependent CDKs, CDK4 and CDK6, while p27^{Kip1} and p21^{Waf/Cip1} inhibit the cyclin-E and -A -dependent CDK, CDK2. When CDKs are inhibited, and incapable of the forming CDK/cyclin complexes,

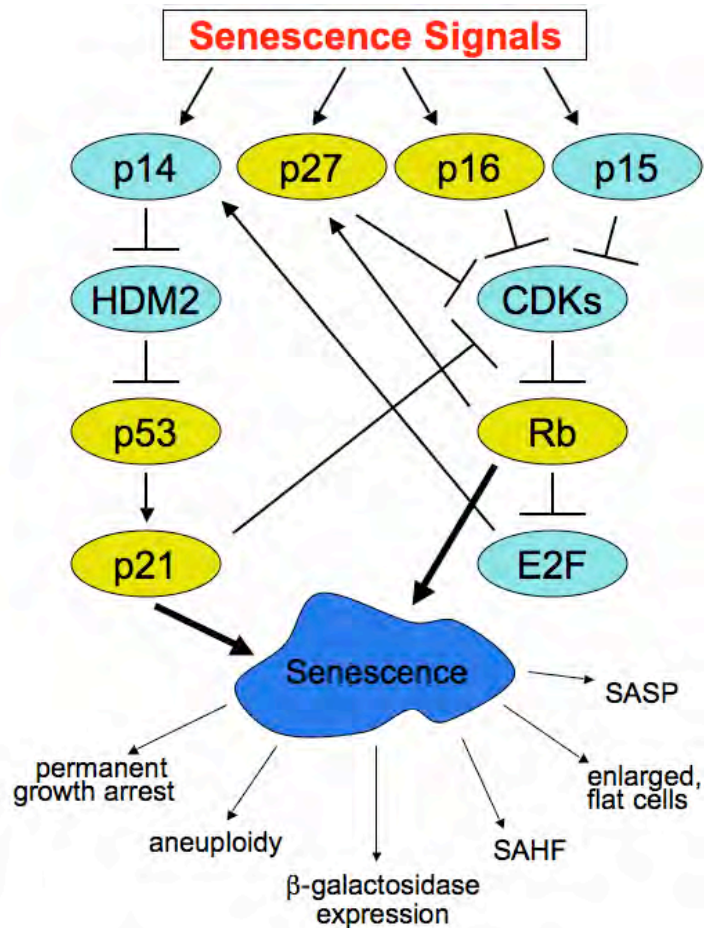


Figure 1.6 **p53 and Rb signaling in senescence.** Signals, such as oncogene overexpression and DNA damage, can activate the senescence pathway. These signals upregulate the expression of cyclin kinase inhibitors (CKIs), such as p14, p27, p16 and p15. p14 results in upregulation of the p53/p21 pathway, while the other CKIs upregulate the Rb pathway. Both p53 and Rb are the main signaling pathways that instigate senescence. The proteins highlighted in yellow are commonly upregulated in senescent cells and expression of these genes is often used as a positive marker for senescence. Senescent cells are also characterized by permanent cell cycle arrest, aneuploidy, β -galactosidase, SAHF, SASP, and enlarged, flat morphologies. Modified from (Campisi and d'Adda di Fagagna, 2007).

Rb is activated (hypophosphorylation) (Giacinti and Giordano, 2006). Rb binds to the transactivation domain of the E2F transcription factor and blocks activity. E2F normally stimulates cell proliferation, and blocking *E2F* transcription induces senescence. Rb can also induce senescence through E2F-independent signaling. Rb activity increases the formation of promyelocytic leukemia (PML) nuclear bodies, which inhibits proliferation and can promote senescence (Fang et al., 2002). Rb can also induce senescence by upregulating expression of and stabilizing p27^{Kip1} through the Rb-Skp2-p27^{Kip1} pathway (Ji et al., 2004). Rb activation is commonly associated with G1 cell cycle arrest, but recent studies have demonstrated that DNA damage can induce Rb-dependent G2 arrest (Jackson et al., 2005; Naderi et al., 2002; Polager and Ginsberg, 2003). Therefore, senescence signals, such as Ras oncogene-induced senescence (OIS), are known to activate both p53 and Rb pathways (Fig. 1.6).

The senescent phenotype

A permanent arrest in cell proliferation is the defining characteristic of senescence. In addition to monitoring cell number, cell cycle arrest can be measured by multiple assays that focus on protein expression or DNA content. A characteristic phenotype of cells that have little or no proliferation is a decrease in the protein levels of either Ki67, which is expressed in actively dividing cells during G1, S, G2, and mitosis, or proliferating cell nuclear antigen (PCNA), which is upregulated during late G1 and S phase (Takahashi and Caviness, 1993). Levels of proliferation can also be measured by the incorporation of the synthetic nucleoside, bromodeoxyuridine (BrdU; 5-bromo-2-

deoxyuridine) into the DNA during the S phase. Senescent and quiescent cells will have no BrdU incorporation. More specific analysis of cell cycle arrest can be analyzed by measuring the levels of propidium iodide (PI) DNA intercalation in permeabilized cells. PI intensity is directly proportional to DNA content and can be used to distinguish cells that are in G1 (one set of chromosomes) versus G2 (two sets of chromosomes), as well as the presence of aneuploidy. Another method to measure growth arrest is with carboxyfluorescein succinimidyl ester (CFSE) label retention. CFSE becomes fluorescent in the cytoplasm, and its intensity progressively decreases by half after each cell division. Therefore, proliferation can be observed by decreased fluorescence, while label-retaining cells make up the non-dividing population. Despite multiple methods to analyze cell proliferation, these measurements will not distinguish senescence from transient phenotypes, such as quiescence or decreased proliferation.

The most common measurement for senescence is the expression of senescence associated (SA)- β -galactosidase. SA- β -galactosidase expression occurs almost exclusively in senescent cells, and can be analyzed both *in vitro* and *in vivo* (Debacq-Chainiaux et al., 2009). Staining for SA- β -galactosidase is pH-dependent. This phenotype is poorly understood, but is believed to be due to increased levels of endogenous lysosomal β -galactosidase in senescent cells. It has been shown that β -galactosidase expression is not required for induction of senescence (Lee et al., 2006a). Knockdown of β -galactosidase does not inhibit the induction of a permanent cell cycle arrest. In addition, senescent cells often form senescence associated heterochromatin foci (SAHF) (Narita et al., 2003). Heterochromatin is made up of condensed regions of chromosomes

that are transcriptionally silent. SAHF is a form of facultative heterochromatin that forms due to a change in a cell's phenotype (Zhang and Adams, 2007). Senescent, human cells stained with 4'-6-Diamidino-2-phenylindole (DAPI) present with 30 to 50 DNA aggregates of SAHF. Each individual SAHF is formed from a single chromosome, and possess foci for HP1, HIRA and macroH2A. Another phenotype of senescence is a flattened morphology and increased cell size; however, this phenotype has not been confirmed *in vivo* and may only apply to human adherent cultures. Senescent cultures also have an increase in aneuploidy (Walen, 2008).

In addition to the above phenotypes, induction of senescence by replicative senescence, OIS, and the DDR upregulates the secretion of many factors involved in cellular signaling, such as growth factors, proteases, and cytokines (Coppe et al., 2008; Freund et al., 2010). This secretion profile is known as the senescence associated secretory phenotype (SASP). Of particular interest are the increased levels of inflammatory cytokines. The robustly secreted factors include interleukin (IL)-8, IL-6, IL-1, granulocyte/macrophage colony stimulating factor (GM-CSF), and monocyte chemotactic proteins (MCPs) (Freund et al., 2010). In combination with other senescent phenotypes, such as growth arrest, SA- β -galactosidase expression, and SAHF formation, the SASP can be used to determine if cells have entered senescence.

Senescence and cancer

Senescence has been attributed to four major biological roles, which include aging, tissue repair, tumor suppression and tumor promotion (Rodier and Campisi, 2011).

There are several features of senescence that might deter cancer growth. First, senescence is common in many benign tumors, suggesting that senescence acts as a barrier to prevent pre-cancerous lesions from becoming malignant (Braig et al., 2005; Collado et al., 2005; Majumder et al., 2008; Michaloglou et al., 2005; Zhuang et al., 2008). Second, senescence is associated with blocking initial tumor formation because many tumor-causing signals lead to senescence in normal cells. These include the overexpression of many oncogenes, including *Ras*, *BRAF*, *E2F1*, and *c-Myc* (Grandori et al., 2003; Lazzarini Denchi et al., 2005; Michaloglou et al., 2005; Serrano et al., 1997), the loss of tumor suppressors, such as *PTEN* (Alimonti et al., 2010; Lin et al., 2010a) and *NF1* (Courtois-Cox et al., 2006). This suggests that a cell must evade senescence in order to establish a malignant tumor. Indeed, the main pathways in senescence, p53 and Rb, are tumor suppressor pathways that are commonly inactivated in cancers (Sherr and McCormick, 2002). Also, tumor cells commonly express *hTERT*, or can combat replicative telomere shortening through a mechanism called alternative lengthening of telomeres (Muntoni and Reddel, 2005; Shay and Bacchetti, 1997; Silvestre et al., 2011). A third link between senescence and tumor suppression is the occurrence of therapy-induced senescence (TIS). TIS is a new mechanism to target cancer cells. Recent studies have found that many current therapies, including chemotherapy (Gunther et al., 2003; Mhaidat et al., 2007; Schmitt et al., 2002) and radiation (Mirzayans et al., 2005; Suzuki and Boothman, 2008) induce senescence. Specifically, in some gliomas, TMZ treatment can induce senescence in a subset of the tumor cells (Gunther et al., 2003; Sato et al., 2009). There are several new cancer drug treatments that rely on TIS and have proved

promising in preclinical studies (Ewald et al., 2010; Huck et al., 2010; Ota et al., 2006). Finally, the fourth concept supporting senescence as a tumor-suppressing mechanism is that the induction of senescence and the SASP may play a role in activating the immune response that is commonly suppressed in tumors. In addition, senescence has been shown to stimulate tumor clearance (Xue et al., 2007). Induction of senescence in a liver carcinoma model resulted in a SASP. These tumors had increased infiltration of immune cells, which resulted in a decrease in tumor volume.

Senescence can also play a supportive role in tumor growth (Coppe et al., 2010). Although contradictory to the role of tumor clearance, the SASP can also contribute to tumor promotion. Many of the secreted factors are pro-proliferative, such as CXCL1, IL-8, and IL-6, and pro-angiogenic, such as vascular endothelial growth factor (VEGF) (Bavik et al., 2006; Coppe et al., 2006; Krtolica et al., 2001; Ksiazek et al., 2008). SASP can also lead to epithelial-mesenchymal transition (EMT) and invasiveness (Coppe et al., 2008). The theory that senescence is cancer-promoting has been demonstrated in mouse xenograft models, in which the co-injection of senescent cells with malignant cancer cells greatly increases tumor formation (Bhatia et al., 2008; Krtolica et al., 2001; Liu and Hornsby, 2007). The antagonistic pleiotropy of senescence implies that the benefits of therapy-induced senescence may lead to deleterious effects at later stages. Therefore, if cells can escape the initial tumor suppressive properties, senescence may support tumor growth during later stages. This suggests that TIS from chemotherapy and IR may promote aggressive tumor recurrence. Therefore, TIS will be the most efficient when it directly targets the population of cells capable of tumor recurrence.

Senescence and Notch

The signals that control the reversibility of quiescence and keep cells from entering an irreversible senescent state remain elusive. Insight into the difference between these two types of cell cycle arrest became available when Sang et al. (2008) demonstrated that quiescent fibroblast cells require an active Notch pathway to maintain their transient cell cycle arrest. The Notch target, *Hes1*, is upregulated in quiescent fibroblasts, and loss of either Notch signaling by DAPT treatment or dominant negative (dn) *Hes1* expression shifts the quiescent cells into a permanent arrested state. These cells express increased SA- β -galactosidase and formed SAHF. In addition, re-expression of *wtHes1* inhibits the cells from entering senescence, while *dnHes1* expression keeps cells in an arrested state. These data demonstrate that Notch is a key pathway that modulates cells between reversible quiescence and irreversible senescence.

Research Framework and Objectives

There is a dire need for new glioma therapies. Combination therapies will likely provide the highest success by targeting the bulk of the tumor with cytotoxic-inducing treatments, such as chemotherapy and IR, while target-directed treatments can be used against the resistant population. This preclinical study described herein focuses on the combination of TMZ treatment and inhibition of the Notch pathway with GSIs. The theory for this thesis research developed from two studies described above. First, TMZ is not curative in glioma patients and only yields short-term results. We were particularly interested in our laboratory's previous results, demonstrating that TMZ induces a

temporary cell cycle arrest in the tumor-propagating population (Mihaliak et al., 2010). The next study of interest was from Sang et al. (2008), which stated that active Notch signaling is essential to maintain the quiescent state of fibroblast cells. When the Notch pathway is blocked, the cells were converted from a reversible cell cycle arrest into an irreversible cell cycle arrest, known as senescence. This study will analyze the assimilation of these two concepts and test our hypothesis that the treatment combination of TMZ with a GSI leads to therapy-induced senescence in glioma cells.

CHAPTER II:

**Gamma-Secretase Inhibitors Enhance Temozolomide Treatment by Inhibiting
Neurosphere Repopulation and Xenograft Recurrence**

Parts of this chapter represent work submitted as:

Candace A. Gilbert, Marie-Claire Daou, Richard P. Moser, and Alonzo H. Ross. Gamma-Secretase Inhibitors Enhance Temozolomide Treatment of Human Gliomas by Inhibiting Neurosphere Repopulation and Xenograft Recurrence. *Cancer Research*. 2010 Sep 1; 70(17):6870-9.

Contributions:

Marie-Claire Daou first converted the U373MG adherent line to our neurosphere culture, U373NS.

Li Li, Ph.D., did sequence analysis on the cell cultures for p53.

Richard Moser, M.D., provided us with patient samples from surgery.

Alonzo Ross, Ph.D., contributed intellectual guidance and editing.

CHAPTER II:

**Gamma-Secretase Inhibitors Enhance Temozolomide Treatment by Inhibiting
Neurosphere Repopulation and Xenograft Recurrence**

The combination of surgery, IR and TMZ is currently the most successful treatment for gliomas. The inclusion of TMZ as the standard chemotherapy treatment has resulted in a median 2-month increase to patient survival rates (Stupp et al., 2005). Gliomas possess a population of cells that are resistant to current therapies and drive tumor recurrence. Development of combination therapies that will target both the bulk of the tumor cells and the tumor-propagating CSCs is the most promising direction for future glioma treatments. Our laboratory previously developed an *in vitro* neurosphere recovery assay to specifically analyze the glioma cells that evade chemotherapy treatments and study drug combinations to target these cells.

Neurosphere cultures are a good model to study gliomas, because the cells maintain genetic profiles similar to the patients' tumors and form invasive intracranial xenografts in immunocompromised mice (Ernst et al., 2009; Lee et al., 2006b; Singh et al., 2004). Our neurosphere recovery assay measures neurosphere formation at three time points to assess the capacity of the culture to repopulate after chemotherapy (Mihaliak et al., 2010). First, we assess the ability of the cells to form neurospheres shortly after treatment. Second, we count the number of neurospheres that form during a one-week recovery period to determine if the surviving cells resume neurosphere formation. Third, we dissociate the neurospheres and count the number of secondary neurospheres that

form to measure self-renewal (Reynolds and Weiss, 1996). This neurosphere recovery assay provides a quantitative assessment of culture repopulation following drug treatment, and is highly relevant to tumor recurrence in the clinic. Utilizing the neurosphere recovery assay, we previously demonstrated that TMZ drastically diminished initial neurosphere formation in many glioma cultures; however, these cultures eventually recovered and formed a robust number of secondary neurospheres (Mihaliak et al., 2010). The ability of TMZ-treated neurospheres to recover and repopulate the culture suggests that some cells undergo a transient cell cycle arrest, allowing them to evade cell death and eventually resume proliferation.

Notch signaling is a promising pathway to target the glioma cells that recover after TMZ treatment. Inhibition of the Notch pathway, by either shRNA or GSIs, can target neurosphere- and tumor-propagating cells by increasing cell death and sensitizing the cells to IR (Fan et al., 2010; Purow et al., 2005; Wang et al., 2010a). In this study, we analyze if the combination of TMZ and GSIs enhances glioma therapy by inhibiting tumor repopulation and recurrence. In contrast to TMZ-only treatment, the TMZ + GSI treatment strongly inhibits neurosphere recovery. This was confirmed by a loss of secondary neurosphere formation in cultures treated with TMZ + GSI. We confirm the involvement of the Notch pathway in the response to our drug treatments by demonstrating that TMZ + GSI treatment does not inhibit recovery and secondary neurosphere formation in glioma cells expressing the constitutively active NICD. In addition, we show that the response to TMZ + GSI treatment is schedule-dependent. Recovery of neurosphere formation is inhibited when TMZ is administered first, followed

by GSI treatment 24 hrs later. If a single dose of GSI is administered prior to, or concurrently with TMZ, the culture is able to recover and form secondary neurospheres. We also observed the effects of TMZ + GSI treatment on tumor formation and progression in a mouse xenograft model. *Ex vivo* and *in vivo* TMZ + GSI treatment decreased tumor formation and progression. These data demonstrate the importance of the Notch pathway for chemoprotection in malignant gliomas. The addition of GSIs to the current care regimens for GBM patients is a promising new approach to decrease brain tumor recurrence.

Results

Establishment of glioma neurosphere cultures

As a first step to test the effects of TMZ and GSI treatments on glioma cultures, we converted adherent glioma cell lines to serum-free neurosphere cultures and established primary neurosphere cultures from patient tissues. Neurosphere morphology ranged from very dense neurospheres in the primary lines, such as GS7-2, GS7-25, and GS9-6, to less dense neurospheres in the U87NS and U373NS converted lines, as well as irregularly shaped, loosely formed aggregates, as seen in the GS1-7 culture (Fig. 2.1 A). The percentage of cells that are capable of forming neurospheres when plated at low clonal density, termed neurosphere-initiating cells, varies across cultures (Fig. 2.1 B). The converted cultures, U87NS and U373NS, had the largest percent of neurosphere-initiating cells. Although neurosphere formation is commonly used to analyze the presence of CSCs and progenitor cells, it is important to note that survival, self-renewal

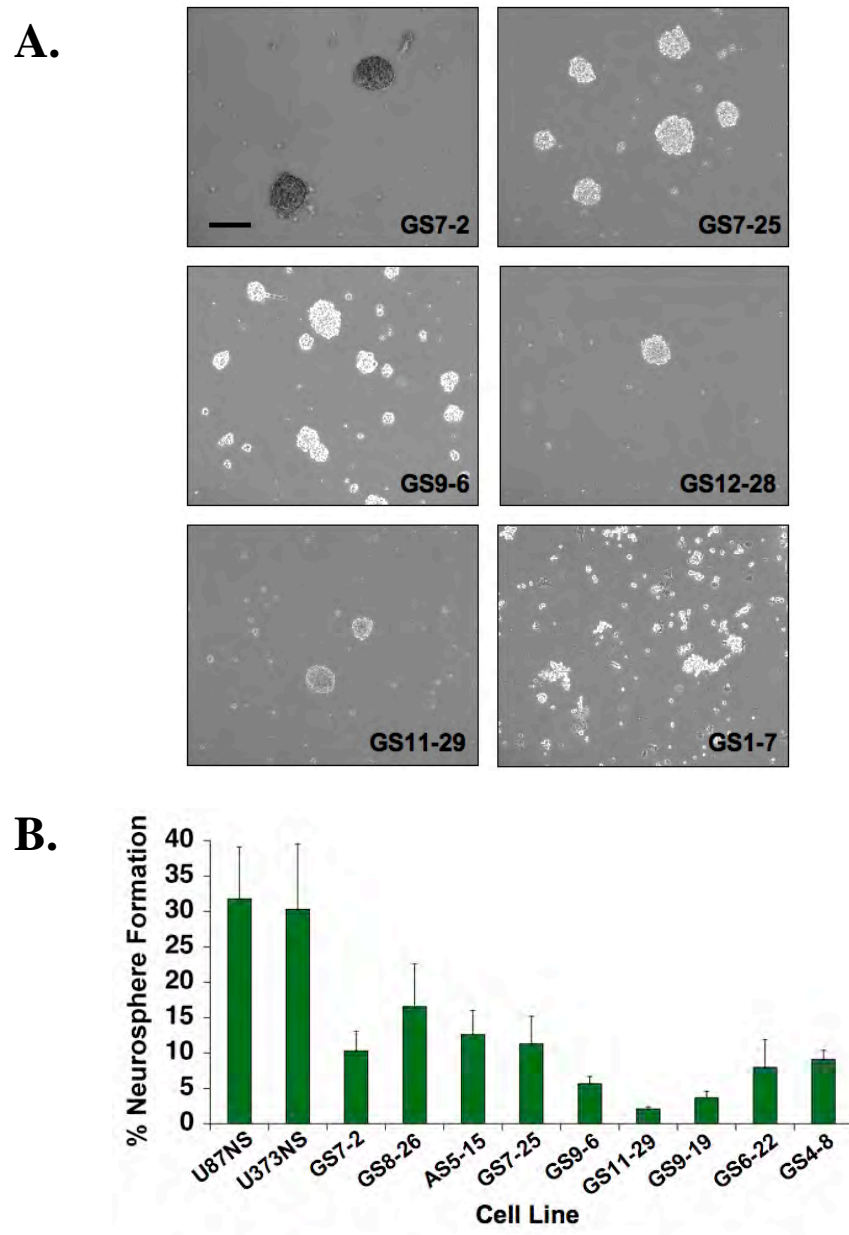


Figure 2.1 **Neurosphere formation in established primary neurosphere cultures.** A) Micrographs of select primary neurosphere cultures. Primary lines established from patient glioma tissues form neurospheres in defined serum-free medium. The morphology of these neurospheres can vary greatly among cultures. Bar = 50 μ m. B) The percent of neurosphere-initiating cells varies among converted and primary neurosphere cultures. The percent neurosphere formation is calculated based on the number of neurospheres formed divided by the number of single cells plated.

and proliferation are all aspects of the neurosphere formation assays (Lathia et al., 2011). In addition, the analysis of neurospheres should not be used to postulate *in vivo* tumor formation or growth, because the *in vitro* setting is meant to enhance growth and survival, and is lacking many factors from the niche that regulate the balance between growth and quiescence. The established lines, U87NS and U373NS, are convenient models to study gliomas, but one must take into account that long-term culture systems are both prone to selection and additional mutations (Venere et al., 2011). All of the neurosphere cultures tested had the potential to form subcutaneous tumors in immunocompromised NU/NU nude mice when 1×10^6 live cells were injected (Table 2.1), but they have not been compared based on *in vivo* limiting dilutions. When possible, the p53 sequences were analyzed in the primary neurosphere cultures to determine if they expressed wild type p53. Finally, MGMT expression was analyzed (Table 2.1). The majority of the cell lines expressed low to negative levels of MGMT, which is known to promote sensitivity to TMZ treatment. The neurosphere cultures demonstrate various sensitivities to TMZ treatment (Table 2.1). Cultures classified as resistant lines did not have any decrease in initial neurosphere formation with TMZ concentrations up to 200 μM . Highly sensitive lines had a significant decrease in initial neurosphere formation with as low as 5 μM TMZ, and were not capable of recovery. Sensitive lines were those that showed a significant decrease in initial neurosphere formation, but were capable of neurosphere recovery. Although MGMT status, in regards to TMZ sensitivity is very important in the clinic, since this proposal focuses on the enhancement of TMZ treatment and inhibiting

Table 2.1 Neurosphere cultures established from patient gliomas

CULTURE	ORIGIN	PASSAGE	NS FORMATION CAPABILITY	XENOGRAFT FORMATION	MGMT	p53	TMZ RESPONSE
U373NS	serum line/GBM	>40	high	s.c	negative	mutant	Sensitive
U87NS	serum line/GBM	>40	high	s.c	negative	wild type	Sensitive
GS7-2	GBM	>30	medium	s.c	negative	mutant	Sensitive
AS5-15	AA	>20	medium	s.c	negative	wild type	Sensitive
GS8-26	GBM	>20	high	TBD	negative	TBD	Sensitive
GS4-8	GBM	>15	medium	TBD	TBD	mutant	Sensitive
GS6-22	GBM	>30	high	TBD	negative	mutant	Highly Sensitive
GS9-6	GBM	>30	high	s.c, i.c	negative	wild type	Highly Sensitive
GS9-19	GBM	>15	low	TBD	TBD	wild type	Highly Sensitive
GS11-29	GBM	>20	medium	s.c	TBD	TBD	Resistant
GS7-25	GBM	>30	high	s.c	positive	wild type	Resistant
GS9-10	GBM	>5	medium	TBD	TBD	TBD	TBD
RGS9-10	recurrent GBM	>5	medium	TBD	TBD	TBD	TBD
RGS6-20	recurrent GBM	>5	medium	TBD	TBD	TBD	TBD
GS12-28	GBM	>15	low	TBD	TBD	TBD	TBD
GS1-7	GBM	>10	low/abnormal	TBD	TBD	TBD	TBD
GS10-18	GBM	<5	-	-	-	-	-
GS1-15	GBM	<3	-	-	-	-	-
GS6-25	GBM	<3	-	-	-	-	-
GS9-4	GBM	<5	-	-	-	-	-

Key:

s.c: subcutaneous

i.c.: intracranial

TBD: to be determined

regrowth after treatment, we concentrated our studies on a subset of the TMZ-sensitive glioma lines, including U87NS, U373NS, GS7-2, GS8-26 and AS5-15.

Glioma neurosphere cell lines express Notch receptors and downstream targets

Characterized serum glioma cultures (U87MG, U373MG), converted cell lines (U87NS, U373NS) and primary neurosphere cultures established from patients' GBMs (GS7-2, GS8-26) and AAs (AS5-15) express the transcripts for Notch1-4 and the downstream targets, Hes1 and Hey1 (Fig. 2.2 A). Notch1, Notch2 and Notch4 expression is comparable between the serum lines and the corresponding serum-free neurosphere cell lines. Interestingly, Notch3 expression is consistently higher in the converted neurosphere cultures, compared to their corresponding serum cultures, while expression of the targets, Hes1 and Hey1, varies. In both the converted neurosphere cell lines and the primary cultures, the highest expression is for Notch2, Notch3 and Hes1 transcripts. Although these results demonstrate the presence of an active Notch pathway, more detailed experimentation would be required to analyze the differences between the serum lines and serum-free neurosphere cultures. Since Notch activation is a cell-cell contact-dependent, it is expected that the level of cell confluency in the adherent cultures and the size of the neurospheres will affect expression levels of the Notch receptors and downstream targets. Treatment with DAPT downregulated the mRNA levels of Hes1 and Hey1 (Fig. 2.2 B), demonstrating that the GSI blocks the Notch pathway. The DAPT concentration used was determined based on a 50% or greater decrease of Notch target

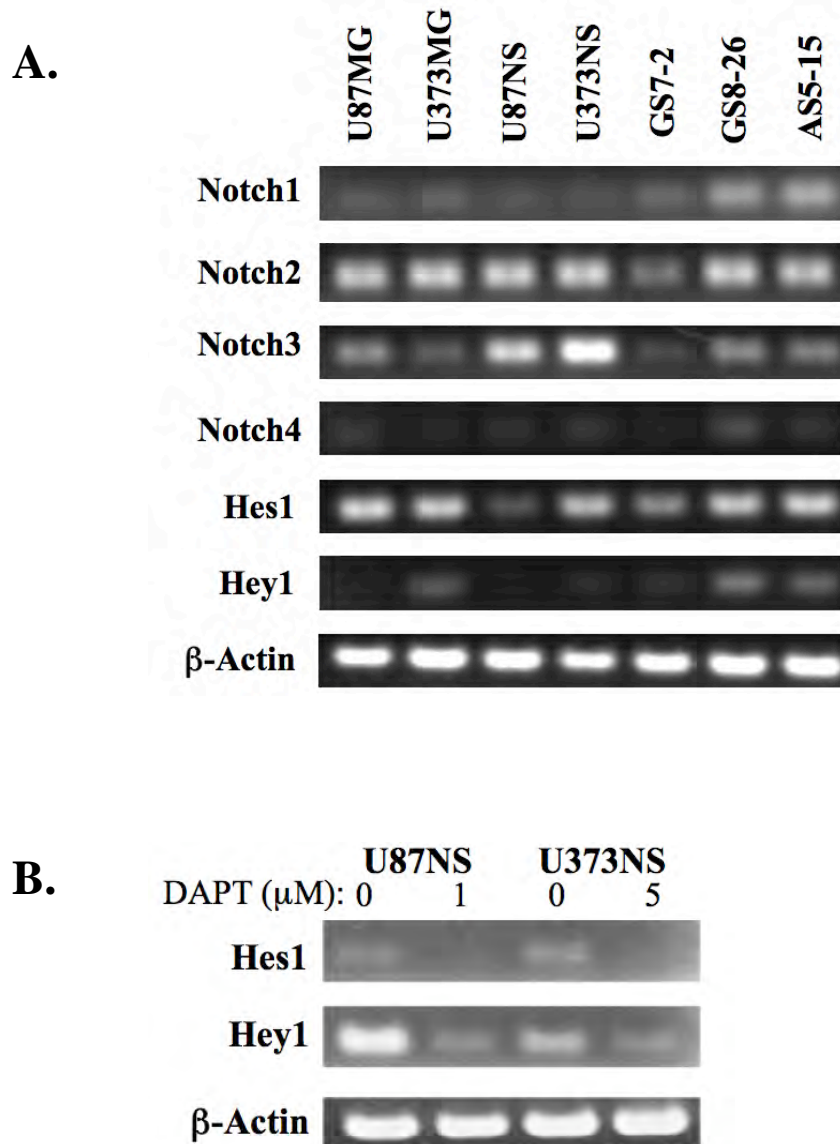


Figure 2.2 **Notch pathway gene expression in glioma cultures.** The Notch pathway is active in neurosphere cultures and is blocked with DAPT treatment. A) mRNA levels of the Notch receptors and downstream targets were measured by RT-PCR. Notch1-4, Hes1, and Hey1 were detected in each neurosphere culture. β -Actin was used for the loading control. B) Hes1 and Hey1 expression were analyzed by RT-PCR 48 hours after DAPT treatment. DAPT treatment decreased Hes1 and Hey1 mRNA levels by 72% and 76% in U87NS (1 μ M), and by 76% and 51% in U373NS (5 μ M).

transcripts. For subsequent experiments, U87NS and GS7-2 cultures were treated with 1 μM DAPT, while U373NS, GS8-26, and AS5-15 cultures were treated with 5 μM DAPT.

TMZ + DAPT treatment inhibits neurosphere recovery and secondary neurosphere formation

Neurosphere recovery was analyzed after TMZ-only, DAPT-only, and TMZ + DAPT treatments (Fig. 2.3). When administered alone, low concentrations of DAPT (1-5 μM) decreased Notch pathway signaling (Fig. 2.2 B), but had little to no effect on the number of neurospheres (Fig. 2.4 A). In addition, low concentrations of DAPT did not affect the size of the neurospheres (Fig. 2.5). In U87NS, U373NS, and GS7-2 cultures, treatment with 10 μM DAPT decreased neurosphere formation by 41%, 39%, and 49%, respectively, compared to DMSO controls (Fig. 2.4 A); however, the DAPT treated cells resumed proliferation and formed secondary neurospheres, even at high concentrations (Fig. 2.4 B).

To determine if DAPT enhances TMZ therapy, we examined the effect of combined treatment on neurosphere recovery. Cultures treated with TMZ-only and TMZ + DAPT, had similar effects on neurosphere size and initial neurosphere formation (Fig. 2.5 and 2.6, red bars). TMZ-only and TMZ + DAPT treatments decreased initial neurosphere formation by 80-98% and 83-99%, respectively. Cultures were given an additional 7 or 10 days to recover in the absence of drugs. During this recovery period, the neurospheres that formed after TMZ-only treatment increased in size; however, the TMZ + DAPT treated neurospheres remained the same size (Fig. 2.5). The number of

Neurosphere Assay

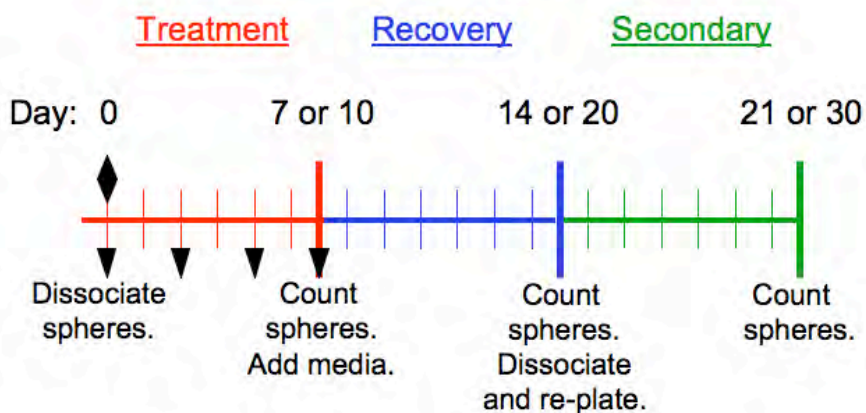


Figure 2.3 **Neurosphere Recovery Assay Schematic.** The neurosphere recovery assay can be used to assess drug treatments. On day 0, neurosphere cultures are pH dissociated and plated as single cells. TMZ (diamond) is administered on day 0. DAPT (inverted triangle) is administered on days 0, 2, 4, and 7. Converted neurosphere cultures, U87NS and U373NS are counted on day 7, 14, and 21, while the primary neurosphere cultures, GS7-2, GS8-26, and AS5-15 are counted on day 10, 20, and 30.

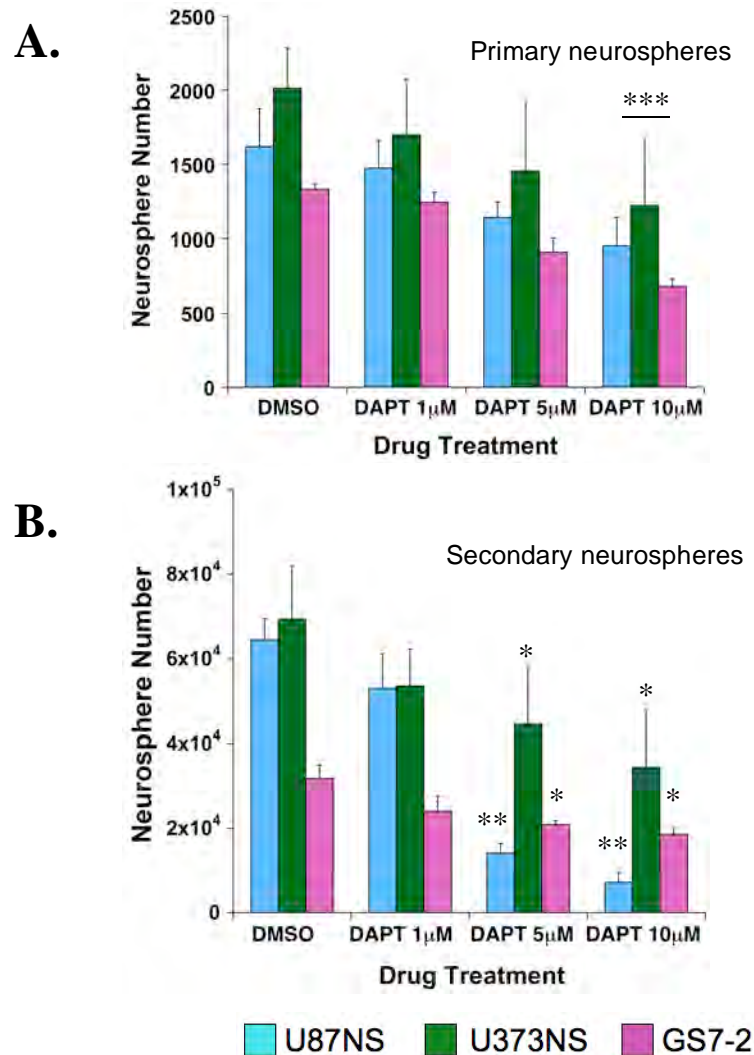


Figure 2.4 **DAPT does not significantly decrease neurosphere formation.** A) The DAPT titration curve demonstrated that low concentrations (1-5 μ M) of DAPT-only treatment had minimal inhibition of neurosphere formation (mean \pm SD) in U87NS, U373NS, or GS7-2 cultures. DAPT administered at higher concentrations (10 μ M) significantly decreased neurosphere formation. Neurospheres were counted on day 7 for U87NS and U373NS and on day 10 for GS7-2. The t-test was used to calculate statistical significance. B) Secondary neurosphere formation for cells treated with varying concentrations of DAPT. U87NS, U373NS, and GS7-2 cells were treated with DMSO (0 μ M DAPT) or DAPT-only at concentrations of 1, 5, and 10 μ M. Neurospheres were dissociated on day 14 for U87NS and U373NS cultures or on day 20 for GS7-2 cultures and re-plated for secondary neurosphere formation. Despite a decrease in secondary neurosphere formation a higher concentrations of DAPT, the treated cells are capable of repopulating the culture. *, $P < 0.01$. **, $P < 0.001$. ***, $P < 0.0001$

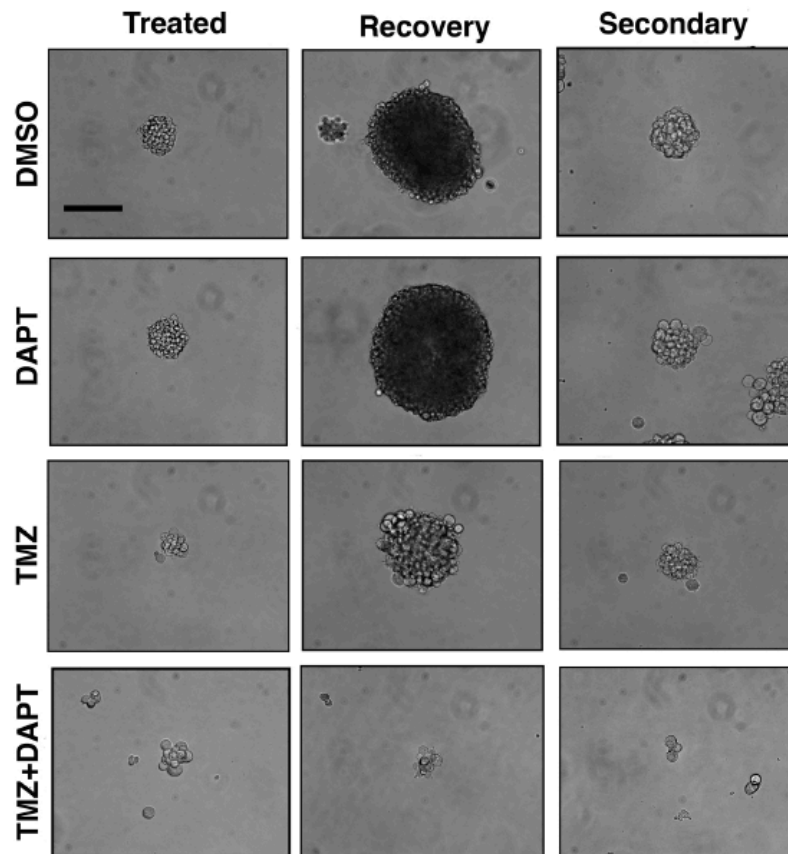


Figure 2.5 Neurosphere size is inhibited by TMZ + DAPT treatment. Representative micrographs of U87NS neurospheres with control DMSO, DAPT (1 μ M) TMZ (200 μ M) and TMZ + DAPT (TMZ (200 μ M) combined with DAPT (1 μ M)) treatment. Neurospheres treated with DAPT display a similar size compared to DMSO control cultures at treatment (day 7), recovery (day 14) and secondary (day 21) time points. After the initial treatment (day 7), TMZ-only and TMZ + DAPT treated neurospheres are smaller than the control cultures. TMZ-only treated neurospheres increased in size during the recovery period (day 14) and formed secondary neurospheres (day 21), while TMZ + DAPT treated neurospheres did not increase in size or form secondary neurospheres. Bar = 50 μ m.

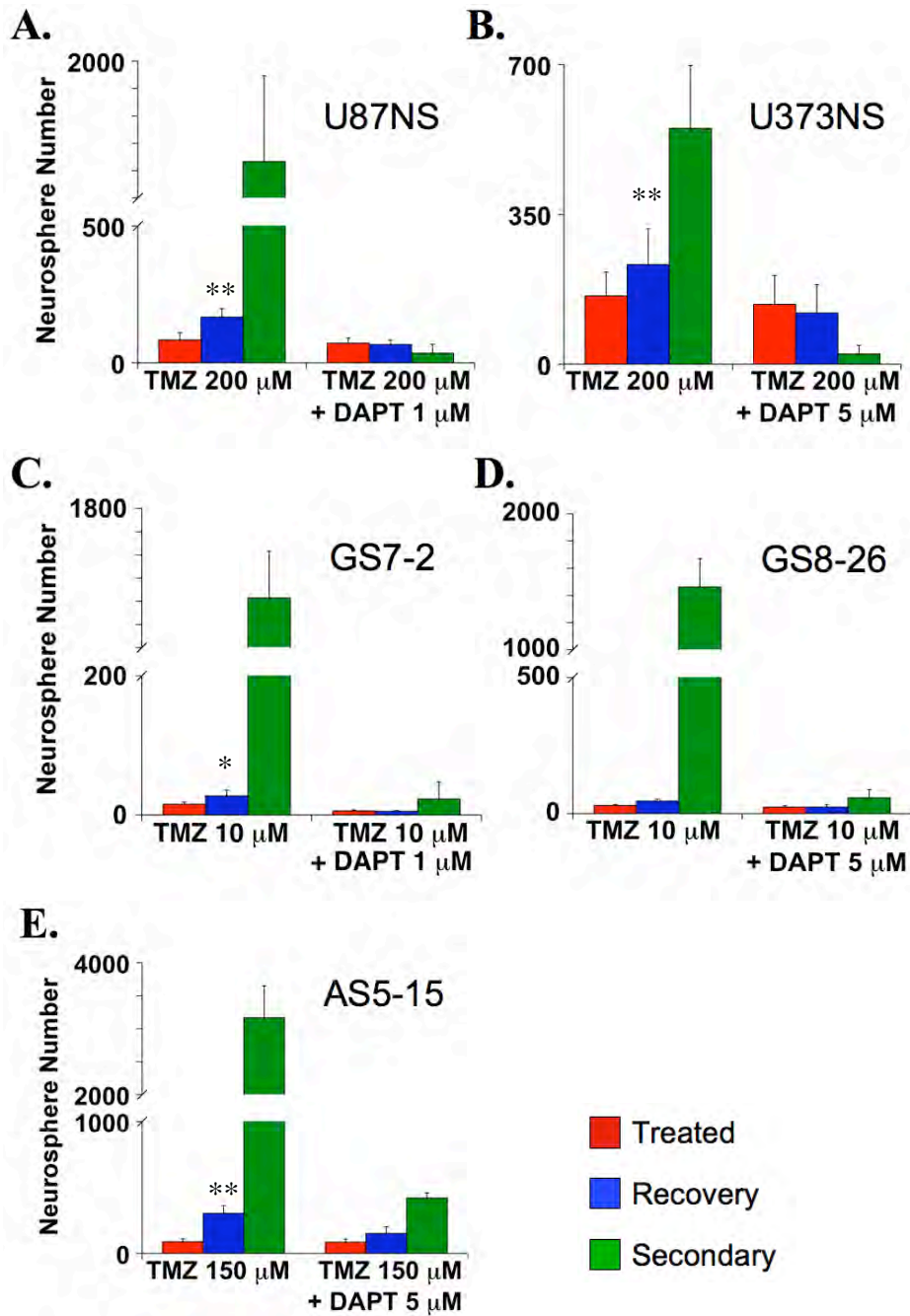


Figure 2.6 TMZ + DAPT treatment blocks recovery and secondary neurosphere formation. The neurosphere recovery assay demonstrates that TMZ + DAPT treatment inhibits recovery and secondary neurosphere formation. Initial treated neurospheres (mean \pm SD) were counted on day 7 for A) U87NS; and B) U373NS cultures; or on day 10 for C) GS7-2, D) GS8-26, and E) AS5-15 cultures. Recovery neurospheres were counted on day 14 or 20, and secondary neurospheres were counted on day 21 or 30. *, $P < 0.001$. **, $P < 0.0001$.

neurospheres also increased after recovery in the TMZ-only treated cultures, but this recovery was not observed in the TMZ + DAPT treated cultures. After recovery from the TMZ-only treatment, U87NS showed a 2-fold increase and U373NS showed a 1.5-fold increase in the number of neurospheres (Fig. 2.6 A and B, blue bars). The primary neurosphere cultures also showed a recovery from the TMZ-only treatment: the number of GS7-2 neurospheres increased by 1.8-fold, GS8-26, by 1.6-fold and AS5-15, by 3.4-fold (Fig. 2.6 C-E, blue bars). In contrast, TMZ + DAPT effectively inhibited recovery for U87NS, U373NS, GS7-2 and GS8-26 (Fig. 2.6 A-D, blue bars). The number of neurospheres in these cultures was essentially the same after recovery on day 14 or 20 relative to the number of initial neurospheres counted on day 7 or 10. Only AS5-15 displayed a small recovery (1.7-fold) when treated with TMZ + DAPT, but this recovery was not statistically significant (Figure 2.6 E, blue bar).

To assess if the cultures retained cells capable of self-renewal, the initial neurospheres were dissociated to single cells and re-plated to measure secondary neurosphere formation. TMZ-only treated cultures readily formed secondary neurospheres, but secondary neurosphere formation for TMZ + DAPT treated cultures was significantly diminished. U87NS secondary neurosphere formation in the TMZ-only treated culture was 36-fold greater ($P < 0.0001$) than secondary neurosphere formation in the TMZ + DAPT treated culture (Fig. 2.6 A, green bar), and U373NS secondary neurosphere formation in the TMZ-only treated culture was 23-fold greater ($P < 0.001$) than in the TMZ + DAPT treated culture (Fig. 2.6 B, green bar). The primary cultures also had profuse secondary neurosphere formation after TMZ-only treatments, but

minimal secondary neurosphere formation after TMZ + DAPT treatments. Secondary neurosphere formation was 45-fold greater ($P < 0.001$) in the GS7-2 TMZ-only treated culture (Fig. 2.6 C, green bar), 25-fold greater ($P < 0.001$) in the GS8-26 TMZ-only treated culture (Fig. 2.6 D, green bar), and 7-fold greater in the AS5-15 treated culture (Fig. 2.6 E, green bar), when compared to the TMZ + DAPT treated cultures.

The number of cells in each neurosphere capable of self-renewal can be calculated by dividing the number of secondary neurospheres by the number of neurospheres formed during the recovery period. After recovery from TMZ-only treatment, there were an average of 8 and 3 cells per neurosphere that maintained self-renewal properties in the U87NS and U373NS cultures, respectively; however, in the TMZ + DAPT treated cultures there were only approximately 0.5 cells per neurosphere that were capable of self-renewal after the recovery period. In the primary lines treated with TMZ-only, each neurosphere from the GS7-2, GS8-26 and AS5-15 cultures contained a large number of cells capable of self-renewal, an average of 38, 31, and 9 cells, respectively. In contrast, the average number of cells capable of self-renewal after TMZ + DAPT treatment decreased to only 2 cells per neurosphere in the GS7-2, GS8-26, and AS5-15 cultures.

To demonstrate that the lack of recovery and secondary neurosphere formation after TMZ + DAPT treatment was a specific response to the inhibition of gamma-secretase activity, we repeated the neurosphere recovery assay with LY411,575 (LY) (Fauq et al., 2007). When LY was administered to U87NS and U373NS cultures at various concentrations, there was a dose-dependent decrease in neurosphere formation (Fig. 2.7 A); however, the LY-only treated cultures retained the ability to form a robust

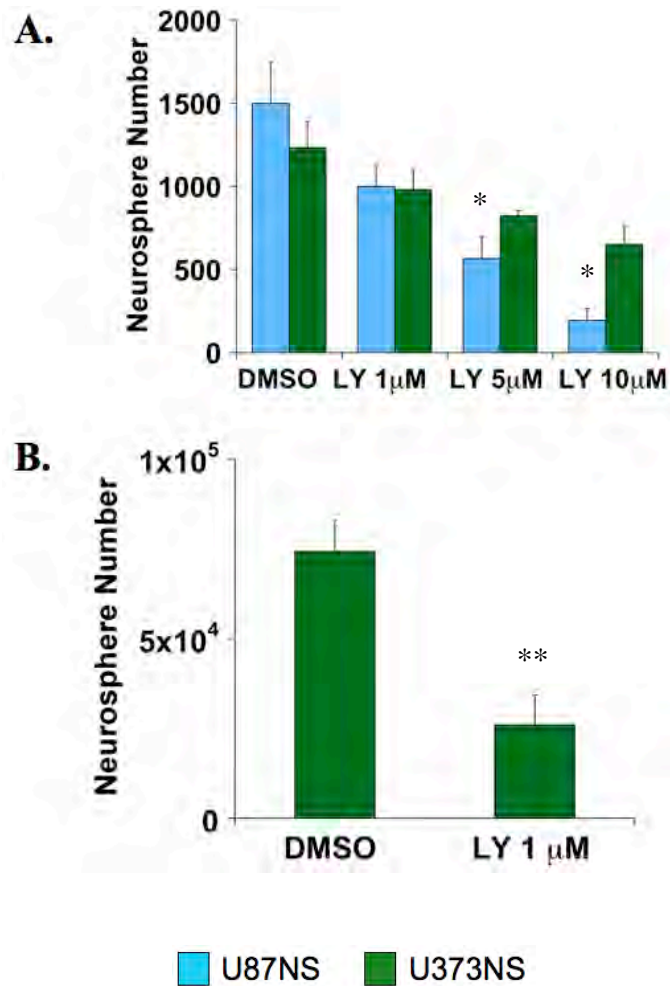


Figure 2.7 **LY411,575 alone does not significantly decrease neurosphere formation.** LY targets the Notch pathway and synergizes with TMZ treatment to inhibit neurosphere recovery. A) U87NS and U373NS cells were treated with varying concentrations of LY, and neurospheres were counted after 7 days. B) U373NS LY treated cultures have decreased secondary neurosphere formation, when compared to DMSO treated samples; however, secondary neurosphere formation was still robust. *, $P < 0.01$. **, $P < 0.001$.

number of secondary neurospheres (Fig. 2.7 B). In contrast, the combination of TMZ + LY significantly repressed neurosphere recovery secondary neurosphere formation (Fig. 2.8 A and B, red and green bars).

It was previously shown that cells expressing MGMT have an increased resistance to TMZ, because they are can repair the O⁶-methyl-guanine lesion (Fukushima et al., 2009). Therefore, we analyzed MGMT expression by real time PCR. Each of our neurosphere lines studied had low to negative MGMT expression, except for the primary line, GS7-25 (Fig. 2.9). Compared to the other lines, GS7-25 had minimal response to TMZ treatment. There was only a 24% decrease in neurosphere formation with TMZ-only treatment (Fig. 2.10 A). Therefore, it appeared that no cells were entering the quiescent state due to TMZ treatment. There was no increase in neurosphere formation during the recovery period for either the TMZ-only or the TMZ + DAPT treated cultures (Fig. 2.10 B). This demonstrates that MGMT-positive lines are unresponsive to the double treatment.

Serum cultures are more sensitive to TMZ and do not recovery

To determine if this recovery was specific to the neurosphere cultures, we tested the combined drug treatment in the original serum cultures, U87MG and U373MG. After treatments, proliferation was analyzed based on the number of live cells present on days 7, 14, and 21. The low concentrations of DAPT (1 μ M for U87MG and 5 μ M U373MG) used in the previously described neurosphere assays had minimal affect on cell number when administered alone (Fig. 2.11 A and B). We found that the adherent glioma cell

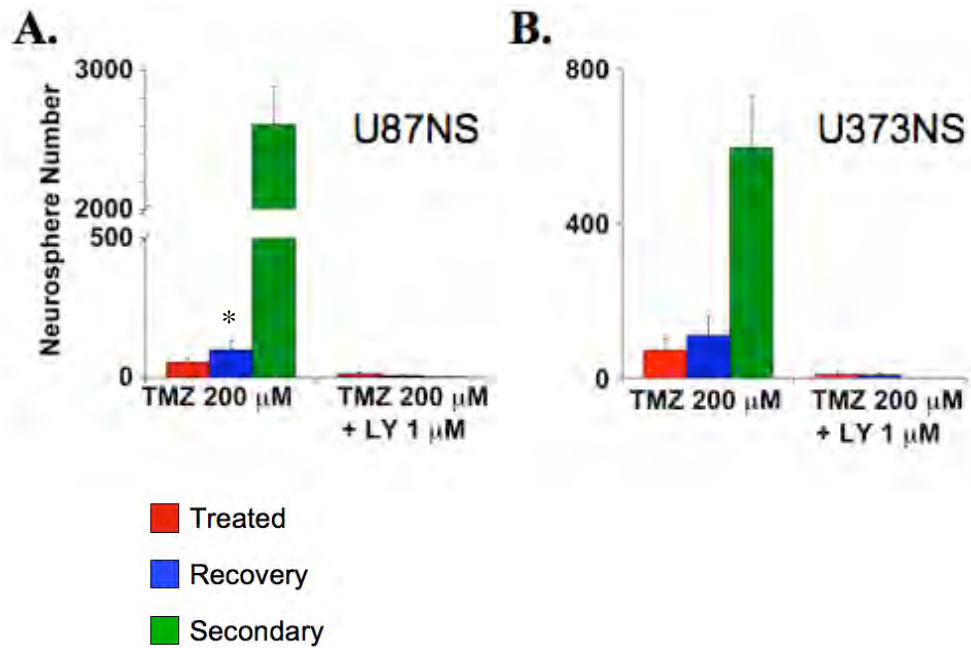


Figure 2.8 TMZ + LY blocks neurosphere recovery and secondary neurosphere formation. The recovery assay for A) U87NS and B) U373NS cells demonstrated that combined treatment with TMZ + LY inhibited neurosphere recovery and secondary neurosphere formation. The t-test was used to calculate statistical significance. Initial treated neurospheres (mean \pm SD) were counted on day 7. Recovery neurospheres were counted on day 14, and secondary neurospheres were counted on day 21. *, $P < 0.01$.

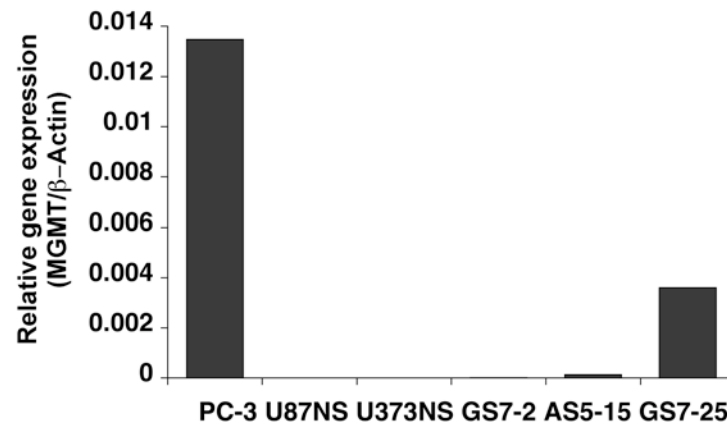


Figure 2.9 **MGMT expression levels by real time PCR in neurosphere converted cultures and primary lines.** PC-3 is a human prostate cancer cell line is used here as a positive control because of it's high expression of MGMT. Of the tested lines, U87NS, U373NS and GS7-2 had no detectable levels of MGMT transcript. AS5-15 displayed minimal levels of MGMT transcript, and GS7-25 was positive for MGMT expression.

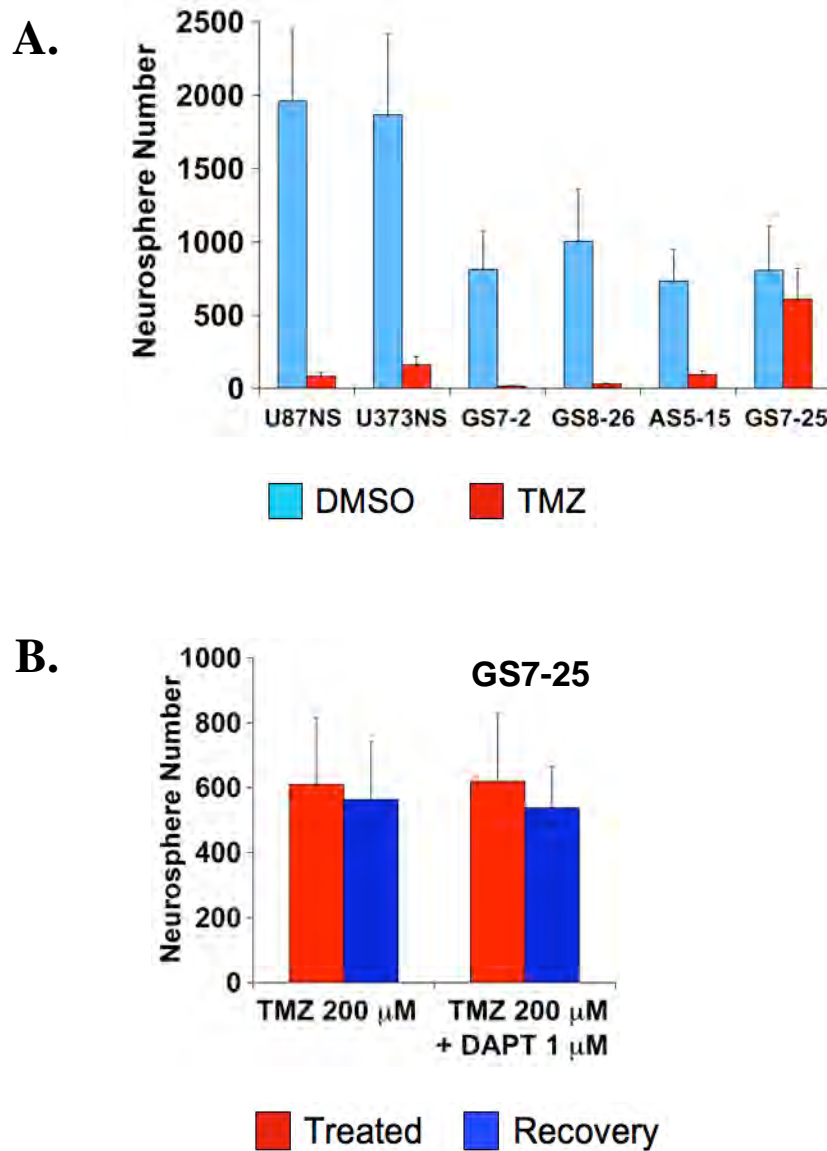


Figure 2.10 **MGMT+ lines are not responsive to TMZ treatment.** A) Neurosphere assay to test TMZ sensitivity among cultures. Converted lines, U87NS and U373NS, were counted on day 7, and the primary lines, GS7-2, GS8-26, AS5-15, and GS7-25 were counted on day 10. All the lines with negative or low MGMT expression were sensitive to TMZ treatment at 200 μ M, while the MGMT-positive line, GS7-25 was resistant. B) The addition of DAPT did not enhance TMZ treatment in the GS7-25 MGMT-positive culture. There was no increase in neurosphere formation between the treated day 7 cultures and the recovery on day 14 for either TMZ-only or TMZ + DAPT treatments.

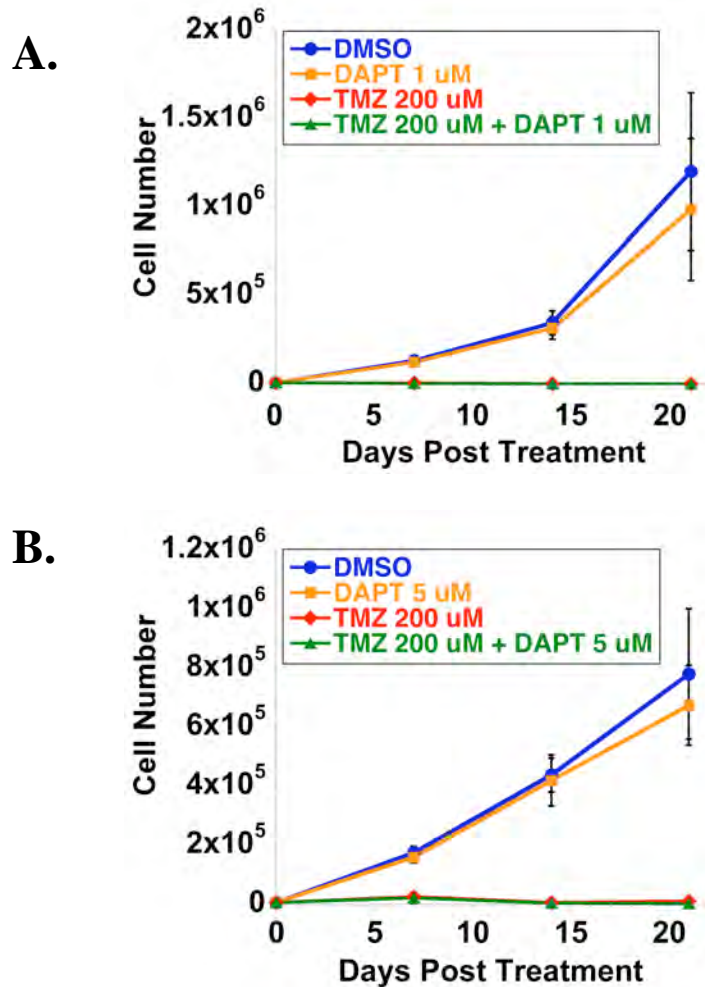


Figure 2.11 **Adherent glioma cultures do not recover after TMZ or TMZ + DAPT treatments.** Cell survival was analyzed in the serum cultures A) U87MG and B) U373MG. DAPT treatment did not significantly affect cell growth in either culture. However, TMZ treatment was highly affective in the adherent lines. TMZ treatment resulted in a decrease in cell number, and no recovery occurred in either the U87MG or U373MG cultures. TMZ + DAPT treatment showed the same effect as TMZ-only treatment.

lines are more sensitive to 200 μ M TMZ than the neurosphere cultures. Both adherent cultures demonstrate a loss of cell number by day 14, and there is no recovery observed. Due to the high efficiency of TMZ treatment alone in the serum-grown, adherent lines, there was no detectable enhancement of treatment when TMZ was combined with Notch inhibition. It is possible that lower concentrations of TMZ may uncover a subpopulation of cells in the adherent culture that are capable of recovery. However, these data demonstrate that the neurosphere cultures have a more heterogeneous response to TMZ than the adherent cultures, demonstrating the benefit of using neurosphere cultures as the *in vitro* model to study the resistant subpopulations within gliomas.

Constitutive expression of NICD protects neurosphere cultures from TMZ + DAPT treatment

In addition to the Notch receptors, gamma-secretase can cleave other substrates (Beel and Sanders, 2008). To establish that DAPT enhances TMZ treatment by targeting the Notch pathway, we infected U87NS and GS7-2 cells with a retrovirus to express the constitutively active NICD1 (Pui et al., 1999). Expression of the GFP reporter gene was used to sort the cells infected with NICD or the empty control vector pMIG. Expression of functional NICD was confirmed by measuring increased mRNA levels of the downstream targets, Hes1 and Hey1 (Fig. 2.12 A). When NICD is constitutively expressed, the Notch pathway is not inhibited by DAPT treatment (Fig 2.12 B). NICD-expressing U87NS and GS7-2 cells treated with TMZ-only were capable of recovery and robust secondary neurosphere formation, similar to the control cells expressing the empty

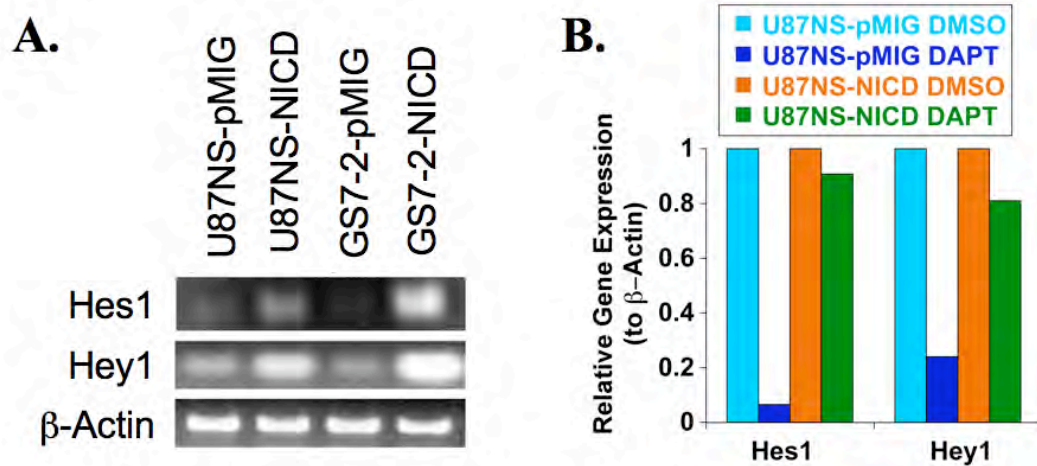


Figure 2.12 **Expression of constitutively active NICD blocks GSI knockdown of Notch targets.** A) RT-PCR analysis of Hes1 and Hey1 expression was used to confirm NICD activity. Hes1 and Hey1 expression increased in U87NS-NICD and GS7-2-NICD cultures compared to cultures expressing the empty vector (pMIG). B) DAPT does not inhibit the Notch pathway in neurospheres constitutively expressing NICD. U87NS-pMIG and U87NS-NICD cells were treated with 1 μ M DAPT and collected 48 hours after treatment. qRT-PCR analysis demonstrated that Hes1 and Hey1 expression decreased in the representative DAPT treated samples. However, U87NS-NICD culture had a minimal decrease of Hes1 and Hey1 expression in the DMSO and DAPT treated samples.

vector (pMIG) (Fig. 2.13 A and B). Importantly, NICD expression attenuated the effects of TMZ + DAPT treatment, and the culture demonstrated neurosphere recovery and robust secondary neurosphere formation. The control U87NS-pMIG TMZ-only treated cells had a 1.9-fold recovery, but no increase was seen in the TMZ + DAPT treated culture (Fig. 2.13 A, blue bars). U87NS-NICD cells showed a 2.3-fold recovery in TMZ-only treated cultures and a 1.8-fold recovery in TMZ + DAPT treated cultures. GS7-2-pMIG TMZ-only treated cells showed a 2.1-fold increase in neurospheres during recovery, while TMZ + DAPT treated cells showed no recovery (Fig. 2.13 C, blue bars). GS7-2-NICD cells showed a 2.6-fold recovery after TMZ-only and a 2.8-fold recovery after TMZ + DAPT treatment.

Similar to the parental lines, U87NS-pMIG and GS7-2-pMIG cultures treated with TMZ-only had robust secondary neurosphere formation, but cultures treated with TMZ + DAPT had minimal secondary neurosphere formation (Fig. 2.13 A and B). In contrast, U87NS-NICD and GS7-2-NICD cultures had robust secondary neurosphere formation for both TMZ-only and TMZ + DAPT treatments. When treated with TMZ + DAPT, U87NS-NICD secondary neurosphere formation was 61.2-fold greater ($P < 0.0001$) than U87NS-pMIG secondary neurosphere formation (Fig. 2.13 A, green bars). In the GS7-2-NICD TMZ + DAPT treated cultures, secondary neurosphere formation was 47.8-fold greater ($P < 0.0001$) than secondary neurosphere formation in the GS7-2-pMIG TMZ + DAPT treated cultures (Fig. 2.13 B, green bars). Hence, constitutive NICD expression eliminates GSI enhancement of TMZ therapy, identifying the Notch pathway as the relevant GSI target.

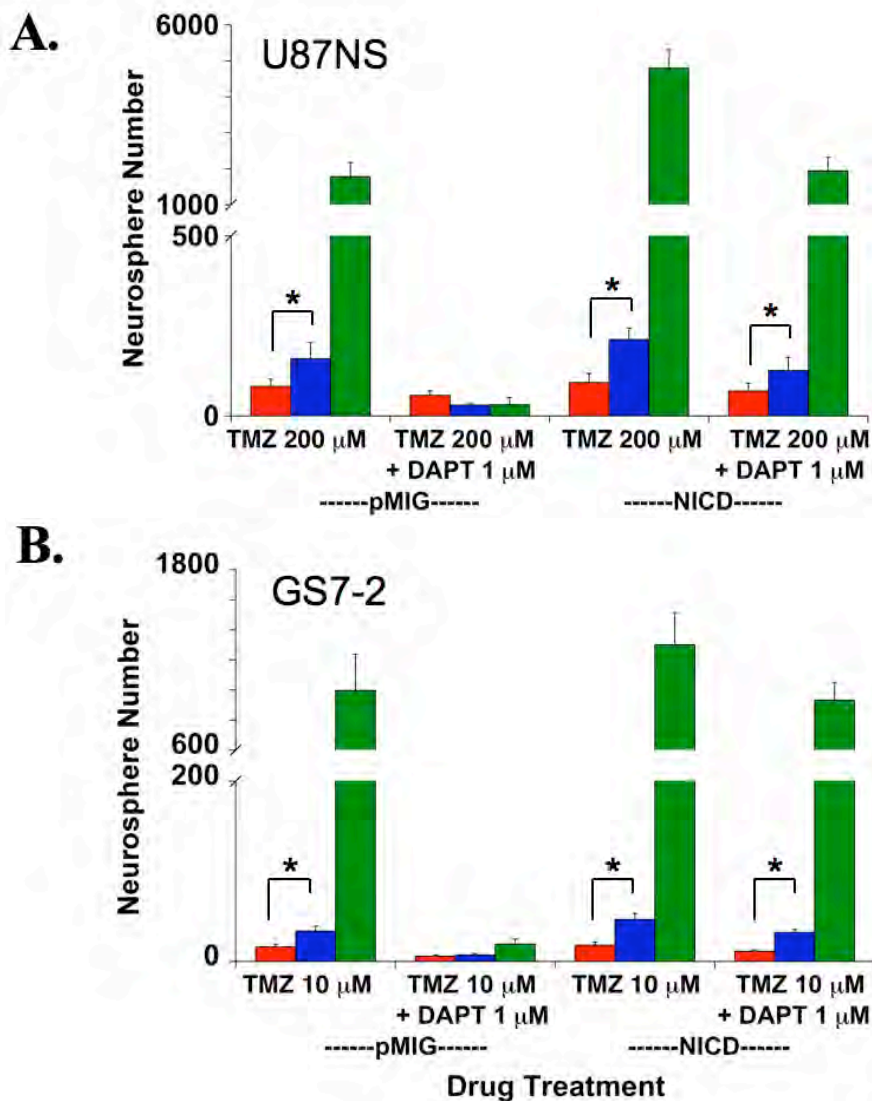


Figure 2.13 **Expression of constitutively active NICD attenuates the TMZ + DAPT treatment synergy.** NICD-expressing cultures resume neurosphere formation following TMZ + DAPT treatment. A) Treating U87NS-pMIG with TMZ + DAPT inhibited recovery, but U87NS-NICD cultures recovered after both TMZ-only and TMZ + DAPT treatment. B) In GS7-2-pMIG and GS7-2-NICD cultures treated with TMZ-only or TMZ + DAPT, cultures constitutively expressing NICD, but not the empty vector, were able to recover after TMZ + DAPT treatment. *, $P < 0.0001$.

TMZ + DAPT treatment response is schedule-dependent

We tested if single DAPT doses administered before, during, or after TMZ treatment would have distinct effects. TMZ and DAPT were administered to U87NS, U373NS and GS7-2 neurosphere cultures with three treatment schedules (Fig. 2.14). Interestingly, pre-treatment with DAPT decreased the efficacy of TMZ. Initial neurosphere formation was 7.2-fold, 1.7-fold and 2.7-fold greater than neurosphere formation in TMZ-only treated U87NS, U373NS and GS7-2 cultures, respectively (Fig. 2.15 A-C, red bars). When dissociated, the pre-treated and co-treated samples formed a large number of secondary neurospheres; however, post-treated samples had minimal secondary neurosphere formation (Fig. 2.15 A-C, green bars). Secondary neurosphere formation was significantly greater in TMZ-only, pre-treated and co-treated cultures compared to post-treated cultures. Secondary neurosphere formation in U87NS cultures was 5.7-fold greater ($P < 0.001$) with TMZ-only treatment, 8.1-fold greater ($P < 0.001$) with DAPT pre-treatment, and 4.8-fold greater ($P < 0.01$) with co-treatment, relative to secondary neurosphere formation after DAPT post-treatment (Fig. 2.15 A, green bars). For U373NS secondary neurosphere formation, TMZ-only treatment was 5.7-fold greater ($P < 0.01$), DAPT pre-treatment was 8.1-fold greater ($P < 0.01$), and co-treatment was 4.8-fold greater ($P < 0.01$) than to secondary neurosphere formation in DAPT post-treated samples (Fig. 2.15 B, green bars). The inhibition of GS7-2 secondary neurosphere formation was also greatest with post-treatment. Secondary neurosphere formation in the GS7-2 cultures was 85.7-fold greater ($P < 0.0001$) with TMZ-only treatment, 98.5-fold greater ($P < 0.0001$) with DAPT pre-treatment, and 72.8-fold greater ($P < 0.0001$) with

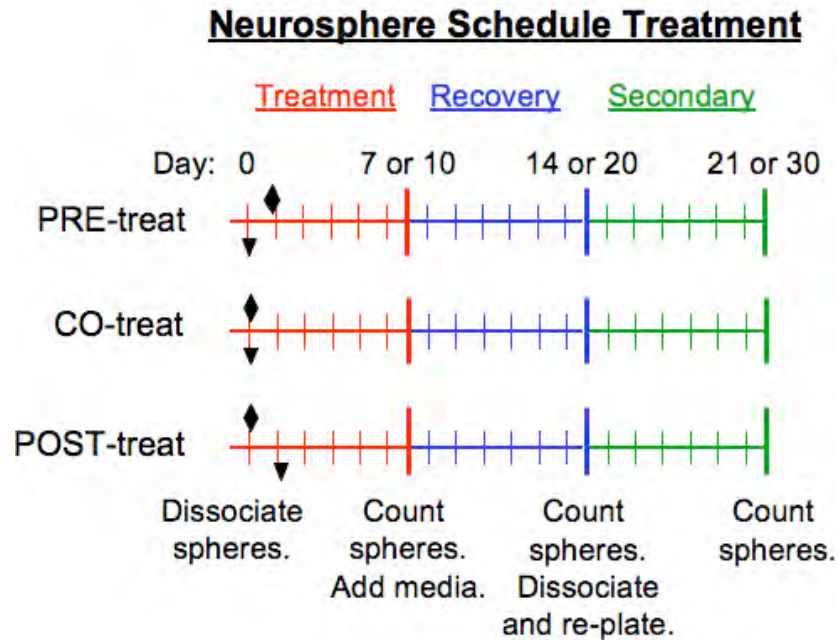


Figure 2.14 **Neurosphere recovery assay drug schedule treatment schematic.** The neurosphere recovery assay was used to analyze single dose GSI treatments and the effect of schedule treatment with TMZ + DAPT on neurosphere secondary neurosphere formation. TMZ (diamond) and DAPT (inverted triangle) treatments were either administered with DAPT 24 hours prior to TMZ (pre-treat), simultaneously with TMZ (co-treat), or 24 hours after TMZ (post-treat).

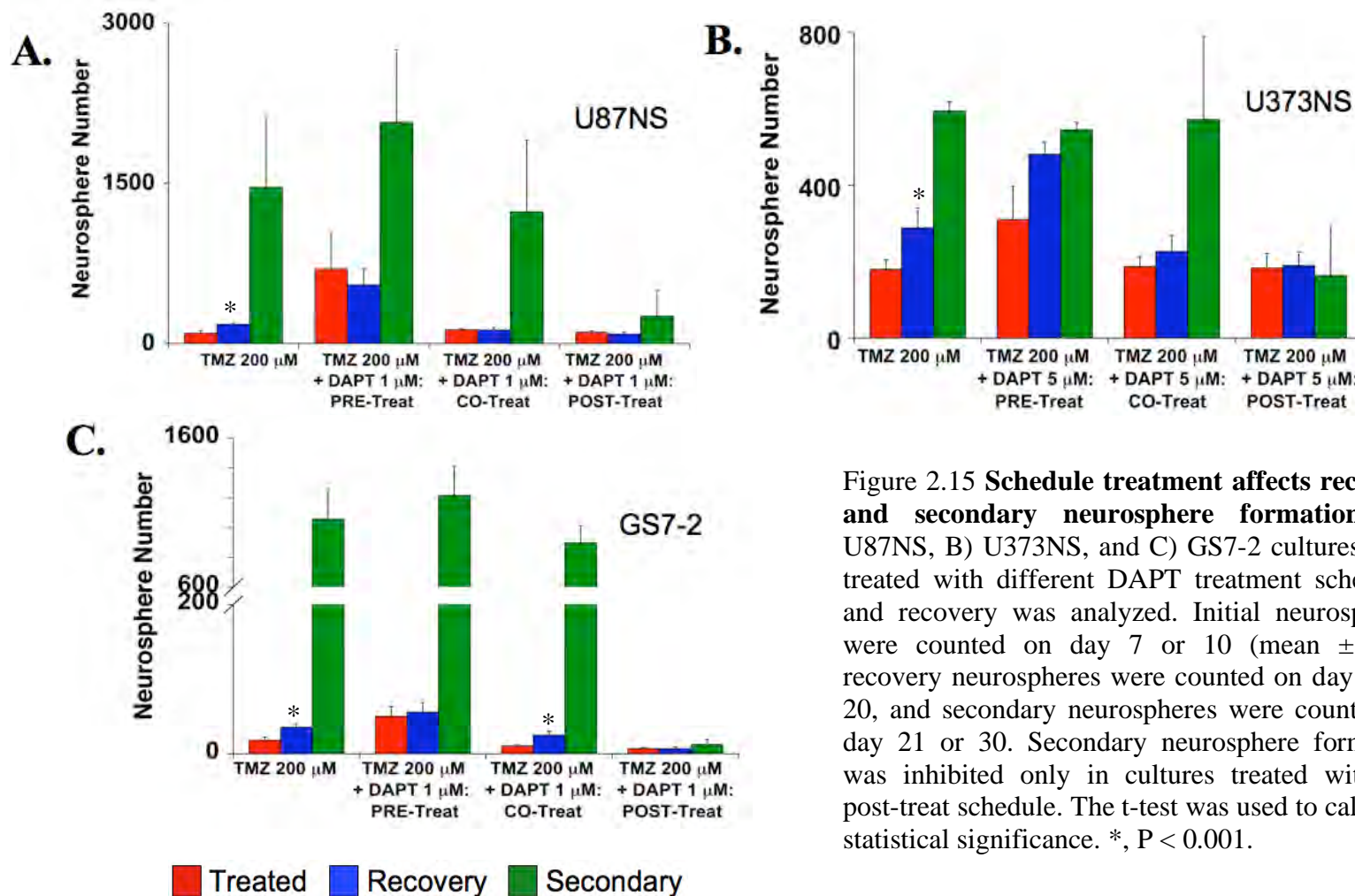


Figure 2.15 **Schedule treatment affects recovery and secondary neurosphere formation.** A) U87NS, B) U373NS, and C) GS7-2 cultures were treated with different DAPT treatment schedules and recovery was analyzed. Initial neurospheres were counted on day 7 or 10 (mean \pm SD), recovery neurospheres were counted on day 14 or 20, and secondary neurospheres were counted on day 21 or 30. Secondary neurosphere formation was inhibited only in cultures treated with the post-treat schedule. The t-test was used to calculate statistical significance. *, $P < 0.001$.

co-treatment, when compared to the DAPT post-treatment (Fig. 2.15 C, green bars). The differences of neurosphere growth and secondary neurosphere formation among the various TMZ and DAPT treatment schedules could also be observed by neurosphere size (Fig. 2.16). In general, the neurospheres present on day 7 were of similar size in all three treatment schedules; however, at day 14, there were more neurospheres that had increased in size in the DAPT pre-treated and co-treated samples. In addition, at day 21, secondary neurospheres for DAPT pre-treatment and co-treatment were normal sized, while most of the DAPT post-treatment sample consisted of single cells.

The number of cells per neurosphere that were capable of secondary neurosphere formation were similar for TMZ-only, pre-treatment, and co-treatment, while the self-renewal capacity was greatly reduced in the DAPT post-treated samples. After recovery from TMZ-only treatment, there were an average of 8, 3, and 29 cells per neurosphere that maintained self-renewal properties in the U87NS, U373NS and GS7-2 cultures, respectively. The number of cells capable of self-renewal in the pre-treated U87NS, U373NS and GS7-2 cultures were 4, 1, and 22 cells per neurosphere, respectively. Similarly, co-treated samples had 10, 3, and 36 cells per neurosphere, for U87NS, U373NS, and GS7-2, respectively. However, for the post-treated samples, only 2, 0.8, and 2 cells per neurosphere formed secondary neurospheres, demonstrating a decrease in self-renewal. Overall, these results led to two observations. First, TMZ + DAPT treatment acts through a specific, sequence-dependent mechanism. Second, these results provide insight for *in vivo* treatment schedule.

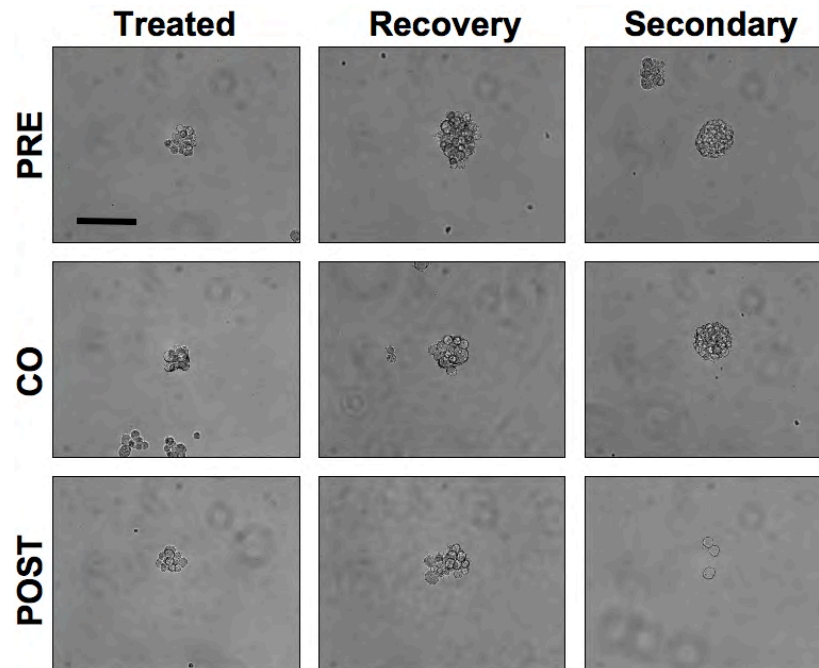


Figure 2.16 **Neurosphere size after schedule treatment assay.** Representative micrographs of U87NS neurospheres with schedule treatments administered either with DAPT 24 hours prior to TMZ (pre-treat), simultaneously with TMZ (co-treat), or 24 hours after TMZ (post-treat). Pre-treated and co-treated neurospheres displayed an increase in neurosphere size treatment (day 7) to recovery (day 14). These treated spheres also demonstrated normal secondary neurosphere formation (day 21). In contrast, post-treated U87NS cells did not have an increase in neurosphere size from the treatment period (day 7) to the recovery period (day 14). After dissociation, the post-treated samples contained mostly single cells and did not form secondary neurospheres (day 21), Bar = 50 μm .

TMZ + DAPT ex vivo treatment greatly reduces tumor formation

We tested if neurosphere recovery correlated with the ability of cells to initiate tumors in a subcutaneous xenograft model. The converted neurosphere cultures, U87NS and U373NS, were used for xenograft experiments, because they have a high incidence of tumor formation and short tumor latency. Primary lines will be ideal for future experiments, but were not used for these mouse studies, due to their significantly longer time required for tumor formation and limitations with cell number availability. U87NS cultures were treated with DMSO, DAPT-only, TMZ-only or TMZ + DAPT. Since TMZ-only and TMZ + DAPT treatments lead to an increase in the percentage of dead cells, it is important to use the same number of live cells for the subcutaneous injections from each treatment cohort. This is assessed using trypan blue staining. Immunocompromised NU/NU nude mice were subcutaneously injected in the right flank with 2.5×10^5 live cells, and tumor initiation was scored when a palpable tumor formed. DMSO and DAPT-only *ex vivo* treated cells showed similar tumor incidence (6/7 and 7/7, respectively) and average latencies of 15 and 14 days, respectively. TMZ-only treated cells had an increased tumor latency of 32 days, but the tumor incidence (6/7 mice) was similar to control xenografts (Fig. 2.17 A; Table 2.2). Impressively, none of the mice injected with TMZ + DAPT treated cells (0/7 mice) formed tumors, even after 90 days. When a higher number of live U87NS cells (3×10^6) were injected, we saw a similar trend (Table 2.2). Mice with 3×10^6 cells for U87NS DMSO (2/2 mice) and DAPT-only (2/2 mice) xenografts developed palpable tumors at 3 and 4 days, respectively, and 3/4 mice formed tumors in TMZ-only treated cells with an average latency of 25 days. With this higher

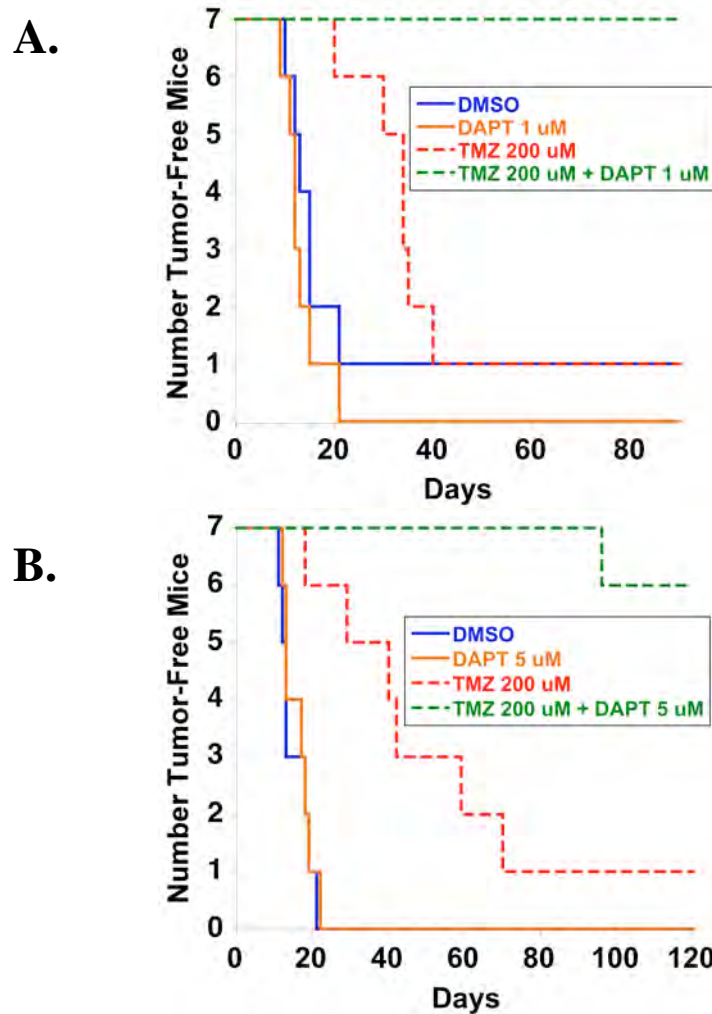


Figure 2.17 *Ex vivo* TMZ + DAPT treatment decreases tumorigenicity. TMZ + DAPT treatment decreases tumorigenicity. A) U87NS cells were treated *ex vivo* with DMSO, DAPT 1 μ M, TMZ 200 μ M or TMZ 200 μ M + DAPT 1 μ M, and 7 days post-treatment, mice were subcutaneously injected with 2.5×10^5 live cells. TMZ treatment increased latency, but xenografts still formed. TMZ + DAPT inhibited xenograft formation. B) U373NS cells were treated *ex vivo*, and mice were subcutaneously injected with 3×10^6 live cells. TMZ 200 μ M treatment increased latency, but tumors still formed. TMZ 200 μ M + DAPT 5 μ M treatment decreased xenograft formation.

Table 2.2 Tumor formation in subcutaneous xenografts after *ex vivo* drug treatment

<i>Ex vivo</i> Treated Xenografts Tumor Incidence and Average Latency (days)			
	U87NS		U373NS
	2.5×10^5	3×10^6	3×10^6
DMSO	6/7 (15)	2/2 (3)	7/7 (15)
DAPT	7/7 (14)	2/2 (4)	7/7 (16)
TMZ	6/7 (32)	3/4 (25)	6/7 (45)
TMZ + DAPT	0/7 (-)	1/4 (43)	1/7 (96)

number of cells injected, U87NS TMZ + DAPT xenografts formed tumors in only 1/4 mice with a longer latency of 43 days.

U373NS cultures were treated with DMSO, DAPT-only, TMZ-only or TMZ + DAPT, and 3×10^6 live cells were injected subcutaneously into NU/NU nude mice (Fig. 2.17 B; Table 2.2). The control DMSO cells formed palpable tumors in an average of 15 days for 7/7 xenografts, and DAPT-only treated cells formed tumors in an average of 16 days for 7/7 xenografts. *Ex vivo* treatment with TMZ-only increased the latency of tumor formation; however, the tumor incidence was similar to the DMSO control xenografts. Palpable tumors formed for 6/7 TMZ-treated U373NS xenografts in an average of 43 days. *Ex vivo* treatment with TMZ + DAPT greatly reduced tumor formation in mice. Only 1/7 mice formed a tumor in the TMZ + DAPT U373NS xenografts with an extended latency of 96 days. The tumor-free mice were observed for up to 120 days before sacrifice. These *ex vivo* experiments demonstrate the potency of TMZ + DAPT combined treatment in reducing tumor formation.

TMZ + LY in vivo treatment inhibits tumor regrowth

Although DAPT greatly enhances TMZ treatment *in vitro*, it has a poor potency *in vivo*, and requires high doses to target to observe an effect (Dovey et al., 2001; Lanz et al., 2004). In contrast, LY411,575 (LY) is a potent GSI both *in vitro* and *in vivo*. We tested the effect of *in vivo* TMZ + GSI treatments on pre-existing subcutaneous glioma xenografts with two i.p. injections of TMZ (20 mg/kg/day) alone, or combined with a ten-day diet of LY411,575 chow (Samon et al., 2008). During drug administration,

toxicity was determined by weight loss. TMZ-only and TMZ + LY chow cohorts initially showed a slight weight loss after TMZ injections (Fig. 2.18 A). However, the TMZ-only and TMZ + LY chow mice returned to their starting body weight, and no significant weight difference was observed throughout the remainder of the treatment. This demonstrates that the mice tolerated the LY chow alone and the combination of the TMZ + LY chow. The lack of overall weight loss also suggests that the mice on LY chow diets did not significantly reduce their food consumption compared to control mice and received the estimated average dose of 5 mg/kg/day of LY (Samon et al., 2008). The ten-day diet of LY chow significantly decreased the mRNA levels of the Notch targets *Hes1* and *Hey1* (Fig. 2.18 B). Mice were subcutaneously injected with 1×10^6 U87NS cells and treated when the tumors reached a volume of approximately 150 mm^3 . When the tumor reached a volume that was double the original volume measured at the start of the drug treatments, we judged the xenograft as progressing. The DMSO control and LY chow-only cohorts did not have any delay in tumor progression (Fig. 2.19 A). TMZ treatment initially decreased tumor volumes (Fig. 2.19 B and 2.20 A). However, the TMZ-only treated tumors eventually progressed in 8/8 xenografts, and tumor volume doubled in an average of 23 ± 7 days after treatment (Fig. 2.19 A, C and 2.20 A). These tumors had a normal growth rate and were sacrificed between 23 to 39 days post-treatment. Impressively, 4/8 the mice treated with TMZ + LY chow displayed no tumor progression (Fig. 2.19 A). In the other 4/8 mice treated with TMZ + LY chow, tumor progression occurred in an average of 26 ± 3 days (Fig. 2.20 B), and mice were euthanized between 24 to 33 days post-treatment. The TMZ + LY chow mice that did not have tumor

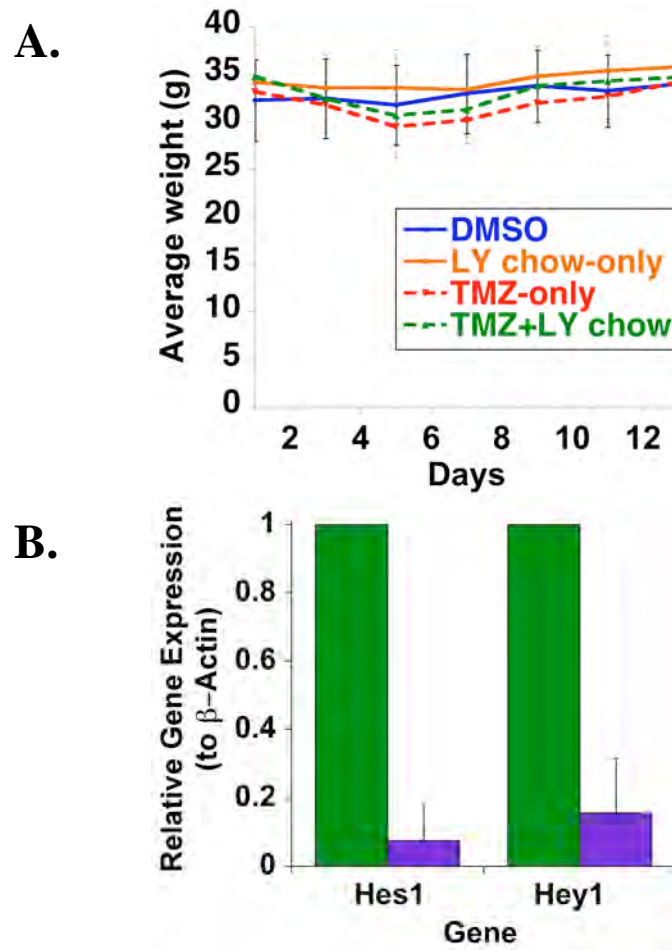


Figure 2.18 *In vivo* TMZ and LY chow treatment effects on toxicity and gene expression. A) Tolerance of the drug treatments was determined by measuring the weight of the mice during the period of drug administration. Initially, TMZ-only and TMZ + LY chow cohorts demonstrate a slight decrease in body weight, but the mice quickly recover. There was no significant change in the final weight of the mice for any of the drug treatments. For DMSO, n = 4; LY chow, n = 5; TMZ-only, n = 6; and TMZ + LY chow, n = 6. B) LY chow significantly decreased the mRNA levels of the Notch targets Hes1 and Hey1 in glioblastoma tumors. Immunocompromised NU/NU nude mice with pre-existing U87NS xenografts were given a diet of normal chow (n = 4) or LY chow (n = 4) for ten consecutive days. After LY treatment, mRNA was isolated from the xenografts and Notch activity was analyzed by qRT-PCR. Hes1 and Hey1 expression significantly decreased in the LY chow cohorts. ***, P < 0.0001.

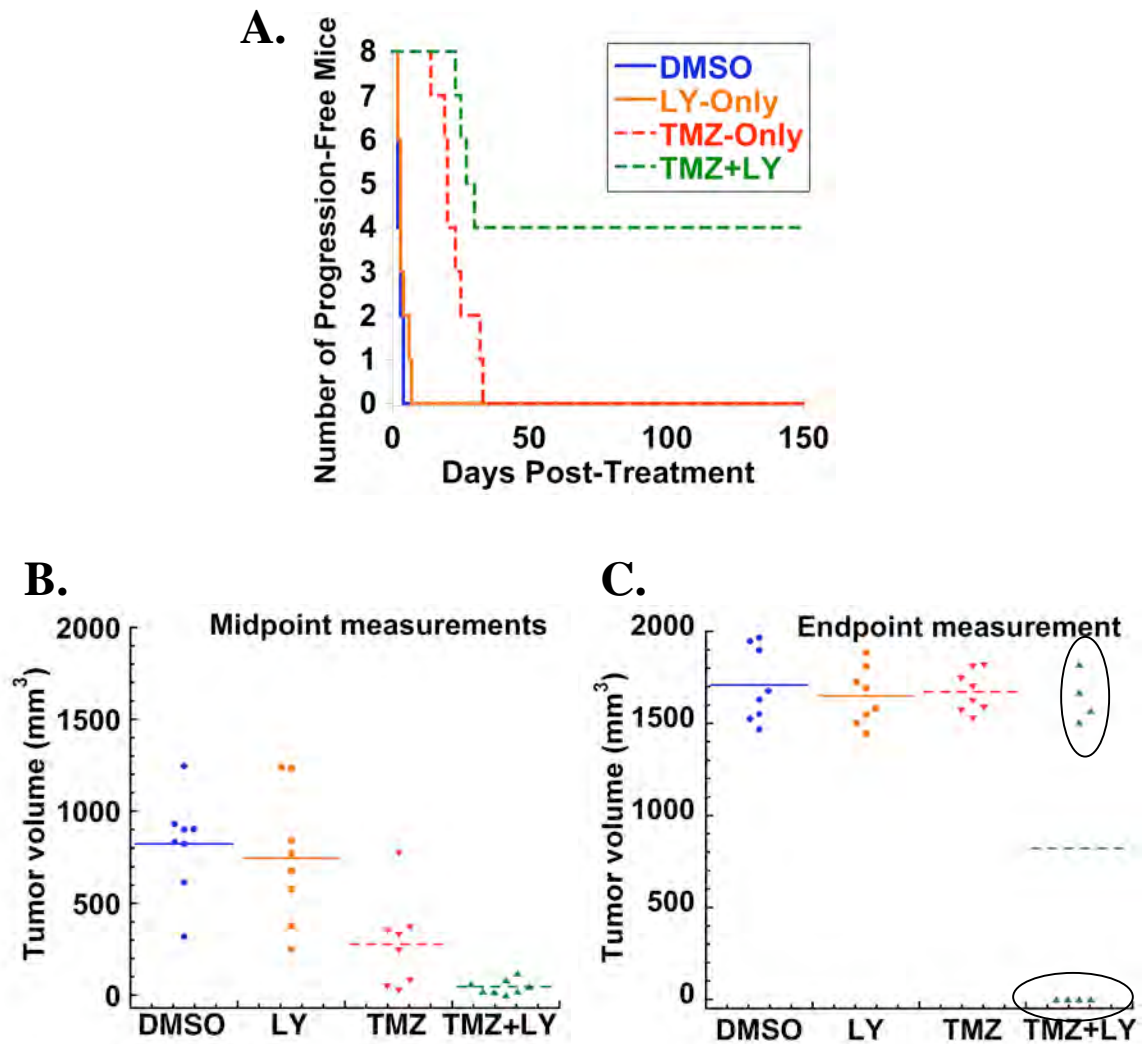


Figure 2.19 *In vivo* TMZ + LY treatment blocks tumor progression. A) *In vivo* TMZ treatment increased the tumor latency in U87NS xenografts, but 100% of the mice succumbed to progression. TMZ + LY chow treatment completely blocked progression in 50% of the mice. B) Tumor volumes at the midpoint, measured between drug treatment and mouse sacrifice. No significant difference in tumor volume is observed between DMSO and LY chow cohort at the midpoint measurement. TMZ-only treated mice possess smaller tumors at the midpoint measurement, while TMZ + LY chow treated mice present with the lowest tumor volume. C) Tumor volumes at the time sacrifice. In the TMZ + LY chow treated mice, two separate groups were observed at the endpoint measurement. 50% of the mice showed full progression, while the remaining 50% had no progression. The U87NS TMZ + LY chow treated xenografts that lacked progression had no palpable tumor at 150 days post-treatment.

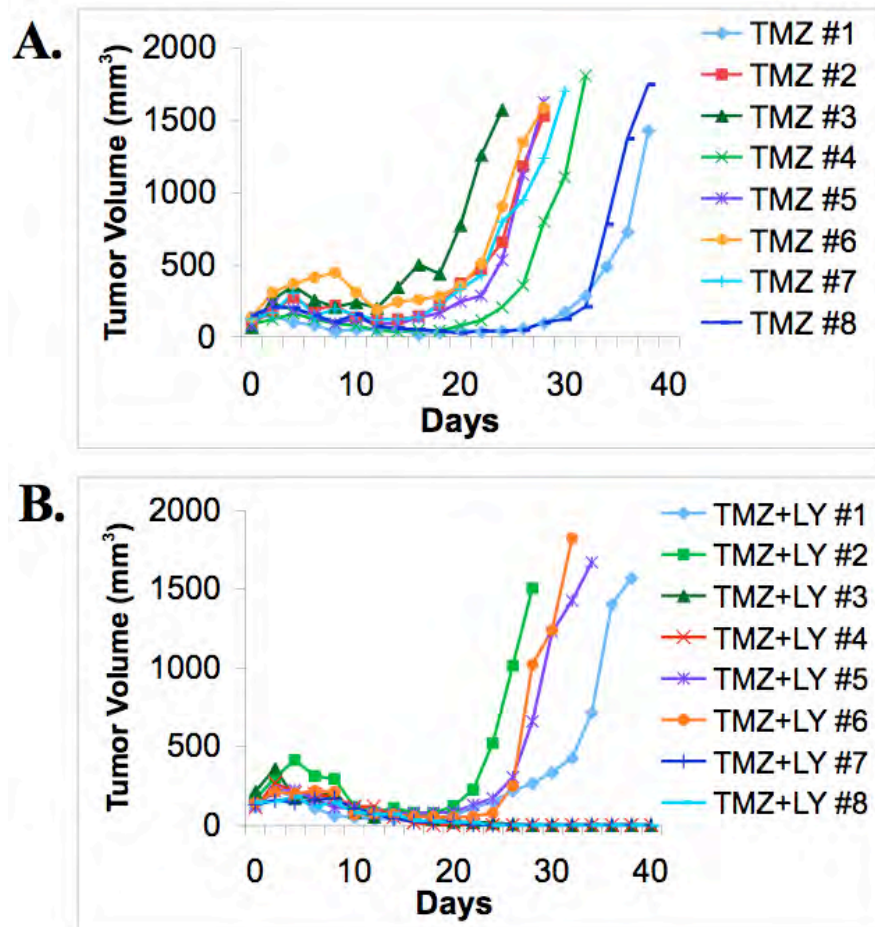


Figure 2.20 **Individual tumor volumes from *in vivo* TMZ + LY treatment.** A) Mice with pre-existing tumors were treated *in vivo* with TMZ-only when tumors reached approximately 150 mm³ and observed for tumor progression, which was classified as the point when the tumor doubled in volume, approximately 300 mm³. Tumors initially began to decrease in volume 5 days after the beginning of treatment. Although all TMZ-only tumors demonstrated regrowth, the time until tumor progression varied greatly between 14 to 32 days after treatment. B) Mice with pre-existing tumors were treated with TMZ + LY chow when the tumors reached approximately 150 mm³. Tumors initially decreased in volume 5 days after the beginning of treatments. 4/8 mice demonstrated tumor progression between 23 to 30 days. The other 4/8 mice demonstrated a complete loss of tumor mass and remained at 0 mm³ for 150 days after treatment until the mice were sacrificed.

progression displayed a complete loss of a palpable tumor and remained tumor-free until euthanized at 150 days (Fig. 2.19 A, C and 2.20 B). In these mice, no tumor masses were evident by gross dissection and examination of H&E stained sections (Fig. 2.21). Hence, the TMZ + LY chow treatment had a dramatic effect on pre-existing tumors by curing 50% of the mice. It is important to note that the *in vivo* drug administration recapitulated the GSI post-treatment used for studying the affect of treatment schedules on neurosphere recovery *in vitro*.

Discussion

With current AA and GBM treatment, tumor recurrence is highly probable. Our laboratory's neurosphere recovery assay demonstrates that glioma cells that survive chemotherapy can repopulate neurosphere cultures and form tumors (Mihaliak et al., 2010). Neurosphere cultures are useful to study glioma responses to drug treatments, since the neurospheres have similar phenotypes and genotypes to patient tumors (Ernst et al., 2009; Lee et al., 2006b). When neurospheres established from patient gliomas are treated with clinically relevant concentrations of TMZ, a small number of cells survive, recover from the chemotherapy and repopulate the cultures. In converted cell lines, this recovery was also observed with high TMZ drug concentrations. These results resemble tumor recurrence in the clinic after glioma patients are treated with TMZ. The quick tumor recurrence observed in the clinic, and the repopulation of neurosphere cultures after TMZ treatment, demonstrate the dire need for combination therapies to target the cells that recover from chemotherapy.

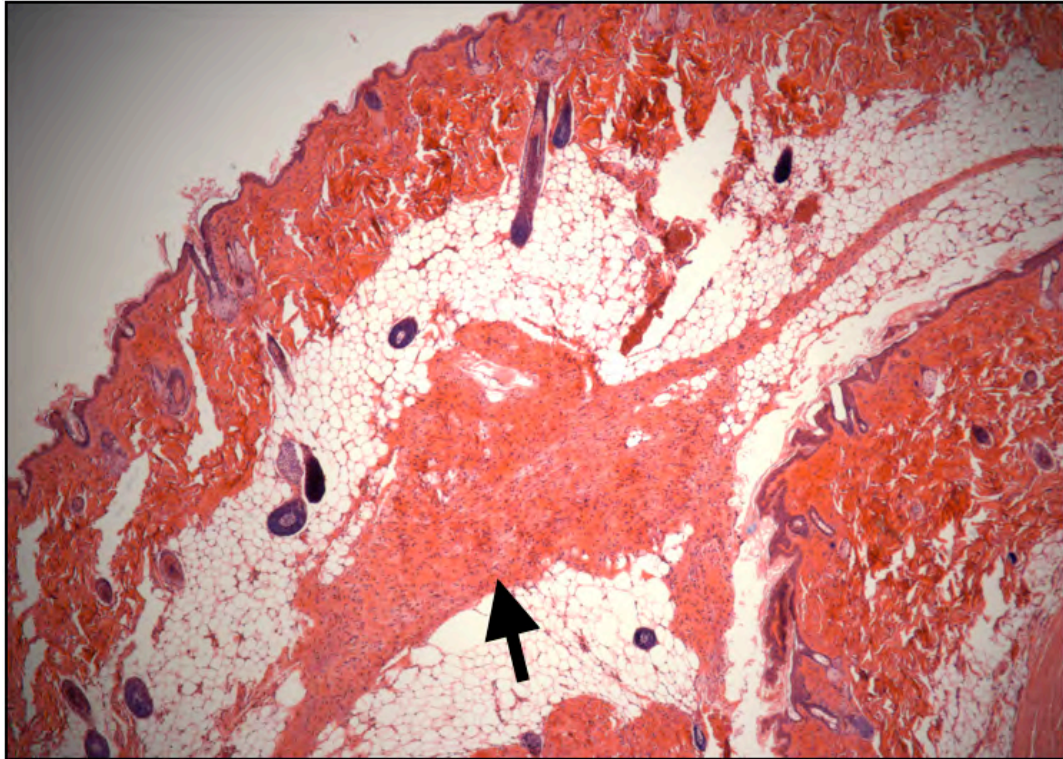


Figure 2.21 *In vivo* TMZ + LY treatment leads to tumor regression in 50% of treated mice. H&E staining of mouse skin paraffin sections shows xenograft loss in TMZ + LY treated mice (4x objective). After gross dissection, strips of skin at the location where the tumor originally formed were fixed and placed in paraffin. When sections were stained with H&E, a small region of scar tissue (arrow) with low cell density remained from the original U87NS xenograft.

The Notch pathway is active in gliomas, and can be inhibited with GSI treatment. In culture, we demonstrated that low concentrations of GSIs alone (1 μM and 5 μM) did not have a significant effect on neurosphere formation. These results are consistent with Wang et al. (2010a), who demonstrated that low concentrations of DAPT or L685,458 only moderately reduced cell growth. However, a recent publication demonstrated that the potent GSI-18 inhibited neurosphere formation and xenograft growth (Fan et al., 2010). GSI-18 is more effective at blocking the Notch pathway and less toxic than DAPT (Yu et al., 2008), which may be the cause of the decreased neurosphere growth with GSI-18 treatment alone. In the presence of higher concentrations of DAPT or LY411,575, a dose-dependent response was observed. At 10 μM , the GSIs had a moderate effect on initial neurosphere formation; however, following drug removal, these cells retained their ability to form secondary neurospheres. It appears that high concentrations of GSIs impede the proliferation of neurosphere cells, but these cells retain the ability to repopulate the culture. On the other hand, we demonstrated that low concentrations of two GSIs, DAPT and LY411,575, enhanced TMZ treatment. Neurosphere recovery was inhibited, and tumor formation was greatly reduced with TMZ + GSI treatment. This response was most drastic when analyzing the secondary neurosphere formation after treatment. TMZ-only treated cultures were capable of robust secondary neurosphere formation, while TMZ + GSI treated cultures were no longer capable of self-renewal, based on their inability to form secondary neurospheres. This supports the hypothesis that TMZ treatment induces a transient cell cycle arrest in neurosphere-initiating cells that block them from forming initial neurospheres, but they can recover and repopulate the

culture. One interesting question is whether the cells that form the original neurospheres after initial TMZ treatment and after recovery are part of the neurosphere-initiating cell population during secondary neurosphere formation. This question could be studied using single-cell, clonal neurosphere assays and lineage tracking experiments. A caveat to the secondary neurosphere formation in the recovery assay is that the cells are not re-counted after dissociation and same number of cells are not plated for each treatment cohort. Therefore, the cells, specifically in DMSO and GSI-only treatments, are not plated at a clonal density. Plating the cells for secondary neurosphere formation at clonal density would also allow the comparison of the percent of neurosphere-initiating cells before and after treatments.

The specific population of cells that is targeted by TMZ + GSI treatment is unknown. Research in the CSC field shows that glioma CSCs exhibit chemo- and radio-resistance (Bao et al., 2006a; Kang and Kang, 2007; Liu et al., 2006). Since Notch activity is associated with glioma CSC function and survival (Jeon et al., 2008; Shih and Holland, 2006), and the cells that survive TMZ-only treatment are capable of self-renewal and tumor initiation, it is probable that the cells targeted by TMZ + GSI treatment possess a CSC phenotype. There is controversy about the current glioma CSC markers, such as CD133 (Gilbert and Ross, 2009), and further progress in the field will be necessary to determine if the TMZ + GSI responsive cells and the CSCs are the same population.

Combined drug treatment with TMZ and GSIs targets tumor-propagating cells and inhibits tumor progression, consistent with the targeting of a CSC population. Our

mouse experiments demonstrate that the addition of GSIs to TMZ treatment can significantly enhance the survival of mice with glioma xenografts. *Ex vivo* treatment of U87NS and U373NS cultures with TMZ + DAPT greatly decreased tumorigenicity. The *in vivo* treatments demonstrated that TMZ-only treatment of pre-existing only temporarily blocked tumor progression. In contrast, 50% of the TMZ + LY chow treated mice had a complete lack of tumor progression, which culminated with the loss of a palpable tumor. In the other 50% of treated mice, there was substantial tumor volume at the time of sacrifice. This variability may result from several sources. In the mice that have a shorter latency the TMZ concentration may not be high enough to induce a cell cycle arrest in all of the cells capable of recovery, which would hinder GSI enhancement. Also, a slight variability in the food consumption between mice in the TMZ + LY chow cohort could explain the heterogeneous response. To circumvent this variability, future experiments will utilize drug administration by gavage to control the LY dosing in each mouse. These observations emphasize the need for personalized treatment and drug dosing. The response to the *in vivo* treatment schedule was analogous to the DAPT post-treatment schedule in the neurosphere recovery assay, which demonstrated that TMZ + GSI treatments permanently blocked culture repopulation and tumor regrowth. These studies suggest a role for TMZ + GSI therapy to reduce recurrences in patients with low tumor burden after surgical resection of the bulk tumor.

The advantage of the subcutaneous xenograft model is it is easy to establish the tumor and quantify tumor volume. It is also more cost effective to quantify tumor burden of subcutaneous xenografts by measure the diameter than the methods to measure

intracranial xenograft tumor burden, such as xenogen cameras and MRI. Due to the constant observation of the tumor burden over a large time period (up to 150 days), it was most practical to begin TMZ + GSI *in vitro* and *in vivo* studies using the subcutaneous xenograft model. The subcutaneous assays were acceptable for this study, because it allows a visible analysis of tumor regrowth after TMZ treatment; however, the weaknesses of testing drug response in the subcutaneous xenograft model include the lack of the tumor microenvironment and the lack of the blood brain barrier. Drug treatments on pre-existing intracranial xenografts would help to overcome these limitations.

Inhibiting the repopulation of the neurosphere cultures is dependent on the sequence of TMZ and GSI treatments. With single doses of DAPT, secondary neurosphere formation was inhibited only when TMZ was administered prior to DAPT (post-treated). Simultaneous treatment of TMZ and DAPT did not significantly inhibit self-renewal. When DAPT was administered before TMZ (pre-treated), secondary neurosphere formation was similar to the TMZ-only treated cells. Pre-treatment also resulted in a higher number of initial neurospheres forming. Although the explanation for this was not examined in further detail, dividing cells are the population normally sensitive to TMZ-induced cytotoxicity, and it is possible that pre-treatment with DAPT slows down the cell cycle enough to decrease the efficiency of TMZ treatment (Jing et al., 2010; Suwanjune et al., 2008). These results were important in determining *in vivo* treatment schedules for mice, and will be valuable to translate this research into the clinic. Since current treatments also include radiotherapy, we ultimately need to add IR to

our TMZ + GSI treatment schedule. Recently, it was found that TMZ and IR are additive when TMZ is administered prior to IR (Chalmers et al., 2009).

An additional benefit of the combined treatment with TMZ + GSI is that lower concentrations of the GSI can be used, and in culture, a single dose of GSI is sufficient to enhance TMZ therapy. These may be important clinical factors, because GSIs can cause cytotoxicity in the gastrointestinal tract (Barten et al., 2006); however, the combination of TMZ with low GSI doses and intermittent treatment schedules will diminish the chances of these side effects (Rizzo et al., 2008). Previous clinical studies in Alzheimer patients demonstrated that achievable GSI (LY450139) levels in the CSF ranged between 0.8 to 2.3 μM , and the half life of the studied GSI was approximately 2.5 hours (Siemers et al., 2005; Siemers et al., 2006). It is also possible that more specific inhibitors, such as anti-Notch receptor antibodies (Wu et al., 2010b), could be utilized in conjunction with TMZ.

Materials and Methods

Cell culture

U373MG (Dr. Larry Recht, Stanford University) and U87MG (ATCC) were cultured in high glucose DMEM (GIBCO, Carlsbad, CA) with supplemented with 1X sodium pyruvate (GIBCO, Carlsbad, CA), 10% fetal bovine serum (Sigma-Aldrich, St. Louis, MO) and 1% penicillin-streptomycin (GIBCO, Carlsbad, CA). To convert the U87MG adherent serum culture into the U87NS neurosphere culture, cells were trypsinized and immediately plated in serum-free, defined medium consisting of DMEM/F12 1:1 (GIBCO, Carlsbad, CA), B27 (GIBCO, Carlsbad, CA), 15 mM HEPES

(GIBCO, Carlsbad, CA), 20 ng/ml EGF (Invitrogen, Carlsbad, CA), and 20 ng/ml bFGF (Invitrogen, Carlsbad, CA) and 1% penicillin-streptomycin (GIBCO, Carlsbad, CA). To convert the U373MG adherent serum culture into the U373NS neurosphere culture, cells were propagated in DMEM/F12 1:1 (GIBCO, Carlsbad, CA) containing 20% FBS until confluent and adherent neurospheres formed. The media was then switched to serum-free, defined media and the cells grew as suspension neurospheres.

The University of Massachusetts Medical School Tissue Bank Core supplied resected brain tumor tissues after surgery. All procedures had Institutional Review Board approval. Tumor tissue was cut into small sections and incubated at 37°C in a 1:1 mixture of defined medium and crude trypsin. The tissue was triturated every 10 minutes to obtain single cell suspensions. After one hour, the cells were washed with PBS and plated in defined medium. The first neurospheres formed within two to three weeks. We classify primary cultures from grade III AAs or IV GBMs and named them AS or GS, respectively (Tom Smith, University of Massachusetts Medical School). The primary neurosphere cultures, GS7-2 and GS7-25, were received from Brent Cochran (Tufts School of Medicine) (Sherry et al., 2009). All primary neurosphere experiments were carried out with cultures between passages 10 and 20.

Glioma cell lines converted to neurosphere cultures and primary GBM lines were grown in serum-free defined medium consisting of DMEM/F12 1:1 (GIBCO, Carlsbad, CA), B27 (GIBCO, Carlsbad, CA), 15 mM HEPES (GIBCO, Carlsbad, CA), 20 ng/ml EGF (Invitrogen, Carlsbad, CA), and 20 ng/ml bFGF (Invitrogen, Carlsbad, CA) and 1% penicillin-streptomycin (GIBCO, Carlsbad, CA). Cultures were passaged using a pH

dissociation method (Sen et al., 2004). There are several methods of neurosphere dissociation. The most common means of obtaining single cell suspensions from neurospheres are mechanical and enzymatic dissociations. Our lab has had greater success in maintaining primary cultures through multiple passages when neurospheres are dissociated by brief exposure to a strong alkaline solution and gentle trituration (Sen et al., 2004). The alkaline solution, pH 11.6, is prepared by adding 1 ml of 1.0 N NaOH to 20 ml of defined neurosphere media. The neurospheres are pelleted and resuspended in 200 μ l of unaltered defined media, followed by the addition of 200 μ l of the alkaline solution. The neurospheres are then gently pipetted, and incubated at room temperature for 2 min. The neurospheres are then triturated a second time, incubated at room temperature for 3 min, triturated a third time, and incubated an additional 2 min. The neurospheres are triturated for a final time, and then 200 μ l of an acidic solution (pH 1.7; 1 ml of 1.0 N HCl in 20 ml of defined media) is added to return the solution to a neutral pH. This pH dissociation method is less harsh on the cells than traditional mechanical dissociation and does not affect the stem cell properties of the culture. Using the pH dissociation method, we have successfully established 14 primary neurosphere cultures from 18 received glioma tissues (Table 1.1).

Drug treatment

TMZ and N-[N-(3,5-difluorophenacetyl)-L-alanyl]-5-phenylglycine t-butyl ester (DAPT) were purchased from Sigma-Aldrich (St. Louis, MO). N-2((2S)-2-(3,5-difluorophenyl)-2-hydroxyethanoyl)-N1-((7S)-5-methyl-6-oxo-6,7-dihydro-5H-dibenzo

[b,d]azepin-7-yl)-L-alaninamide (LY411,575) (Fauq et al., 2007) was a gift from Lisa Minter and Barbara Osborne (University of Massachusetts, Amherst).

TMZ concentrations for each culture were selected based on two factors: 1) at least an 80% decrease of initial neurosphere formation; and 2) the ability of the culture to recover after treatment and form secondary neurospheres. DAPT and LY concentrations were chosen for each culture based on the decrease in Hes1 and Hey1 expression. RNA was isolated from the cultures 48 hours after DAPT treatment, and Hes1 and Hey1 cDNA expression levels were analyzed by PCR or qPCR.

RT-PCR and RT-qPCR

Neurosphere cultures were pelleted and tumor tissues from subcutaneous xenografts were broken into a powder using a BioPulverizer (Biospec Products, Inc., Bartlesville, OK). RNA was isolated from neurosphere cultures and frozen tumor samples using TRIzol Reagent (Invitrogen, Carlsbad, CA) following the manufacturer's protocol. RNA was treated with DNase I, Amplification Grade (Invitrogen, Carlsbad, CA). cDNA was made using the SuperScript II Reverse Transcription (RT) Kit with Oligo(dT)₁₂₋₁₈ primers (Invitrogen, Carlsbad, CA), followed by a 20 minute incubation at 37 °C with RNaseH. PCR was carried out using Platinum Taq DNA Polymerase, following the manufacturer's protocol (Invitrogen, Carlsbad, CA). Real time qPCR was carried out using QuantiTect SYBR Green (QIAGEN, Valencia, CA). Hes1 and β -Actin primers were developed using Primer3 (Rozen and Skaletsky, 2000), while previously published primer sequences include primers for Hey1 (Osipo et al., 2008), Notch1 (Lefort

et al., 2007), Notch2 (O'Neill et al., 2007), Notch3 (Buchler et al., 2005) and Notch4 (Buchler et al., 2005) (Table 2.3). The RT-PCR products were analyzed on 2% agarose gels. Quantification of band intensity for DAPT treated lines was determined using ImageJ (Rasband, 1997-2004). cDNA levels for qRT-PCR products were calculated using the PFAFFL method (Pfaffl, 2001). p53 transcripts were amplified to analyze the sequences for mutation as previously described (Mihaliak et al., 2010). Briefly, mRNA was extracted using a QuickPrep micro mRNA purification kit (GE Healthcare, Piscataway, NJ) and was incubated for 2 h at 37 °C with 1 µl of Oligo(dT)12–18 (500 µg/ml), 4 µl of 5x First strand cDNA buffer, 2 µl of 0.1 mM DTT and 1 µl of 10 mM dNTP mix. SuperScriptII Reverse Transcriptase (1 µl) was added and incubated for 50 min at 42 °C, followed by heat inactivation for 15 min at 70 °C. The cDNA was amplified using Platinum Taq DNA Polymerase (Invitrogen Carlsbad, CA). The two primer sets were used for amplification and sequencing of the human p53 cDNA (Table 2.3). The PCR products were analyzed in both directions using automated DNA sequencing (GENEWIZ, South Plainfield, NJ).

Neurosphere recovery and secondary neurosphere assays

Neurosphere cultures were dissociated to single cell suspensions by pH dissociation followed by filtration through 40 µm filters. For the neurosphere assay, 3,000 cells/ml of defined medium were seeded in 6-well plates. Immediately after plating, cells were treated with DMSO (Research Organics, Cleveland, OH) carrier control, TMZ-only, DAPT-only, or TMZ + DAPT. Additional DAPT was added on days

Table 2.3 List of PCR primer sequences

Gene	Forward primer (5' - 3')	Reverse primer (5' - 3')
Hes1	CTAAACTCCCCAACCCACCT	AAGGCGCAATCCAATATGAACATAT
Hey1	AGCTCCTCGGACAGCGAGCTG	TACCAGCCTTCTCAGCTCAGACA
Notch1	GAACCAATACAACCCTCTGC	AGTCATCATCTGGGACAGG
Notch2	CACAGAGGCTGGGAAAGGATGATA	GGCCACCTGAAGGGAAGCACATA
Notch3	AGATTCTCATCCGAAACCGCTCTA	GGGGTCTCCTCCTTGCTATCCTG
Notch4	GCGGAGGCAGGGTCTCAACGGATG	AGGAGGCGGGATCGGAATGT
p53	ATGGAGGAGCCGCAGTCAGAT AAGGAAATTTGCGTGTGGAGT	TGCGCCGGTCTCTCCAGGAC CAGTCGGAGTCAGGCCCTTCT
β -Actin (RT-PCR)	GCTCGTCGACAACGGCT	CAAACATGATCTGGGTCATCTTCTC
β -Actin (qRT-PCR)	TTGCCGACAGGATGCAGAAGGA	AGGTGGACAGCGAGGCCAGGAT

2 and 4. Neurospheres consisting of 10 or more cells were counted under a light microscope on day 7 for the converted cell lines. Primary lines have a slightly longer doubling time and were counted on day 10. After counting the neurospheres from the initial treatment, 2 ml of fresh defined medium was added to each well. DAPT was also added once more to the DAPT-only and TMZ + DAPT samples, and the cells were incubated for an additional 7 or 10 days. Neurospheres from the recovery period were counted on day 14 or day 20. To analyze secondary neurosphere formation, cells were collected, pelleted and dissociated to a single cell suspension by the pH method (Sen et al., 2004). DMSO and DAPT-only samples were split at 1:30 and reseeded into 6-well plates with 2 ml of defined medium, while TMZ-only and TMZ + DAPT were split at 1:1, and all cells were reseeded into 6-well plates with 2 ml of defined medium. The number of secondary neurospheres formed by converted cell lines and primary cultures were counted on day 21 or day 30, respectively. All recovery assays were repeated with a minimum of 6 data sets. For the LY experiments, LY411,575 was administered in place of DAPT using the same regimen.

For the samples labeled 'pre-treat', a single dose of DAPT was administered when the cells were plated, and then TMZ was added to the medium 24 hours later. For the 'co-treat' samples, single doses of TMZ and DAPT were added simultaneously when the cells were plated. Finally, samples labeled 'post-treat' were treated with TMZ, and then DAPT was added 24 hours later.

Cell proliferation assay

To analyze the effect of drug treatment on the adherent lines, U87MG and U373MG were plated in 6-well plates at 3,000 cells/ml in 2 ml DMEM, supplemented with 10% fetal bovine serum and 1% penicillin-streptomycin. Cultures were treated with DMSO-only, DAPT-only (1 μ M for U87MG and 5 μ M for U373MG), TMZ-only (200 μ M) or TMZ + DAPT. As described for the neurosphere recovery assay, TMZ was administered on day 0, and DAPT was administered on days 0, 2, 4, and 7. Cultures were trypsinized on day 7, 14 and 21 to count the total number of live cells using trypan blue. On days 7 and 14, cells were reseeded in fresh 6-well plates. DMSO and DAPT-only treated cultures were split 1:10 due to high levels of proliferation, while TMZ-only and TMZ + DAPT treated cultures were split 1:1 and all cells were re-plated.

Virus infections

NICD-pMIG (Pui et al., 1999) or pMIG vectors were co-transfected with retrovirus envelope and gag-pol vectors into HEK293T cells, with FuGENE 6 (Roche Applied Science, Indianapolis, IN). Retrovirus was collected after 48 hours. Neurosphere cultures were infected in non-coated bacterial dishes to avoid the cells becoming adherent in the presence of serum. Cells were incubated with virus and 8 μ g/ml polybrene (Sigma-Aldrich, St. Louis, MO) at 37°C for 6 hours. GFP-positive cells were sorted on a FACS Aria (BD Biosciences, Franklin Lakes, NJ).

Subcutaneous xenografts: ex vivo drug treatment

U87NS and U373NS neurospheres were dissociated and 2.5×10^4 cells/ml were plated in defined media and treated with DMSO, TMZ-only (200 μ M), DAPT-only (1 μ M or 5 μ M), or TMZ + DAPT as described for recovery assays. After 7 days, 2.5×10^5 or 3×10^6 live cells were counted using trypan blue and re-suspended in 100 μ l PBS. Cells were subcutaneously injected into the flanks of nude mice. Mice were monitored for tumor formation for up to 120 days post-injection and euthanized when tumors reached volumes of 1.5 to 2 cm^3 .

Subcutaneous xenografts: in vivo drug treatment

For the *in vivo* experiments, we used LY411,575 incorporated into 7012 Teklad LM-485 rodent chow (LY chow) at a concentration of 0.0275 g/kg (Harlan Laboratories Inc, Madison, WI) (Samon et al., 2008). U87NS cells (1×10^6) re-suspended in 100 μ l PBS were subcutaneously injected into the flanks of male nude mice. When the tumor reached approximately 150 mm^3 (volume = $(\frac{3}{4}) \times (\pi) \times (\text{length}/2) \times (\text{width}/2)^2$), we began the following treatments: 1) DMSO control: two days of 100 μ l DMSO/PBS (1:1) intraperitoneal (i.p.) injections; 2) TMZ-only: i.p. injections of TMZ (20 mg/kg) in 100 μ l DMSO/PBS on days one and two; 3) LY chow-only: two days of 100 μ l DMSO/PBS i.p. injections. The mice were fed LY chow from day 3 to 12; 4) TMZ + LY chow: i.p. injections of TMZ (20 mg/kg) in 100 μ l DMSO/PBS on days one and two. The mice were fed LY chow from day 3 to 12. Mice were observed for up to 150 days and euthanized when the tumor reached 1.5 to 2 cm.

CHAPTER III:

**Combined Treatment with Temozolomide and Gamma-Secretase Inhibitors Targets
Glioma-Propagating Cells by Inducing Senescence**

Parts of this chapter represent work submitted as:

Candace A. Gilbert, Yulian P. Ramirez, Jessica L. Weatherbee, Christ MacKay, Evelyn A. Kurt-Jones, and Alonzo H. Ross. Enhancing Temozolomide Treatment by Inhibition of Notch Signaling Induces Senescence in Gliomas. Manuscript in preparation.

Contributions:

Yulian Ramirez conducted all the IHC staining and photographs for Ki67 and assisted in counting. She also provided intellectual guidance and problem shooting.

Jessica Weatherbee provided assistance with cell culture set up for the propidium iodide/cell death experiments.

Christine St. Pierre assisted and provided training for the confocal experiments.

Evelyn Kurt-Jones provided guidance for the immunology aspect of the project.

Alonzo Ross provided intellectual support for the project, experimental ideas and editing.

CHAPTER III:

Combined Treatment with Temozolomide and Gamma-Secretase Inhibitors Targets Glioma-Propagating Cells by Inducing Senescence

Glioma cultures contain a population of cells that escape TMZ-induced cytotoxicity. This population includes neurosphere-initiating and tumor-propagating cells. We have demonstrated that blocking the Notch pathway with low concentrations of GSIs has a minimal affect on neurosphere formation and tumor formation, but when combined with TMZ, they greatly enhance TMZ efficacy. The combined TMZ + GSI treatment targets the TMZ-resistant cells and inhibits both neurosphere recovery and tumor growth. After demonstrating the success of TMZ + GSI treatments, our laboratory was interested in studying the biological mechanism of combined treatment with TMZ + GSIs.

The Notch pathway was previously implicated in regulating the switch between a reversible quiescent state and an irreversible senescent state (Sang et al., 2008). We have demonstrated that TMZ induces a temporary cell cycle arrest in neurosphere-initiating and tumor-propagating cells (Mihaliak et al., 2010) and that TMZ + GSI treatment enhances the TMZ efficiency when administered after TMZ treatment, in a schedule-dependent manner (Gilbert et al., 2010). Together, these data demonstrate that the induction of a transient cell cycle arrest by TMZ treatment must precede GSI administration to enhance the therapy's efficiency. This suggests that TMZ and GSI treatment inhibits neurosphere recovery and tumor progression of glioma cultures

through therapy-induced senescence (TIS). In addition to arresting tumor cell growth, TIS has been shown to stimulate tumor clearance. This occurs due to the secretion of secreted pro-inflammatory proteins by senescent cells, which are part of the SASP (Coppe et al., 2008; Freund et al., 2010). This can activate an innate immune response and result in tumor clearance (Xue et al., 2007).

In this study, we analyze the biological mechanism of TMZ + GSI treatment *in vitro* and *in vivo*. We found that TMZ + GSI treatment does not increase cell death in neurosphere cultures. Instead, when glioma cells are treated with TMZ + GSI the majority of the cultures enters into a permanent senescent state. The cells show characteristics of senescence, including a temporary growth arrest and SA- β -galactosidase expression. These data demonstrate that TMZ + GSI treatment induces a permanent growth arrest that blocks regrowth of glioma cultures and xenografts. In addition, we demonstrate that *in vitro* TMZ + GSI treatment stimulates macrophage phagocytosis of the neurosphere cells. This treatment has the potential to greatly reduce glioma recurrence in the clinic by TIS.

Results

TMZ + DAPT treatment does not increase cell death in neurosphere cultures

PI staining was used to analyze cell death in U87NS cultures after drug treatment. Control neurosphere samples treated with DMSO had a baseline PI⁺ population of $14.2 \pm 4.0\%$ on day 3 of the neurosphere recovery assay. There was no significant difference observed on day 3 between the DMSO control and the other treatments (Fig. 3.1 A and

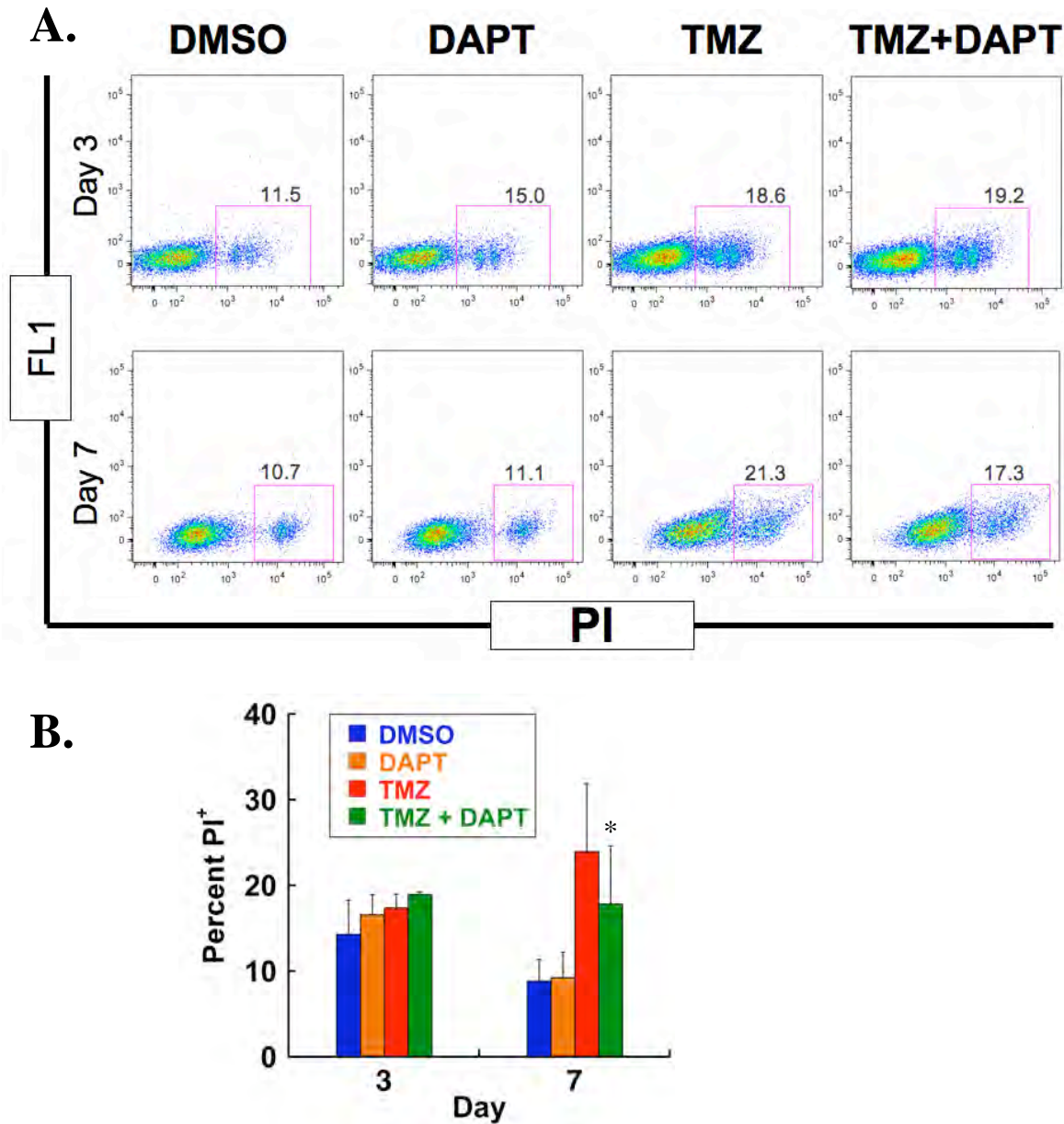


Figure 3.1 **TMZ + DAPT treatment does not increase cell death.** A) Representative dot plots for PI-uptake 3 days and 7 days after treatment of the U87NS neurosphere culture. Events are gated for PI⁺ expression against the unstained FL1 channel to select for the dead cell population capable of PI-uptake. B) Quantification of the PI⁺ population in the U87NS treated cultures on day 3 and day 7. (mean \pm SD; n = 6). There is no difference between the different treatments on day 3. On day 7, TMZ-only and TMZ + DAPT treated cultures have higher cell death than the controls, but there is a significant decrease in the PI⁺ population from the TMZ-only to the TMZ + DAPT treated populations. *, P < 0.01

B). The average percentage of PI⁺ cells in DAPT-only, TMZ-only, and TMZ + DAPT treated cultures was $16.7 \pm 2.3\%$, $17.5 \pm 1.6\%$, and $19.0 \pm 0.3\%$ (Fig. 3.1 A). On day 7, the DMSO and DAPT-only treatments were similar with $8.9 \pm 2.5\%$ and $9.3 \pm 3.1\%$, respectively. A 2.7-fold increase ($P < 0.01$) in cell death was observed in the TMZ-only treated cultures on day 7, compared to the DMSO controls. The PI⁺ population in the TMZ-only treated U87NS culture was $24.0 \pm 7.9\%$. Interestingly, the PI⁺ population for the TMZ + DAPT treated neurospheres was only $17.9 \pm 6.8\%$, which was significantly less than the cell death observed in the TMZ-only treated culture ($P < 0.01$).

SA- β -galactosidase expression is increased in TMZ + DAPT treated cultures

To determine if the inhibition of neurosphere recovery in TMZ + DAPT treated cultures is due to an induction of senescence, SA- β -galactosidase expression was analyzed in U87NS and U373NS treated cultures on day 7 and day 21 (Fig. 3.2 A and B). On day 7, DMSO and DAPT-only treated U87NS samples had a minimal number of cells with SA- β -galactosidase expression, $2.2 \pm 0.9\%$ and $2.4 \pm 1.0\%$, respectively (Fig. 3.3 A). TMZ-only treated U87NS cells stained $36.3 \pm 11.1\%$ SA- β -galactosidase positive on day 7 (Fig 3.3 A). TMZ + DAPT treated neurospheres showed a 1.8-fold increase ($P < 0.00001$) of SA- β -galactosidase expression on day 7, with $64.0 \pm 9.5\%$. This trend was also observed in the U373NS treated culture on day 7 (Fig. 3.2 B). U373NS DMSO and DAPT-only treated cultures had $1.9 \pm 1.8\%$ and $1.9 \pm 1.7\%$, respectively (Fig. 3.3 B). TMZ-only treatment increased SA- β -galactosidase expression, but SA- β -galactosidase expression in TMZ + DAPT treated cultures was 1.7 fold greater ($P < 0.0001$). U373NS

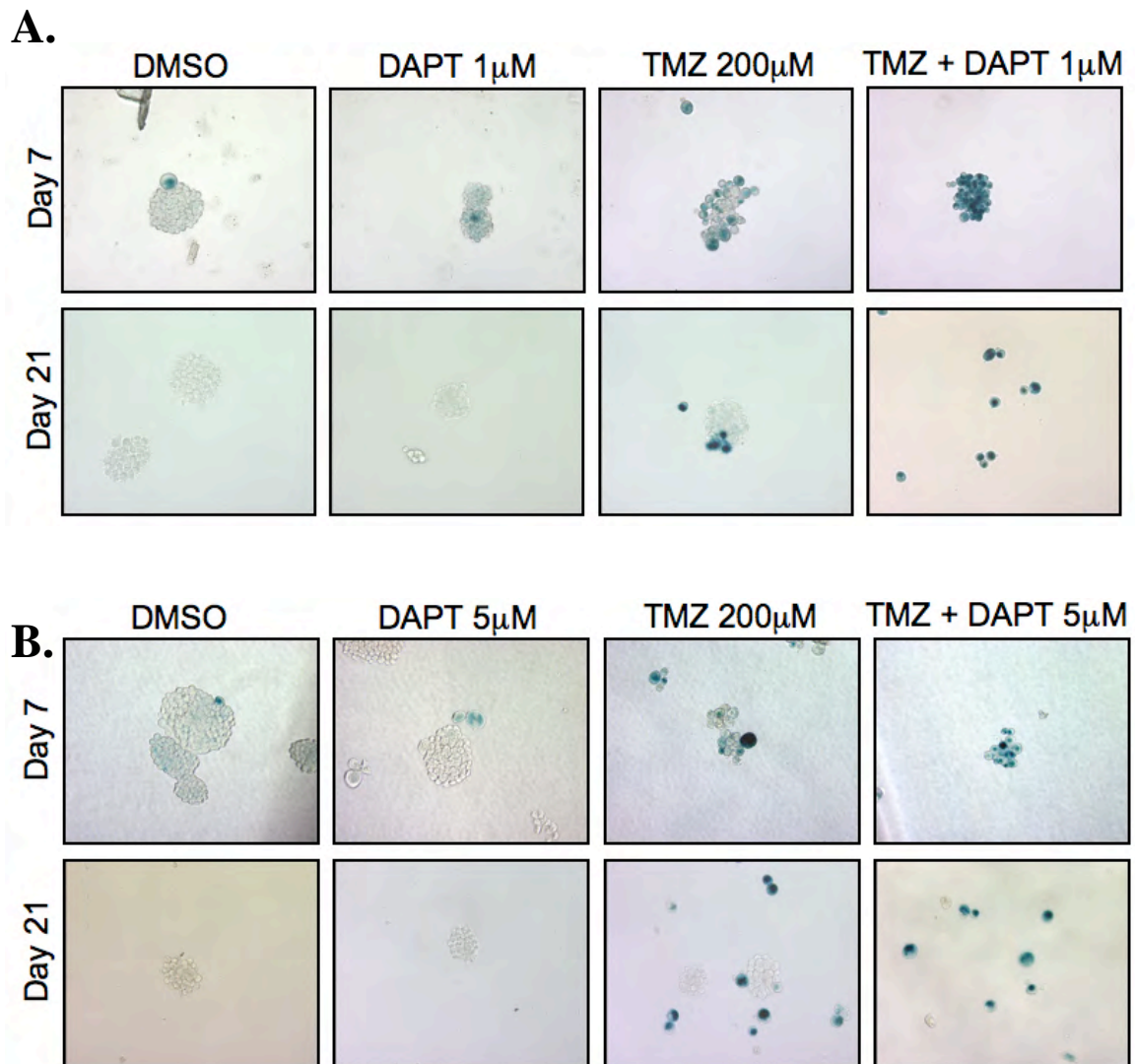


Figure 3.2 **TMZ + DAPT induces SA- β -galactosidase in neurosphere cultures.** Senescence was analyzed using SA- β -galactosidase expression in A) U87NS and B) U373NS cultures with DMSO, DAPT-only, TMZ-only, and TMZ + DAPT treatments. SA- β -galactosidase positive cells stain blue. DMSO and DAPT treated cultures have minimal SA- β -galactosidase positive on both day 7 and day 21. TMZ-only and TMZ + DAPT treated cultures have an initial induction of SA- β -galactosidase positive on day 7. However, after secondary neurosphere formation, TMZ-only samples on day 21 have a reduced number of SA- β -galactosidase positive, and there are SA- β -galactosidase negative neurospheres present. In contrast, the TMZ + DAPT samples on day 21 consist largely of single cell that are SA- β -galactosidase positive.

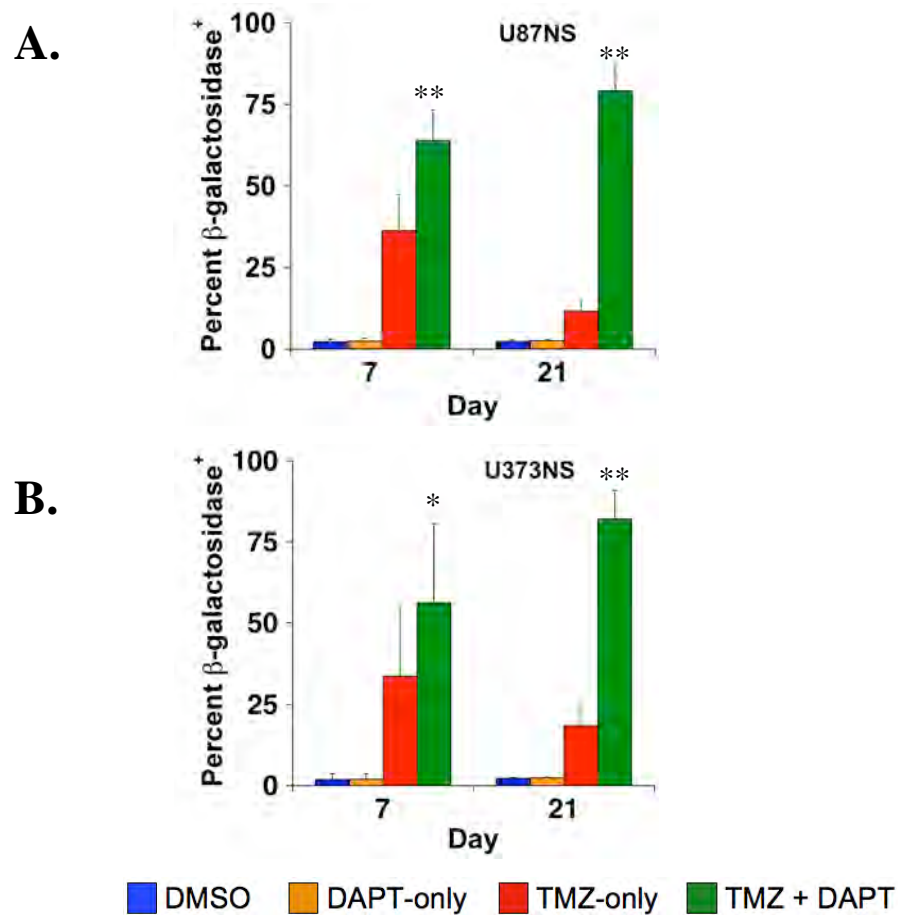


Figure 3.3 **TMZ + DAPT induces SA- β -galactosidase in U87NS and U373NS cultures.** SA- β -galactosidase expression was quantified for A) U87NS and B) U373NS cultures with DMSO, DAPT-only, TMZ-only, and TMZ + DAPT treatments. DMSO and DAPT treated cultures have minimal levels of SA- β -galactosidase on both day 7 and day 21. TMZ-only and TMZ + DAPT treated cultures have an initial induction of SA- β -galactosidase positive on day 7. However, after secondary neurosphere formation, TMZ-only samples on day 21 have a reduced percentage of SA- β -galactosidase positive cells, while the TMZ + DAPT samples remain mostly SA- β -galactosidase positive. In both U87NS and U373NS cultures, the TMZ + DAPT treatments induce a significantly greater percentage of SA- β -galactosidase positive cells compared to the TMZ-only treatments on day 7 and 21. (mean \pm SD) *, $P < 0.0001$; **, $P < 0.00001$

TMZ-only treated cultures showed $33.8 \pm 22.2\%$ SA- β -galactosidase expression and TMZ + DAPT treated cultures showed $56.3 \pm 24.4\%$.

To analyze the long-term effects of the drug treatments, neurosphere cultures were dissociated on day 14, and SA- β -galactosidase expression was analyzed in secondary neurospheres on day 21. The percent of SA- β -galactosidase-positive cells in DMSO and DAPT-only treated U87NS cultures remained low with only $2.3 \pm 0.5\%$ and $2.6 \pm 0.3\%$, respectively (Fig. 3.3 A). Neurospheres from day 21 TMZ-only treated cultures demonstrated a decrease in the overall SA- β -galactosidase expression compared to day 7 samples (Fig. 3.2 and 3.3). In U87NS cultures, the percentage of SA- β -galactosidase positive cells dropped to $11.6 \pm 3.4\%$, demonstrating that the cells negative for SA- β -galactosidase on day 7 were capable of repopulating the culture (Fig. 3.3 A). In contrast, SA- β -galactosidase expression in the TMZ + DAPT treated neurospheres remained high and was 6.8-fold greater ($P < 0.00001$) than expression in the TMZ-only treated culture. TMZ + DAPT treated samples on day 21 were $79.2 \pm 7.6\%$ SA- β -galactosidase positive. Similarly, U373NS showed minimal SA- β -galactosidase at day 21 for DMSO and DAPT-only samples, $2.3 \pm 0.3\%$ and $2.4 \pm 0.3\%$, respectively (Fig. 3.3 B). SA- β -galactosidase expression decreased in the TMZ-only treated U373NS samples on day 21, with only $18.5 \pm 6.6\%$ positive, but high expression persisted in the TMZ + DAPT U373NS samples, with $82.1 \pm 8.8\%$. At day 21, SA- β -galactosidase expression in TMZ + DAPT treated U373NS cultures was 4.4-fold greater ($P < 0.00001$) than the expression in TMZ-only treated cultures. This demonstrates that TMZ + DAPT treatment induces a persistent SA- β -galactosidase expression.

We previously demonstrated that endogenous expression of the constitutively active NICD attenuates the effects of TMZ + DAPT treatment in neurosphere cultures (Gilbert et al., 2010). To determine if NICD expression will also block an increase in SA- β -galactosidase expression, the U87NS-pMIG and U87NS-NICD cultures were administered DMSO, DAPT-only, TMZ-only and TMZ + DAPT treatments. In the DMSO treated controls, the baseline expression of SA- β -galactosidase on day 7 increased by 4.0-fold ($P < 0.01$), from $3.3 \pm 1.3\%$ in the U87NS-pMIG cultures to $13.2 \pm 5.2\%$ in the U87NS-NICD cultures (Fig. 3.4). A 3.8-fold increase ($P < 0.01$) was also observed in the DAPT-treated cultures, from $3.3 \pm 1.3\%$ in the U87NS-pMIG cultures to $12.5 \pm 6.7\%$ in the U87NS-NICD cultures. This data corresponds with a recent publication demonstrating that Notch overexpression can induce senescence (Venkatesh et al., 2011). Expression of SA- β -galactosidase in the U87NS-pMIG culture was $47.9 \pm 2.5\%$ positive in the TMZ-only treated cultures and $77.1 \pm 5.8\%$ positive in the TMZ + DAPT treated cultures (Fig. 3.4). While the U87NS-pMIG culture displayed a 1.6-fold ($P < 0.00001$) increase in SA- β -galactosidase when treated with TMZ + DAPT compared to TMZ-only, no significant fold increase of SA- β -galactosidase expression was observed between the U87NS-NICD TMZ-only and TMZ + DAPT treated cultures, with $62.1 \pm 6.9\%$ and $69.3 \pm 8.1\%$ positive, respectively. Although NICD expression increases the baseline levels of SA- β -galactosidase expression, the U87NS-NICD cells did not show an increase of SA- β -galactosidase between TMZ-only and TMZ + DAPT treatments. Since NICD-expression cultures are capable of robust secondary neurosphere formation after TMZ + DAPT treatment, this suggests that Notch signaling protects the neurosphere-initiating

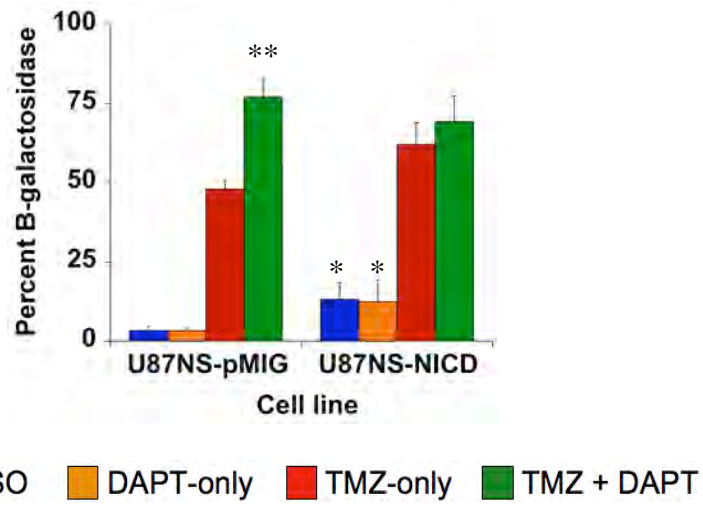


Figure 3.4 **SA- β -galactosidase in the U87NS NICD-expressing culture** SA- β -galactosidase expression was analyzed on day 7 after DMSO, DAPT-only, TMZ-only, and TMZ + DAPT treatments NICD-expressing U87NS culture displays an increased SA- β -galactosidase expression ($P < 0.01$) in the control treatments compared to the U87NS-pMIG cell line. SA- β -galactosidase expression in the U87-pMIG is induced in TMZ-only and further enhanced in TMZ + DAPT treatments; however, there is no difference between TMZ-only and TMZ + DAPT treated samples in the U87NS-NICD culture. (mean \pm SD). *, $P < 0.01$; **, $P < 0.0001$

cells that enter the TMZ-induced transient cell cycle arrest from switching to the permanent senescent state after GSI treatment.

TMZ + DAPT-induced senescence is schedule-dependent in vitro

The response of neurospheres to TMZ + DAPT is dependent on the drug treatment schedule (Gilbert et al., 2010) (Fig. 2.14). We previously demonstrated that pre-treatment with DAPT, followed 24 hours later by TMZ treatment, or co-treatment with single doses of TMZ and DAPT, do not inhibit secondary neurosphere formation. In contrast, the post-treatment schedule, which consists of initial TMZ treatment, followed by DAPT treatment 24 hours afterwards, has a large affect and inhibits secondary neurosphere formation (Gilbert et al., 2010). Consistent with the neurosphere formation on day 7, TMZ-only, pre-treatment with DAPT, and TMZ + DAPT co-treatment has similar SA- β -galactosidase expression levels, while post-treatment with DAPT shows an increase in SA- β -galactosidase (Fig. 3.5 and 3.6). For SA- β -galactosidase expression in U87NS cultures, TMZ-only treatment resulted in $36.3 \pm 8.2\%$ positive, pre-treatment resulted in $50.5 \pm 7.5\%$ positive, co-treatment resulted in $59.5 \pm 3.8\%$ positive and post-treatment resulted in $79.1 \pm 2.4\%$ positive (Fig. 3.7 A). The pre-treatment SA- β -galactosidase expression was not significantly greater than expression levels observed after TMZ-only treatment. SA- β -galactosidase expression in U87NS co-treated samples was 1.6-fold greater ($P < 0.01$), while expression in the post-treated samples was 2.2-fold greater ($P < 0.01$). In U373NS treated cultures, levels of SA- β -galactosidase positive cells on day 7 was $55.4 \pm 3.5\%$ for TMZ-only, $58.3 \pm 3.5\%$ for pre-treatment, $61.2 \pm$

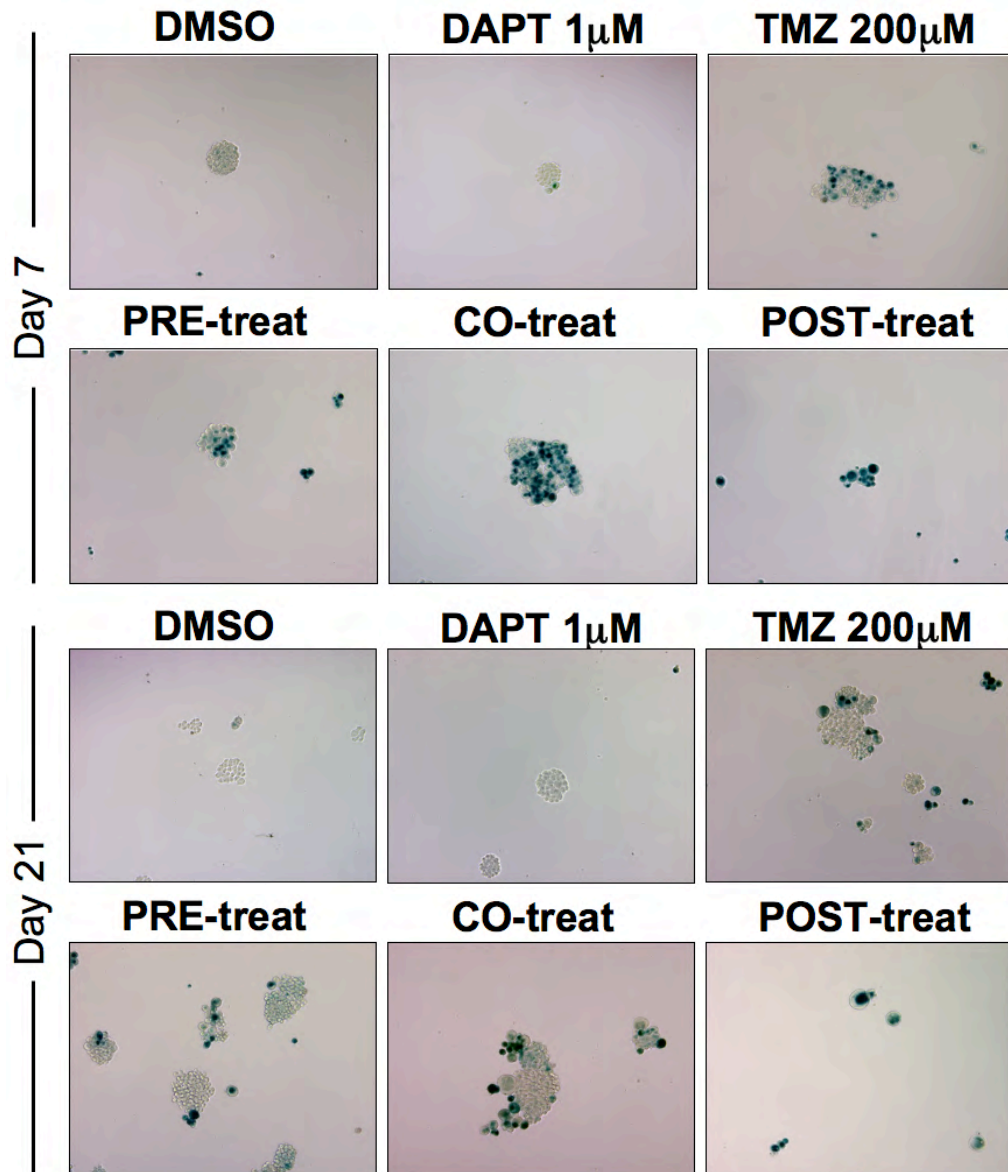


Figure 3.5 Therapy-induced senescence in the neurosphere assay schedule treatment is unique to DAPT post-treatment in U87NS. Senescence was analyzed using SA-β-galactosidase expression in U87NS cultures treated with TMZ + DAPT treatment schedules. SA-β-galactosidase positive cells stain blue. DMSO and DAPT treated cultures have minimal SA-β-galactosidase positive cells on both day 7 and day 21. TMZ-only and pre-treated, co-treated and post-treated cultures have an initial induction of SA-β-galactosidase on day 7. However, after secondary neurosphere formation, day 21 samples for TMZ-only, pre-treatment, and co-treatment have a reduced number of SA-β-galactosidase positive cells, and neurospheres are present that are the majority SA-β-galactosidase negative. In contrast, the DAPT post-treated samples on day 21 consist largely of single cell that are SA-β-galactosidase positive.

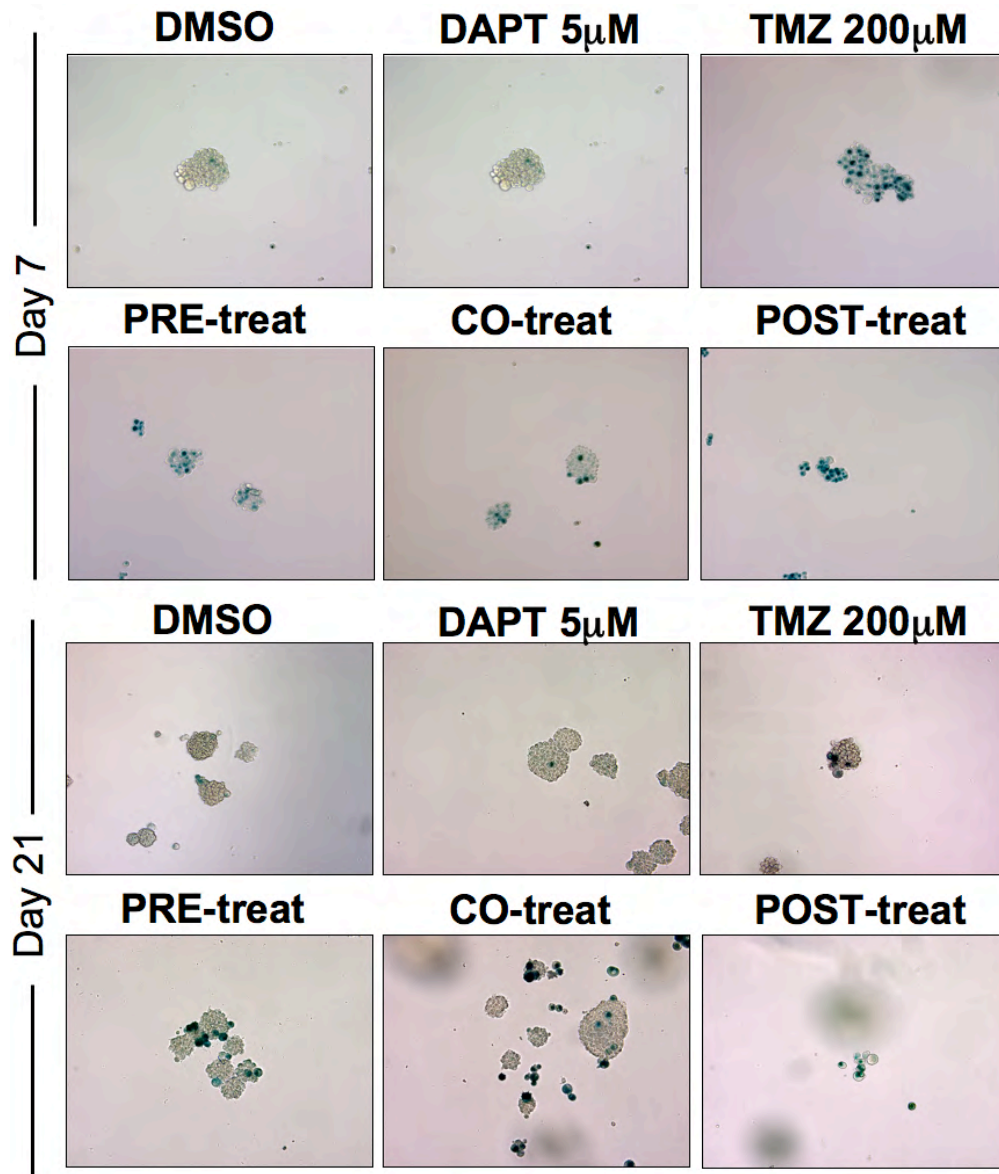


Figure 3.6 Therapy-induced senescence in the neurosphere assay schedule treatment is unique to DAPT post-treatment in U373NS. Senescence was analyzed using SA-β-galactosidase expression in U373NS cultures treated with TMZ + DAPT treatment schedules. SA-β-galactosidase positive cells stain blue. DMSO and DAPT treated cultures have minimal SA-β-galactosidase positive cells on both day 7 and day 21. TMZ-only and pre-treated, co-treated and post-treated cultures have an initial induction of SA-β-galactosidase on day 7. However, after secondary neurosphere formation, day 21 samples for TMZ-only, pre-treatment, and co-treatment have a reduced number of SA-β-galactosidase positive cells, and neurospheres are present that are the majority SA-β-galactosidase negative. In contrast, the DAPT post-treated samples on day 21 consist largely of single cell that are SA-β-galactosidase positive.

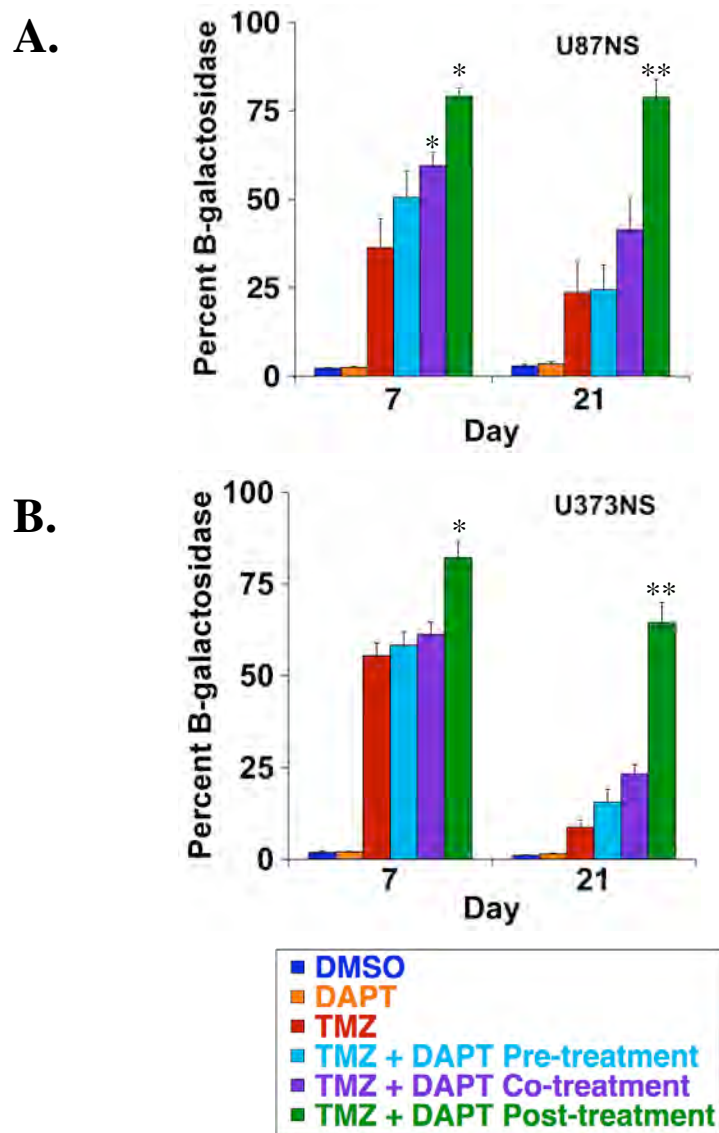


Figure 3.7 **Therapy-induced senescence in the neurosphere assay schedule treatment is unique to DAPT post-treatment.** SA- β -galactosidase expression was quantified in A) U87NS and B) U373NS cultures treated with TMZ + DAPT treatment schedules. TMZ-only and pre-treated, co-treated and post-treated cultures have an initial induction of SA- β -galactosidase on day 7. However, after secondary neurosphere formation, day 21 samples for TMZ-only, pre-treatment, and co-treatment have a reduced number of SA- β -galactosidase positive. In contrast, the DAPT post-treated samples on day 21 maintain the higher percentage of SA- β -galactosidase positive cells. Compared to TMZ-only samples, DAPT post-treated samples consistently showed significantly greater levels of SA- β -galactosidase expression. *, $P < 0.01$. **, $P < 0.001$.

3.5% for co-treatment, and $82.2 \pm 4.5\%$ for post-treatment (Fig. 3.7 B). In the day 7 U373NS schedule treatment samples, only the post-treated samples demonstrated increased SA- β -galactosidase expression compared to TMZ-only treatment, with a 1.4-fold increase ($P < 0.01$). By day 21, SA- β -galactosidase expression decreased in TMZ-only, pre-treatment, and co-treatment. U87NS TMZ-only showed $23.6 \pm 8.7\%$ positive, pre-treatment showed $24.4 \pm 7.1\%$ positive, and co-treatment showed $41.5 \pm 9.0\%$ positive (Fig. 3.7 A). The percent SA- β -galactosidase positive in U373NS demonstrated the same trend, TMZ-only, $8.8 \pm 1.9\%$, pre-treatment, $15.6 \pm 3.6\%$, and co-treatment, $23.3 \pm 2.5\%$ (Fig. 3.7 B). However, the samples administered the post-treatment schedule maintained high levels of SA- β -galactosidase expression at day 21. Post-treatment resulted in $78.8 \pm 5.0\%$ positive in U87NS secondary neurospheres (Fig. 3.7 A) and $64.5 \pm 5.4\%$ in U373NS secondary neurospheres on day 21 (Fig. 3.7 B). SA- β -galactosidase expression in post-treated samples was 3.3-fold ($P < 0.001$) and 7.3-fold ($P < 0.001$) greater than SA- β -galactosidase in the TMZ-only treated samples for U87NS and U373NS cultures, respectively.

TMZ + LY treated xenografts have decreased proliferation

Ki67 staining was used to determine the number of proliferating cells in the subcutaneous U87NS xenografts after *in vivo* treatment. Decreased proliferation is expected based on the increase in the percent of senescent cells. In tumors harvested on 13 days after the beginning of treatment, there was no significant difference of Ki67 expression between the control DMSO and LY chow-only groups (Fig. 3.8 and 3.9).

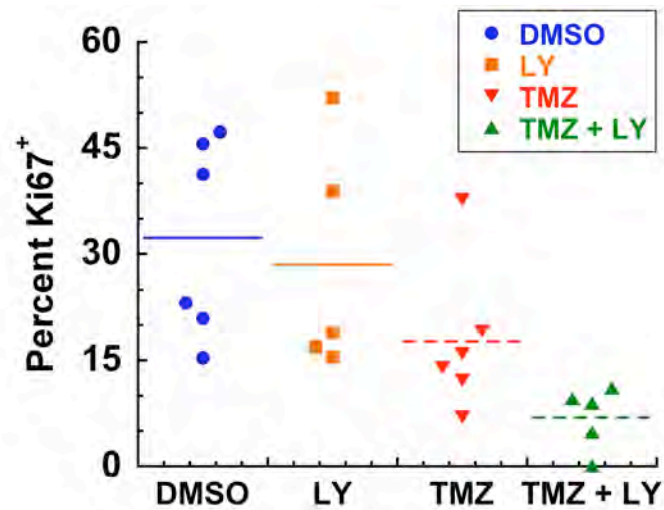


Figure 3.8 **Ki67 expression decreases in TMZ + LY treated U87NS xenografts.** Ki67 expression was analyzed to determine the levels of proliferation in U87NS *in vivo* treated xenografts. Quantification of percent Ki67⁺ demonstrates a range of Ki67 levels for each treatment cohort. Each point represents the average Ki67 expression from five fields for an individual tumor. DMSO and LY chow-only mice have the highest percent of Ki67⁺ cells. TMZ-treatment decreased Ki67 staining in the majority of the treated mice, while TMZ + LY chow cohorts had the greatest decrease in Ki67⁺ cells.

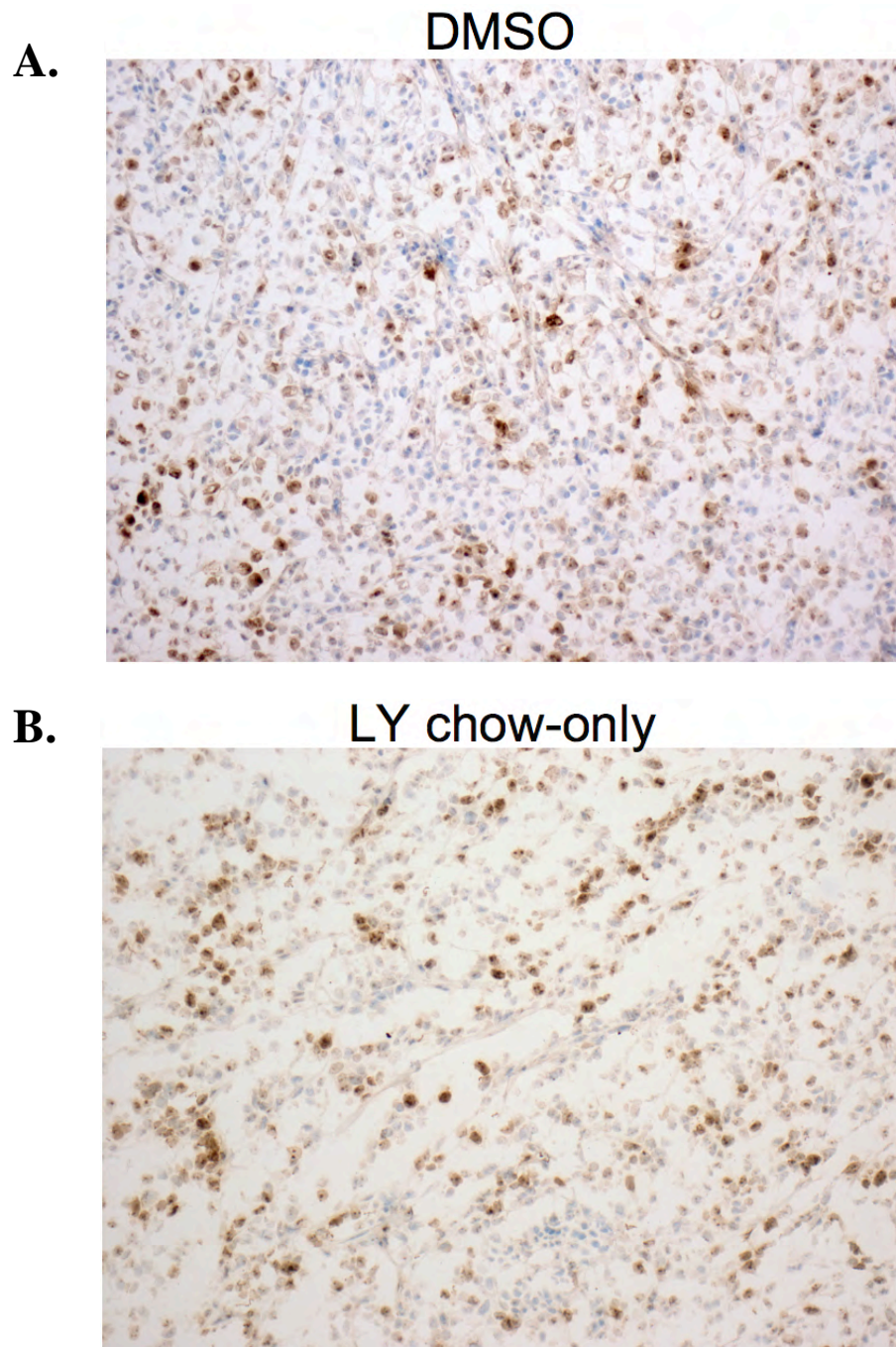


Figure 3.9 **Ki67 expression in DMSO and LY chow treated U87NS xenografts.** Ki67 expression was analyzed to determine the levels of proliferation in U87NS *in vivo* treated xenografts. Representative micrographs for Ki67 staining 13 days after the start of treatment. A) DMSO and B) LY chow-only treated xenografts have the highest number cells staining positive for Ki67.

DMSO treated samples were $32.3 \pm 13.6\%$ (Fig. 3.8 and Fig. 3.9 A) positive and LY chow-only samples were $28.5 \pm 15.4\%$ (Fig. 3.9 B). Xenografts treated with TMZ-only showed a significant ($P < 0.00001$) decrease in proliferation compared to DMSO, with only $18.2 \pm 10.4\%$ positive for Ki67 (Fig. 3.8 and Fig. 3.10 A). TMZ + LY chow samples had the greatest decrease of Ki67 expression ($P < 0.00001$). Only $6.9 \pm 4.3\%$ of the cells were positive for Ki67 in the TMZ + LY chow tissue, a 2.6-fold decrease ($P < 0.00001$) in expression compared to the TMZ-only tissue (Fig. 3.8 and 3.10 B).

SA- β -galactosidase is induced in xenografts by *in vivo* TMZ + LY treatment

Next we tested if SA- β -galactosidase expression is induced after *in vivo* treatment in mice with pre-existing subcutaneous U87NS xenografts. Previously, we demonstrated that 50% of mice had complete tumor regression when treated *in vivo* with TMZ + LY411,575 (LY) chow (Gilbert et al., 2010). All mice treated *in vivo* with DMSO, LY chow-only and TMZ-only showed 100% tumor progression. SA- β -galactosidase expression was grouped into four categories depending on the number of positive, blue cells in each microscope field. The 'negative' category has less than 10 SA- β -galactosidase-positive cells per field, 'low' has between 11 to 50 positive cells, 'medium' has between 51 to 100 positive cells, and 'high' has greater than 101 positive cells. When tumor sections were excised and analyzed 13 days after *in vivo* treatment began, DMSO, LY chow-only and TMZ-only samples had minimal SA- β -galactosidase staining (Fig. 3.11, 3.12, and 3.13). In DMSO tumor sections, 85% of the fields of view were negative and 15% low (Fig. 3.11). LY chow-only treated mice showed similar levels of SA- β -

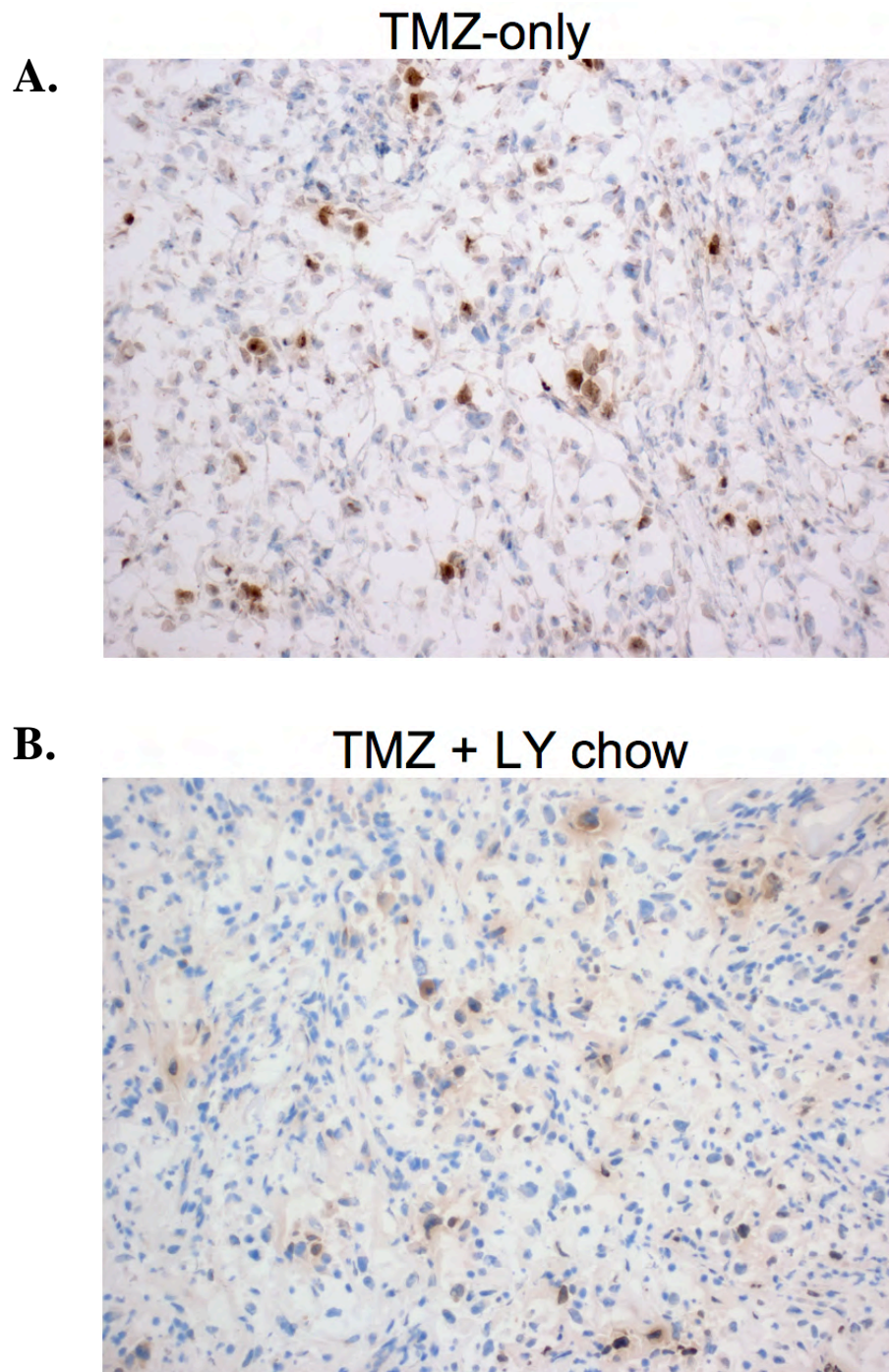


Figure 3.10 **Ki67 expression in TMZ-only and TMZ + LY treated U87NS xenografts.** Ki67 expression was analyzed to determine the levels of proliferation in U87NS *in vivo* treated xenografts. Representative micrographs for Ki67 staining 13 days after the start of treatment. The number of Ki67⁺ cells is greatly reduced in A) TMZ-only and B) TMZ + LY chow xenografts.

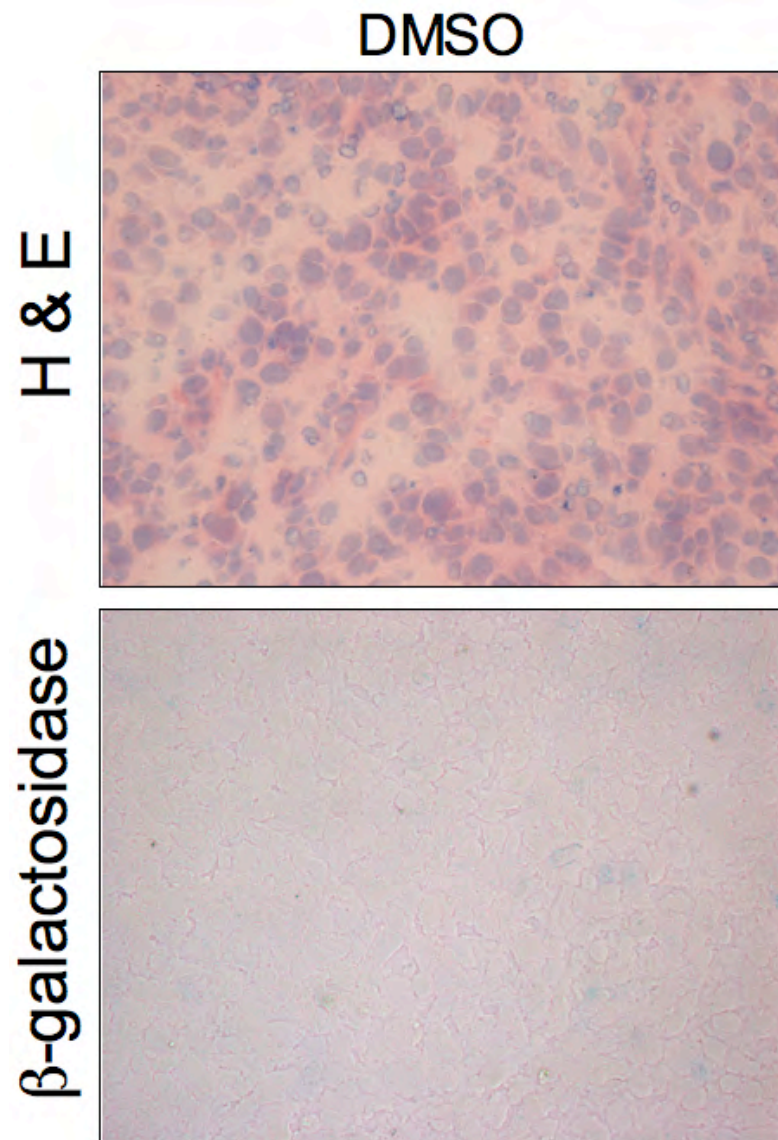


Figure 3.11 **DMSO *in vivo* control treatment and SA- β -galactosidase staining.** Tumor sections collected from U87NS xenografts, 13 days after the start of treatment, were analyzed by microscopy for H&E and SA- β -galactosidase staining (40x). DMSO treated mice possess xenografts with minimal SA- β -galactosidase-positive staining.

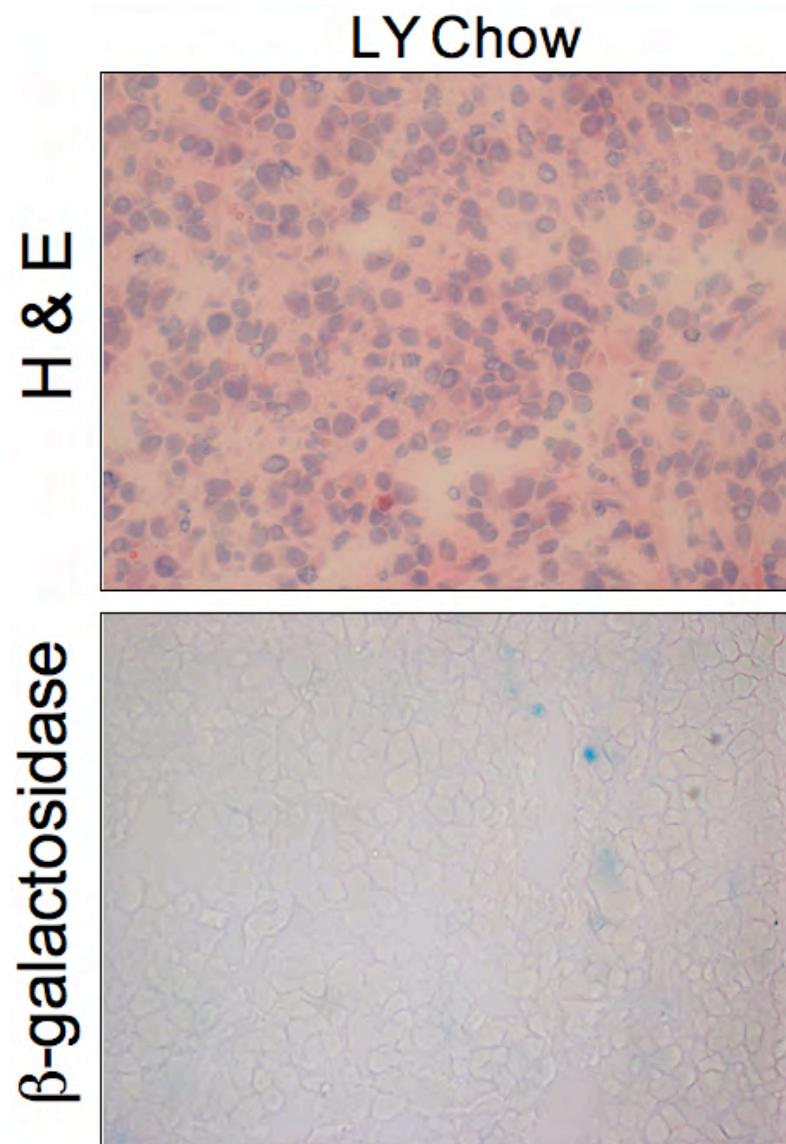


Figure 3.12 **LY chow-only *in vivo* treatment and SA- β -galactosidase.** Tumor sections collected from U87NS xenografts, 13 days after the start of treatment, were analyzed by microscopy for H&E and SA- β -galactosidase staining (40x). There is a small increase in the number of SA- β -galactosidase-positive cells after LY chow-only treatment.

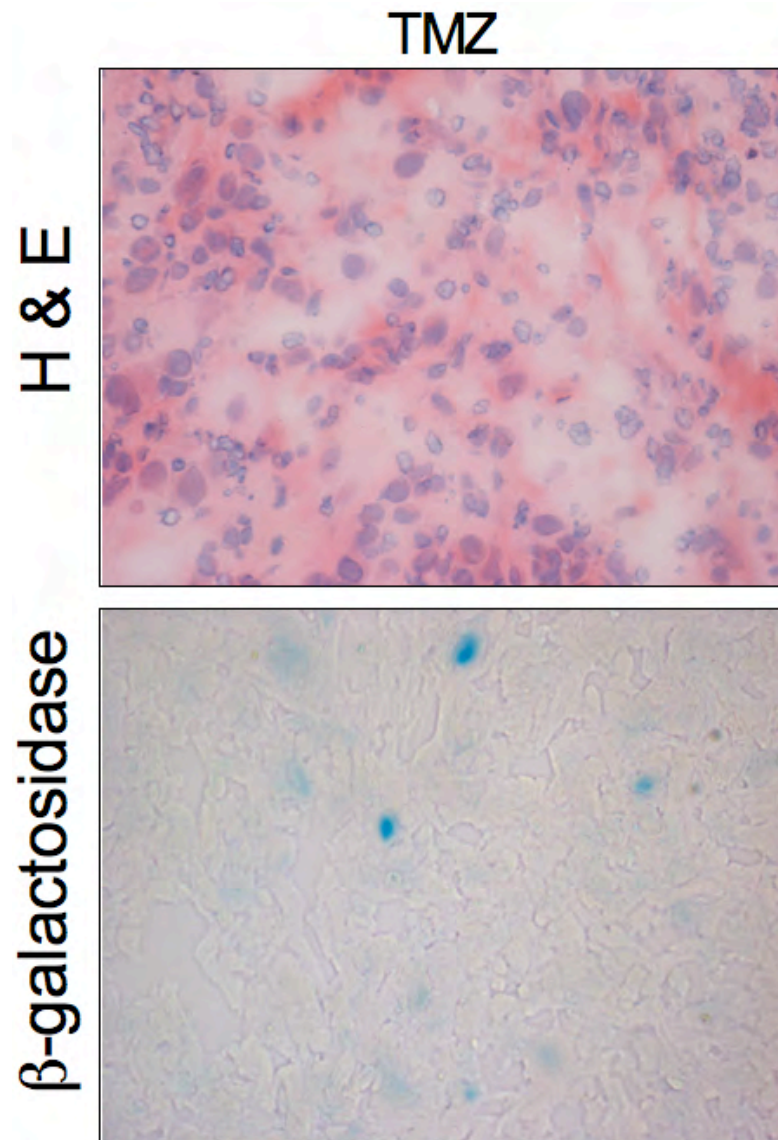


Figure 3.13 **TMZ *in vivo* treatment induces SA- β -galactosidase.** Tumor sections collected from U87NS xenografts, 13 days after the start of treatment, were analyzed by microscopy for SA- β -galactosidase staining (40x). H&E staining shows a slight decrease in cellular density in the TMZ-only treated xenografts. SA- β -galactosidase staining is increased in the TMZ-only samples.

galactosidase as TMZ-only samples. LY chow-only sections were 37% negative, 55% low and 8% medium (Fig. 3.15). Tumor sections from TMZ + LY chow treated mice have a large number of SA- β -galactosidase positive cells (Fig. 3.14). In contrast to other treated groups, only 4% of the view fields were classified as negative (Fig. 3.15). 26% of the view fields were SA- β -galactosidase low and 35% were SA- β -galactosidase medium. Only the mice treated with TMZ + LY chow yielded tumor sections with high levels of SA- β -galactosidase (greater than 101 cells). 35% of the fields classified as high SA- β -galactosidase (Fig. 3.15). These data demonstrate that TMZ + LY chow induces SA- β -galactosidase *in vitro* and *in vivo*.

TMZ + DAPT treatment enhances macrophage phagocytosis of the neurosphere cells

Based on the reports that macrophages can clear senescent cells, we investigated the interactions of macrophages with our glioma neurosphere cultures. Drug treated neurosphere cultures from 7 and 14 days after treatment were labeled with Alexa 647 and co-cultured with mouse macrophages labeled with Alexa 488. Cultures were analyzed for co-expression of Alexa 647 and Alexa 488 by flow cytometry to observe phagocytosis. On day 7 and 14 days after treatment, U87NS DMSO and DAPT treated cultures showed similar baseline levels of phagocytosis (Fig. 3.16 A). TMZ-only treatment increased the phagocytosis of U87NS cells 2.4-fold in the day 7 samples and 1.9-fold in the day 14 samples. U87NS cultures treated with TMZ + DAPT had the highest phagocytosis. The population of cells from the TMZ + DAPT treated culture phagocytosed by mouse

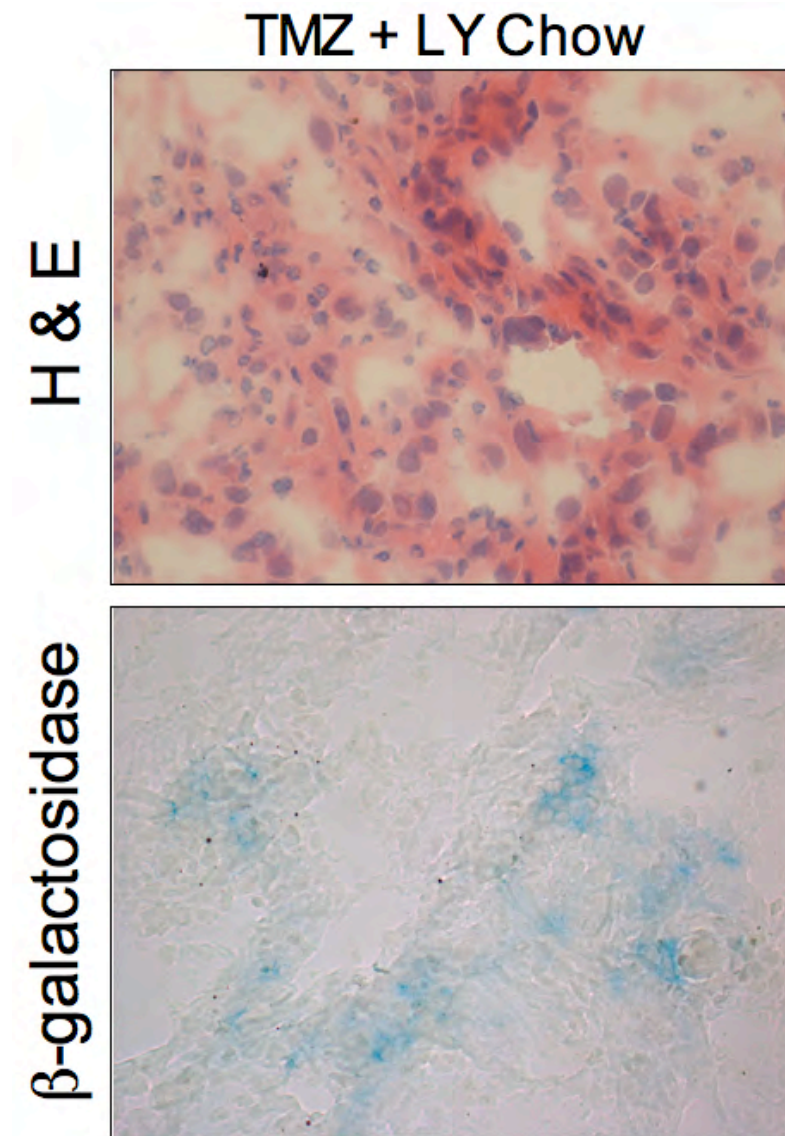


Figure 3.14 **TMZ + LY *in vivo* treatment induces SA- β -galactosidase.** Tumor sections collected from U87NS xenografts, 13 days after the start of treatment, were analyzed by microscopy for SA- β -galactosidase staining (40x). H&E staining shows a slight decrease in cellular density in the TMZ + LY chow treated xenografts. SA- β -galactosidase-positive staining is greatly increased in the TMZ + LY chow samples.

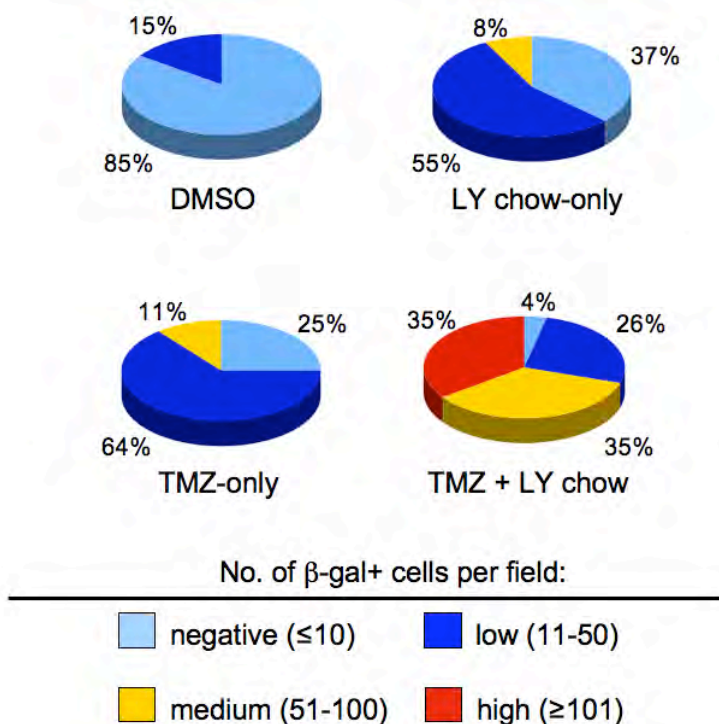


Figure 3.15 SA- β -galactosidase *in vivo* quantification. Quantification of the number of positive SA- β -galactosidase cells per view. The majority of DMSO treated xenografts have negative levels (≤ 10 positive cells) of SA- β -galactosidase expression. Interestingly, the LY chow-only xenografts have similar levels of SA- β -galactosidase expression, with over half of the views having low expression (11 – 50 positive cells), and a small percent of the views had medium expression (51 – 100 positive cells). The xenografts treated with TMZ + LY chow showed a significant upregulation of SA- β -galactosidase expression. Thirty-five percent of the views displayed medium expression. In addition, TMZ + LY chow xenografts were the only cohort to have any views that had high expression (≥ 101 positive cells), thirty-five percent of the views displaying high expression of SA- β -galactosidase levels.

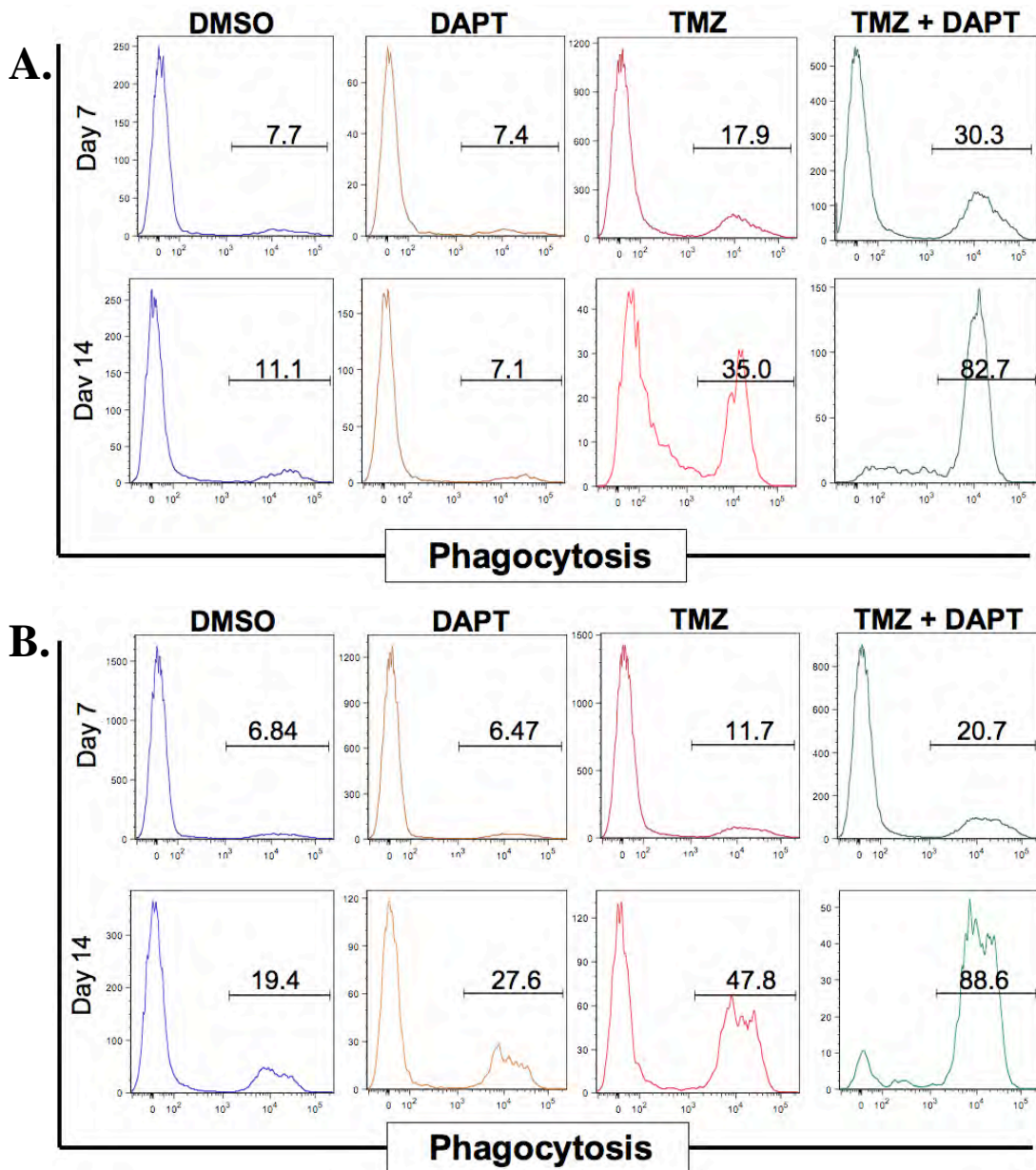


Figure 3.16 **TMZ + DAPT treated cells are more susceptible to macrophage phagocytosis.** Representative histograms displaying macrophage phagocytosis of A) U87NS and B) U373NS cultures. Neurospheres were treated, collected on either day 7 or 14, and labeled with Alexa 647. After co-culture with Alexa 488-labeled macrophages, cells were analyzed for phagocytosis by flow cytometry. Neurosphere cells were gated for Alexa 647⁺ staining, and analyzed for co-expression with Alexa 488. Co-expression is represented the occurrence of phagocytosis. TMZ-only treatment induces some levels of phagocytosis; however, TMZ + DAPT treated neurospheres induce the highest percentage of phagocytosis.

macrophages was 3.9-fold and 3.8-fold higher than the DMSO samples. In the U373NS cultures, DMSO and DAPT treated cells showed similar levels of phagocytosis when co-cultured with macrophages 7 and 14 days after treatments. Phagocytosis of the TMZ-only treated U373NS cells is increased by 1.7-fold and 2.6-fold in day 7 and day 14 cultures, when compared to DMSO controls (Fig. 3.16 B). TMZ + DAPT treated samples co-cultured with macrophages induced the highest phagocytosis, with a 2.5-fold increase on day 7 and a 6.1-fold increase on day 14, compared to DMSO controls (Fig. 3.16 B). Next, day 21 U87NS Alexa 647 neurospheres were co-cultured with the Alexa 488-labeled macrophages and analyzed by confocal microscopy, many neurospheres that remained single positive were present in the DMSO and DAPT-only treated samples, while TMZ-only and TMZ + DAPT treated samples showed a high number of macrophages that contained double-positive foci, representative of phagocytosis (Fig. 3.17).

Discussion

While TMZ treatment induces cell death and senescence (Gunther et al., 2003), some cancer cells survive by entering a transient cell cycle arrest (Mihaliak et al., 2010). We have demonstrated that the combined treatment of TMZ + GSI greatly enhances glioma therapy by blocking neurosphere recovery and tumor progression. We believe that the loss of Notch signaling triggers the arrested cells to enter a permanent senescent state. We have demonstrated that TMZ + GSI treatment increases senescence in neurosphere cultures and glioma xenografts. These cultures display decreased levels of proliferation, as measured by cell growth and Ki67 expression. TMZ + DAPT treatment increases SA-

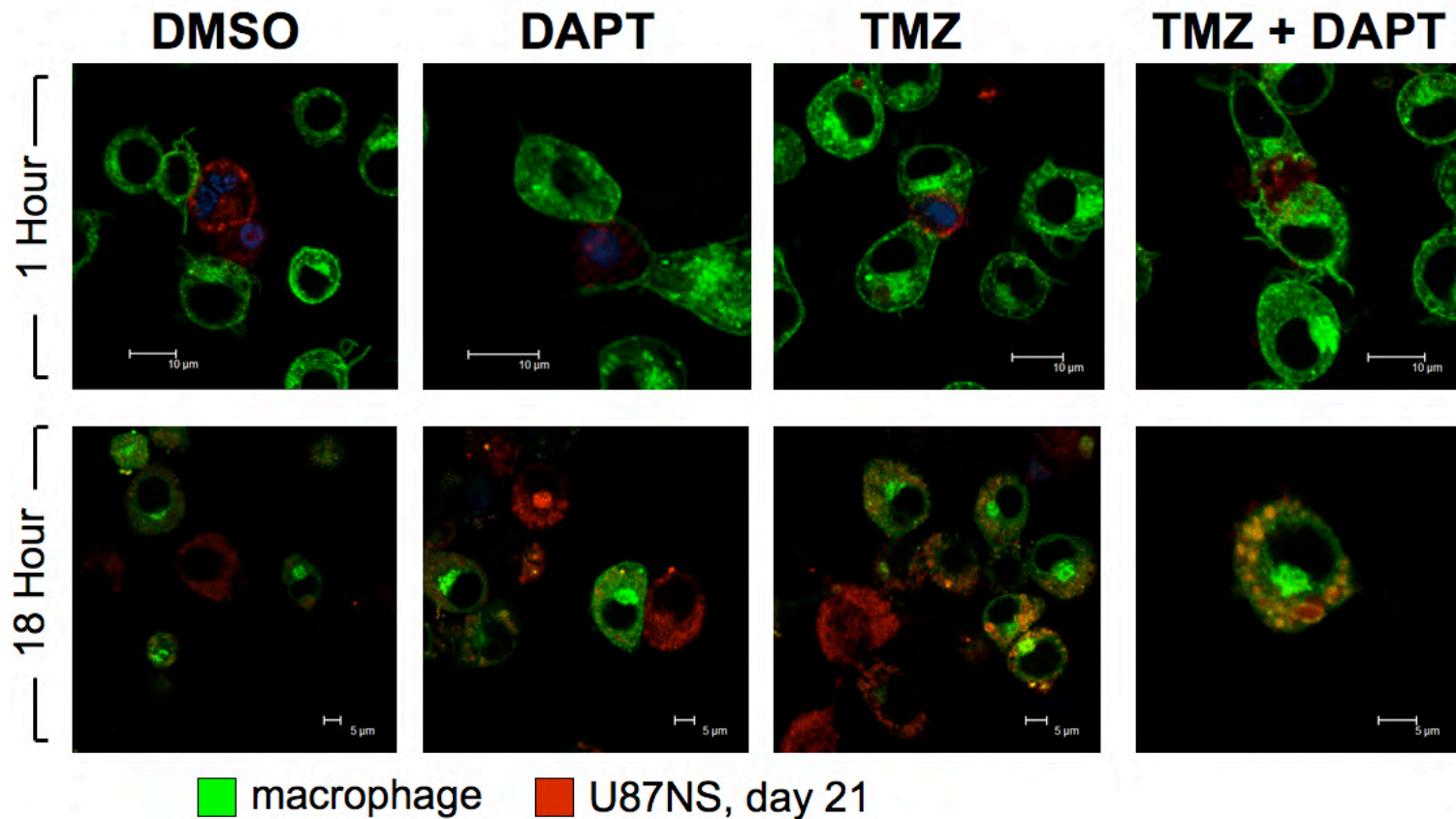


Figure 3.17 **TMZ + DAPT treated cells are more susceptible to macrophage phagocytosis.** U87NS labeled with Alexa 647 (red) and Hoechst 33342 (blue, in 1 hour samples) were co-cultured with Alexa 488 labeled macrophages (green) and analyzed by confocal microscopy. After 1 hour, macrophages were in contact with the neurospheres from each treated sample. However, after 18 hours of co-culture, the majority DMSO and DAPT-only treated neurospheres remained single-positive for Alexa 647. In contrast, the TMZ-treated neurospheres were both double-positive and single-positive. In the TMZ + DAPT treated samples, the majority of the cells were double-positive. These cells appeared as Alexa 488 labeled macrophages, with compartments co-labeled with Alexa 647, reminiscent of phagosomes in phagocytic macrophages.

β -galactosidase expression in neurosphere cultures. When these treated neurospheres are dissociated and re-plated, the cells neither proliferate nor form neurospheres, but remain as single viable cells expressing SA- β -galactosidase. Senescence cells in adherent cultures are classically characterized by a flattened morphology, an increase in vacuoles and increased cell size. Due to the non-adherent nature of the neurosphere cultures, we do not observe the flattened morphology in the SA- β -galactosidase-positive cells. It is interesting to note, however, that a percentage of the SA- β -galactosidase-positive appear to have an increased size and an increase in vacuoles. This feature was not used to further characterize the cells, but it would be interesting to sort the cells by flow cytometry after TMZ + GSI treatment based on size and granularity to see if there are differences in expression levels of senescence-associated genes, such as *p21* and *p27*.

Our data supports the hypothesis that TMZ + DAPT treatment targets both the, as the bulk tumor cells and the cell cycle arrested tumor-propagating population through TIS. First, we demonstrate that that TMZ + DAPT treatment does not increase cell death. In contrast, TMZ + DAPT treated neurospheres show decreased levels of cell death, suggesting some cells that undergo cell death with TMZ-only treatment enter into senescence with TMZ + DAPT treatment. TMZ treatment alone induces senescence in a subpopulation of glioma cells. These cells are likely the non-tumorigenic cells, because the cancer progresses after TMZ treatment. Since we demonstrated that the upregulation of SA- β -galactosidase expression occurs specifically when GSI is administered after TMZ treatment, this implies that the GSI can only induce senescence if the cells have first entered a transient cell cycle arrest.

Our TMZ + DAPT schedule treatment assay suggests that treatments must be administered in a schedule-specific manner. We hypothesize that GSIs will be beneficial when administered after initial concurrent and adjuvant TMZ treatments to enhance TIS. However, GSIs can also enhance IR-induced cell death when administered within 24 hours before or after radiotherapy (Wang et al., 2010a). Further experiments are necessary to determine how IR will contribute to combination therapy with TMZ and GSIs and the sequence of treatments that will provide the most efficient therapy. GSI treatment concurrent with IR may further enhance the proposed efficacy of TMZ + GSI adjuvant treatments, however, it may hinder the TMZ efficacy as we observed in our DAPT pre-treatment experiments.

TIS has the potential to increase patient progression-free survival and overall survival rates. Our TMZ + GSI treatment regimen is promising because it stimulated TIS to directly target the population of cells capable of tumor progression, while also inducing cell death and senescence in the bulk tumor cells. Under normal conditions, senescence is a permanent cell cycle arrest; however, genetic mutations can interfere with the senescence pathways (Beausejour et al., 2003; Dirac and Bernards, 2003). Therefore, it is possible that over time a senescent cancer cell could exit the senescent state, become resistant to TMZ + GSI treatment, and drive tumor recurrence. In this scenario, a promising feature of senescence is that it produces a SASP that activates tumor clearance by the innate immune system (Coppe et al., 2008; Freund et al., 2010; Xue et al., 2007). Indeed, we found that TMZ + DAPT treated neurosphere cells are more likely to be phagocytosed by macrophages *in vitro* than TMZ-only, DAPT-only and DMSO treated

cells. Interestingly, we previously observed that TMZ + GSI *in vivo* treatment of subcutaneous xenografts resulted in complete tumor loss in 50% of the treated mice (Gilbert et al., 2010). Since TMZ + GSI treatment induces a cytostatic senescent state in the xenograft cells, and there is no increase in cell death compared to the TMZ-only treated cultures, it was expected that the tumor progression would halt, but the pre-existing xenograft would remain after treatment. These data, combined with the *in vitro* phagocytosis assay, suggest that the senescent cells are cleared by the innate immune system *in vivo*, which further enhances the efficacy of the TMZ + GSI treatment.

Materials and Methods

Cell Culture

U87MG (ATCC) and U373MG (Dr. Larry Recht, Stanford University) serum cultures were converted to neurosphere cultures, U87NS, U87NS-luc and U373NS, as described in the previous chapter. All neurosphere cultures are maintained in defined media consisting of DMEM/F12 1:1 (GIBCO, Carlsbad, CA), supplemented with 1X B27, without vitamin A (GIBCO, Carlsbad, CA), 15 mM HEPES (GIBCO, Carlsbad, CA), 20 ng/ml EGF (Invitrogen, Carlsbad, CA), and 20 ng/ml bFGF (Invitrogen, Carlsbad, CA) and 1% penicillin-streptomycin (GIBCO, Carlsbad, CA). All cultures were passaged using a pH dissociation method with brief exposure to a strong alkaline solution and gentle trituration (Sen et al., 2004). Cells were incubated at 37°C with 5% CO₂. Mouse immortalized macrophages were provided by Evelyn Kurt-Jones (University of

Massachusetts Medical School, Department of Medicine). Mouse macrophages are maintained in DMEM supplemented with 10% FBS and 1% penicillin-streptomycin.

Drug Concentrations

TMZ (Sigma-Aldrich, St. Louis, MO) was dissolved in DMSO (Research Organics, Cleveland, OH) to a stock concentration of 10 mM and stored at -20°C. TMZ concentrations for each culture were selected based on previous experiments (Mihaliak et al., unpublished), i.e., high enough to produce an 80% or greater decrease in neurosphere formation, but low enough to allow recovery of neurosphere formation after treatment. U87NS and U373NS cultures were treated with 200 μ M TMZ. DAPT (Sigma-Aldrich, St. Louis, MO) concentrations were chosen for each culture by the decrease in Hes1 and Hey1 expression as previously described (Gilbert et al., 2010). U87NS was treated with 1 μ M DAPT and U373NS was treated with 5 μ M DAPT.

Neurosphere Recovery and Secondary Neurosphere Assays

Neurosphere cultures were dissociated to single cell suspensions by pH dissociation followed by filtration through 40 μ m screens. Neurospheres were seeded at either 3,000 cells/ml or 6,000 cells/ml in defined neurosphere medium. Immediately after plating, cells were treated with DMSO carrier control, TMZ-only, DAPT-only, or TMZ + DAPT. Additional DAPT was added on days 2 and 4. On day 7, fresh defined neurosphere medium was added to each sample, DAPT was administered to the DAPT-only and TMZ + DAPT samples, and the cells were incubated for an additional 7 days.

For secondary neurosphere formation, cells were collected on day 14, dissociated to a single cell suspension by the pH method, and re-seeded in defined neurosphere medium. Secondary neurospheres were cultured for an additional 7 days.

For the TMZ + DAPT schedule treatment, neurosphere assays were plated as described above. Pre-treated samples were administered a single dose of DAPT immediately after plating, and TMZ was added 24 hours later. For co-treated samples, single doses of TMZ and DAPT were administered together, immediately after plating. For post-treated samples, TMZ was added to the culture immediately after plating, and DAPT was added 24 hours later.

Subcutaneous Xenografts: in vivo Drug Treatment

As previously described (Gilbert et al., 2010), 1×10^6 U87NS cells were pH dissociated and re-suspended in 100 μ l PBS. Cells were subcutaneously injected into the right flank of male nude mice. Tumor volume was calculated as $(\frac{3}{4}) \times (\pi) \times (\text{length}/2) \times (\text{width}/2)^2$. When the tumor reached approximately 200 mm³ we began the following *in vivo* treatments: 1) DMSO control mice received 2 days of 100 μ l DMSO/PBS (1:1) i.p. injections; 2) TMZ-only mice received i.p. injections of 20 mg/kg of TMZ in 100 μ l 1:1 DMSO/PBS on days one and two; 3) LY chow-only mice received i.p. injections of 100 μ l of DMSO carrier on days one and two. Beginning on day three, the mice were fed 7012 Teklad LM-485 rodent chow infused with LY411,575 at a concentration of 0.0275 g/kg (Harlan Laboratories Inc, Madison, WI) (Samon et al., 2008). At this concentration, the estimated dosage of LY411,575 ingested by the mice is 5 mg/kg/day (Samon et al.,

2008); 4) TMZ + LY chow mice received i.p. injections of 20 mg/kg of TMZ in 100 μ l 1:1 DMSO/PBS on days one and two. Beginning on day three, the mice were fed LY chow for 10 consecutive days. Mice were euthanized 13 days after the beginning of treatment and tumor tissue was extracted. Tumors were embedded in O.C.T Compound (Sakura, Torrance, CA) and stored at -80 °C.

PI staining for cell death

U87NS cells were plated at 3,000 cells/ml in 15 ml of defined neurosphere medium and treated with DMSO, DAPT-only, TMZ-only, and TMZ + DAPT, as described above. Cells were harvested on either day 3 or day 7, pH dissociated, and resuspended at 1×10^6 cells/ml PBS. Cells were incubated at room temperature for 15 minutes with PI (BD Biosciences, Franklin Lakes, NJ) at a final concentration of 0.5 μ g/ml. PI uptake was detected by flow cytometry analysis on a BD™ LSRII (BD Bioscience, Franklin Lakes, NJ).

β -galactosidase staining

SA- β -galactosidase expression was measured using the Senescence Detection Kit (Calbiochem, San Diego, CA). For *in vitro* staining, 6,000 cells were plated in 12-well plates in 1 ml of defined neurosphere medium. DMSO, TMZ-only, DAPT-only and TMZ + DAPT treatments were repeated as described for the neurosphere assays. On days 7 and 21, the 12-well plates were centrifuged at 2,000 rpm for 10 minutes to attach the neurospheres to the plates. Wells were then washed with PBS and centrifuged to save any

dislodged cells. The cells were fixed with 0.5 ml of the fixative solution and incubated at room temperature for 15 min. The plates were centrifuged briefly, the fixative solution was removed, and cells were washed twice. A staining mixture, containing staining solution, staining supplement and X-gal (20 mg/ml) were added to each well and incubated at 37°C, as described in the manufacturer's protocol. After 12 hours, the staining solution was removed and cells were washed with PBS. β -galactosidase positive and negative cells were counted by light microscopy, and the percentage of positive cells was calculated based on the total number of cells.

To analyze SA- β -galactosidase expression in tumors treated *in vivo*, O.C.T. frozen samples were sectioned at 8 μ m by the Tissue Bank Core at the University of Massachusetts Medical School. The Senescence Detection Kit (Calbiochem, San Diego, CA) staining mixture, containing staining solution, staining supplement and X-gal (20 mg/ml) was added to each slide (200 μ l), incubated at 37°C for 12 hours, and then washed with PBS. Under blind conditions, β -galactosidase positive cells (blue) were counted using a light microscope, and the number of senescent cells per field was quantified from a total of . The percentage of fields with either 0 - 10 (negative), 11 - 50 (low), 51 - 100 (intermediate) and greater than 100 (high) β -galactosidase positive cells were quantified for each set of tumors from mice treated with DMSO (n = 5), LY chow-only (n = 4), TMZ-only (n = 5) and TMZ + LY chow (n = 5). For each mouse, 6 tumor sections were stained and 5 views were counted at 40X for SA- β -galactosidase positive.

Immunohistochemistry staining

Subcutaneous tumors were extracted 13 days after the start of treatment and embedded in O.C.T. reagent. All sections were cut at a 6 μm thickness. Frozen sections were fixed with ice-cold 100% methanol at room temperature for 5 min. Antigen retrieval was carried out in Tris-EDTA pH 9.0. Antibodies were used as follows: Ki67 (1:1000; Nova-Castra, Newcastle, UK) and biotinylated anti-rabbit IgG (1:200; Vector Laboratories, Burlingame, CA). Sections were stained with Ki67 antibody overnight at 4°C, followed by secondary antibody for one hour at room temperature. To visualize the Ki67 expression, Vectastain Elite ABC reagent and diaminobenzidine tetrachloride (DAB) kits were used, following manufacturer protocols, to produce a brown stain (Vector Laboratories, Burlingame, CA). Five random fields at 20X were analyzed and quantified for positive expression of Ki67 in day 13 tumors from DMSO (n = 6), LY chow-only (n = 5), TMZ-only (n = 6), and TMZ + LY chow (n = 5). Ki67 stained sections were counted blind by two laboratory members.

In vitro phagocytosis assay

U87NS and U373NS cultures were plated at 25,000 cells/ml in 20 ml of defined neurosphere medium in flasks and treated with DMSO, DAPT-only, TMZ-only, and TMZ + DAPT as described above. Neurosphere cells were harvested and pH dissociated on days 7, 14, and 21. Mouse immortalized macrophages were harvested and labeled with cholera toxin subunit B (CT-B) conjugated to Alexa Fluor® 488 (Invitrogen Molecular Probes, Eugene, OR), which attaches to the cell surface through the pentasaccharide

chain of ganglioside GM1. Mouse macrophages were stained with 5 $\mu\text{g/ml}$ CT-B-Alexa 488 in PBS/B27/HEPES staining buffer at room temperature for 30 minutes. Macrophages were washed three times with PBS to remove free CT-B. 6,000 cells were seeded onto 35 mm glass bottom dishes (MatTek, Ashland, MA) in DMEM supplemented with 10% FBS and incubated at 37°C for 1 hour. Simultaneously, the pH dissociated neurosphere cells were labeled with 5 $\mu\text{g/ml}$ CT-B-Alexa Fluor® 647 (Invitrogen Molecular Probes, Eugene, OR) and 5 $\mu\text{g/ml}$ Hoechst 33342 (Invitrogen Molecular Probes, Eugene, OR) at room temperature for 30 minutes. The neurosphere cells were then washed three times with PBS to remove free CT-B and Hoechst 33347 dye. The serum media was removed from the macrophages and 300,000 Alexa 647-labeled neurosphere cells were co-cultured with the Alexa 488-labeled macrophages in defined medium for 1, 10 or 18 hours. For flow cytometry analysis, cells were harvested after 10 hours of co-culture, resuspended in PBS/B27/HEPES staining buffer and run on a BD™ LSRII (BD Biosciences, Franklin Lakes, NJ). Flow cytometry data was analyzed using FlowJo (TreeStar, Inc, Ashland, OR). Debris and doublets were not included in data analysis. Alexa 488 events were gated to select for the labeled neurosphere population, and co-expression of Alexa 488 and Alexa 647 were analyzed to quantify phagocytosis. Co-cultures were also analyzed by confocal microscopy at 1 hour and 18 hours time points on a DM-IRE2 inverted microscope (Leica, Mannheim, Germany).

CHAPTER IV:

Final Conclusions and Future Directions

CHAPTER IV:

Final Conclusions and Future Directions

Previous studies in T-ALL and multiple myeloma, have demonstrated synergistic effects between chemotherapy and GSI treatment (De Keersmaecker et al., 2008; Liu et al., 2009; Nefedova et al., 2008). GSIs have been shown to sensitize glioma cells, specifically the tumor-propagating CSC population, to IR treatment (Lin et al., 2010b; Wang et al., 2010a). Our laboratory was the first to combine TMZ chemotherapy with GSI treatment in gliomas (Gilbert et al., 2010; Gilbert et al., unpublished). While the effects of GSI-only and TMZ-only treatments are only temporary and do not inhibit tumor regrowth, we have demonstrated that TMZ + GSI treatment blocks neurosphere and tumor formation, and inhibits tumor progression through TIS. This response has the potential to enhance TMZ therapy in the clinic by inhibiting glioma recurrence. We propose that the cells that evade TMZ cytotoxicity do so by entering a temporary reversible cell cycle arrest. Notch activity appears to prevent these cells from entering a permanent senescent state, while GSI treatment, when administered after TMZ treatment, induces senescence (Fig. 4.1).

What population is targeted by TMZ + GSI treatment?

Glioma cancer stem cells

One of the largest caveats to this study is that we have not characterized the specific population that is targeted by the TMZ + GSI treatment. Since the TMZ + GSI

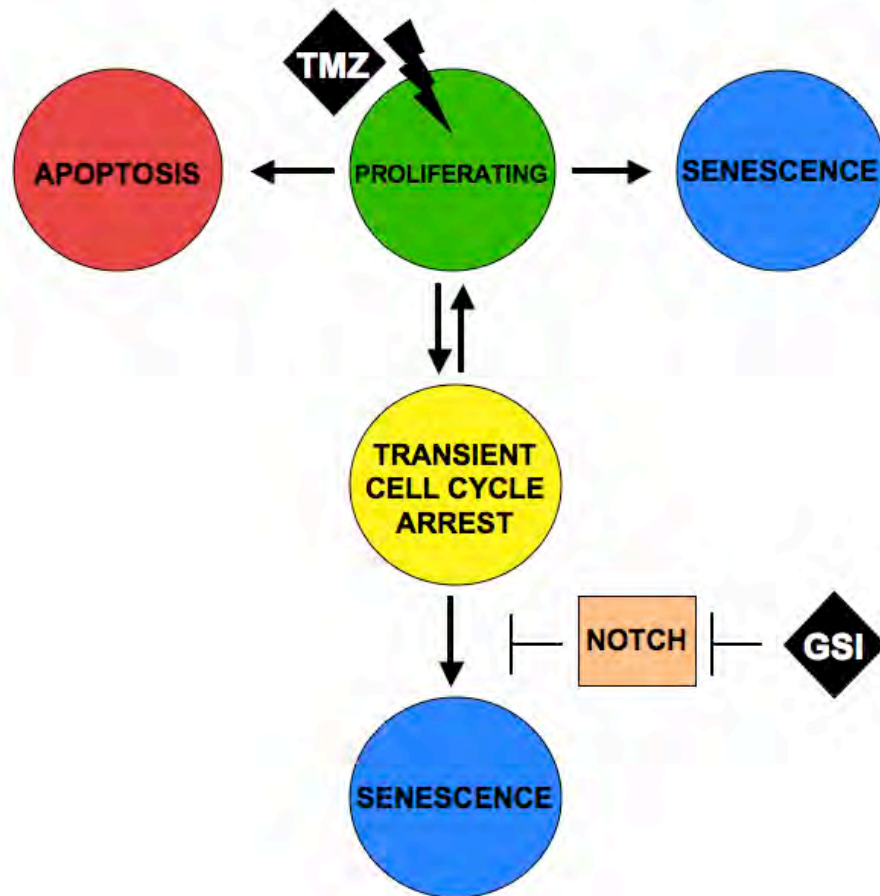


Figure 4.1 TMZ + GSI Treatment Mechanism. TMZ treatment targets proliferating cells, which leads to either apoptosis, senescence or a transient cell cycle arrest. Unfortunately, the cells that enter the transient cell cycle arrest include tumor-propagating cells. These cells eventually re-enter the cell cycle, and are responsible for tumor recurrence. We have demonstrated that these cells can be targeted by combination treatment with TMZ and GSI, in a sequence-dependent manner. When the cell enters the transient cell cycle state, Notch signaling protects the cell from the permanent cell cycle arrested, senescent state. Therefore, after TMZ treatment, we can target the chemoevasive cells by blocking Notch pathway with GSI treatment.

treatment induces senescence and blocks neurosphere recovery and tumor growth, we believe that CSCs are the targeted cells. However, to confirm that TMZ + GSI treatment induces senescence in the CSC population requires the isolation of the CSC population. Cell surface markers are commonly used to identify and isolate different cell types by fluorescence-activated cell sorting or magnetic bead isolation. Leukemias currently are the most accepted models of CSCs due to an excellent set of markers for the lineages of both normal hematopoietic and leukemia cells (Ratajczak, 2008). Unfortunately, a definitive set of markers to delineate all glioma CSCs has not been described. The most commonly used cell surface marker for glioma CSCs has traditionally been CD133 (Bao et al., 2006a; Hemmati et al., 2003; Singh et al., 2003; Wang et al., 2010a), but despite many successes using this cell surface marker, it has become increasingly clear that individual gliomas are very heterogeneous and vary greatly from patient to patient (Phillips et al., 2006). Although this heterogeneity may be an example of the stochastic model and acquired mutations, differences in expression of stem cell markers among gliomas may also be explained by variability in the hierarchy of the original tumor-initiating cells for different tumors, such as CSCs, progenitors, or further differentiated cells (Lottaz et al., 2010). Cells isolated from CD133⁺ tumors are more likely to express a “proneural” gene signature and resemble fetal neural stem cells, while cells from CD133⁻ tumors have “mesenchymal” genes and resemble adult neural stem cells (Phillips et al., 2006). Collectively, these data demonstrate that CD133 is not a universal stem cell marker for GBMs and highlight the limits of selecting for glioma CSCs using CD133. Researchers in the field have recognized the caveats of using a single CSC marker, such

as CD133, and new work has been published on markers CD15, A2B5, podoplanin, and integrin alpha 6.

An additional way to determine whether the cells targeted by TMZ + GSI treatment *in vivo* are part of a CSC population, is to analyze if the senescent cells are associated with a CSC niche. If the SA- β -galactosidase-positive in the TMZ + GSI treated mice were CSCs, it is expected that they would localize to regions of hypoxia and the perivascular niche (Calabrese et al., 2007; Heddleston et al., 2009).

Since there is not a single marker consistent for all patients that can be used to successfully isolate a pure and inclusive population of CSCs, it is likely that isolation of glioma CSCs will require the use of a set of markers to identify and purify CSCs in all gliomas. Until we are able to definitively isolate the glioma CSCs using stem cell markers, we will use the following criteria to support the hypothesis that the TMZ + GSI treatment targets CSCs: the targeted population includes 1) neurosphere-initiating cells; 2) tumor-propagating cells; 3) chemoresistant cells; and 4) cells capable of self-renewal.

Notch-expressing subpopulation

We have demonstrated that Notch is an active target in TMZ + GSI treatment, since expression of constitutively active NICD attenuates the inhibition of neurosphere recovery. Therefore, the cells that escape TMZ treatment, but respond to TMZ + DAPT treatment, should express one or multiple Notch receptors. To determine if the cells expressing Notch receptors make up the entire population that escapes TMZ toxicity, glioma cells can be sorted for Notch1-4 expression. If only cells with active Notch

signaling escape TMZ treatment, then a Notch-negative population will not be capable of recovery or secondary neurosphere formation after TMZ-only treatment. In addition, a Notch-positive population will recover and form secondary neurospheres with TMZ-only treatment, but not with TMZ + DAPT treatment. Since the TMZ + DAPT treatment is so effective, I would hypothesize that the cells that evade TMZ treatment will only be present in the Notch-positive population. The correlation between Notch status and TMZ response could be further analyzed based on the expression of individual Notch receptors to determine if there any of the four receptors play a specific role in TMZ + GSI treatment. We know Notch1 is involved in the biologic response of TMZ + GSI treatment, because our NICD1 reconstitution experiments attenuate the effects of the combined treatment. In gliomas, Notch1 and Notch2 have been shown to play the largest role in growth and survival. Knockdown of Notch1 by RNAi resulted in decreased cell growth through cell cycle arrest and apoptosis, and decreased tumorigenicity (Chen et al., 2010a; Purow et al., 2005; Xu et al., 2010; Zhao et al., 2010). Knockdown of Notch2 also decreases cell growth (Chen et al., 2010a). RNAi techniques or specific inhibitory antibodies could also be used to examine the importance of each individual Notch receptor when combined with TMZ treatment. However, according to the TMZ + GSI treatment schedule data, TMZ treatment must precede Notch knockdown to induce senescence. Therefore, inducible vectors will be necessary to analyze the effects of knocking down individual Notch receptors.

Despite the high level of secondary neurosphere formation in NICD-expressing cells treated with TMZ + GSI, it is possible that a unique population responds to TMZ +

GSI treatment through a pathway other than Notch. If any Notch-negative cells can evade TMZ toxicity, but respond to TMZ + GSI treatment, this would suggest that additional gamma-secretase substrates play a role in TMZ + GSI treatment. To test this, Notch-sparing GSIs can be utilized (Augelli-Szafran et al., 2010). If Notch is the only important target in TMZ + GSI treatment, administration of Notch-sparing GSIs will not enhance TMZ treatment and there will be no inhibition of neurosphere recovery or tumor progression.

Multifaceted effects of TMZ + GSI treatment

TMZ + GSI treatment is a promising glioma therapy in MGMT-negative because it permanently blocks cell proliferation by inducing senescence in the neurosphere-initiating and tumor-propagating cells. In addition to growth arrest, the combination treatment has the potential to target the tumor by other mechanisms. First, senescence is known to stimulate an immune response, resulting in tumor clearance (Xue et al., 2007). Since we demonstrated that TMZ + GSI treatment increases phagocytosis *in vitro*, and *in vivo* treatment results in dissipation of the tumor, TMZ + GSI treatment may activate the innate immune system for tumor clearance (Fig. 4.2). The second mechanism is that the inhibition of Notch in the TMZ + GSI treatment also targets the tumor vasculature. Other laboratories have demonstrated that Notch signaling is important for angiogenesis, and Notch inhibition can decrease glioma growth by targeting the endothelial cells (Bae et al., 2011; Hovinga et al., 2010; Noguera-Troise et al., 2006; Ridgway et al., 2006; Wang et al., 2010b).

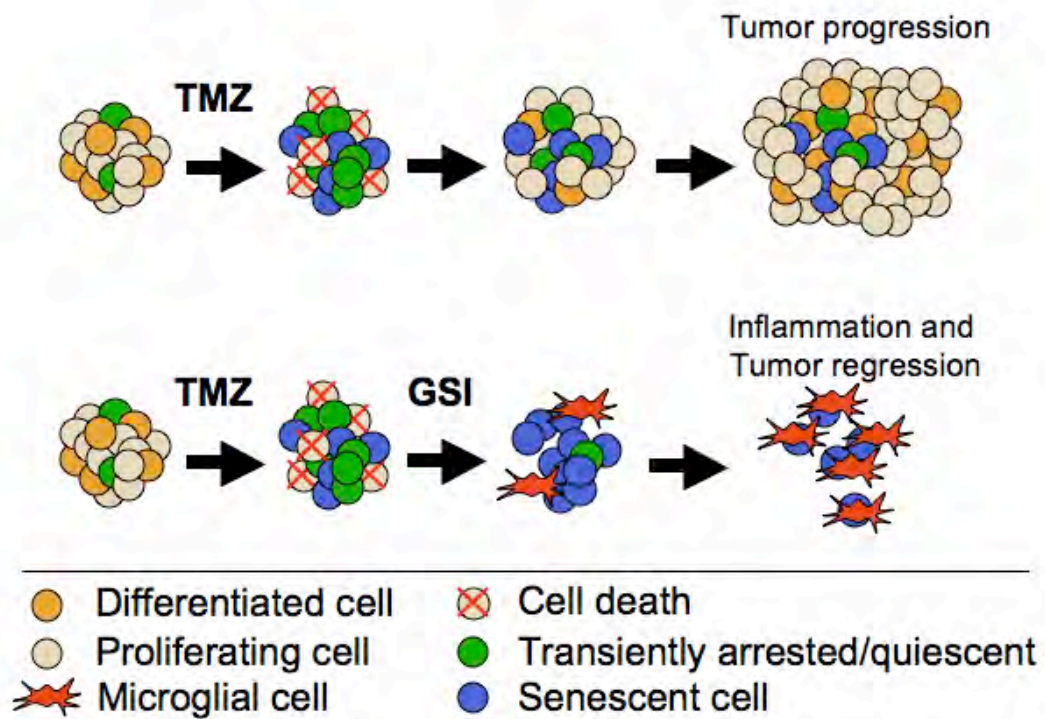


Figure 4.2 **TMZ + GSI treatment model.** TMZ treatment has a heterogeneous affect, resulting in apoptosis, senescence and reversible cell cycle arrest. With TMZ treatment alone, a population of the cells enters the transient cell cycle arrest and evades chemotoxicity. These cells eventually re-enter the cell cycle and drive tumor progression. When the tumor is treated with TMZ first, followed by a GSI, the transiently arrested cells enter a senescent state. The TIS stimulates an innate immune response, and the remaining tumor cells are cleared by the microglia.

Senescence and the immune system in gliomas

Although the TMZ + DAPT treatment induces cytostasis in the tumor cells, the ultimate result is a loss of tumor volume. We believe this is due to tumor clearance through by the immune system. Our TMZ + GSI treatment has the potential to influence the immune system and enhance therapy through two methods. First, the TMZ + GSI treatment may target the CSC population, which is responsible for immunosuppression in gliomas, and second, the treatment increases senescence, resulting in a SASP, which can prompt an immune response.

Although the brain is commonly considered immune privileged, there are active immune responses in normal brain and brain tumors (Carson et al., 2006). The most prevalent immune cells infiltrating gliomas are microglia. In GBMs, up to 30% of the tumor can be microglia (Hanisch and Kettenmann, 2007). Microglia are the macrophage counterpart in the brain and are part of the innate immune system. Like macrophages, microglia are polarized and exist in M1 and M2 states. M1 is the classically-activated state, in which the microglia are capable of phagocytosis and secrete cytotoxic and pro-inflammatory factors. However, tumor-associated microglia (TAMs) are in an alternatively-activated M2 state (Rodrigues et al., 2010). TAMs are also capable of phagocytosis, but are known to promote cancer growth, angiogenesis and invasion in gliomas and other cancers (Pollard, 2004; Sliwa et al., 2007). There is also a high incidence of neutrophils in gliomas (Fossati et al., 1999). Neutrophils are white blood cells that function in the innate immune system by phagocytosis. Natural killer (NK) cells are present in brain and glioma tissue; however, they are relatively rare and likely play a

minimal role in gliomas (Stevens et al., 1988; Yamasaki, 2004). Peripheral blood mononuclear cells (PBMCs), including T-cells, are also relatively rare in gliomas (McVicar et al., 1992). In addition, since our *in vivo* TMZ + GSI treatments were performed in athymic nude mice, which lack functional T cells, we know that T cell activity is not necessary for tumor clearance in our system. In recent studies, the host model has been demonstrating to play an important role on tumor formation and maintenance (Quintana et al., 2008). Therefore, further studies focusing on the role the immune system plays in tumor clearance after TMZ + GSI treatment must be diligently carried out. To avoid the limitations of host models, it would be best to test the role of the immune system in endogenous glioma mouse models or in humanized mouse models.

The capacity to evade tumor surveillance by the immune system is a key step in the development of cancer (Jaiswal et al., 2010). In gliomas, CSCs appear to play a large role in immunosuppression. Glioma CSCs secrete immunosuppressive factors, including IL-10, TGF- β 2, VEGF, and CCL-2 (Qiu et al., 2010; Wei et al., 2010a; Wei et al., 2010b). Glioma CSC cultures inhibited T-cell proliferation and induces T regulatory cells (Tregs) (Di Tomaso et al., 2010; Wei et al., 2010a). Tregs can suppress the functions of T-cells, B-cells, dendritic cells, monocytes, macrophages and natural killer (NK) cells. Glioma CSCs also directly induce an immunosuppressive phenotype in microglia (Wu et al., 2010a). Factors secreted by glioma CSCs that induce immunosuppressive microglia include sCSF-1, TGF- β 1, and MIC-1. These microglia secrete IL-10, possess a M2 polarization, and are not capable of phagocytosis. Since CSCs strongly influence

immunosuppression in gliomas, targeting the CSCs with TMZ + GSI treatment may dampen immunosuppression, and allow the immune system to target the malignant cells.

While the immune system defends against microorganism infections and tumor cells and can promote the clearance of debris and dead cells, an immune response can also be triggered in damaged and malignant tissues in response to senescent cells (Krizhanovsky et al., 2008; Xue et al., 2007). Senescent cells in fibrotic livers are targeted by NK cells (Krizhanovsky et al., 2008). In addition to NK cells, there is a high incidence of other infiltrating immune cells near the senescent tissue, including macrophages and neutrophils. This senescence-induced immune response has also been detected in a murine liver carcinoma model (Xue et al., 2007). p53 restoration induces senescence in these tumor cells, and leads to an upregulation of the SASP and infiltration of immune cells. Xue and colleagues found that inhibiting macrophage, neutrophil or natural killer cell functions significantly delayed tumor regression, demonstrating that the innate immune system plays an active role in senescence-driven tumor clearance.

In gliomas, the high prevalence of microglia makes them a strong candidate as a driver of tumor clearance after TMZ + GSI treatment. Microglia are capable of both phagocytosis and cytotoxic activity against foreign bodies (Gehrmann et al., 1995; Graeber and Streit, 2010; Hanisch and Kettenmann, 2007; Yang et al., 2010). We have demonstrated that macrophages have an enhanced phagocytosis *in vitro* when co-cultured with TMZ + DAPT treated glioma neurosphere cells. Senescent cells are known to have a SASP, which includes production of pro-inflammatory cytokines. We have preliminary data demonstrating that the TMZ + DAPT treated glioma cultures have an significant

increase in secretion of IL-6 and IL-8 (See Appendix, Fig. A.2). These data help demonstrate that the induction of senescence supports an pro-immune response in the TMZ + GSI treated gliomas and that the decreased tumor volume observed in the *in vivo* treated mice is due to tumor clearance, at least in part, through macrophage phagocytosis of senescent cells (Fig. 4.2). To further study this, it will be necessary to analyze immune cell infiltration in glioma xenografts with and without treatments. TMZ + GSI treatment may enhance the percentage of infiltrating innate immune cells, such as microglia; however, it is also possible that there is no increase in the number microglia after TMZ + GSI treatment, but the cells shift from TAMs in the M2 state, to classically-activated microglia in the M1 state. We propose to study this in an intracranial xenograft system (see Appendix, Fig. A.3), in which we can analyze infiltration of microglia, and the levels of secreted cytokines specific to classically-activated microglia, such as IL-12, versus cytokines specific to alternatively-activated TAMs, such as IL-10 (Wang et al., 2010c). Compounds that induce microglial toxicity or inhibit microglial maturation, such as clodronate or gadolinium chloride (Xue et al., 2007; Zeisberger et al., 2006), could also be administered in conjunction with TMZ + GSI treatments. If macrophages and microglia are responsible for tumor clearance after the induction of senescence, these compounds would delay tumor regression. It is important to be aware when studying this system *in vivo*, that there are differences between species reactivity, and not all human cytokines will activate mouse cells, nor will all mouse cytokines activate human cells (Cayphas et al., 1987; Schoenhaut et al., 1992).

Interestingly, Notch signaling is known to affect the activity of macrophages and microglial cells. Active Notch signaling in microglia stimulates phagocytosis (Grandbarbe et al., 2007). In macrophages, Notch signaling regulates their M1 versus M2 status (Wang et al., 2010c). Notch signaling promotes the classically-activated M1 macrophages, while blocking Notch leads to alternatively-activated M2 macrophages. Therefore, macrophages that have Notch signaling have enhanced tumor clearance activity. At first glance, these data are counterintuitive for TMZ + GSI treatment inducing tumor clearance. However, the most robust tumor regression in the TMZ + GSI treated mice that have complete tumor clearance occurs after the GSI treatment ceased. This would imply that an added benefit to short-term GSI treatment in a clinical setting would be the enhancement of tumor clearance.

Notch signaling and the glioma vasculature

Notch signaling is necessary for normal angiogenesis (Bae et al., 2011; Krebs et al., 2000). In addition, Notch plays a significant role in tumor angiogenesis. Blocking the Notch pathway can inhibit growth of different types of cancers by disrupting the tumor's vasculature system (Noguera-Troise et al., 2006; Ridgway et al., 2006). In gliomas, DAPT treatment greatly decreased the presence of endothelial cells in special 'tumor slice' cultures (Hovinga et al., 2010). Interestingly, this disturbed the CSC vascular niche, which resulted in a decreased number of CD133⁺ cells and neurosphere-initiating cells in the 'tumor slice' cultures. These data demonstrate that blocking the Notch pathway can inhibit glioma growth by disruption of angiogenesis, which in turn affects the CSC

vascular niche. Therefore, we propose that in addition to TIS and enhanced tumor clearance, the TMZ + GSI treatment has the potential to inhibit glioma growth by disrupting the tumors vasculature system.

Furthermore, it was recently demonstrated that tumor vascularization can occur through the differentiation of glioma CSCs into endothelial cells (Ricci-Vitiani et al., 2010; Wang et al., 2010b). Theoretically, endothelial cells derived from CSCs may be a mechanism for tumor cells to 'hide' from treatment. If these CSC-derived endothelial cells survive chemotherapy and IR, they might have the ability to de-differentiate and initiate tumor recurrence. Wang and colleagues (2010b) found that the differentiation of the CSCs into endothelial cells required Notch signaling. Therefore, in addition to potentially depleting the tumor-associated endothelial cells, the TMZ + GSI treatment may target the CSC-derived endothelial cells.

Future Directions

Our studies demonstrate that the combination of TMZ + GSI is a promising new treatment to induce senescence in glioma cells that evade TMZ-only treatment. However the mechanism by which this occurs has not been elucidated. We demonstrate that there is a sequence-dependent mechanism that requires the induction of a temporary cell cycle arrest. Previous studies in fibroblasts have demonstrated that blocking the Notch pathway will target quiescent cells and induce senescence (Sang et al., 2008). Our laboratory previously demonstrated that TMZ treatment leads to a G2/M arrest in neurosphere cultures (Mihaliak et al., 2010); however, we have not determined if all of the cells

capable of recovery and secondary neurosphere formation after TMZ-only treatment fall into this G2/M arrest, or if they are in a G0, or G1 transient arrest. As a future direction, cell cycle profiles of TMZ-only and TMZ + GSI treated samples will be compared at early time points and after secondary neurosphere formation. Then, live cell sorting of TMZ-only treatment samples will be employed using DNA content to isolate cells in the G1/G0, S, and G2/M phases. Analysis of the recovery and secondary neurosphere formation in each sorted population will help determine which phase the chemoresistant cells arrest in. Additional future experiments will focus on inducing specific cell cycle arrests, such as G1/G0 arrest by overexpression of exogenous p27^{Kip1} (Li et al., 2000), to determine if the combination of p27^{Kip1} overexpression and Notch inhibition can induce senescence. This will be an important study, because it will test whether Notch inhibition can cause neurosphere cells to transition from a transient cell cycle arrest to a permanent senescent in the absence of DNA damage. Conversely, future studies can also analyze if other DNA damaging agents, such as IR, ultra-violet light exposure and other alkylating agents, such as BCNU, can be combined with GSIs to induce senescence. This will help to elucidate if the TIS from TMZ + GSI treatment is specific to TMZ, if it is unique to alkylating agents, or if any form of DNA damage is sufficient.

Final Thoughts

The CSC model has had a positive effect on cancer research, leading to a renewed examination of tumor heterogeneity and therapy resistance. An important question for the clinic is whether the glioma CSCs are the cells resistant to therapy and hence, drive tumor

recurrence? We believe that the population of glioma cells that escapes chemotherapy-induced cell death and senescence do include CSCs (Mihaliak et al., 2010). Advocates for the CSC model suggested that therapy should be specifically directed against glioma CSCs, and the remainder of the tumor cells will eventually wither away (Cheng et al., 2010). However, since it is possible for differentiated tumor cells to dedifferentiate into stem cell-like cells (Chen et al., 2010b; Gupta et al., 2009), targeting just the glioma CSCs may only delay tumor recurrence. Therefore, long-term survival of glioma patients will require combination therapies that target both the bulk of the tumor and the glioma CSCs (Cheng et al., 2010). Our TMZ + GSI treatments offer a promising glioma therapy because both populations are targeted.

The TMZ + GSI treatment may be further enhanced by directly targeting other proteins in the Notch pathway. The most relevant downstream Notch target is Hes1, which was shown to be necessary for maintenance of the quiescent status (Sang et al., 2008). Currently, we hypothesize that the TMZ + GSI treatment will only be effective in gliomas with MGMT-negative or low expression levels. Although TMZ treatment provides some benefit to MGMT-positive cases in the clinic, we did not observe the induction of a transient cell cycle arrest in our MGMT-positive neurosphere cultures. Since MGMT can repair the O6-methyl-guanine product after TMZ treatment, new imidazotetrazine derivatives synthesized by a collaborator result in DNA damage that cannot be repaired by MGMT (Wheelhouse, RT, personal communication). A future direction is to test if treatment with these imidazotetrazine derivatives induces the transient cell cycle arrest in both MGMT-positive and -negative gliomas cultures, and

then determine if they can be combined with GSI treatment to induce senescence. Using a chemotherapy drug that does not rely on the MGMT status would broaden the pool of patients that could benefit from the TMZ + GSI regimen.

In conclusion, the TMZ + GSI treatment was highly successful at eliciting TIS. Specifically, we were able to target the cells that evade current treatment by shifting the cells that enter the TMZ-induced transient arrested state into a permanent senescent state. In addition, the TIS may cooperate with the innate immune system to induce tumor clearance. Therefore, TMZ + GSI treatment has the potential to decrease glioma recurrence when combined with surgical debulking. We believe that these studies will be successful for clinical translation, because TMZ is already the chemotherapy drug of choice for GBMs (Stupp et al., 2005), and GSIs are currently in being tested in clinical trials (Fleisher et al., 2008; Kreft et al., 2009; Olson and Albright, 2008; Rizzo et al., 2008).

APPENDIX

Preliminary Data

Contributions:

Jessica Weatherbee was involved with the real time PCR experiments.

Christine St. Pierre set up the ELISA experiments.

Evelyn Kurt-Jones provided guidance for the immunology aspect of the project.

Alonzo Ross provided intellectual support for the project and editing of the thesis.

APPENDIX:
Preliminary Data

p21 is persistently upregulated in TMZ + DAPT treated neurosphere cultures

One of the most commonly upregulated members of the senescence pathway is p21. Therefore, we were interested in analyzing p21 transcript levels in the neurosphere treated cultures. U87NS cells were treated with DMSO, DAPT-only, TMZ-only and TMZ + DAPT as previously described. Fresh media was added to the cultures on day 7, and the neurospheres were pH dissociated and re-plated for secondary neurosphere formation on day 14. Cells were harvested on days 2, 6, 10, 16, and 18. cDNA was made using the SuperScript II Reverse Transcription (RT) Kit (Invitrogen, Carlsbad, CA). Real time qPCR was carried out using QuantiTect SYBR Green (QIAGEN, Valencia, CA) following the manufacturer protocol. p21 forward primer: 5' CACCTCACC TGCTCTGCTG 3' and reverse primer: 5' GGCGTTTGGAGTGGTAGAAA 3'. β -Actin forward primer: 5' TTGCCGACAGGATGCAGAAGGA 3' and reverse primer: 5' AGGTGGACAGCGAGGCCAGGAT 3'. These preliminary experiments were drug treated in duplicate.

p21 levels were normalized to the DMSO control samples for each individual time point. The p21 transcript levels in DMSO and DAPT-only treated cultures remained low for all time points (Fig. A.1). Day 2 demonstrated a slight increase of p21 levels in both the TMZ-only and TMZ + DAPT treated cells. Transcript levels peaked on day 6 and remained upregulated in both TMZ-only and TMZ + DAPT treated samples on day

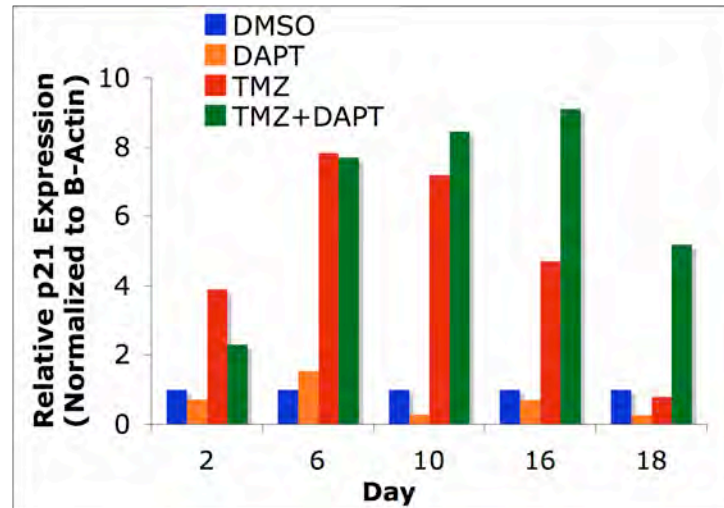


Figure A.1 **TMZ + DAPT treatment induces a persistent upregulation of p21 transcript levels.** U87NS neurosphere cultures were treated with DMSO, DAPT 1 μ M, TMZ 200 μ M and TMZ 200 μ M + DAPT 1 μ M. p21 expression levels were analyzed by real time RT-qPCR. TMZ-only and TMZ + DAPT treatments induced p21 expression; however, p21 upregulation was transient in the TMZ-only cultures and persistent in the TMZ + DAPT cultures. This correlates with the difference between the TMZ-only induction of a transient cell cycle arrest and the TMZ + DAPT induction of senescence.

10. However, while the p21 expression remained high through day 18 for the TMZ + DAPT samples, the TMZ-only samples had decreased p21 levels on day 16, and expression returned to control levels by day 18. This data demonstrates that p21 is temporarily increased in TMZ-only treatments, but is persistently upregulated in the TMZ + DAPT treatments (Fig. A.1). p21 expression is also associated with reversible cell cycle arrests. The decreased levels of p21 in the TMZ-only samples corresponds the cell cycle re-entry of cells during secondary neurosphere formation. In contrast, the persistent p21 expression in the TMZ + DAPT treated culture is consistent with the maintenance of senescence.

Cytokine secretion is upregulated in TMZ + GSI treated cultures

Senescent cells secrete cytokines as part of the SASP (Coppe et al., 2010; Freund et al., 2010). Two important factors in the SASP are IL-6 and IL-8, which are major mediators of the immune system and associated with inflammation. We analyzed the secretion of IL-6 and IL-8 to determine if there was an upregulation in the TMZ + DAPT treated cultures that correlated with the increase in senescent cells. U87NS cells were plated at 50,000 cells/ml in 3 ml of defined media. Cultures were treated as previously described, with TMZ and multiple doses of DAPT. On day 14, cultures were dissociated. DMSO and DAPT-only cultures were reseeded at a 1:30 ratio, while TMZ-only and TMZ + DAPT cultures were seeded at a 1:1 ratio. Supernatants were collected on days 15, 16, 17, 18, 19, 20 and 21. Supernatants were assayed for human IL-6 or IL-8 with ELISA kits (BD Biosciences, Franklin Lakes, NJ) according to manufacturer's instructions. These

experiments represent data from only one biological experiment analyzed in duplicate by ELISA.

In the neurosphere cultures treated with DMSO or DAPT-only, secretion of IL-6 and IL-8 remained low with no difference between the two treatments, consistent with low levels of senescence (Fig. A.2). TMZ-only and TMZ + DAPT samples showed a large increase in secretion of IL-6 and IL-8, compared to DMSO controls. The greatest difference between TMZ-only and TMZ + DAPT treatments was observed in day 21 supernatants. Compared to the supernatant from U87NS TMZ-only treated cultures, the TMZ + DAPT supernatants expressed IL-6 levels that were 1.7-fold greater (Fig. A.2 A), The IL-8 levels were 3.1-fold greater in the TMZ + DAPT treated cultures compared the TMZ-only treated cultures (Fig. A.2 B). These levels of secreted IL-6 and IL-8 are not normalized to cell number. Since the TMZ-only population greatly recovers during the secondary neurosphere formation, while the cell number remains low in the TMZ + DAPT treated cultures, the difference between the stimulation of IL-6 and IL-8 is even greater in the TMZ + DAPT samples than observed. This preliminary data suggests that the TMZ + DAPT treatment upregulates secretion of cytokines, as seen with SASP.

TMZ-only treated gliomas progress after in vivo treatment in an intracranial xenograft model

The most accurate model to test the TMZ + GSI treatments is in an intracranial xenograft model. To do this, we first analyzed the proof-of-concept with our DMSO and TMZ-only treatments. U87MG-luciferase cells (provided by Dario Altieri, Wistar

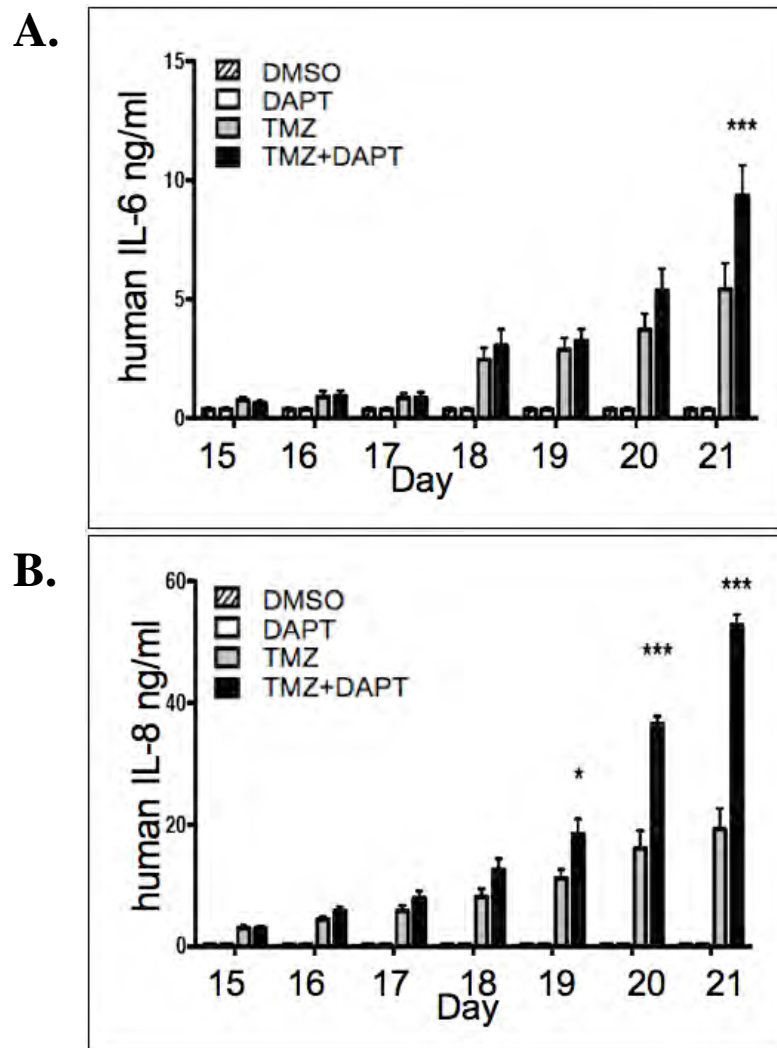


Figure A.2 Secretion of IL-6 and IL-8 are highest in TMZ + DAPT treated cultures. In U87NS treated cultures, DMSO and DAPT-only treatment do not stimulate A) IL-6 or B) IL-8 production. TMZ-only and TMZ + DAPT treatment induce IL-6 and IL-8 production during secondary neurosphere formation, with a significantly greater production from the TMZ + DAPT treated samples. ***, $P < 0.0001$

Institute) were converted to neurosphere cultures in defined serum-free medium under G418 selection. 1×10^6 U87NS-luciferase cells were pH dissociated and resuspended in 5 μ l of medium. The mice were anesthetized by i.p. injection with Ketamine-xylazine. Using sterile techniques, the cells were injected into the striatum of immunocompromised NU/NU nude mice by stereotaxic surgery. The coordinates from bregma are lateral +2.3, anterior 0.7, and distal 3.0. Tumors were allowed to form for 7 days. Then mice were treated with luciferin to image the U87NS-luciferase cells on an IVIS xenogen camera (Caliper Life Sciences, Hopkinton, MA). Mice were then treated randomly with either DMSO carrier (n = 3) or TMZ 20 mg/kg (n = 2) by i.p. injection, on day 0. Mice were given a second DMSO or TMZ 20 mg/kg i.p. injection on day 1. Mice were analyzed 5 days after the start of treatment. DMSO control mice (n = 3) presented with robust luciferase signals on day 5 (Fig. A.3 A). These mice also possessed neurological symptoms (decreased motility) and loss of weight. All DMSO mice demonstrated significant tumor progression and were sacrificed. In contrast, the TMZ-only treated mice showed a decrease of the luciferase signal on day 5 (Fig. A.3 B). These mice were healthy and had no visible neurological symptoms. The TMZ-only mice were observed up to 27 days after the drug treatment, at which point, the mice showed significant loss of motility, appetite and weight. Luciferase expression was increased on day 27, compared to day measurements (Fig. A.3 B), demonstrating that the tumor can recover after TMZ-only treatment in an intracranial xenograft model. The future direction for this experiment is to analyze the combination of TMZ + LY411,575 treatment on intracranial xenografts. Due to the symptoms of intracranial tumors (including decreased motility and

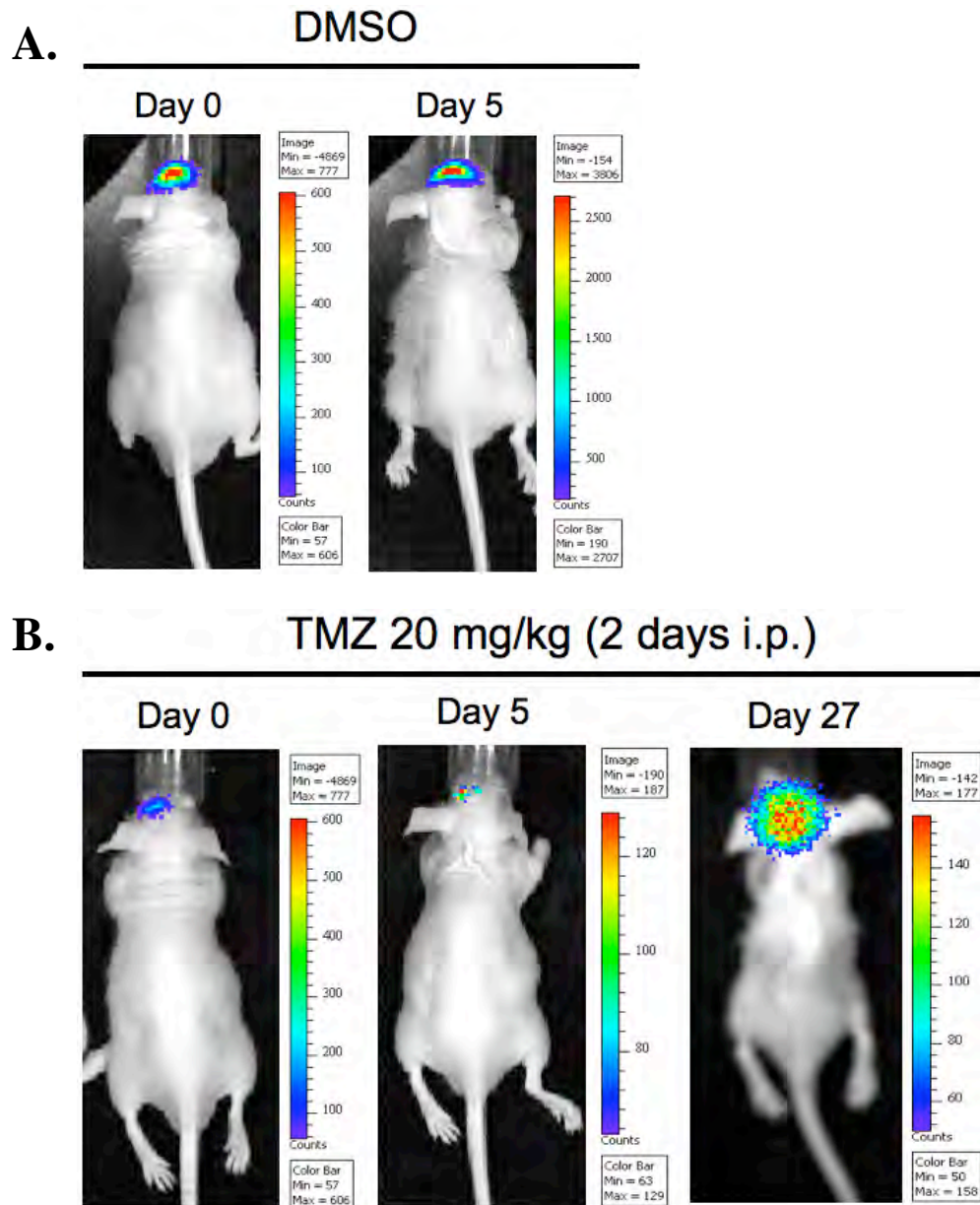


Figure A.3 **TMZ-only treated intracranial xenografts are capable of tumor progression.** U87NS-luciferase cells were injected intracranially into immunocompromised mice. Day 0 began one week after the tumor injection. DMSO treated mice ($n = 3$) had very quick tumor progression, and were sacrificed on day 5. In contrast, TMZ-only mice ($n = 2$) showed an initial decrease of tumor volume, followed by tumor regrowth. The TMZ-only treated mice were sacrificed on day 27.

loss of appetite) the synthetically infused LY chow is not an ideal form of GSI administration. Therefore, oral administration of LY411,575 solution by gavage will need to be tested for dosage and schedule treatment.

References

- Abbas, T., and Dutta, A. (2009). p21 in cancer: intricate networks and multiple activities. *Nat Rev Cancer* 9, 400-414.
- Ables, J.L., Decarolis, N.A., Johnson, M.A., Rivera, P.D., Gao, Z., Cooper, D.C., Radtke, F., Hsieh, J., and Eisch, A.J. (2010). Notch1 is required for maintenance of the reservoir of adult hippocampal stem cells. *J Neurosci* 30, 10484-10492.
- Ahmed, S. (2009). The culture of neural stem cells. *J Cell Biochem* 106, 1-6.
- Akala, O.O., Park, I.K., Qian, D., Pihalja, M., Becker, M.W., and Clarke, M.F. (2008). Long-term haematopoietic reconstitution by Trp53^{-/-}p16Ink4a^{-/-}p19Arf^{-/-} multipotent progenitors. *Nature* 453, 228-232.
- Al-Hajj, M., Wicha, M.S., Benito-Hernandez, A., Morrison, S.J., and Clarke, M.F. (2003). Prospective identification of tumorigenic breast cancer cells. *Proc Natl Acad Sci U S A* 100, 3983-3988.
- Alimonti, A., Nardella, C., Chen, Z., Clohessy, J.G., Carracedo, A., Trotman, L.C., Cheng, K., Varmeh, S., Kozma, S.C., Thomas, G., *et al.* (2010). A novel type of cellular senescence that can be enhanced in mouse models and human tumor xenografts to suppress prostate tumorigenesis. *J Clin Invest* 120, 681-693.
- Allenspach, E.J., Maillard, I., Aster, J.C., and Pear, W.S. (2002). Notch signaling in cancer. *Cancer Biol Ther* 1, 466-476.
- Altman, J. (1963). Autoradiographic investigation of cell proliferation in the brains of rats and cats. *Anat Rec* 145, 573-591.
- Altman, J., and Das, G.D. (1965). Autoradiographic and histological evidence of postnatal hippocampal neurogenesis in rats. *J Comp Neurol* 124, 319-335.
- Augelli-Szafran, C.E., Wei, H.X., Lu, D., Zhang, J., Gu, Y., Yang, T., Osenkowski, P., Ye, W., and Wolfe, M.S. (2010). Discovery of notch-sparing gamma-secretase inhibitors. *Curr Alzheimer Res* 7, 207-209.
- Aviv, H., Khan, M.Y., Skurnick, J., Okuda, K., Kimura, M., Gardner, J., Priolo, L., and Aviv, A. (2001). Age dependent aneuploidy and telomere length of the human vascular endothelium. *Atherosclerosis* 159, 281-287.
- Bachoo, R.M., Maher, E.A., Ligon, K.L., Sharpless, N.E., Chan, S.S., You, M.J., Tang, Y., DeFrances, J., Stover, E., Weissleder, R., *et al.* (2002). Epidermal growth factor receptor and Ink4a/Arf: convergent mechanisms governing terminal differentiation and transformation along the neural stem cell to astrocyte axis. *Cancer Cell* 1, 269-277.
- Bae, Y.H., Park, H.J., Kim, S.R., Kim, J.Y., Kang, Y., Kim, J.A., Wee, H.J., Kageyama, R., Jung, J.S., Bae, M.K., *et al.* (2011). Notch1 mediates visfatin-induced FGF-2 up-regulation and endothelial angiogenesis. *Cardiovasc Res* 89, 436-445.
- Baker, S.D., Wirth, M., Statkevich, P., Reidenberg, P., Alton, K., Sartorius, S.E., Dugan, M., Cutler, D., Batra, V., Grochow, L.B., *et al.* (1999). Absorption, metabolism, and excretion of ¹⁴C-temozolomide following oral administration to patients with advanced cancer. *Clin Cancer Res* 5, 309-317.

- Bao, S., Wu, Q., McLendon, R.E., Hao, Y., Shi, Q., Hjelmeland, A.B., Dewhirst, M.W., Bigner, D.D., and Rich, J.N. (2006a). Glioma stem cells promote radioresistance by preferential activation of the DNA damage response. *Nature* 444, 756-760.
- Bao, S., Wu, Q., Sathornsumetee, S., Hao, Y., Li, Z., Hjelmeland, A.B., Shi, Q., McLendon, R.E., Bigner, D.D., and Rich, J.N. (2006b). Stem cell-like glioma cells promote tumor angiogenesis through vascular endothelial growth factor. *Cancer Res* 66, 7843-7848.
- Barabe, F., Kennedy, J.A., Hope, K.J., and Dick, J.E. (2007). Modeling the initiation and progression of human acute leukemia in mice. *Science* 316, 600-604.
- Barker, N., Ridgway, R.A., van Es, J.H., van de Wetering, M., Begthel, H., van den Born, M., Danenberg, E., Clarke, A.R., Sansom, O.J., and Clevers, H. (2009). Crypt stem cells as the cells-of-origin of intestinal cancer. *Nature* 457, 608-611.
- Barraud, P., Stott, S., Mollgard, K., Parmar, M., and Bjorklund, A. (2007). In vitro characterization of a human neural progenitor cell coexpressing SSEA4 and CD133. *J Neurosci Res* 85, 250-259.
- Barten, D.M., Meredith, J.E., Jr., Zaczek, R., Houston, J.G., and Albright, C.F. (2006). Gamma-secretase inhibitors for Alzheimer's disease: balancing efficacy and toxicity. *Drugs R D* 7, 87-97.
- Bavik, C., Coleman, I., Dean, J.P., Knudsen, B., Plymate, S., and Nelson, P.S. (2006). The gene expression program of prostate fibroblast senescence modulates neoplastic epithelial cell proliferation through paracrine mechanisms. *Cancer Res* 66, 794-802.
- Beausejour, C.M., Krtolica, A., Galimi, F., Narita, M., Lowe, S.W., Yaswen, P., and Campisi, J. (2003). Reversal of human cellular senescence: roles of the p53 and p16 pathways. *EMBO J* 22, 4212-4222.
- Beel, A.J., and Sanders, C.R. (2008). Substrate specificity of gamma-secretase and other intramembrane proteases. *Cell Mol Life Sci* 65, 1311-1334.
- Beier, D., Hau, P., Proescholdt, M., Lohmeier, A., Wischhusen, J., Oefner, P.J., Aigner, L., Brawanski, A., Bogdahn, U., and Beier, C.P. (2007). CD133(+) and CD133(-) glioblastoma-derived cancer stem cells show differential growth characteristics and molecular profiles. *Cancer Res* 67, 4010-4015.
- Beier, D., Rohrl, S., Pillai, D.R., Schwarz, S., Kunz-Schughart, L.A., Leukel, P., Proescholdt, M., Brawanski, A., Bogdahn, U., Trampe-Kieslich, A., *et al.* (2008). Temozolomide preferentially depletes cancer stem cells in glioblastoma. *Cancer Res* 68, 5706-5715.
- Bhatia, B., Multani, A.S., Patrawala, L., Chen, X., Calhoun-Davis, T., Zhou, J., Schroeder, L., Schneider-Broussard, R., Shen, J., Pathak, S., *et al.* (2008). Evidence that senescent human prostate epithelial cells enhance tumorigenicity: cell fusion as a potential mechanism and inhibition by p16INK4a and hTERT. *Int J Cancer* 122, 1483-1495.
- Blagosklonny, M.V. (2006). Cell senescence: hypertrophic arrest beyond the restriction point. *J Cell Physiol* 209, 592-597.
- Blagosklonny, M.V. (2011). Cell cycle arrest is not senescence. *Aging (Albany NY)* 3, 94-101.

- Bleau, A.M., Hambarzumyan, D., Ozawa, T., Fomchenko, E.I., Huse, J.T., Brennan, C.W., and Holland, E.C. (2009). PTEN/PI3K/Akt pathway regulates the side population phenotype and ABCG2 activity in glioma tumor stem-like cells. *Cell Stem Cell* 4, 226-235.
- Bonnet, D., and Dick, J.E. (1997). Human acute myeloid leukemia is organized as a hierarchy that originates from a primitive hematopoietic cell. *Nat Med* 3, 730-737.
- Bower, M., Newlands, E.S., Bleehen, N.M., Brada, M., Begent, R.J., Calvert, H., Colquhoun, I., Lewis, P., and Brampton, M.H. (1997). Multicentre CRC phase II trial of temozolomide in recurrent or progressive high-grade glioma. *Cancer Chemother Pharmacol* 40, 484-488.
- Brada, M., Judson, I., Beale, P., Moore, S., Reidenberg, P., Statkevich, P., Dugan, M., Batra, V., and Cutler, D. (1999). Phase I dose-escalation and pharmacokinetic study of temozolomide (SCH 52365) for refractory or relapsing malignancies. *Br J Cancer* 81, 1022-1030.
- Braig, M., Lee, S., Loddenkemper, C., Rudolph, C., Peters, A.H., Schlegelberger, B., Stein, H., Dorken, B., Jenuwein, T., and Schmitt, C.A. (2005). Oncogene-induced senescence as an initial barrier in lymphoma development. *Nature* 436, 660-665.
- Brandes, A.A., Franceschi, E., Tosoni, A., Bartolini, S., Bacci, A., Agati, R., Ghimenton, C., Turazzi, S., Talacchi, A., Skrap, M., *et al.* (2010). O(6)-methylguanine DNA-methyltransferase methylation status can change between first surgery for newly diagnosed glioblastoma and second surgery for recurrence: clinical implications. *Neuro Oncol* 12, 283-288.
- Breunig, J.J., Silbereis, J., Vaccarino, F.M., Sestan, N., and Rakic, P. (2007). Notch regulates cell fate and dendrite morphology of newborn neurons in the postnatal dentate gyrus. *Proc Natl Acad Sci U S A* 104, 20558-20563.
- Buatti, J., Ryken, T.C., Smith, M.C., Sneed, P., Suh, J.H., Mehta, M., and Olson, J.J. (2008). Radiation therapy of pathologically confirmed newly diagnosed glioblastoma in adults. *J Neurooncol* 89, 313-337.
- Buchler, P., Gazdhar, A., Schubert, M., Giese, N., Reber, H.A., Hines, O.J., Giese, T., Ceyhan, G.O., Muller, M., Buchler, M.W., *et al.* (2005). The Notch signaling pathway is related to neurovascular progression of pancreatic cancer. *Ann Surg* 242, 791-800, discussion 800-791.
- Buick, R.N., Minden, M.D., and McCulloch, E.A. (1979). Self-renewal in culture of proliferative blast progenitor cells in acute myeloblastic leukemia. *Blood* 54, 95-104.
- Cahill, D.P., Levine, K.K., Betensky, R.A., Codd, P.J., Romany, C.A., Reavie, L.B., Batchelor, T.T., Futreal, P.A., Stratton, M.R., Curry, W.T., *et al.* (2007). Loss of the mismatch repair protein MSH6 in human glioblastomas is associated with tumor progression during temozolomide treatment. *Clin Cancer Res* 13, 2038-2045.
- Calabrese, C., Poppleton, H., Kocak, M., Hogg, T.L., Fuller, C., Hamner, B., Oh, E.Y., Gaber, M.W., Finklestein, D., Allen, M., *et al.* (2007). A perivascular niche for brain tumor stem cells. *Cancer Cell* 11, 69-82.
- Campisi, J., and d'Adda di Fagagna, F. (2007). Cellular senescence: when bad things happen to good cells. *Nat Rev Mol Cell Biol* 8, 729-740.

- Canoll, P., and Goldman, J.E. (2008). The interface between glial progenitors and gliomas. *Acta Neuropathol* 116, 465-477.
- Carson, M.J., Doose, J.M., Melchior, B., Schmid, C.D., and Ploix, C.C. (2006). CNS immune privilege: hiding in plain sight. *Immunol Rev* 213, 48-65.
- Cayphas, S., Van Damme, J., Vink, A., Simpson, R.J., Billiau, A., and Van Snick, J. (1987). Identification of an interleukin HP1-like plasmacytoma growth factor produced by L cells in response to viral infection. *J Immunol* 139, 2965-2969.
- CBTRUS (2010). CBTRUS Statistical Report: Primary Brain and Central Nervous System Tumors Diagnosed in the United States in 2004-2006. (Hinsdale, IL, Central Brain Tumor Registry of the United States).
- Chaichana, K.L., Kosztowski, T., Niranjan, A., Olivi, A., Weingart, J.D., Lattera, J., Brem, H., and Quinones-Hinojosa, A. (2010). Prognostic significance of contrast-enhancing anaplastic astrocytomas in adults. *J Neurosurg* 113, 286-292.
- Chalmers, A.J., Ruff, E.M., Martindale, C., Lovegrove, N., and Short, S.C. (2009). Cytotoxic effects of temozolomide and radiation are additive- and schedule-dependent. *Int J Radiat Oncol Biol Phys* 75, 1511-1519.
- Chamberlain, M.C., Wei-Tsao, D.D., Blumenthal, D.T., and Glantz, M.J. (2008). Salvage chemotherapy with CPT-11 for recurrent temozolomide-refractory anaplastic astrocytoma. *Cancer* 112, 2038-2045.
- Chen, J., Kesari, S., Rooney, C., Strack, P.R., Shen, H., Wu, L., and Griffin, J.D. (2010a). Inhibition of Notch Signaling Blocks Growth of Glioblastoma Cell Lines and Tumor Neurospheres. *Genes Cancer* 1, 822-835.
- Chen, R., Nishimura, M.C., Bumbaca, S.M., Kharbanda, S., Forrest, W.F., Kasman, I.M., Greve, J.M., Soriano, R.H., Gilmour, L.L., Rivers, C.S., *et al.* (2010b). A hierarchy of self-renewing tumor-initiating cell types in glioblastoma. *Cancer Cell* 17, 362-375.
- Cheng, L., Bao, S., and Rich, J.N. (2010). Potential therapeutic implications of cancer stem cells in glioblastoma. *Biochem Pharmacol* 80, 654-665.
- Chin, L., Meyerson, M., Aldape, K., Bigner, D., Mikkelsen, T., VandenBerg, S., Kahn, A., Penny, R., Ferguson, M.L., Gerhard, D.S., *et al.* (2008). Comprehensive genomic characterization defines human glioblastoma genes and core pathways. *Nature* 455, 1061-1068.
- Christensen, K., Aaberg-Jessen, C., Andersen, C., Goplen, D., Bjerkvig, R., and Kristensen, B.W. (2010). Immunohistochemical expression of stem cell, endothelial cell, and chemosensitivity markers in primary glioma spheroids cultured in serum-containing and serum-free medium. *Neurosurgery* 66, 933-947.
- Clarke, M.F., Dick, J.E., Dirks, P.B., Eaves, C.J., Jamieson, C.H., Jones, D.L., Visvader, J., Weissman, I.L., and Wahl, G.M. (2006). Cancer stem cells--perspectives on current status and future directions: AACR Workshop on cancer stem cells. *Cancer Res* 66, 9339-9344.
- Collado, M., Gil, J., Efeyan, A., Guerra, C., Schuhmacher, A.J., Barradas, M., Benguria, A., Zaballos, A., Flores, J.M., Barbacid, M., *et al.* (2005). Tumour biology: senescence in premalignant tumours. *Nature* 436, 642.
- Coller, H.A., Sang, L., and Roberts, J.M. (2006). A new description of cellular quiescence. *PLoS Biol* 4, e83.

- Coppe, J.P., Desprez, P.Y., Krtolica, A., and Campisi, J. (2010). The senescence-associated secretory phenotype: the dark side of tumor suppression. *Annu Rev Pathol* 5, 99-118.
- Coppe, J.P., Kauser, K., Campisi, J., and Beausejour, C.M. (2006). Secretion of vascular endothelial growth factor by primary human fibroblasts at senescence. *J Biol Chem* 281, 29568-29574.
- Coppe, J.P., Patil, C.K., Rodier, F., Sun, Y., Munoz, D.P., Goldstein, J., Nelson, P.S., Desprez, P.Y., and Campisi, J. (2008). Senescence-associated secretory phenotypes reveal cell-nonautonomous functions of oncogenic RAS and the p53 tumor suppressor. *PLoS Biol* 6, 2853-2868.
- Cortez, M.A., Nicoloso, M.S., Shimizu, M., Rossi, S., Gopisetty, G., Molina, J.R., Carlotti, C., Jr., Tirapelli, D., Neder, L., Brassesco, M.S., *et al.* (2010). miR-29b and miR-125a regulate podoplanin and suppress invasion in glioblastoma. *Genes Chromosomes Cancer*.
- Coskun, V., Wu, H., Bianchi, B., Tsao, S., Kim, K., Zhao, J., Biancotti, J.C., Hutnick, L., Krueger, R.C., Jr., Fan, G., *et al.* (2008). CD133+ neural stem cells in the ependyma of mammalian postnatal forebrain. *Proc Natl Acad Sci U S A* 105, 1026-1031.
- Counter, C.M., Meyerson, M., Eaton, E.N., Ellisen, L.W., Caddle, S.D., Haber, D.A., and Weinberg, R.A. (1998). Telomerase activity is restored in human cells by ectopic expression of hTERT (hEST2), the catalytic subunit of telomerase. *Oncogene* 16, 1217-1222.
- Courtois-Cox, S., Genter Williams, S.M., Reczek, E.E., Johnson, B.W., McGillicuddy, L.T., Johannessen, C.M., Hollstein, P.E., MacCollin, M., and Cichowski, K. (2006). A negative feedback signaling network underlies oncogene-induced senescence. *Cancer Cell* 10, 459-472.
- Dang, T.P., Gazdar, A.F., Virmani, A.K., Sepetavec, T., Hande, K.R., Minna, J.D., Roberts, J.R., and Carbone, D.P. (2000). Chromosome 19 translocation, overexpression of Notch3, and human lung cancer. *J Natl Cancer Inst* 92, 1355-1357.
- De Keersmaecker, K., Lahortiga, I., Mentens, N., Folens, C., Van Neste, L., Bekaert, S., Vandenberghe, P., Odero, M.D., Marynen, P., and Cools, J. (2008). In vitro validation of gamma-secretase inhibitors alone or in combination with other anti-cancer drugs for the treatment of T-cell acute lymphoblastic leukemia. *Haematologica* 93, 533-542.
- Debacq-Chainiaux, F., Erusalimsky, J.D., Campisi, J., and Toussaint, O. (2009). Protocols to detect senescence-associated beta-galactosidase (SA-beta-gal) activity, a biomarker of senescent cells in culture and in vivo. *Nat Protoc* 4, 1798-1806.
- Desjardins, A., Reardon, D.A., Herndon, J.E., 2nd, Marcello, J., Quinn, J.A., Rich, J.N., Sathornsumetee, S., Gururangan, S., Sampson, J., Bailey, L., *et al.* (2008). Bevacizumab plus irinotecan in recurrent WHO grade 3 malignant gliomas. *Clin Cancer Res* 14, 7068-7073.
- Di Tomaso, T., Mazzoleni, S., Wang, E., Sovena, G., Clavenna, D., Franzin, A., Mortini, P., Ferrone, S., Doglioni, C., Marincola, F.M., *et al.* (2010). Immunobiological characterization of cancer stem cells isolated from glioblastoma patients. *Clin Cancer Res* 16, 800-813.

- Diehn, M., and Majeti, R. (2010). Metastatic cancer stem cells: an opportunity for improving cancer treatment? *Cell Stem Cell* 6, 502-503.
- Dievart, A., Beaulieu, N., and Jolicoeur, P. (1999). Involvement of Notch1 in the development of mouse mammary tumors. *Oncogene* 18, 5973-5981.
- Dirac, A.M., and Bernards, R. (2003). Reversal of senescence in mouse fibroblasts through lentiviral suppression of p53. *J Biol Chem* 278, 11731-11734.
- Doetsch, F., Caille, I., Lim, D.A., Garcia-Verdugo, J.M., and Alvarez-Buylla, A. (1999). Subventricular zone astrocytes are neural stem cells in the adult mammalian brain. *Cell* 97, 703-716.
- Doetsch, F., Garcia-Verdugo, J.M., and Alvarez-Buylla, A. (1997). Cellular composition and three-dimensional organization of the subventricular germinal zone in the adult mammalian brain. *J Neurosci* 17, 5046-5061.
- Dovey, H.F., John, V., Anderson, J.P., Chen, L.Z., de Saint Andrieu, P., Fang, L.Y., Freedman, S.B., Folmer, B., Goldbach, E., Holsztynska, E.J., *et al.* (2001). Functional gamma-secretase inhibitors reduce beta-amyloid peptide levels in brain. *J Neurochem* 76, 173-181.
- Dresemann, G. (2010). Temozolomide in malignant glioma. *Onco Targets Ther* 3, 139-146.
- Eaves, C.J. (2008). Cancer stem cells: Here, there, everywhere? *Nature* 456, 581-582.
- Ellisen, L.W., Bird, J., West, D.C., Soreng, A.L., Reynolds, T.C., Smith, S.D., and Sklar, J. (1991). TAN-1, the human homolog of the Drosophila notch gene, is broken by chromosomal translocations in T lymphoblastic neoplasms. *Cell* 66, 649-661.
- Ernst, A., Hofmann, S., Ahmadi, R., Becker, N., Korshunov, A., Engel, F., Hartmann, C., Felsberg, J., Sabel, M., Peterziel, H., *et al.* (2009). Genomic and expression profiling of glioblastoma stem cell-like spheroid cultures identifies novel tumor-relevant genes associated with survival. *Clin Cancer Res* 15, 6541-6550.
- Evan, G.I., and d'Adda di Fagagna, F. (2009). Cellular senescence: hot or what? *Curr Opin Genet Dev* 19, 25-31.
- Ewald, J.A., Desotelle, J.A., Wilding, G., and Jarrard, D.F. (2010). Therapy-induced senescence in cancer. *J Natl Cancer Inst* 102, 1536-1546.
- Fan, X., Khaki, L., Zhu, T.S., Soules, M.E., Talsma, C.E., Gul, N., Koh, C., Zhang, J., Li, Y.M., Maciaczyk, J., *et al.* (2010). NOTCH pathway blockade depletes CD133-positive glioblastoma cells and inhibits growth of tumor neurospheres and xenografts. *Stem Cells* 28, 5-16.
- Fang, W., Mori, T., and Cobrinik, D. (2002). Regulation of PML-dependent transcriptional repression by pRB and low penetrance pRB mutants. *Oncogene* 21, 5557-5565.
- Fauq, A.H., Simpson, K., Maharvi, G.M., Golde, T., and Das, P. (2007). A multigram chemical synthesis of the gamma-secretase inhibitor LY411575 and its diastereoisomers. *Bioorg Med Chem Lett* 17, 6392-6395.
- Fischer, A., and Gessler, M. (2007). Delta-Notch--and then? Protein interactions and proposed modes of repression by Hes and Hey bHLH factors. *Nucleic Acids Res* 35, 4583-4596.

- Fleisher, A.S., Raman, R., Siemers, E.R., Becerra, L., Clark, C.M., Dean, R.A., Farlow, M.R., Galvin, J.E., Peskind, E.R., Quinn, J.F., *et al.* (2008). Phase 2 safety trial targeting amyloid beta production with a gamma-secretase inhibitor in Alzheimer disease. *Arch Neurol* 65, 1031-1038.
- Fortini, M.E. (2009). Notch signaling: the core pathway and its posttranslational regulation. *Dev Cell* 16, 633-647.
- Fossati, G., Ricevuti, G., Edwards, S.W., Walker, C., Dalton, A., and Rossi, M.L. (1999). Neutrophil infiltration into human gliomas. *Acta Neuropathol* 98, 349-354.
- Freund, A., Orjalo, A.V., Desprez, P.Y., and Campisi, J. (2010). Inflammatory networks during cellular senescence: causes and consequences. *Trends Mol Med* 16, 238-246.
- Friedman, H.S., McLendon, R.E., Kerby, T., Dugan, M., Bigner, S.H., Henry, A.J., Ashley, D.M., Krischer, J., Lovell, S., Rasheed, K., *et al.* (1998). DNA mismatch repair and O6-alkylguanine-DNA alkyltransferase analysis and response to Temodal in newly diagnosed malignant glioma. *J Clin Oncol* 16, 3851-3857.
- Friedman, H.S., Prados, M.D., Wen, P.Y., Mikkelsen, T., Schiff, D., Abrey, L.E., Yung, W.K., Paleologos, N., Nicholas, M.K., Jensen, R., *et al.* (2009). Bevacizumab alone and in combination with irinotecan in recurrent glioblastoma. *J Clin Oncol* 27, 4733-4740.
- Fukuda, S., Kato, F., Tozuka, Y., Yamaguchi, M., Miyamoto, Y., and Hisatsune, T. (2003). Two distinct subpopulations of nestin-positive cells in adult mouse dentate gyrus. *J Neurosci* 23, 9357-9366.
- Fukushima, T., Takeshima, H., and Kataoka, H. (2009). Anti-glioma therapy with temozolomide and status of the DNA-repair gene MGMT. *Anticancer Res* 29, 4845-4854.
- Gaiano, N., Nye, J.S., and Fishell, G. (2000). Radial glial identity is promoted by Notch1 signaling in the murine forebrain. *Neuron* 26, 395-404.
- Galli, R., Binda, E., Orfanelli, U., Cipelletti, B., Gritti, A., De Vitis, S., Fiocco, R., Foroni, C., Dimeco, F., and Vescovi, A. (2004). Isolation and characterization of tumorigenic, stem-like neural precursors from human glioblastoma. *Cancer Res* 64, 7011-7021.
- Gehrmann, J., Matsumoto, Y., and Kreutzberg, G.W. (1995). Microglia: intrinsic immuneffector cell of the brain. *Brain Res Brain Res Rev* 20, 269-287.
- Gerson, S.L. (2002). Clinical relevance of MGMT in the treatment of cancer. *J Clin Oncol* 20, 2388-2399.
- Ghods, A.J., Irvin, D., Liu, G., Yuan, X., Abdulkadir, I.R., Tunici, P., Konda, B., Wachsmann-Hogiu, S., Black, K.L., and Yu, J.S. (2007). Spheres isolated from 9L gliosarcoma rat cell line possess chemoresistant and aggressive cancer stem-like cells. *Stem Cells* 25, 1645-1653.
- Giacinti, C., and Giordano, A. (2006). RB and cell cycle progression. *Oncogene* 25, 5220-5227.
- Gilbert, C.A., Daou, M., Moser, R.P., and Ross, A.H. (2010). γ -Secretase Inhibitors Enhance Temozolomide Treatment of Human Gliomas by Inhibiting Neurosphere Repopulation and Xenograft Recurrence. *Cancer Res* 70, 6870-6879.

- Gilbert, C.A., Ramirez, Y.P., Weatherbee, J., MacKay, C., Kurt-Jones, E.A., and Ross, A.H. (unpublished). Enhancement of Temozolomide Treatment by Inhibition of Notch Signaling is due to Therapy-Induced Senescence
- Gilbert, C.A., and Ross, A.H. (2009). Cancer stem cells: cell culture, markers, and targets for new therapies. *J Cell Biochem* 108, 1031-1038.
- Gong, X., Schwartz, P.H., Linskey, M.E., and Bota, D.A. (2011). Neural stem/progenitors and glioma stem-like cells have differential sensitivity to chemotherapy. *Neurology*.
- Graeber, M.B., and Streit, W.J. (2010). Microglia: biology and pathology. *Acta Neuropathol* 119, 89-105.
- Grandbarbe, L., Michelucci, A., Heurtaux, T., Hemmer, K., Morga, E., and Heuschling, P. (2007). Notch signaling modulates the activation of microglial cells. *Glia* 55, 1519-1530.
- Grandori, C., Wu, K.J., Fernandez, P., Ngouenet, C., Grim, J., Clurman, B.E., Moser, M.J., Oshima, J., Russell, D.W., Swisshelm, K., *et al.* (2003). Werner syndrome protein limits MYC-induced cellular senescence. *Genes Dev* 17, 1569-1574.
- Grey, B.R., Oates, J.E., Brown, M.D., and Clarke, N.W. (2009). Cd133: a marker of transit amplification rather than stem cell phenotype in the prostate? *BJU Int* 103, 856-858.
- Grossman, S.A., Reinhard, C., Colvin, O.M., Chasin, M., Brundrett, R., Tamargo, R.J., and Brem, H. (1992). The intracerebral distribution of BCNU delivered by surgically implanted biodegradable polymers. *J Neurosurg* 76, 640-647.
- Gunther, H.S., Schmidt, N.O., Phillips, H.S., Kemming, D., Kharbanda, S., Soriano, R., Modrusan, Z., Meissner, H., Westphal, M., and Lamszus, K. (2008). Glioblastoma-derived stem cell-enriched cultures form distinct subgroups according to molecular and phenotypic criteria. *Oncogene* 27, 2897-2909.
- Gunther, W., Pawlak, E., Damasceno, R., Arnold, H., and Terzis, A.J. (2003). Temozolomide induces apoptosis and senescence in glioma cells cultured as multicellular spheroids. *Br J Cancer* 88, 463-469.
- Guo, D., Ye, J., Dai, J., Li, L., Chen, F., Ma, D., and Ji, C. (2009). Notch-1 regulates Akt signaling pathway and the expression of cell cycle regulatory proteins cyclin D1, CDK2 and p21 in T-ALL cell lines. *Leuk Res* 33, 678-685.
- Gupta, P.B., Chaffer, C.L., and Weinberg, R.A. (2009). Cancer stem cells: mirage or reality? *Nat Med* 15, 1010-1012.
- Hanisch, U.K., and Kettenmann, H. (2007). Microglia: active sensor and versatile effector cells in the normal and pathologic brain. *Nat Neurosci* 10, 1387-1394.
- Haraguchi, N., Utsunomiya, T., Inoue, H., Tanaka, F., Mimori, K., Barnard, G.F., and Mori, M. (2006). Characterization of a side population of cancer cells from human gastrointestinal system. *Stem Cells* 24, 506-513.
- Harley, C.B., Futcher, A.B., and Greider, C.W. (1990). Telomeres shorten during ageing of human fibroblasts. *Nature* 345, 458-460.
- Hartwell, L.H., Culotti, J., Pringle, J.R., and Reid, B.J. (1974). Genetic control of the cell division cycle in yeast. *Science* 183, 46-51.

- Hayflick, L., and Moorhead, P.S. (1961). The serial cultivation of human diploid cell strains. *Exp Cell Res* 25, 585-621.
- Heddleston, J.M., Li, Z., McLendon, R.E., Hjelmeland, A.B., and Rich, J.N. (2009). The hypoxic microenvironment maintains glioblastoma stem cells and promotes reprogramming towards a cancer stem cell phenotype. *Cell Cycle* 8, 3274-3284.
- Heitzler, P., and Simpson, P. (1993). Altered epidermal growth factor-like sequences provide evidence for a role of Notch as a receptor in cell fate decisions. *Development* 117, 1113-1123.
- Hemmati, H.D., Nakano, I., Lazareff, J.A., Masterman-Smith, M., Geschwind, D.H., Bronner-Fraser, M., and Kornblum, H.I. (2003). Cancerous stem cells can arise from pediatric brain tumors. *Proc Natl Acad Sci U S A* 100, 15178-15183.
- Hill, R.P., and Perris, R. (2007). "Destemming" cancer stem cells. *J Natl Cancer Inst* 99, 1435-1440.
- Hirose, Y., Berger, M.S., and Pieper, R.O. (2001). p53 effects both the duration of G2/M arrest and the fate of temozolomide-treated human glioblastoma cells. *Cancer Res* 61, 1957-1963.
- Hitoshi, S., Alexson, T., Tropepe, V., Donoviel, D., Elia, A.J., Nye, J.S., Conlon, R.A., Mak, T.W., Bernstein, A., and van der Kooy, D. (2002). Notch pathway molecules are essential for the maintenance, but not the generation, of mammalian neural stem cells. *Genes Dev* 16, 846-858.
- Holland, E.C., Celestino, J., Dai, C., Schaefer, L., Sawaya, R.E., and Fuller, G.N. (2000). Combined activation of Ras and Akt in neural progenitors induces glioblastoma formation in mice. *Nat Genet* 25, 55-57.
- Holland, E.C., Hively, W.P., DePinho, R.A., and Varmus, H.E. (1998). A constitutively active epidermal growth factor receptor cooperates with disruption of G1 cell-cycle arrest pathways to induce glioma-like lesions in mice. *Genes Dev* 12, 3675-3685.
- Holyoake, T., Jiang, X., Eaves, C., and Eaves, A. (1999). Isolation of a highly quiescent subpopulation of primitive leukemic cells in chronic myeloid leukemia. *Blood* 94, 2056-2064.
- Hope, K.J., Jin, L., and Dick, J.E. (2004). Acute myeloid leukemia originates from a hierarchy of leukemic stem cell classes that differ in self-renewal capacity. *Nat Immunol* 5, 738-743.
- Hovinga, K.E., Shimizu, F., Wang, R., Panagiotakos, G., Van Der Heijden, M., Moayedpardazi, H., Correia, A.S., Soulet, D., Major, T., Menon, J., *et al.* (2010). Inhibition of notch signaling in glioblastoma targets cancer stem cells via an endothelial cell intermediate. *Stem Cells* 28, 1019-1029.
- Huck, J.J., Zhang, M., McDonald, A., Bowman, D., Hoar, K.M., Stringer, B., Ecsedy, J., Manfredi, M.G., and Hyer, M.L. (2010). MLN8054, an inhibitor of Aurora A kinase, induces senescence in human tumor cells both in vitro and in vivo. *Mol Cancer Res* 8, 373-384.
- Humphries, W., Wei, J., Sampson, J.H., and Heimberger, A.B. (2010). The role of tregs in glioma-mediated immunosuppression: potential target for intervention. *Neurosurg Clin N Am* 21, 125-137.

- Hunter, C., Smith, R., Cahill, D.P., Stephens, P., Stevens, C., Teague, J., Greenman, C., Edkins, S., Bignell, G., Davies, H., *et al.* (2006). A hypermutation phenotype and somatic MSH6 mutations in recurrent human malignant gliomas after alkylator chemotherapy. *Cancer Res* 66, 3987-3991.
- Iso, T., Kedes, L., and Hamamori, Y. (2003). HES and HERP families: multiple effectors of the Notch signaling pathway. *J Cell Physiol* 194, 237-255.
- Jackson, M.W., Agarwal, M.K., Yang, J., Bruss, P., Uchiumi, T., Agarwal, M.L., Stark, G.R., and Taylor, W.R. (2005). p130/p107/p105Rb-dependent transcriptional repression during DNA-damage-induced cell-cycle exit at G2. *J Cell Sci* 118, 1821-1832.
- Jacobsen, T.L., Brennan, K., Arias, A.M., and Muskavitch, M.A. (1998). Cis-interactions between Delta and Notch modulate neurogenic signalling in *Drosophila*. *Development* 125, 4531-4540.
- Jaiswal, S., Chao, M.P., Majeti, R., and Weissman, I.L. (2010). Macrophages as mediators of tumor immunosurveillance. *Trends Immunol* 31, 212-219.
- Jaksch, M., Munera, J., Bajpai, R., Terskikh, A., and Oshima, R.G. (2008). Cell cycle-dependent variation of a CD133 epitope in human embryonic stem cell, colon cancer, and melanoma cell lines. *Cancer Res* 68, 7882-7886.
- Jeon, H.M., Jin, X., Lee, J.S., Oh, S.Y., Sohn, Y.W., Park, H.J., Joo, K.M., Park, W.Y., Nam, D.H., DePinho, R.A., *et al.* (2008). Inhibitor of differentiation 4 drives brain tumor-initiating cell genesis through cyclin E and notch signaling. *Genes Dev* 22, 2028-2033.
- Ji, P., Jiang, H., Rekhtman, K., Bloom, J., Ichetovkin, M., Pagano, M., and Zhu, L. (2004). An Rb-Skp2-p27 pathway mediates acute cell cycle inhibition by Rb and is retained in a partial-penetrance Rb mutant. *Mol Cell* 16, 47-58.
- Jiang, L., Wu, J., Chen, Q., Hu, X., Li, W., and Hu, G. (2011). Notch1 expression is upregulated in glioma and is associated with tumor progression. *J Clin Neurosci* 18, 387-390.
- Jing, W., Xiong, Z., Cai, X., Huang, Y., Li, X., Yang, X., Liu, L., Tang, W., Lin, Y., and Tian, W. (2010). Effects of gamma-secretase inhibition on the proliferation and vitamin D(3) induced osteogenesis in adipose derived stem cells. *Biochem Biophys Res Commun* 392, 442-447.
- Johansson, C.B., Momma, S., Clarke, D.L., Risling, M., Lendahl, U., and Frisen, J. (1999a). Identification of a neural stem cell in the adult mammalian central nervous system. *Cell* 96, 25-34.
- Johansson, C.B., Svensson, M., Wallstedt, L., Janson, A.M., and Frisen, J. (1999b). Neural stem cells in the adult human brain. *Exp Cell Res* 253, 733-736.
- Johnson, M.A., Ables, J.L., and Eisch, A.J. (2009). Cell-intrinsic signals that regulate adult neurogenesis in vivo: insights from inducible approaches. *BMB Rep* 42, 245-259.
- Jude, C.D., Gaudet, J.J., Speck, N.A., and Ernst, P. (2008). Leukemia and hematopoietic stem cells: balancing proliferation and quiescence. *Cell Cycle* 7, 586-591.
- Kanamori, M., Kawaguchi, T., Nigro, J.M., Feuerstein, B.G., Berger, M.S., Miele, L., and Pieper, R.O. (2007). Contribution of Notch signaling activation to human glioblastoma multiforme. *J Neurosurg* 106, 417-427.
- Kang, M.K., and Kang, S.K. (2007). Tumorigenesis of chemotherapeutic drug-resistant cancer stem-like cells in brain glioma. *Stem Cells Dev* 16, 837-847.

- Kawaguchi, A., Miyata, T., Sawamoto, K., Takashita, N., Murayama, A., Akamatsu, W., Ogawa, M., Okabe, M., Tano, Y., Goldman, S.A., *et al.* (2001). Nestin-EGFP transgenic mice: visualization of the self-renewal and multipotency of CNS stem cells. *Mol Cell Neurosci* 17, 259-273.
- Kelly, P.N., Dakic, A., Adams, J.M., Nutt, S.L., and Strasser, A. (2007). Tumor growth need not be driven by rare cancer stem cells. *Science* 317, 337.
- Kennedy, J.A., Barabe, F., Poepl, A.G., Wang, J.C., and Dick, J.E. (2007). Comment on "Tumor growth need not be driven by rare cancer stem cells". *Science* 318, 1722; author reply 1722.
- Koch, U., and Radtke, F. (2007). Notch and cancer: a double-edged sword. *Cell Mol Life Sci* 64, 2746-2762.
- Krebs, L.T., Xue, Y., Norton, C.R., Shutter, J.R., Maguire, M., Sundberg, J.P., Gallahan, D., Closson, V., Kitajewski, J., Callahan, R., *et al.* (2000). Notch signaling is essential for vascular morphogenesis in mice. *Genes Dev* 14, 1343-1352.
- Kreft, A.F., Martone, R., and Porte, A. (2009). Recent advances in the identification of gamma-secretase inhibitors to clinically test the Abeta oligomer hypothesis of Alzheimer's disease. *J Med Chem* 52, 6169-6188.
- Kreisl, T.N., Kim, L., Moore, K., Duic, P., Royce, C., Stroud, I., Garren, N., Mackey, M., Butman, J.A., Camphausen, K., *et al.* (2009). Phase II trial of single-agent bevacizumab followed by bevacizumab plus irinotecan at tumor progression in recurrent glioblastoma. *J Clin Oncol* 27, 740-745.
- Kriegstein, A., and Alvarez-Buylla, A. (2009). The glial nature of embryonic and adult neural stem cells. *Annu Rev Neurosci* 32, 149-184.
- Krizhanovsky, V., Yon, M., Dickins, R.A., Hearn, S., Simon, J., Miething, C., Yee, H., Zender, L., and Lowe, S.W. (2008). Senescence of activated stellate cells limits liver fibrosis. *Cell* 134, 657-667.
- Krtolica, A., Parrinello, S., Lockett, S., Desprez, P.Y., and Campisi, J. (2001). Senescent fibroblasts promote epithelial cell growth and tumorigenesis: a link between cancer and aging. *Proc Natl Acad Sci U S A* 98, 12072-12077.
- Ksiazek, K., Jorres, A., and Witowski, J. (2008). Senescence induces a proangiogenic switch in human peritoneal mesothelial cells. *Rejuvenation Res* 11, 681-683.
- Lanz, T.A., Hosley, J.D., Adams, W.J., and Merchant, K.M. (2004). Studies of Abeta pharmacodynamics in the brain, cerebrospinal fluid, and plasma in young (plaque-free) Tg2576 mice using the gamma-secretase inhibitor N2-[(2S)-2-(3,5-difluorophenyl)-2-hydroxyethanoyl]-N1-[(7S)-5-methyl-6-oxo-6,7-dihydro-5H-dibenzo[b,d]azepin-7-yl]-L-alaninamide (LY-411575). *J Pharmacol Exp Ther* 309, 49-55.
- Lathia, J.D., Gallagher, J., Heddleston, J.M., Wang, J., Eyler, C.E., Macswords, J., Wu, Q., Vasanthi, A., McLendon, R.E., Hjelmeland, A.B., *et al.* (2010). Integrin alpha 6 regulates glioblastoma stem cells. *Cell Stem Cell* 6, 421-432.
- Lathia, J.D., Venere, M., Rao, M.S., and Rich, J.N. (2011). Seeing is Believing: Are Cancer Stem Cells the Loch Ness Monster of Tumor Biology? *Stem Cell Rev* 7, 227-237.
- Lazzerini Denchi, E., Attwooll, C., Pasini, D., and Helin, K. (2005). Deregulated E2F activity induces hyperplasia and senescence-like features in the mouse pituitary gland. *Mol Cell Biol* 25, 2660-2672.

- Lee, B.Y., Han, J.A., Im, J.S., Morrone, A., Johung, K., Goodwin, E.C., Kleijer, W.J., DiMaio, D., and Hwang, E.S. (2006a). Senescence-associated beta-galactosidase is lysosomal beta-galactosidase. *Aging Cell* 5, 187-195.
- Lee, J., Kotliarova, S., Kotliarov, Y., Li, A., Su, Q., Donin, N.M., Pastorino, S., Purow, B.W., Christopher, N., Zhang, W., *et al.* (2006b). Tumor stem cells derived from glioblastomas cultured in bFGF and EGF more closely mirror the phenotype and genotype of primary tumors than do serum-cultured cell lines. *Cancer Cell* 9, 391-403.
- Lefort, K., Mandinova, A., Ostano, P., Kolev, V., Calpini, V., Kolfschoten, I., Devgan, V., Lieb, J., Raffoul, W., Hohl, D., *et al.* (2007). Notch1 is a p53 target gene involved in human keratinocyte tumor suppression through negative regulation of ROCK1/2 and MRCKalpha kinases. *Genes Dev* 21, 562-577.
- Lendahl, U., Zimmerman, L.B., and McKay, R.D. (1990). CNS stem cells express a new class of intermediate filament protein. *Cell* 60, 585-595.
- Li, J., Cui, Y., Gao, G., Zhao, Z., Zhang, H., and Wang, X. (2011). Notch1 is an independent prognostic factor for patients with glioma. *J Surg Oncol*.
- Li, J., Yang, X.K., Yu, X.X., Ge, M.L., Wang, W.L., Zhang, J., and Hou, Y.D. (2000). Overexpression of p27(KIP1) induced cell cycle arrest in G(1) phase and subsequent apoptosis in HCC-9204 cell line. *World J Gastroenterol* 6, 513-521.
- Li, L., Dutra, A., Pak, E., Labrie, J.E., 3rd, Gerstein, R.M., Pandolfi, P.P., Recht, L.D., and Ross, A.H. (2009a). EGFRvIII expression and PTEN loss synergistically induce chromosomal instability and glial tumors. *Neuro Oncol* 11, 9-21.
- Li, Z., Bao, S., Wu, Q., Wang, H., Eyler, C., Sathornsumetee, S., Shi, Q., Cao, Y., Lathia, J., McLendon, R.E., *et al.* (2009b). Hypoxia-inducible factors regulate tumorigenic capacity of glioma stem cells. *Cancer Cell* 15, 501-513.
- Lin, H.K., Chen, Z., Wang, G., Nardella, C., Lee, S.W., Chan, C.H., Yang, W.L., Wang, J., Egia, A., Nakayama, K.I., *et al.* (2010a). Skp2 targeting suppresses tumorigenesis by Arf-p53-independent cellular senescence. *Nature* 464, 374-379.
- Lin, J., Zhang, X.M., Yang, J.C., Ye, Y.B., and Luo, S.Q. (2010b). gamma-secretase inhibitor-I enhances radiosensitivity of glioblastoma cell lines by depleting CD133+ tumor cells. *Arch Med Res* 41, 519-529.
- Liu, D., and Hornsby, P.J. (2007). Senescent human fibroblasts increase the early growth of xenograft tumors via matrix metalloproteinase secretion. *Cancer Res* 67, 3117-3126.
- Liu, G., Yuan, X., Zeng, Z., Tunici, P., Ng, H., Abdulkadir, I.R., Lu, L., Irvin, D., Black, K.L., and Yu, J.S. (2006). Analysis of gene expression and chemoresistance of CD133+ cancer stem cells in glioblastoma. *Mol Cancer* 5, 67.
- Liu, S., Breit, S., Danckwardt, S., Muckenthaler, M.U., and Kulozik, A.E. (2009). Downregulation of Notch signaling by gamma-secretase inhibition can abrogate chemotherapy-induced apoptosis in T-ALL cell lines. *Ann Hematol* 88, 613-621.
- Logeat, F., Bessia, C., Brou, C., LeBail, O., Jarriault, S., Seidah, N.G., and Israel, A. (1998). The Notch1 receptor is cleaved constitutively by a furin-like convertase. *Proc Natl Acad Sci U S A* 95, 8108-8112.
- Lottaz, C., Beier, D., Meyer, K., Kumar, P., Hermann, A., Schwarz, J., Junker, M., Oefner, P.J., Bogdahn, U., Wischhusen, J., *et al.* (2010). Transcriptional profiles of

CD133+ and CD133- glioblastoma-derived cancer stem cell lines suggest different cells of origin. *Cancer Res* 70, 2030-2040.

Lu, C., and Shervington, A. (2008). Chemoresistance in gliomas. *Mol Cell Biochem* 312, 71-80.

Lugert, S., Basak, O., Knuckles, P., Haussler, U., Fabel, K., Gotz, M., Haas, C.A., Kempermann, G., Taylor, V., and Giachino, C. (2010). Quiescent and active hippocampal neural stem cells with distinct morphologies respond selectively to physiological and pathological stimuli and aging. *Cell Stem Cell* 6, 445-456.

Ma, S., Lee, T.K., Zheng, B.J., Chan, K.W., and Guan, X.Y. (2008). CD133+ HCC cancer stem cells confer chemoresistance by preferential expression of the Akt/PKB survival pathway. *Oncogene* 27, 1749-1758.

Majumder, P.K., Grisanzio, C., O'Connell, F., Barry, M., Brito, J.M., Xu, Q., Guney, I., Berger, R., Herman, P., Bikoff, R., *et al.* (2008). A prostatic intraepithelial neoplasia-dependent p27 Kip1 checkpoint induces senescence and inhibits cell proliferation and cancer progression. *Cancer Cell* 14, 146-155.

Mao, X.G., Zhang, X., Xue, X.Y., Guo, G., Wang, P., Zhang, W., Fei, Z., Zhen, H.N., You, S.W., and Yang, H. (2009). Brain Tumor Stem-Like Cells Identified by Neural Stem Cell Marker CD15. *Transl Oncol* 2, 247-257.

McCormack, M.P., Young, L.F., Vasudevan, S., de Graaf, C.A., Codrington, R., Rabbitts, T.H., Jane, S.M., and Curtis, D.J. (2010). The Lmo2 oncogene initiates leukemia in mice by inducing thymocyte self-renewal. *Science* 327, 879-883.

McVicar, D.W., Davis, D.F., and Merchant, R.E. (1992). In vitro analysis of the proliferative potential of T cells from patients with brain tumor: glioma-associated immunosuppression unrelated to intrinsic cellular defect. *J Neurosurg* 76, 251-260.

Medema, R.H., Klompaker, R., Smits, V.A., and Rijksen, G. (1998). p21waf1 can block cells at two points in the cell cycle, but does not interfere with processive DNA-replication or stress-activated kinases. *Oncogene* 16, 431-441.

Mellor, H.R., Ferguson, D.J., and Callaghan, R. (2005). A model of quiescent tumour microregions for evaluating multicellular resistance to chemotherapeutic drugs. *Br J Cancer* 93, 302-309.

Mhaidat, N.M., Zhang, X.D., Allen, J., Avery-Kiejda, K.A., Scott, R.J., and Hersey, P. (2007). Temozolomide induces senescence but not apoptosis in human melanoma cells. *Br J Cancer* 97, 1225-1233.

Michaloglou, C., Vredeveld, L.C., Soengas, M.S., Denoyelle, C., Kuilman, T., van der Horst, C.M., Majoor, D.M., Shay, J.W., Mooi, W.J., and Peeper, D.S. (2005).

BRAFE600-associated senescence-like cell cycle arrest of human naevi. *Nature* 436, 720-724.

Miele, L. (2006). Notch signaling. *Clin Cancer Res* 12, 1074-1079.

Mihaliak, A.M., Gilbert, C.A., Li, L., Daou, M., Moser, R.P., Reeves, A., Cochran, B.H., and Ross, A.H. (2010). Clinically relevant doses of chemotherapy agents reversibly block formation of glioblastoma neurospheres. *Cancer Lett* 296, 168-177.

- Mirzayans, R., Scott, A., Cameron, M., and Murray, D. (2005). Induction of accelerated senescence by gamma radiation in human solid tumor-derived cell lines expressing wild-type TP53. *Radiat Res* 163, 53-62.
- Muntoni, A., and Reddel, R.R. (2005). The first molecular details of ALT in human tumor cells. *Hum Mol Genet* 14 *Spec No. 2*, R191-196.
- Naderi, S., Hunton, I.C., and Wang, J.Y. (2002). Radiation dose-dependent maintenance of G(2) arrest requires retinoblastoma protein. *Cell Cycle* 1, 193-200.
- Namihira, M., Kohyama, J., Semi, K., Sanosaka, T., Deneen, B., Taga, T., and Nakashima, K. (2009). Committed neuronal precursors confer astrocytic potential on residual neural precursor cells. *Dev Cell* 16, 245-255.
- Narita, M., Nunez, S., Heard, E., Lin, A.W., Hearn, S.A., Spector, D.L., Hannon, G.J., and Lowe, S.W. (2003). Rb-mediated heterochromatin formation and silencing of E2F target genes during cellular senescence. *Cell* 113, 703-716.
- Nefedova, Y., Sullivan, D.M., Bolick, S.C., Dalton, W.S., and Gabrilovich, D.I. (2008). Inhibition of Notch signaling induces apoptosis of myeloma cells and enhances sensitivity to chemotherapy. *Blood* 111, 2220-2229.
- Newlands, E.S., Blackledge, G.R., Slack, J.A., Rustin, G.J., Smith, D.B., Stuart, N.S., Quarterman, C.P., Hoffman, R., Stevens, M.F., Brampton, M.H., *et al.* (1992). Phase I trial of temozolomide (CCRG 81045: M&B 39831: NSC 362856). *Br J Cancer* 65, 287-291.
- Newlands, E.S., Stevens, M.F., Wedge, S.R., Wheelhouse, R.T., and Brock, C. (1997). Temozolomide: a review of its discovery, chemical properties, pre-clinical development and clinical trials. *Cancer Treat Rev* 23, 35-61.
- Niculescu, A.B., 3rd, Chen, X., Smeets, M., Hengst, L., Prives, C., and Reed, S.I. (1998). Effects of p21(Cip1/Waf1) at both the G1/S and the G2/M cell cycle transitions: pRb is a critical determinant in blocking DNA replication and in preventing endoreduplication. *Mol Cell Biol* 18, 629-643.
- Noguera-Troise, I., Daly, C., Papadopoulos, N.J., Coetzee, S., Boland, P., Gale, N.W., Lin, H.C., Yancopoulos, G.D., and Thurston, G. (2006). Blockade of Dll4 inhibits tumour growth by promoting non-productive angiogenesis. *Nature* 444, 1032-1037.
- O'Brien, C.A., Pollett, A., Gallinger, S., and Dick, J.E. (2007). A human colon cancer cell capable of initiating tumour growth in immunodeficient mice. *Nature* 445, 106-110.
- O'Neill, C.F., Urs, S., Cinelli, C., Lincoln, A., Nadeau, R.J., Leon, R., Toher, J., Mouta-Bellum, C., Friesel, R.E., and Liaw, L. (2007). Notch2 signaling induces apoptosis and inhibits human MDA-MB-231 xenograft growth. *Am J Pathol* 171, 1023-1036.
- O'Reilly, S.M., Newlands, E.S., Glaser, M.G., Brampton, M., Rice-Edwards, J.M., Illingworth, R.D., Richards, P.G., Kennard, C., Colquhoun, I.R., Lewis, P., *et al.* (1993). Temozolomide: a new oral cytotoxic chemotherapeutic agent with promising activity against primary brain tumours. *Eur J Cancer* 29A, 940-942.
- Ogden, A.T., Waziri, A.E., Lochhead, R.A., Fusco, D., Lopez, K., Ellis, J.A., Kang, J., Assanah, M., McKhann, G.M., Sisti, M.B., *et al.* (2008). Identification of A2B5+CD133-tumor-initiating cells in adult human gliomas. *Neurosurgery* 62, 505-514; discussion 514-505.

- Olson, R.E., and Albright, C.F. (2008). Recent progress in the medicinal chemistry of gamma-secretase inhibitors. *Curr Top Med Chem* 8, 17-33.
- Osipo, C., Patel, P., Rizzo, P., Clementz, A.G., Hao, L., Golde, T.E., and Miele, L. (2008). ErbB-2 inhibition activates Notch-1 and sensitizes breast cancer cells to a gamma-secretase inhibitor. *Oncogene* 27, 5019-5032.
- Ostermann, S., Csajka, C., Buclin, T., Leyvraz, S., Lejeune, F., Decosterd, L.A., and Stupp, R. (2004). Plasma and cerebrospinal fluid population pharmacokinetics of temozolomide in malignant glioma patients. *Clin Cancer Res* 10, 3728-3736.
- Oswald, F., Liptay, S., Adler, G., and Schmid, R.M. (1998). NF-kappaB2 is a putative target gene of activated Notch-1 via RBP-Jkappa. *Mol Cell Biol* 18, 2077-2088.
- Ota, H., Tokunaga, E., Chang, K., Hikasa, M., Iijima, K., Eto, M., Kozaki, K., Akishita, M., Ouchi, Y., and Kaneki, M. (2006). Sirt1 inhibitor, Sirtinol, induces senescence-like growth arrest with attenuated Ras-MAPK signaling in human cancer cells. *Oncogene* 25, 176-185.
- Palmer, T.D., Willhoite, A.R., and Gage, F.H. (2000). Vascular niche for adult hippocampal neurogenesis. *J Comp Neurol* 425, 479-494.
- Palomero, T., Lim, W.K., Odom, D.T., Sulis, M.L., Real, P.J., Margolin, A., Barnes, K.C., O'Neil, J., Neuberg, D., Weng, A.P., *et al.* (2006). NOTCH1 directly regulates c-MYC and activates a feed-forward-loop transcriptional network promoting leukemic cell growth. *Proc Natl Acad Sci U S A* 103, 18261-18266.
- Pannuti, A., Foreman, K., Rizzo, P., Osipo, C., Golde, T., Osborne, B., and Miele, L. (2010). Targeting Notch to target cancer stem cells. *Clin Cancer Res* 16, 3141-3152.
- Pardee, A.B. (1974). A restriction point for control of normal animal cell proliferation. *Proc Natl Acad Sci U S A* 71, 1286-1290.
- Patrawala, L., Calhoun, T., Schneider-Broussard, R., Zhou, J., Claypool, K., and Tang, D.G. (2005). Side population is enriched in tumorigenic, stem-like cancer cells, whereas ABCG2+ and ABCG2- cancer cells are similarly tumorigenic. *Cancer Res* 65, 6207-6219.
- Pfaffl, M.W. (2001). A new mathematical model for relative quantification in real-time RT-PCR. *Nucleic Acids Res* 29, e45.
- Pfenninger, C.V., Roschupkina, T., Hertwig, F., Kottwitz, D., Englund, E., Bengzon, J., Jacobsen, S.E., and Nuber, U.A. (2007). CD133 is not present on neurogenic astrocytes in the adult subventricular zone, but on embryonic neural stem cells, ependymal cells, and glioblastoma cells. *Cancer Res* 67, 5727-5736.
- Phillips, H.S., Kharbanda, S., Chen, R., Forrest, W.F., Soriano, R.H., Wu, T.D., Misra, A., Nigro, J.M., Colman, H., Soroceanu, L., *et al.* (2006). Molecular subclasses of high-grade glioma predict prognosis, delineate a pattern of disease progression, and resemble stages in neurogenesis. *Cancer Cell* 9, 157-173.
- Piccirillo, S.G., Reynolds, B.A., Zanetti, N., Lamorte, G., Binda, E., Broggi, G., Brem, H., Olivi, A., Dimeco, F., and Vescovi, A.L. (2006). Bone morphogenetic proteins inhibit the tumorigenic potential of human brain tumour-initiating cells. *Nature* 444, 761-765.
- Polager, S., and Ginsberg, D. (2003). E2F mediates sustained G2 arrest and down-regulation of Stathmin and AIM-1 expression in response to genotoxic stress. *J Biol Chem* 278, 1443-1449.

- Pollard, J.W. (2004). Tumour-educated macrophages promote tumour progression and metastasis. *Nat Rev Cancer* 4, 71-78.
- Pollard, S.M., Yoshikawa, K., Clarke, I.D., Danovi, D., Stricker, S., Russell, R., Bayani, J., Head, R., Lee, M., Bernstein, M., *et al.* (2009). Glioma stem cell lines expanded in adherent culture have tumor-specific phenotypes and are suitable for chemical and genetic screens. *Cell Stem Cell* 4, 568-580.
- Ponti, D., Costa, A., Zaffaroni, N., Pratesi, G., Petrangolini, G., Coradini, D., Pilotti, S., Pierotti, M.A., and Daidone, M.G. (2005). Isolation and in vitro propagation of tumorigenic breast cancer cells with stem/progenitor cell properties. *Cancer Res* 65, 5506-5511.
- Pruszek, J., Sonntag, K.C., Aung, M.H., Sanchez-Pernaute, R., and Isacson, O. (2007). Markers and methods for cell sorting of human embryonic stem cell-derived neural cell populations. *Stem Cells* 25, 2257-2268.
- Pui, J.C., Allman, D., Xu, L., DeRocco, S., Karnell, F.G., Bakkour, S., Lee, J.Y., Kadesch, T., Hardy, R.R., Aster, J.C., *et al.* (1999). Notch1 expression in early lymphopoiesis influences B versus T lineage determination. *Immunity* 11, 299-308.
- Purow, B.W., Haque, R.M., Noel, M.W., Su, Q., Burdick, M.J., Lee, J., Sundaresan, T., Pastorino, S., Park, J.K., Mikolaenko, I., *et al.* (2005). Expression of Notch-1 and its ligands, Delta-like-1 and Jagged-1, is critical for glioma cell survival and proliferation. *Cancer Res* 65, 2353-2363.
- Qiang, L., Yang, Y., Ma, Y.J., Chen, F.H., Zhang, L.B., Liu, W., Qi, Q., Lu, N., Tao, L., Wang, X.T., *et al.* (2009). Isolation and characterization of cancer stem like cells in human glioblastoma cell lines. *Cancer Lett* 279, 13-21.
- Qiu, B., Zhang, D., Wang, C., Tao, J., Tie, X., Qiao, Y., Xu, K., Wang, Y., and Wu, A. (2010). IL-10 and TGF-beta2 are overexpressed in tumor spheres cultured from human gliomas. *Mol Biol Rep*.
- Quintana, E., Shackleton, M., Sabel, M.S., Fullen, D.R., Johnson, T.M., and Morrison, S.J. (2008). Efficient tumour formation by single human melanoma cells. *Nature* 456, 593-598.
- Radaelli, E., Ceruti, R., Patton, V., Russo, M., Degrassi, A., Croci, V., Caprera, F., Stortini, G., Scanziani, E., Pesenti, E., *et al.* (2009). Immunohistopathological and neuroimaging characterization of murine orthotopic xenograft models of glioblastoma multiforme recapitulating the most salient features of human disease. *Histol Histopathol* 24, 879-891.
- Radtke, F., and Raj, K. (2003). The role of Notch in tumorigenesis: oncogene or tumour suppressor? *Nat Rev Cancer* 3, 756-767.
- Rasband, W.S. (1997-2004). ImageJ, U. S. National Institutes of Health, Bethesda, Maryland, USA.
- Ratajczak, M.Z. (2008). Phenotypic and functional characterization of hematopoietic stem cells. *Curr Opin Hematol* 15, 293-300.
- Reynolds, B.A., Tetzlaff, W., and Weiss, S. (1992). A multipotent EGF-responsive striatal embryonic progenitor cell produces neurons and astrocytes. *J Neurosci* 12, 4565-4574.

- Reynolds, B.A., and Weiss, S. (1992). Generation of neurons and astrocytes from isolated cells of the adult mammalian central nervous system. *Science* 255, 1707-1710.
- Reynolds, B.A., and Weiss, S. (1996). Clonal and population analyses demonstrate that an EGF-responsive mammalian embryonic CNS precursor is a stem cell. *Dev Biol* 175, 1-13.
- Ricci-Vitiani, L., Lombardi, D.G., Pilozzi, E., Biffoni, M., Todaro, M., Peschle, C., and De Maria, R. (2007). Identification and expansion of human colon-cancer-initiating cells. *Nature* 445, 111-115.
- Ricci-Vitiani, L., Pallini, R., Biffoni, M., Todaro, M., Invernici, G., Cenci, T., Maira, G., Parati, E.A., Stassi, G., Larocca, L.M., *et al.* (2010). Tumour vascularization via endothelial differentiation of glioblastoma stem-like cells. *Nature* 468, 824-828.
- Rich, J.N. (2008). The Implications of the Cancer Stem Cell Hypothesis for Neuro-Oncology and Neurology. *Future Neurol* 3, 265-273.
- Ridgway, J., Zhang, G., Wu, Y., Stawicki, S., Liang, W.C., Chantry, Y., Kowalski, J., Watts, R.J., Callahan, C., Kasman, I., *et al.* (2006). Inhibition of Dll4 signalling inhibits tumour growth by deregulating angiogenesis. *Nature* 444, 1083-1087.
- Rizzo, P., Osipo, C., Foreman, K., Golde, T., Osborne, B., and Miele, L. (2008). Rational targeting of Notch signaling in cancer. *Oncogene* 27, 5124-5131.
- Robbins, J., Blondel, B.J., Gallahan, D., and Callahan, R. (1992). Mouse mammary tumor gene int-3: a member of the notch gene family transforms mammary epithelial cells. *J Virol* 66, 2594-2599.
- Rodier, F., and Campisi, J. (2011). Four faces of cellular senescence. *J Cell Biol*.
- Rodrigues, J.C., Gonzalez, G.C., Zhang, L., Ibrahim, G., Kelly, J.J., Gustafson, M.P., Lin, Y., Dietz, A.B., Forsyth, P.A., Yong, V.W., *et al.* (2010). Normal human monocytes exposed to glioma cells acquire myeloid-derived suppressor cell-like properties. *Neuro Oncol* 12, 351-365.
- Ronchini, C., and Capobianco, A.J. (2001). Induction of cyclin D1 transcription and CDK2 activity by Notch(ic): implication for cell cycle disruption in transformation by Notch(ic). *Mol Cell Biol* 21, 5925-5934.
- Roy, M., Pear, W.S., and Aster, J.C. (2007). The multifaceted role of Notch in cancer. *Curr Opin Genet Dev* 17, 52-59.
- Rozen, S., and Skaletsky, H. (2000). Primer3 on the WWW for general users and for biologist programmers. *Methods Mol Biol* 132, 365-386.
- Salmaggi, A., Boiardi, A., Gelati, M., Russo, A., Calatozzolo, C., Ciusani, E., Sciacca, F.L., Ottolina, A., Parati, E.A., La Porta, C., *et al.* (2006). Glioblastoma-derived tumorspheres identify a population of tumor stem-like cells with angiogenic potential and enhanced multidrug resistance phenotype. *Glia* 54, 850-860.
- Samon, J.B., Champhekar, A., Minter, L.M., Telfer, J.C., Miele, L., Fauq, A., Das, P., Golde, T.E., and Osborne, B.A. (2008). Notch1 and TGFbeta1 cooperatively regulate Foxp3 expression and the maintenance of peripheral regulatory T cells. *Blood* 112, 1813-1821.
- Sanai, N., Alvarez-Buylla, A., and Berger, M.S. (2005). Neural stem cells and the origin of gliomas. *N Engl J Med* 353, 811-822.

- Sanai, N., and Berger, M.S. (2008). Glioma extent of resection and its impact on patient outcome. *Neurosurgery* 62, 753-764; discussion 264-756.
- Sanalkumar, R., Dhanesh, S.B., and James, J. (2010). Non-canonical activation of Notch signaling/target genes in vertebrates. *Cell Mol Life Sci* 67, 2957-2968.
- Sang, L., Collier, H.A., and Roberts, J.M. (2008). Control of the reversibility of cellular quiescence by the transcriptional repressor HES1. *Science* 321, 1095-1100.
- Sarkaria, J.N., Kitange, G.J., James, C.D., Plummer, R., Calvert, H., Weller, M., and Wick, W. (2008). Mechanisms of chemoresistance to alkylating agents in malignant glioma. *Clin Cancer Res* 14, 2900-2908.
- Sato, Y., Kurose, A., Ogawa, A., Ogasawara, K., Traganos, F., Darzynkiewicz, Z., and Sawai, T. (2009). Diversity of DNA damage response of astrocytes and glioblastoma cell lines with various p53 status to treatment with etoposide and temozolomide. *Cancer Biol Ther* 8, 452-457.
- Schafer, K.A. (1998). The cell cycle: a review. *Vet Pathol* 35, 461-478.
- Schmitt, C.A., Fridman, J.S., Yang, M., Lee, S., Baranov, E., Hoffman, R.M., and Lowe, S.W. (2002). A senescence program controlled by p53 and p16INK4a contributes to the outcome of cancer therapy. *Cell* 109, 335-346.
- Schoenhaut, D.S., Chua, A.O., Wolitzky, A.G., Quinn, P.M., Dwyer, C.M., McComas, W., Familletti, P.C., Gately, M.K., and Gubler, U. (1992). Cloning and expression of murine IL-12. *J Immunol* 148, 3433-3440.
- Scopelliti, A., Cammareri, P., Catalano, V., Saladino, V., Todaro, M., and Stassi, G. (2009). Therapeutic implications of Cancer Initiating Cells. *Expert Opin Biol Ther* 9, 1005-1016.
- Sen, A., Kallos, M.S., and Behie, L.A. (2004). New tissue dissociation protocol for scaled-up production of neural stem cells in suspension bioreactors. *Tissue Eng* 10, 904-913.
- Seri, B., Garcia-Verdugo, J.M., Collado-Morente, L., McEwen, B.S., and Alvarez-Buylla, A. (2004). Cell types, lineage, and architecture of the germinal zone in the adult dentate gyrus. *J Comp Neurol* 478, 359-378.
- Serrano, M., Lin, A.W., McCurrach, M.E., Beach, D., and Lowe, S.W. (1997). Oncogenic ras provokes premature cell senescence associated with accumulation of p53 and p16INK4a. *Cell* 88, 593-602.
- Shackleton, M., Quintana, E., Fearon, E.R., and Morrison, S.J. (2009). Heterogeneity in cancer: cancer stem cells versus clonal evolution. *Cell* 138, 822-829.
- Shafee, N., Smith, C.R., Wei, S., Kim, Y., Mills, G.B., Hortobagyi, G.N., Stanbridge, E.J., and Lee, E.Y. (2008). Cancer stem cells contribute to cisplatin resistance in Brca1/p53-mediated mouse mammary tumors. *Cancer Res* 68, 3243-3250.
- Sharma, V.M., Calvo, J.A., Draheim, K.M., Cunningham, L.A., Hermance, N., Beverly, L., Krishnamoorthy, V., Bhasin, M., Capobianco, A.J., and Kelliher, M.A. (2006). Notch1 contributes to mouse T-cell leukemia by directly inducing the expression of c-myc. *Mol Cell Biol* 26, 8022-8031.
- Shay, J.W., and Bacchetti, S. (1997). A survey of telomerase activity in human cancer. *Eur J Cancer* 33, 787-791.

- Shay, J.W., Pereira-Smith, O.M., and Wright, W.E. (1991). A role for both RB and p53 in the regulation of human cellular senescence. *Exp Cell Res* 196, 33-39.
- Sherr, C.J., and McCormick, F. (2002). The RB and p53 pathways in cancer. *Cancer Cell* 2, 103-112.
- Sherry, M.M., Reeves, A., Wu, J.K., and Cochran, B.H. (2009). STAT3 is required for proliferation and maintenance of multipotency in glioblastoma stem cells. *Stem Cells* 27, 2383-2392.
- Shih, A.H., and Holland, E.C. (2006). Notch signaling enhances nestin expression in gliomas. *Neoplasia* 8, 1072-1082.
- Shin, D.M., Zuba-Surma, E.K., Wu, W., Ratajczak, J., Wysoczynski, M., Ratajczak, M.Z., and Kucia, M. (2009). Novel epigenetic mechanisms that control pluripotency and quiescence of adult bone marrow-derived Oct4(+) very small embryonic-like stem cells. *Leukemia* 23, 2042-2051.
- Siemers, E., Skinner, M., Dean, R.A., Gonzales, C., Satterwhite, J., Farlow, M., Ness, D., and May, P.C. (2005). Safety, tolerability, and changes in amyloid beta concentrations after administration of a gamma-secretase inhibitor in volunteers. *Clin Neuropharmacol* 28, 126-132.
- Siemers, E.R., Quinn, J.F., Kaye, J., Farlow, M.R., Porsteinsson, A., Tariot, P., Zoulnouni, P., Galvin, J.E., Holtzman, D.M., Knopman, D.S., *et al.* (2006). Effects of a gamma-secretase inhibitor in a randomized study of patients with Alzheimer disease. *Neurology* 66, 602-604.
- Silvestre, D.C., Pineda Marti, J.R., Hoffschir, F., Studler, J.M., Mouthon, M.A., Pflumio, F., Junier, M.P., Chneiweiss, H., and Boussin, F.D. (2011). Alternative Lengthening of Telomeres in Human Glioma Stem Cells. *Stem Cells*.
- Singec, I., Knoth, R., Meyer, R.P., Maciaczyk, J., Volk, B., Nikkhah, G., Frotscher, M., and Snyder, E.Y. (2006). Defining the actual sensitivity and specificity of the neurosphere assay in stem cell biology. *Nat Methods* 3, 801-806.
- Singh, S.K., Clarke, I.D., Terasaki, M., Bonn, V.E., Hawkins, C., Squire, J., and Dirks, P.B. (2003). Identification of a cancer stem cell in human brain tumors. *Cancer Res* 63, 5821-5828.
- Singh, S.K., Hawkins, C., Clarke, I.D., Squire, J.A., Bayani, J., Hide, T., Henkelman, R.M., Cusimano, M.D., and Dirks, P.B. (2004). Identification of human brain tumour initiating cells. *Nature* 432, 396-401.
- Sliwa, M., Markovic, D., Gabrusiewicz, K., Synowitz, M., Glass, R., Zawadzka, M., Wesolowska, A., Kettenmann, H., and Kaminska, B. (2007). The invasion promoting effect of microglia on glioblastoma cells is inhibited by cyclosporin A. *Brain* 130, 476-489.
- Snippert, H.J., van Es, J.H., van den Born, M., Begthel, H., Stange, D.E., Barker, N., and Clevers, H. (2009). Prominin-1/CD133 marks stem cells and early progenitors in mouse small intestine. *Gastroenterology* 136, 2187-2194 e2181.
- Somasundaram, K., Reddy, S.P., Vinnakota, K., Britto, R., Subbarayan, M., Nambiar, S., Hebbar, A., Samuel, C., Shetty, M., Sreepathi, H.K., *et al.* (2005). Upregulation of ASCL1 and inhibition of Notch signaling pathway characterize progressive astrocytoma. *Oncogene* 24, 7073-7083.

- Son, M.J., Woolard, K., Nam, D.H., Lee, J., and Fine, H.A. (2009). SSEA-1 is an enrichment marker for tumor-initiating cells in human glioblastoma. *Cell Stem Cell* 4, 440-452.
- Spiro, T.P., Liu, L., Majka, S., Haaga, J., Willson, J.K., and Gerson, S.L. (2001). Temozolomide: the effect of once- and twice-a-day dosing on tumor tissue levels of the DNA repair protein O(6)-alkylguanine-DNA-alkyltransferase. *Clin Cancer Res* 7, 2309-2317.
- Stevens, A., Kloter, I., and Roggendorf, W. (1988). Inflammatory infiltrates and natural killer cell presence in human brain tumors. *Cancer* 61, 738-743.
- Stockhausen, M.T., Kristoffersen, K., and Poulsen, H.S. (2010). The functional role of Notch signaling in human gliomas. *Neuro Oncol* 12, 199-211.
- Stupp, R., Hegi, M.E., Mason, W.P., van den Bent, M.J., Taphoorn, M.J., Janzer, R.C., Ludwin, S.K., Allgeier, A., Fisher, B., Belanger, K., *et al.* (2009). Effects of radiotherapy with concomitant and adjuvant temozolomide versus radiotherapy alone on survival in glioblastoma in a randomised phase III study: 5-year analysis of the EORTC-NCIC trial. *Lancet Oncol*.
- Stupp, R., Mason, W.P., van den Bent, M.J., Weller, M., Fisher, B., Taphoorn, M.J., Belanger, K., Brandes, A.A., Marosi, C., Bogdahn, U., *et al.* (2005). Radiotherapy plus concomitant and adjuvant temozolomide for glioblastoma. *N Engl J Med* 352, 987-996.
- Suh, H., Consiglio, A., Ray, J., Sawai, T., D'Amour, K.A., and Gage, F.H. (2007). In vivo fate analysis reveals the multipotent and self-renewal capacities of Sox2+ neural stem cells in the adult hippocampus. *Cell Stem Cell* 1, 515-528.
- Suwanjune, S., Wongchana, W., and Palaga, T. (2008). Inhibition of gamma-secretase affects proliferation of leukemia and hepatoma cell lines through Notch signaling. *Anticancer Drugs* 19, 477-486.
- Suzuki, M., and Boothman, D.A. (2008). Stress-induced premature senescence (SIPS)--influence of SIPS on radiotherapy. *J Radiat Res (Tokyo)* 49, 105-112.
- Takahashi, T., and Caviness, V.S., Jr. (1993). PCNA-binding to DNA at the G1/S transition in proliferating cells of the developing cerebral wall. *J Neurocytol* 22, 1096-1102.
- Tamura, K., Aoyagi, M., Wakimoto, H., Ando, N., Nariai, T., Yamamoto, M., and Ohno, K. (2010). Accumulation of CD133-positive glioma cells after high-dose irradiation by Gamma Knife surgery plus external beam radiation. *J Neurosurg* 113, 310-318.
- Tang, D.G., Patrawala, L., Calhoun, T., Bhatia, B., Choy, G., Schneider-Broussard, R., and Jeter, C. (2007). Prostate cancer stem/progenitor cells: identification, characterization, and implications. *Mol Carcinog* 46, 1-14.
- Tavazoie, M., Van der Veken, L., Silva-Vargas, V., Louissaint, M., Colonna, L., Zaidi, B., Garcia-Verdugo, J.M., and Doetsch, F. (2008). A specialized vascular niche for adult neural stem cells. *Cell Stem Cell* 3, 279-288.
- Tchoghandjian, A., Baeza, N., Colin, C., Cayre, M., Metellus, P., Beclin, C., Ouafik, L., and Figarella-Branger, D. (2010). A2B5 Cells from Human Glioblastoma have Cancer Stem Cell Properties. *Brain Pathol* 20, 211-221.

- te Poele, R.H., Okorokov, A.L., Jardine, L., Cummings, J., and Joel, S.P. (2002). DNA damage is able to induce senescence in tumor cells in vitro and in vivo. *Cancer Res* 62, 1876-1883.
- Uchida, N., Buck, D.W., He, D., Reitsma, M.J., Masek, M., Phan, T.V., Tsukamoto, A.S., Gage, F.H., and Weissman, I.L. (2000). Direct isolation of human central nervous system stem cells. *Proc Natl Acad Sci U S A* 97, 14720-14725.
- Ulasov, I.V., Nandi, S., Dey, M., Sonabend, A.M., and Lesniak, M.S. (2011). Inhibition of Sonic Hedgehog and Notch Pathways Enhances Sensitivity of CD133(+) Glioma Stem Cells to Temozolomide Therapy. *Mol Med* 17, 103-112.
- Varghese, M., Olstorn, H., Sandberg, C., Vik-Mo, E.O., Noordhuis, P., Nister, M., Berg-Johnsen, J., Moe, M.C., and Langmoen, I.A. (2008). A comparison between stem cells from the adult human brain and from brain tumors. *Neurosurgery* 63, 1022-1033; discussion 1033-1024.
- Venere, M., Fine, H.A., Dirks, P.B., and Rich, J.N. (2011). Cancer stem cells in gliomas: Identifying and understanding the apex cell in cancer's hierarchy. *Glia*.
- Venkatesh, D., Fredette, N., Rostama, B., Tang, Y., Vary, C.P., Liaw, L., and Urs, S. (2011). RhoA-Mediated Signaling in Notch-Induced Senescence-Like Growth Arrest and Endothelial Barrier Dysfunction. *Arterioscler Thromb Vasc Biol*.
- Walén, K.H. (2008). Genetic stability of senescence reverted cells: genome reduction division of polyploidy cells, aneuploidy and neoplasia. *Cell Cycle* 7, 1623-1629.
- Wang, J., Wakeman, T.P., Lathia, J.D., Hjelmeland, A.B., Wang, X.F., White, R.R., Rich, J.N., and Sullenger, B.A. (2010a). Notch promotes radioresistance of glioma stem cells. *Stem Cells* 28, 17-28.
- Wang, R., Chadalavada, K., Wilshire, J., Kowalik, U., Hovinga, K.E., Geber, A., Fligelman, B., Leversha, M., Brennan, C., and Tabar, V. (2010b). Glioblastoma stem-like cells give rise to tumour endothelium. *Nature* 468, 829-833.
- Wang, Y.C., He, F., Feng, F., Liu, X.W., Dong, G.Y., Qin, H.Y., Hu, X.B., Zheng, M.H., Liang, L., Feng, L., *et al.* (2010c). Notch signaling determines the M1 versus M2 polarization of macrophages in antitumor immune responses. *Cancer Res* 70, 4840-4849.
- Wedge, S.R., Porteous, J.K., Glaser, M.G., Marcus, K., and Newlands, E.S. (1997). In vitro evaluation of temozolomide combined with X-irradiation. *Anticancer Drugs* 8, 92-97.
- Wei, J., Barr, J., Kong, L.Y., Wang, Y., Wu, A., Sharma, A.K., Gumin, J., Henry, V., Colman, H., Priebe, W., *et al.* (2010a). Glioblastoma cancer-initiating cells inhibit T-cell proliferation and effector responses by the signal transducers and activators of transcription 3 pathway. *Mol Cancer Ther* 9, 67-78.
- Wei, J., Barr, J., Kong, L.Y., Wang, Y., Wu, A., Sharma, A.K., Gumin, J., Henry, V., Colman, H., Sawaya, R., *et al.* (2010b). Glioma-associated cancer-initiating cells induce immunosuppression. *Clin Cancer Res* 16, 461-473.
- Weng, A.P., Ferrando, A.A., Lee, W., Morris, J.P.t., Silverman, L.B., Sanchez-Irizarry, C., Blacklow, S.C., Look, A.T., and Aster, J.C. (2004). Activating mutations of NOTCH1 in human T cell acute lymphoblastic leukemia. *Science* 306, 269-271.
- Wolfe, M.S. (2010). Structure, mechanism and inhibition of gamma-secretase and presenilin-like proteases. *Biol Chem* 391, 839-847.

- Wong, G.T., Manfra, D., Poulet, F.M., Zhang, Q., Josien, H., Bara, T., Engstrom, L., Pinzon-Ortiz, M., Fine, J.S., Lee, H.J., *et al.* (2004). Chronic treatment with the gamma-secretase inhibitor LY-411,575 inhibits beta-amyloid peptide production and alters lymphopoiesis and intestinal cell differentiation. *J Biol Chem* 279, 12876-12882.
- Woolard, K., and Fine, H.A. (2009). Glioma stem cells: better flat than round. *Cell Stem Cell* 4, 466-467.
- Wu, A., Wei, J., Kong, L.Y., Wang, Y., Priebe, W., Qiao, W., Sawaya, R., and Heimberger, A.B. (2010a). Glioma cancer stem cells induce immunosuppressive macrophages/microglia. *Neuro Oncol*.
- Wu, Y., Cain-Hom, C., Choy, L., Hagenbeek, T.J., de Leon, G.P., Chen, Y., Finkle, D., Venook, R., Wu, X., Ridgway, J., *et al.* (2010b). Therapeutic antibody targeting of individual Notch receptors. *Nature* 464, 1052-1057.
- Xu, P., Qiu, M., Zhang, Z., Kang, C., Jiang, R., Jia, Z., Wang, G., Jiang, H., and Pu, P. (2010). The oncogenic roles of Notch1 in astrocytic gliomas in vitro and in vivo. *J Neurooncol* 97, 41-51.
- Xue, W., Zender, L., Miething, C., Dickins, R.A., Hernando, E., Krizhanovsky, V., Cordon-Cardo, C., and Lowe, S.W. (2007). Senescence and tumour clearance is triggered by p53 restoration in murine liver carcinomas. *Nature* 445, 656-660.
- Yamasaki, T. (2004). Absence of antitumor natural killer cell-mediated defense in the brain. *Surg Neurol* 61, 227-228.
- Yang, I., Han, S.J., Kaur, G., Crane, C., and Parsa, A.T. (2010). The role of microglia in central nervous system immunity and glioma immunology. *J Clin Neurosci* 17, 6-10.
- Yip, S., Miao, J., Cahill, D.P., Iafrate, A.J., Aldape, K., Nutt, C.L., and Louis, D.N. (2009). MSH6 mutations arise in glioblastomas during temozolomide therapy and mediate temozolomide resistance. *Clin Cancer Res* 15, 4622-4629.
- Yu, X., Zou, J., Ye, Z., Hammond, H., Chen, G., Tokunaga, A., Mali, P., Li, Y.M., Civin, C., Gaiano, N., *et al.* (2008). Notch signaling activation in human embryonic stem cells is required for embryonic, but not trophoblastic, lineage commitment. *Cell Stem Cell* 2, 461-471.
- Yung, W.K., Prados, M.D., Yaya-Tur, R., Rosenfeld, S.S., Brada, M., Friedman, H.S., Albright, R., Olson, J., Chang, S.M., O'Neill, A.M., *et al.* (1999). Multicenter phase II trial of temozolomide in patients with anaplastic astrocytoma or anaplastic oligoastrocytoma at first relapse. Temodal Brain Tumor Group. *J Clin Oncol* 17, 2762-2771.
- Zagouras, P., Stifani, S., Blaumueller, C.M., Carcangiu, M.L., and Artavanis-Tsakonas, S. (1995). Alterations in Notch signaling in neoplastic lesions of the human cervix. *Proc Natl Acad Sci U S A* 92, 6414-6418.
- Zeisberger, S.M., Odermatt, B., Marty, C., Zehnder-Fjallman, A.H., Ballmer-Hofer, K., and Schwendener, R.A. (2006). Clodronate-liposome-mediated depletion of tumour-associated macrophages: a new and highly effective antiangiogenic therapy approach. *Br J Cancer* 95, 272-281.
- Zhang, Q.B., Ji, X.Y., Huang, Q., Dong, J., Zhu, Y.D., and Lan, Q. (2006). Differentiation profile of brain tumor stem cells: a comparative study with neural stem cells. *Cell Res* 16, 909-915.

- Zhang, R., and Adams, P.D. (2007). Heterochromatin and its relationship to cell senescence and cancer therapy. *Cell Cycle* 6, 784-789.
- Zhang, X.P., Zheng, G., Zou, L., Liu, H.L., Hou, L.H., Zhou, P., Yin, D.D., Zheng, Q.J., Liang, L., Zhang, S.Z., *et al.* (2008). Notch activation promotes cell proliferation and the formation of neural stem cell-like colonies in human glioma cells. *Mol Cell Biochem* 307, 101-108.
- Zhao, N., Guo, Y., Zhang, M., Lin, L., and Zheng, Z. (2010). Akt-mTOR signaling is involved in Notch-1-mediated glioma cell survival and proliferation. *Oncol Rep* 23, 1443-1447.
- Zhuang, D., Mannava, S., Grachtchouk, V., Tang, W.H., Patil, S., Wawrzyniak, J.A., Berman, A.E., Giordano, T.J., Prochownik, E.V., Soengas, M.S., *et al.* (2008). C-MYC overexpression is required for continuous suppression of oncogene-induced senescence in melanoma cells. *Oncogene* 27, 6623-6634.
- Zuniga, R.M., Torcuator, R., Jain, R., Anderson, J., Doyle, T., Ellika, S., Schultz, L., and Mikkelsen, T. (2009). Efficacy, safety and patterns of response and recurrence in patients with recurrent high-grade gliomas treated with bevacizumab plus irinotecan. *J Neurooncol* 91, 329-336.